The extra ciliary roles of Meckel-Gruber syndrome proteins

Submitted by **Kate McIntosh**, to the University of Exeter as a thesis for the degree of **Doctor of Philosophy in Biological Sciences, July 2015**.

I certify that all material in this thesis which is not my own work has been identified, and that no material has previously been submitted and approved for the award of a degree by this or any other University.

ABSTRACT

Meckel-Gruber syndrome (MKS) is a recessive genetic disease that is uniformly lethal in affected children due to resultant developmental defects in the kidney and brain. 13 *MKS* genes have been identified, and further candidate genes have been linked to this disease, all encoding unrelated proteins. Their role is believed to be in generation and compartmentalisation of the primary cilium, a microtubule-based organelle that functions in signal transduction of developmentally-crucial pathways. However, recent evidence indicates that these proteins are also likely involved in regulation of the actin cytoskeleton. Furthermore, research is beginning to uncover roles of other ciliopathy proteins in regulation of additional subcellular structures, such as the microtubule cytoskeleton, focal adhesions and the Golgi. To begin to understand the roles of the MKS proteins beyond the cilium, I examined a number of cellular features of patient fibroblasts carrying mutations in *TMEM216* (MKS2) and *TMEM67* (MKS3). In this thesis, I describe the temporal appearance and nature of prominent actin bundles observed in these cells, and analyse the dependency of these on the Rho/ROCK signalling pathway. Furthermore, I identify novel alterations to the microtubule cytoskeleton and organisation of the Golgi complex in MKS patient cells, and subsequently establish a temporal order of these phenotypes, demonstrating microtubule defects as the first to occur in these cells. Finally, I connect these phenotypic defects to Rho/ROCK signalling. In contrast to the prevailing view in the ciliopathy field, I believe that a diffusion barrier at the transition zone is not the primary role of MKS proteins. Instead I propose, supported by these data, that MKS protein complexes play a dual role as effectors of Rho signalling in addition to performing a structural role with particular importance in tethering the cytoskeleton to membranes. I therefore conclude that these, and other ciliopathy protein complexes, may act as important signal transduction and structural components at multiple locations throughout the cell.

TABLE OF CONTENTS

ACKNOWLEDGEMENTS

My deepest gratitude goes to all those who have made doing a PhD that little bit easier and, at times, actually quite a lot of fun. This project would not have been possible without the BBSRC, who I would also like to thank for their financial support.

My thanks particularly extend to:

Helen, my supervisor, for pushing me to my absolute best and enabling me to far exceed my own expectations of myself.

My parents, who have instilled in me their certainty that I could get wherever I wanted to, provided that I tried my best.

My incredibly conscientious brother, Alistair, who has always made me feel wiser than I really am, and whom I wish the absolute best for his current and future scientific endeavours.

Ben, who's been there since the beginning, offering me much-needed support and laughter at some of the worst points.

Those who've provided me with some of the key advice to get me through, both scientific (particularly Martin, Pete and Joe), and pastoral (many thanks specifically to Sam, our lab guru).

Dawe group members, past and present, including David, Amy, Holly and Kat, and to Isabelle Jourdain and James Wakefield, for providing me with incredibly valuable feedback and advice throughout my project.

To my housemates, particularly Sam and Joe, for putting up with my temporary lapses in a sense of humour, and for providing a great distraction in my downtime.

Finally, to all the friends I've met since arriving here, with whom I've laughed so much that I've hurt myself, particularly Charli, Stacey, Kim, Sheera, Nat, Dan, Anna, Andy, and Sarah (and, in fact, all of Lab 211, both past and present). It's been an absolute joy to work with all of you.

LIST OF FIGURES AND TABLES

CHAPTER I: Introduction

CHAPTER II: Materials and Methods

CHAPTER III: MKS patient cells display characteristic prominent actin bundles due to filament turnover defects

CHAPTER V: MKS patient cells show defects in microtubule organisation

CHAPTER VI: Microtubule defects temporally precede, but do not cause, the other cellular defects

CHAPTER I: INTRODUCTION

1.1 Ciliopathies

Diseases termed “ciliopathies” represent a spectrum of inherited, recessive human disorders associated with mutations in proteins that are structural or functional components of the primary cilium. The primary cilium is an organelle involved in mechanosensation, chemosensation, photoreception, olfaction and a plethora of other roles entailing signal transduction. Dysfunction of the primary cilium causes wide-ranging disease phenotypes, including severe developmental abnormalities such as polycystic kidneys, polydactyly and central nervous system (CNS) malformations (Sharma *et al.*, 2008; Szymanska *et al.*, 2014). The cause of a number of these defects remains unexplained, illustrating the importance of clarifying the molecular aetiology of these disorders.

The diseases typically associated with ciliary dysfunction include Joubert syndrome (JBTS), Senior-Løken syndrome (SLS), nephronophthisis (NPHP), Bardet-Biedl syndrome (BBS), orofaciodigital (OFD) syndrome, Jeune syndrome, polycystic kidney disease (PKD), Alström syndrome, and Meckel-Gruber syndrome (MKS) (Sharma *et al.*, 2008; Waters and Beales, 2011). Ciliopathies are relatively common, with estimated worldwide prevalence of 1 in 2,000, based on the three typical disease traits of polydactyly, retinal degeneration, and renal cysts (Quinlan *et al.*, 2008). These diseases are clinically distinct entities but have overlapping clinical presentation (Table 1.1). Simultaneous presentation of a number of these traits is often used as a predictive fingerprint of structural and/or functional ciliary abnormalities. Many ciliopathies also present with brain agenesis (such as of the corpus callosum, or encephalocele), *situs inversus*, and renal disease (Badano *et al.*, 2006b).

In 2011, ciliopathic features were associated with mutations in over 40 genes, and over 1,000 polypeptides were known to fall within the ciliary proteome (Waters and Beales, 2011), but this number has greatly increased in recent years. This is, in part, due to the increasing availability of next-generation methods for nucleic acid sequencing, which make mutation identification much less time-consuming. Presently, mutations in 27 genes have been described as JBTS-associated (Bachmann-Gagescu *et al.*, 2015), and 13 as MKS-causative,

for instance (Shaheen *et al.*, 2015; Szymanska *et al.*, 2014); however, a few other likely candidates have also been identified (Shaheen *et al*., 2013; Szymanska *et al*., 2012). These display allelism with each other and with other ciliopathies.

Ciliopathies are genetically and phenotypically heterogeneous, often demonstrating similar phenotypes in models with mutations in multiple loci as in models with mutations at a single locus. This has presented extreme difficulty in making genotype-phenotype correlations (Szymanska *et al.*, 2014). These similarities have ethical implications: antenatal presentation of BBS appears like MKS, the former of which has a much lower fatality risk, meaning that termination could be inappropriately recommended (Karmous-Benailly *et al.*, 2005).

Although these “ciliopathic” diseases share a dysfunction of the primary cilium or associated structures, a number of other subcellular defects correlate in these diseases, which is the subject of this thesis.

Clinical diagnosis

There is a high degree of phenotypic overlap in clinical presentation of the ciliopathies (*Table 1.1*), and there are a few common features observed across multiple ciliopathies, such as hepatic and renal disease, retinal degeneration, laterality defects, and polydactyly. These defects occur at varying frequency in each disease, and certain ciliopathies are more severe than others. For example, in NPHP patients, childhood end-stage renal failure is estimated at only 5% prevalence in these patients; this is, however, the most common genetic cause of chronic kidney disease up to the third decade of life (Wolf and Hildebrandt, 2011). MKS – the subject of this thesis - is uniformly perinatal lethal (Waters and Beales, 2011; Wolf and Hildebrandt, 2011). As one of the most severe of the ciliopathies, and the most common syndromic cause of neural tube defects (Leitch *et al.*, 2008), MKS is an important focus of investigation from which we may be able to deduce the underlying molecular foundations of ciliopathies. It is for this reason that I have chosen to study MKS as a model of the ciliopathies.

MKS was first reported in 1822 by Johann F. Meckel, and then by C.B. Gruber in 1934 (Salonen and Paavola, 1998). MKS is typically characterised by

TABLE 1.1: Clinical features associated with ciliopathies

Feature	MKS	BBS	JBTS	NPHP	SLS	Jeune	OFD	Alström	PKD
Hepatic disease	✓	✓	✓	✓	✓	✓	✓	✓	✓
Renal disease	✓	✓	✓	✓	✓	✓	✓	✓	✓
Polydactyly	✓	✓	✓			✓	✓		
Posterior fossa defects/encephalocele	✓		✓						
Laterality defects/situs inversus	✓	✓		✓	✓	✓			
Skeletal dysplasia	✓					✓	✓		
Craniofacial defects	✓	✓	✓				✓		
Retinal impairment	?	✓	✓	✓	✓		✓	✓	
Cognitive impairment	?	✓	✓				✓		
Obesity	?	✓						✓	

Adapted from Waters and Beales (2011), Brugmann *et al.* (2010) and Quinlan *et al.* (2008).

renal cysts [estimated at a prevalence of 97.7% of cases (Barisic *et al.*, 2015), making it the most frequent defect], variable CNS defects (particularly occipital encephalocele; 83.8% of cases), and polydactyly (87.3% of cases) (Barisic *et al.*, 2015). It should be noted, however, that the diagnostic triad occasionally incorporates hepatic fibrosis in place of polydactyly, as this is also a common defect (65.5% of cases) (Barisic *et al*., 2015; Dawe *et al.*, 2007b). These defects typically correlate with specific mutations, and phenotypes are often heritable.

MKS is also associated with a number of other defects, including skeletal changes and laterality defects (Alexiev *et al.*, 2006; Salonen, 1984; Salonen and Paavola, 1998). Incidence is estimated to be between 1:13,250 and 1:140,000 live births. Higher incidence is present in groups with higher rates of consanguineous relationships, such as the Gujarati Indians and the Finnish. In Finland, for instance, there is a genetic founder effect, meaning that the same *MKS1* mutation (a deletion, 1408-35_1408-7del29; Szymanska *et al.*, 2012) exists in many of the patients here (Chen, 2007).

Ultrasound diagnosis of the classical MKS presentation of CNS, renal and digital anomalies is typically made before 14 weeks gestation (Barisic *et al.*, 2015; Sepulveda *et al.*, 1997; Tongsong *et al.*, 1999). MKS is unavoidably lethal *in utero* or in the first hours of life (or, rarely, up to a few months), normally due to pulmonary hypoplasia (Ramadani and Nasrat, 1992).

Mutations at the *MKS2* (occurring within the *TMEM216* gene) and at *MKS3/TMEM67* loci, the focus of this thesis, cause fairly typical MKS phenotypes. Mutations at the *MKS2* locus, for instance, cause CNS defects (anencephaly, encephalocele or meningocele) and cystic kidneys, amongst other defects (including bile duct proliferation, polydactyly, cleft palate and bowing of long bones) in patients (Valente *et al.*, 2010).

By contrast, mutations at the *MKS3*/*TMEM67* locus appear to affect the liver in all patients, suggesting that liver disease is a key clinical result of this mutation (Otto *et al.*, 2009). Mutations in *TMEM67* are also the most common cause of COACH syndrome, a Joubert syndrome-related disorder presenting with liver fibrosis, supporting a marked association between this gene and liver involvement (Iannicelli *et al.*, 2010; Szymanska *et al.*, 2014). Notably, it has previously been reported that, compared with patients with mutations at *MKS1* loci, CNS malformations are less common and milder in MKS3 cases, and polydactyly is rarely present (Consugar *et al.*, 2007; Morgan *et al.*, 2002). Thus

far, a clear genotype-phenotype correlation from *MKS2* and *-3* loci to cause MKS has proven difficult to elucidate. However, based the severity of the disease, it is likely that these mutations have dramatic consequences on the MKS proteins.

Animal models of MKS

Mice carrying mutations in *MKS1*, *TMEM67*, *CEP290*, *RPGRIP1L, CC2D2A*, *NPHP3*, *TCTN2*, *B9D1* and *B9D2* have now been established, many of which closely mirror human disease (Chen *et al.*, 2015; Norris and Grimes, 2012; Stratigopoulos *et al.*, 2014).

No mouse models of MKS2 currently exist and animal studies beyond this are limited to investigation of *TMEM216* (of which the *MKS2* locus forms a smaller part) in two zebrafish models. The first was a knockdown of *tmem216*, causing gastrulation defects that are typical of Wnt/planar cell polarity defects, including misshapen somites, broad notochords, and a shortened body axis (Valente *et al.*, 2010). Similar defects were previously demonstrated by a similar, morpholino-based approach in *mks3* knockdown zebrafish, which revealed alterations to somite size, a kinked notochord and a shortened body axis (Leitch *et al.*, 2008). Morpholino knockdown of *tmem216* and *tmem67* also caused defects in convergence to the midline and extension along the anterior-posterior axis; it is of note that this was more pronounced in *tmem67* morphants, however (Valente *et al.*, 2010). The second also used a morpholino knockdown of *tmem216*, revealing similar gastrulation defects; these morphants demonstrated hydrocephalus, left-right heart axis defects and a curved or kinked tail (Lee *et al.*, 2012). These defects, particularly gastrulation defects, are of interest due to the established CNS malformations in MKS2 patients, supporting a necessity of *MKS2* protein product TMEM216 in embryonic development.

MKS3 models are better established, with several examples; these include *Caenorhabditis elegans* and *Paramecium tetraurelia* mutants, the Wpk (Wistar polycystic kidney) rat and the bpck (bilateral polycystic kidney) mouse. *C. elegans mks-3* null mutants displayed reduced chemotaxis, indicative of impaired sensory function, but exhibited no obvious ciliogenesis defects (Williams *et al.*, 2011). *P. tetraurelia* with RNAi knockdown of *MKS3* developed

distortions in the cell and ciliary membranes and, in contrast with the *C. elegans* mutants, demonstrated absence or shortening of cilia (Picariello *et al.*, 2014). The Wpk rat, originally established as a model of autosomal recessive polycystic kidney disease (Nauta *et al.*, 2000), also displays CNS malformations such as severe hydrocephalus (Gauttone *et al.*, 2004). The presence of severe CNS defects mirrors the zebrafish model, but does not reflect human disease – as mentioned previously, CNS defects are less common and typically milder in MKS3 (Consugar *et al.*, 2007; Morgan *et al.*, 2002). The bpck mouse, which is *tmem67*-null, has multiple tissue phenotypes reflective of human disease. These include cystic kidneys and a bowing of bones and a notable absence of polydactyly (Cook *et al.*, 2009; Du *et al.*, 2013). These mice also exhibit features not typically present in human MKS3 but present in multiple ciliopathies, including disorganised stereociliary bundles in the inner ear, retinal degeneration, (Leightner *et al.*, 2013) neural tube defects (Abdelhamed *et al.*, 2013) and hydrocephalus (Cook *et al.*, 2009). Variation in phenotypes is likely due to species differences; versions of human and rat meckelin, the *MKS3* protein have 91% similarity (Smith *et al.*, 2006), for instance. For this reason, it is valuable to study MKS2 and -3 using *in vitro*, human cell models, to optimally recapitulate clinically observed features. However, these animal models can provide insight into how conserved, and crucial, these proteins are in correct embryonic development across multiple species, particularly during gastrulation.

Molecular genetics

The ciliopathies are genetically heterogeneous, and MKS has been associated with mutations at several of the same loci found to be affected in BBS, JBTS, SLS, LCA, OFD and NPHP (Baala *et al.*, 2007; Delous *et al.*, 2007; Edvardson *et al.*, 2010; Gerdes *et al.*, 2009; Gorden *et al.*, 2008; Leitch *et al.*, 2008; Mougou-Zerelli *et al.*, 2009; Online Mendelian Inheritance in Man, 2015; Quinlan *et al.*, 2008; Valente *et al.*, 2010; Valente *et al.*, 2006).

MKS is caused by mutations in 13 known genes, (*Table 1.2*) encoding proteins at numerous subcellular locations. These are present in most fetal and adult tissues, but are expressed at particularly high levels in ciliated tissues. *TMEM216* (*MKS2*) mRNA, for instance, is abundantly expressed in the CNS, limb bud and kidney (Valente *et al.*, 2010). Similarly, *MKS3* transcripts are

TABLE 1.2: Table to summarise the known information about the MKS genes.

Phenotype	**Gene locus**	**Also known as**	**Chromosome location (in humans)**	**Corresponding protein length (amino acid residues)**
Meckel syndrome type 1	*MKS1*	*MKS, BBS13*	17q23	559 a.a.
Protein name and structural features: MKS1. Contains B9 domain.				
Meckel syndrome type 2	*MKS2*	*TMEM216, JBTS2, CORS2*	11q13	148 a.a. (longest splice isoform)
Protein name and structural features: TMEM216. A tetraspan transmembrane protein with one intracellular and two extracellular loops. Forms a complex with TMEM67.				
Meckel syndrome type 3	*MKS3*	*TMEM67, JBTS6, NPHP11*	8q21.13-q22.1	995 a.a.
Protein name and structural features: TMEM67 or Meckelin. Contains a cleavable signal peptide and extracellular region, followed by three to seven predicted transmembrane regions and a short cytoplasmic tail.				
Meckel syndrome type 4	*CEP290*	*KIAA0373, 3H11AG, JBTS5, SLSN6, LCA10, BBS14*	12q21.32-q21.33	2479 a.a.
Protein name and structural features: CEP290/Nephrocystin-6 (NPHP6). Contains 13 putative coiled-coil domains, a region with homology to SMC chromosome segregation ATPases, a bipartite NLS, 6 KID motifs, three tropomyosin homology domains, and an ATP/GTP binding site motif A, and has sites for N-glycosylation, tyrosine sulfation, phosphorylation, N-myristoylation, and amidation.				
Meckel syndrome type 5	*MKS5*	*RPGRIP1L, KIAA1005, JBTS7*	16q12.2	1315 a.a.
Protein name and structural features: RPGRIP1L. Contains an N-terminal region comprising five coiled-coil domains, a C-terminal region homologous to the RPGR-interacting domain of RPGRIP1 and a central region containing two PKC C2 motifs. Interacts with nephrocystin-4.				

Meckel syndrome type 6	*MKS6*	*CC2D2A, KIAA1345*	4p15.3	1561 a.a.
Protein name and structural features: CC2D2A. Contains C2 domain; likely to have three coiled-coils and CaM-binding site. Predicted to be mostly alpha helix and random coil structure.				
Meckel syndrome type 7	*MKS7*	*NPHP3, NPH3, RHPD1*	3q22	1330 a.a.
Protein name and structural features: Nephrocystin-3 (NPHP3). Contains an N-terminal coiled-coil, a C-terminal tetratrico peptide repeat and a tubulin-tyrosine ligase domain. Interacts with nephrocystin-1 (NPHP1).				
Meckel syndrome type 8	*MKS8*	*TCTN2, TECT2*	12q24.31	700 a.a. (in mouse)
Protein name and structural features: Tectonic 2. Contains an N-terminal signal peptide.				
Meckel syndrome type 9	*MKS9*	*B9D1, MKSR1*	17p11.2	115 a.a.
Protein name and structural features: B9 domain-containing protein 1 (B9D1).				
Meckel syndrome type 10	*MKS10*	*B9D2, MKSR2*	19q13.2	175 a.a.
Protein name and structural features: B9 domain-containing protein 2 (B9D2).				
Meckel syndrome type 11	*MKS11*	*TMEM231, JBTS20,*	16q23.1	315 a.a.
Protein name and structural features: TMEM231. Contains both N-terminal and C-terminal transmembrane domains.				
Meckel syndrome type 12	*MKS12*	*KIF14, KIAA0042*	1q32.1	1648 aa. (longest splice isoform)
Protein name and structural features: KIF14. Contains myosin- and kinesin-motor domain.				

Meckel syndrome type 13	*MKS13*	*TMEM107*	17p13.1	139 a.a.
Protein name and structural features: TMEM107. Has 4 transmembrane domains.				

Information sources: Bialas et al., 2009; Chih et al., 2012; Delous et al., 2007; Edvardson et al., 2010; Filges et al., 2014; Frank et al., 2008; Kyttala et al., 2006; Nakagawa et al., 1997; Olbrich et al., 2003; Omran et al., 2000; Online Mendelian Inheritance in Man, 2015; Ota et al., 2004; Reiter and Skarnes, 2006; Sayer et al., 2006; Shaheen et al., 2011; Shaheen et al., 2013a; Shaheen et al., 2015; Smith et al., 2006; Tallila et al., 2008; Valente et al., 2010.

Abbreviations: SMC - structural maintenance of chromosomes; NLS – nuclear localisation signal; KID - kinase-inducible domain; PKC – protein kinase C; C2 – conserved region (Ca2+ dependent) 2; CaM - calmodulin

expressed in agreement with tissue phenotypes observed in this disease, particularly in the hindbrain, the cartilage of developing limbs, the lung, the kidney and the developing retina (Dawe *et al.*, 2007b).

The type of mutation at these loci – i.e. frameshift deletions, splicing mutations, insertions, nonsense or missense mutations from transversion or transition, and from homozygous/heterozygous mutations, or (as "modifier genes") having subsequent epistatic effects from any of these on other loci can cause alternative clinical outcomes from MKS (Arts *et al.*, 2007; Baala *et al.*, 2007; Brancati *et al.*, 2009; Delous *et al.*, 2007; den Hollander *et al.*, 2006; Doherty *et al.*, 2010; Edvardson *et al.*, 2010; Gorden *et al.*, 2008; Leitch *et al.*, 2008; Noor *et al.*, 2008; Otto *et al.*, 2009; Sayer *et al.*, 2006; Srour *et al.*, 2012; Valente *et al.*, 2010; Valente *et al.*, 2006).

The two genetic loci I have concentrated on in my research are *MKS2* and *MKS3*, encoded for by genes *TMEM216* and *TMEM67* (respectively). These were chosen based on the availability of patient cells, and as *TMEM67* is reported to be the most commonly mutated gene in MKS patients (29.8% of cases in the cohort analysed; Szymanska *et al.*, 2012). Aside from causing MKS, mutations at both of these loci can cause Joubert syndrome (Baala *et al.*, 2007; Edvardson *et al.*, 2010; Valente *et al.*, 2010). *TMEM67* mutations can additionally cause COACH syndrome (Brancati *et al.*, 2009; Doherty *et al.*, 2010) or NPHP (Otto *et al.*, 2009), or can have an epistatic effect, acting as a modifier at BBS-associated loci (Leitch *et al.*, 2008).

MKS2 cases are attributable to homozygous deleterious mutations to the *TMEM216* gene on chromosome 11q13, and the *MKS2* locus is proposed to have allelism with *JBTS2* (Roume *et al.*, 1998; Valente *et al.*, 2010). Causative mutations include nonsense, splice site and, most commonly, missense mutations, which led to unstable protein production when transfected into heterologous cells (Valente *et al.*, 2010). Mutations are reported throughout the gene, with no obvious correlation between mutation and clinical outcome. Confusingly, the same *TMEM216* mutation (a homozygous 218G-A transition in exon 4, leading to the same arg73-to-his (R73H) substitution) has been noted in siblings with different disorders (one with JBTS, one with MKS) (Valente *et al.*, 2010). This is likely to be due to modifier genes also present in these patients having an epistatic effect on clinical outcomes.

MKS3 is caused by homozygous or compound heterozygous mutations to the *TMEM67* gene on chromosome 8q21.13-q22.1, including frame-shift, splicing and missense mutations (Consugar *et al.*, 2007; Smith *et al.*, 2006). These mutations are hypothesised to lead to nonsense-mediated decay of transcripts in MKS3 patients (Smith *et al.*, 2006).

The most impactful MKS mutation is that of *MKS4*-associated gene *CEP290*, encoding nephrocystin-6 or CEP290 (Sayer *et al.*, 2006); mutations at this locus are causative of phenotypes associated with SLS, JBTS, NPHP, BBS, LCA and MKS, with no obvious genotype-phenotype correlation (Coppieters *et al.*, 2010; Frank *et al.*, 2008). Mutations in *CEP290* are also, after *TMEM67* and *MKS1*, the third most frequent cause of MKS (Szymanska *et al.*, 2012). Over 100 unique *CEP290* mutations are known to exist, affecting multiple organ systems; these include the eyes (as retinal dystrophy), nose (olfactory dysfunction), ears (particularly otitis media), kidneys, CNS (particularly occipital encephalocele), liver (elevated liver enzymes and abnormal structure are reported), heart (particularly septal defects), in addition to a plethora of other skeletal and other tissue patterning defects, such as diverse craniofacial defects and polydactyly (Coppieters *et al.*, 2010).

Most *CEP290* mutations are nonsense, splice-site, or frameshift mutations, which cause loss of protein function (Frank *et al.*, 2008; Waters and Beales, 2011). It is proposed that the dramatic spectrum of phenotypic heterogeneity associated with these mutations is not due to the function of the CEP290 proteins themselves, but rather disruption of their function as genetic modifiers, or their interaction with other proteins (Coppieters *et al.*, 2010; Gorden *et al.*, 2008). This is the case for *CEP290* and *CC2D2A*, in which the knockdown of each results in concomitant pronephric cyst phenotypes. CEP290 interacts with TCTN1, RPGR, CC2D2A and numerous other proteins at the transition zone (Chang *et al.*, 2006; Garcia-Gonzalo *et al.*, 2011; Gorden *et al.*, 2008), the role of which will be described in a later section.

Mutations in a number of MKS-associated genes, such as *CC2D2A* and *RPGRIP1L*, demonstrate a more obvious genotype-phenotype correlation; the more severe MKS phenotypes result from truncating and resultant loss-of-function mutations at these loci, whilst patients with the milder JBTS tend to have at least one missense mutation (Delous *et al.*, 2007; Mougou-Zerelli *et al.*, 2009).

In a study aiming to make a genotype-phenotype correlation in the ciliopathies, NPHP (with no brain anomaly) was demonstrated to correlate with a missense mutation affecting amino acids C615 or G821, and Joubert syndrome patients all had at least one missense allele but not truncating mutations (Otto *et al.*, 2009). Heterozygous mutations in BBS-related genes and alterations to certain BBS-interacting proteins can modulate penetrance of the BBS phenotype (Badano *et al.*, 2003; Badano *et al.*, 2006a; Beales *et al.*, 2003; Katsanis *et al.*, 2001; Stoetzel *et al.*, 2006). As a BBS-causative gene, *MKS3* mutations are thought to have an epistatic effect on BBS-associated loci (Leitch *et al.*, 2008), i.e., whether BBS or another clinical outcome occurs is dependent on the genetic context of the mutation. It is apparent that making a genotype-phenotype correlation is an incredibly complex issue, which cannot yet be resolved with the information currently available.

The *MKS2* and *-3*-encoded proteins

The *MKS2* locus is present within gene *TMEM216* and and *MKS3* is otherwise known as *TMEM67*, encoding TMEM216 and meckelin proteins, respectively (Smith *et al.*, 2006; Valente *et al.*, 2010).

TMEM216 and meckelin are both considered to be transmembrane proteins. TMEM216 is a tetraspan transmembrane protein, a group of proteins characterised by four hydrophobic putative transmembrane domains (TM1 to TM4), forming two extracellular loops and one intracellular loop (Lee *et al.*, 2012; Valente *et al.*, 2010), but this protein remains uncharacterised. Meckelin consists of a cleavable signal peptide, a 490-residue extracellular region followed by seven transmembrane regions, and a 30-residue cytoplasmic tail (Smith *et al.*, 2006). The structure of the extracellular region and cytoplasmic tail are proposed to be likely indicators of a receptor function of this protein; however, despite topological similarity to the Frizzled receptors, there is limited sequence homology with this or any other proteins (Smith *et al.*, 2006).

Notably, TMEM216 and meckelin form a complex, as demonstrated by an immunoprecipitation study (Valente *et al.*, 2010). This study revealed that TMEM216-GFP could be immunoprecipitated by meckelin antisera containing the N- and C-termini, and that anti-GFP could also pull down a C-terminus-containing isoform of meckelin in a complex with TMEM216-GFP. These

proteins are now established to interact within a larger complex at the transition zone (Garcia-Gonzalo *et al.*, 2011), which will be discussed in the next section.

1.2 Building a cilium

Ciliary structure – an overview

Cilia are categorised as primary or motile, based on their structure and function. Cilia are sensory organelles, acting to detect the extracellular environment, participate in signal transduction to the inside of the cell and link diverse signalling pathways involved in cellular activities such as differentiation, migration and cell growth (Satir and Christensen, 2007; Satir *et al.*, 2010). The primary cilium is presented on the outside of quiescent cells and resorbed during cell division. However, there is evidence that a transient cilium is re-assembled and subsequently disassembled during G_1/S-phase transition (Spalluto *et al.*, 2013; Tucker *et al.*, 1979a; Tucker *et al.*, 1979b), but the exact nature of this cilium remains unknown.

Motile cilia have additional roles in directing fluid flow. This is an important function, for instance, in developing left-right patterning at the embryonic node by generating leftward fluid flow to instigate signalling in primary cilia at the periphery of the node (Babu and Roy, 2013; Satir and Christensen, 2007), or lining the trachea, where they remove mucus from the lungs (Horvath and Sorscher, 2008; Jeffery and Reid, 1975; Sanderson and Sleigh, 1981; Shah *et al.*, 2009). Multiple cilia are more likely to be present in higher numbers than flagella or primary cilia (Dawe *et al.*, 2007a), at least in opisthokonts; the sperm of gymnosperm *Ginkgo biloba*, for instance, are multi-flagellated (Vaughn and Renzaglia, 2006).

All cilia and flagella have a similar structure, consisting of a distinct, specialised membrane, the ciliary membrane, surrounding nine doublet microtubules (MTs). These extend from a centriole of nine triplet MTs, referred to as a basal body (Ishikawa and Marshall, 2011; Scholey, 2003).

Figure 1.1 illustrates the structure of mammalian primary cilia in cross-section, including the components of the transition zone, a region between the basal body and axoneme that is posited to act as a diffusion barrier (discussed later). Primary cilia have a 9+0 structure, meaning that they are lacking a

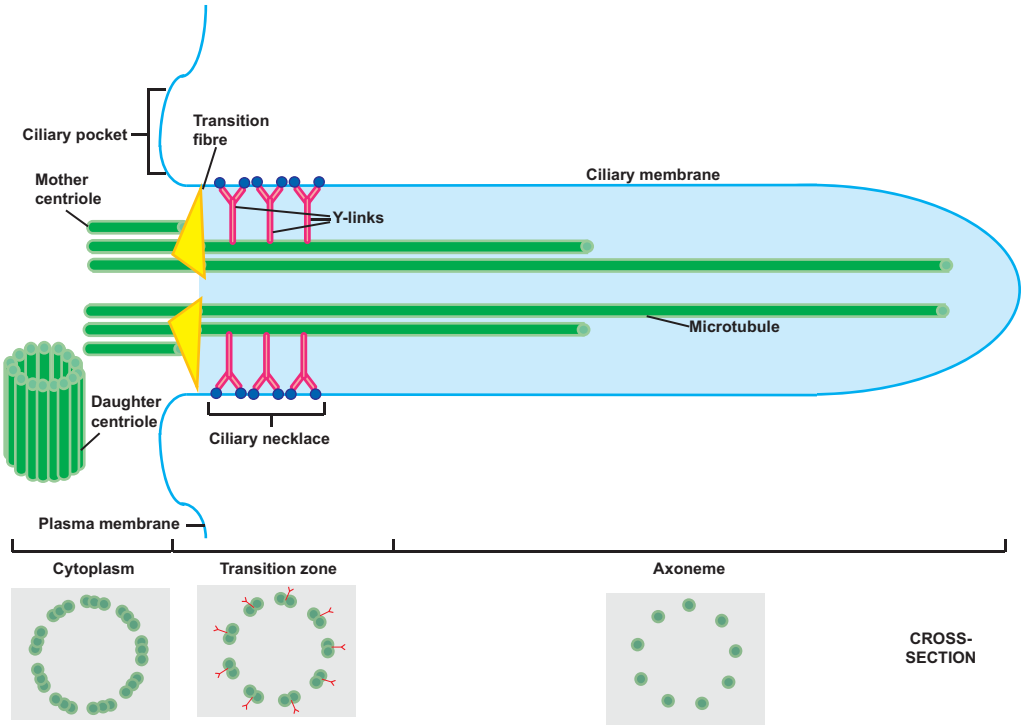

FIGURE 1.1: Longitudinal and transverse structure of a human primary cilium. The cilium has a 9+0 microtubule-based axoneme, beginning as microtubule triplet pairs at the basal body (comprising mother and daughter centrioles), and tapering to microtubule singlets at the end of the axoneme. Separating the basal body from the transition zone are the transition fibres, which begin as distal appendages. Distal to this are the Y-links; these connect each microtubule doublet to the overlying membrane via the ciliary necklace, a set of intramembranous particles. The transition zone is proposed to enable selectivity of diffusion into the cilium, allowing the specialised ciliary membrane and axoneme to develop. Ciliary placement is demonstrated with respect to the ciliary pocket and plasma membrane (Adapted from Reiter *et al.*, 2012).

central pair of MTs (i.e., not 9+2), and lack the dynein and nexin arms, radial spokes and central pair apparatus of motile cilia (Scholey, 2003). *Figure 1.1* also shows these structures in relation to the ciliary pocket, a region embedded within the plasma membrane.

The basal body is, in the case of the primary cilium, derived from the mature centriole of the two, forming the microtubule organising centre (MTOC). Specifically, in the case of eukaryotic cells, this is referred to as the centrosome, and this is an important structure in cell division. When docked, the centrosome is known as a basal body, an analogous structure to the mother centriole (Chapman, 1998). Migration of the centrioles to the apical cell surface marks the start of ciliogenesis and is followed by association with vesicles (proposed to be post-Golgi) and acquisition of accessory structures. Abundant evidence implicates the actin-myosin network in this migration and docking (Dawe *et al.*, 2007a; Garcia-Gonzalo and Reiter, 2012). An MT axoneme is subsequently nucleated from the basal body then elongated to form a cilium through a process known as intraflagellar transport (IFT) (Ishikawa and Marshall, 2011; Rosenbaum and Witman, 2002), discussed later.

Centriole migration

The centriole is a 0.4-μm long, 0.2-μm diameter cylindrical arrangement of MT triplets arrayed with ninefold radial symmetry around a cylindrical core; these triplets consist of α– and β-tubulin heterodimers (Dawe *et al.*, 2007a). An immature centriole, such as the daughter centriole, has a central rod linked to the inner tubule by spokes, referred to as the cartwheel (Vorobjev and Nadezhdina, 1987). The mature (mother) centriole acquires distal and subdistal appendages (Paintrand *et al.*, 1992) with various cellular roles, including in docking the centrosome. The mother and daughter centriole, along with a surrounding dense mass of pericentriolar material (PCM) comprise the centrosome (Dawe *et al.*, 2007a).

Centrosome position is tightly regulated across multiple cellular contexts, based on polarity cues. These can be factors such as cell shape or extracellular signals, which are then transduced through the partitioning (Par) proteins and the Rho GTPases (Goldstein and Macara, 2007). Par proteins and the Rho

GTPases then interact with the cytoskeleton in order to effect this established cell polarity (Cowan and Hyman, 2007).

To initiate cilium formation, the centrioles migrate to the plasma membrane, through a cytoskeleton-dependent mechanism; this movement also appears to be dependent on a number of centrosomal proteins, such as TALPID3 (Stephen *et al*., 2013). Notably, TMEM216 and meckelin are necessary for this stage of ciliogenesis. Cells with an siRNA knockdown of *TMEM67* (Dawe *et al.*, 2007b) and *TMEM216*, and two different patient fibroblast cell lines with mutations in *TMEM216* (Valente *et al.*, 2010) all display defects in ciliogenesis and, specifically, in centriole migration and docking at the apical cell surface. This process has a proposed link to the actin cytoskeleton, and these MKS proteins may be directly involved in centrosome migration during ciliogenesis via action on the cytoskeleton (Abdelhamed *et al.*, 2015; Dawe *et al.*, 2007b; Valente *et al.*, 2010). Recent evidence also supports a role of meckelin in basal body positioning in *Paramecium* (Picariello *et al.*, 2014), suggesting a conserved role of these proteins.

Centriole repositioning is necessary not only for ciliogenesis, but also for cell motility; wounded monolayers of endothelial cells, for example, exhibit MTOC reorganisation between the nucleus and leading edge in 80% of cells within 4 hours of wound formation (Gotlieb *et al.*, 1981). In migrating newt eosinophils, U2OS and PtK2 cells, irradiation-induced centrosome removal led to loss of cell polarisation during directed cell migration, likely linked to concurrent actin- and MT-based changes (Koonce *et al.*, 1984; Wakida *et al.*, 2010). The *MKS2* patient cells examined in this thesis demonstrate centrosome positioning defects (Valente *et al.*, 2010), and siRNA knockdown of *TMEM67* in IMCD3 cells inhibits the apical positioning of centrosomes (Dawe *et al.*, 2007b), as previously mentioned. This is of note as, in unpublished work, these patient lines have been shown to have motility defects; in a wound healing assay, *MKS2*- and *MKS3*-mutated patient cells demonstrated aberrant migratory capabilities through defects in speed and directionality (Barker and Dawe, unpublished). These data may implicate cell migratory defects underlying errors during embryonic development. Moreover, this implies that problems in centrosome positioning may precede or cause these, or a number of other defects. For additional information on centrosome repositioning, see *Appendix 1: Centrosome positioning in non-dividing cells*.

The cytoskeleton is involved during centrosome reorientation and docking. MTs are known to position the centrosome during interphase in a dynein-dependent manner (Burakov *et al.*, 2003) and centriole movement to the cell surface is accompanied by loss of radial MT organisation (Rieder *et al.*, 2001). There is also substantial evidence implicating involvement of the actomyosin network; actin and myosin are known to be associated with the centrioles or centriolar material (Lemullois *et al.*, 1988; Lemullois *et al.*, 1987), and actin- or myosin-blocking drug treatments prevent centriole migration in ciliogenic oviducts (Boisvieux-Ulrich *et al.*, 1987; Boisvieux-Ulrich *et al.*, 1990). Furthermore, interrupting actin remodelling prevents basal body docking (Pan *et al.*, 2007). Precise regulation of the actin cytoskeleton is critical to facilitate ciliogenesis, for instance through stabilisation of the pericentrosomal preciliary compartment by blocking actin assembly at specific subcellular locations (Kim *et al.*, 2010).

The underlying signalling pathways for centrosome reorientation during primary cilium development are slowly being revealed, principally in links to the cytoskeleton. *Foxj1* appears to be involved; *Foxj1*-null mice display aberrant centriole migration (Brody *et al.*, 2000), and Foxj1, dependent on the presence of a cilium, modulates the responsiveness of cells to Shh signalling (Cruz *et al.*, 2010).

As previously mentioned, the Rho GTPases and Par proteins are necessary for centrosome repositioning during both migration and ciliogenesis. For example, in order for the centrosome to reposition in *C. elegans*, Rho1 regulates actomyosin-dependent movement of the centrosome, while Cdc42 enables interaction between the actin cortex and the Par proteins (Cowan and Hyman, 2007). In astrocytes, cell polarity determinants, including Cdc42 and the Par proteins, control centrosome and Golgi orientation in the direction of migration, organised in this way to ensure vesicular trafficking in the correct direction (Cau and Hall, 2005). This is known to occur via a complex consisting of Par6, Par3 and atypical protein kinase C (aPKC) (Etienne-Manneville and Hall, 2001). This aPKC complex also localises to cilia and participates in ciliogenesis by promoting ciliary membrane development (Krock and Perkins, 2014), and intraflagellar transport (Rosenbaum and Witman, 2002; Scholey, 2003), a process discussed in a subsequent section. Inhibition of the activity of this protein complex has been reported to cause a reduction in cilia number and

size in zebrafish photoreceptors, leading to left-right asymmetry defects (Krock and Perkins, 2014). Moreover, Par1 and aPKC have also been revealed to promote and inhibit ciliated cell fates in the developing *Xenopus* ectoderm, respectively (Ossipova *et al.*, 2007), illustrating their powerful influence in cells.

In fibroblasts, the centrosome must remain at the cell centre and the nucleus moves in a dynein-dependent manner (Dujardin *et al.*, 2003; Gomes *et al.*, 2005; Levy and Holzbaur, 2008); for additional details on the nucleus-centrosome interaction, see *Appendix 1*. MTs anchored to the actin cortex are thought to be partially responsible for centrosome positioning by exerting pulling forces; myosin and moesin impart the necessary rigidity on the actin cortex for this to occur (Tang and Marshall, 2012), illustrating a necessity of cross-talk between the actin and MT cytoskeleton for centrosome repositioning.

It is apparent that the cytoskeleton is necessary for centrosome movement during ciliogenesis and cell migration; however, it is unclear how the association of the centrosome with other organelles, such as the Golgi complex, relates to centrosome repositioning. The Golgi is necessarily positioned to enable appropriately directed vesicular trafficking; that is, at the minus ends of microtubules and typically surrounding the centrosome, as it is transported here via microtubule motor proteins (Ho *et al.*, 1989; Thyberg and Moskalewski, 1999). This is so organised in order that ciliary components are trafficked to the ciliary base and membrane during cilium biogenesis. In most cell types and contexts, microtubule cytoskeleton organisation, controlled by polarity determinants and centrosome position, is presumed to affect Golgi position. However, the Golgi complex is also known to nucleate a subset of microtubules used in migration (Chabin-Brion *et al.*, 2001; Miller *et al.*, 2009), and reorientation of the Golgi and centrosome can be independently controlled (Magdalena *et al*., 2003). Furthermore, it has been reported by a previous study that blocking Golgi reorientation can prevent centrosome reorientation (Bisel, 2008), suggesting that movement of other organelles may be an overlooked factor in centrosome repositioning.

Basal body docking

In order to initiate axoneme MT polymerisation for ciliary elongation (Lemullois *et al.*, 1988; Satir and Christensen, 2007), basal bodies must dock

either with the plasma membrane [in a number of epithelial cells (Sorokin, 1962)], or with Golgi-derived ciliary vesicles [in smooth muscle and other epithelial cells (Sorokin, 1968; Sotelo and Trujillo-Cenoz, 1958)]. Docking is thought to be mediated by distal appendages, the precursors for transition fibres (Anderson, 1972), which are discussed later. Fusion of additional vesicles enables ciliary growth into the extracellular medium (Sorokin, 1962).

Focal adhesion proteins FAK, Paxillin and Vinculin, interact in complexes with the actin cytoskeleton to enable cell migration. Furthermore, integrin, another focal adhesion component, interacts with the extracellular matrix during astrocyte cell migration to activate and effect the polarised recruitment of Cdc42 (and thus the mPar6/PKC complex) at the leading edge (Etienne-Manneville and Hall, 2001). All of these proteins are additionally required for basal body migration, docking, and spacing, suggesting that focal adhesion complexes also participate in tethering the centrosome to the cortical actin cytoskeleton in a variety of cellular contexts (Antoniades *et al.*, 2014).

All cilia are extended from a single basal body, or numerous basal bodies in the case of multi-ciliated cells (Dawe *et al.*, 2007a). Multi-ciliated cells do not use typical centriolar duplication; instead basal bodies develop from the pre-existing progenitor daughter centrosome, which nucleates deuterosomes in a cartwheel-shaped structure. The resultant procentrioles grow synchronously before detaching from each other, following which they migrate and dock as usual (Al Jord *et al.*, 2014).

During migration and docking, basal bodies in primary cilia retain an associated procentriole daughter, and acquire a plethora of accessory structures. For instance, Cep164, a centrosomal protein that is required for vesicle docking, recruits and acts as a substrate of Tau tubulin kinase 2 (TTK2), an enzyme involved in distal appendage assembly during primary ciliogenesis (Cajanek and Nigg, 2014; Carvalho *et al.*, Cilia 2014 conference (unpublished); Schmidt et al., 2012). This Cep164-TTK2 interaction, in addition to recruitment of proximal end centriolar satellites such as Cep135 and WDR8, are essential in removal of a proximal CP110 cap, a requirement for axoneme extension (Kurtulmus *et al.*, 2015; Oda *et al.*, 2014).

Membrane trafficking to the primary cilium, inclusive of the ciliary vesicle, is crucial for basal body docking and ciliary elongation. A number of centriolar satellites, such as Cep164, Chibby and Talpid3 are recruited and form

structures at the distal end of the basal body, which then recruit and activate the Rab pathway components in order to form the ciliary vesicle (Burke *et al.*, 2014; Kobayashi *et al.*, 2014). Small GTPases, such as Rab8, are involved in sorting, docking and fusion of post-Golgi vesicles or recycling endosomes containing ciliary proteins at the periciliary membrane of the ciliary base (Li and Hu, 2011; Lim *et al.*, 2011; Nachury *et al.*, 2010; Pazour and Bloodgood, 2008; Rosenbaum and Witman, 2002; Wei *et al.*, 2015).

Defects in components involved in formation of the ciliary vesicle have also been connected to ciliopathy. CC2D2A, a protein altered in some forms of MKS and Joubert syndrome, functions with the centrosomal protein NINL in Rab8-regulated ciliary vesicle docking; knockdown of *cc2d2a* or *ninl* in zebrafish leads to vesicular accumulation and mislocalisation of Rab8, in addition to retinal defects that are reminiscent of symptoms of Joubert syndrome (Bachmann-Gagescu *et al.*, 2015). Furthermore, *EXOC8*, a Joubert syndrome-causative gene, and *EXOC4*, a novel MKS candidate gene encoding Sec8, encode proteins involved in the exocyst, a structure involved in vesicular trafficking to the basal body (Dixon-Salazar *et al.*, 2012; Shaheen *et al*., 2013). Deletion in zebrafish of the Joubert syndrome-contributory interactors of these, Sec10 and Arl13b, leads to the cystic kidney and decreased ciliogenesis phenotypes observed in ciliopathy patients (Seixas *et al.*, 2016), illustrating the necessity of appropriate vesicular trafficking in ciliogenesis.

A number of studies have been conducted regarding the signalling responsible for basal body docking and ciliary vesicle formation. Anchoring of the basal body at the plasma membrane has been linked to planar polarity pathway components inturned (Park *et al.*, 1996) and fuzzy (Collier and Gubb, 1997) through their control of the actin array. Similarly, cytoskeletal calpain, a protease appearing downstream of *Foxj1* and acting on actin-plasma membrane linker protein ezrin, regulates basal body anchoring to the apical cytoskeleton (Gomperts *et al.*, 2004). Cdc42, a downstream effector of the Ca^{2+}-dependent Wnt signalling pathway, is reportedly required for exocyst fusion at the base of the primary cilium, effecting ciliogenesis (Zuo *et al.*, 2011); notably, knockdown of Cdc42 attenuates vesicular trafficking to the primary cilia, leading to ciliogenesis defects and polycystic kidney disease (Choi *et al.*, 2013).

Mutation or loss of many ciliopathy-associated proteins therefore causes defects in the beginning stages of ciliogenesis (Reiter *et al.*, 2012), such as in ciliary vesicular trafficking (Fan *et al.*, 2004; Hsiao *et al.*, 2009) and basal body anchoring (Huang *et al.*, 2011; Valente *et al.*, 2010; Williams *et al.*, 2011), indicative of the importance of these stages in directing appropriate embryonic development.

The basal body and the transition zone

The structurally-unique region separating the basal body and the axoneme is called the transition zone (TZ). The TZ contains a number of important ciliary structures and proteins with vital roles in ciliary function, such as in recruiting IFT components and regulating ciliary composition (Christensen *et al.*, 2012; Garcia-Gonzalo and Reiter, 2012).

In mammalian cells, disruption of the TZ causes plasma membrane proteins GFP-CEACAM1 and GFP-GPI to aberrantly accumulate inside the cilium (Chih *et al.*, 2012); this illustrates how crucial this structure is in maintaining a specialised region within the cilium. Furthermore, emerging bioinformatic evidence has demonstrated that TZ complex proteins are restricted to the proteomes of ciliated organisms (Barker *et al.*, 2014a), implying a necessity of these proteins in ciliary function. The TZ is therefore the focus of a large proportion of research into ciliary function. The localisation of the TZ within the cilium is shown in *Figure 1.1*.

Complicating the proposed role of the TZ, the primary cilium has no basal plate, meaning the boundaries of TZ are harder to define. In primary cilia, the Y-links extend further into the cilium than in motile cilia, meaning the entire primary cilium has been proposed to be analogous to the transition zone of motile cilia (Rohlich, 1975).

An important feature of primary cilia is compartmentalisation, which is achieved through its distinct membrane composition and regulated protein transport. The regulation of protein entry and exit is thought to be via a ‘ciliary gate’ which prevents non-specific movement of protein and allows it to remain a privileged domain for appropriate modulation of certain signalling pathways (Garcia-Gonzalo and Reiter, 2012; Hu *et al.*, 2010; Reiter *et al.*, 2012).

Various structures and systems are proposed to make up this 'ciliary gate', including the ciliary necklace and Y-links (in the TZ), transition fibres (displayed in *Figure 1.1*) and a septin ring (at the periciliary region) and nucleocytoplasmic transport machinery (Reiter *et al.*, 2012).

At the ciliary base, a "ciliary pore complex" is thought to be present, and is proposed to be analogous to the nuclear pore complex. The nuclear pore excludes passage of proteins greater than a certain size, unless bound to importins or exportins, which recognise their targets using nuclear localisation signals (NLSs) or export sequences (NESs) (Garcia-Gonzalo and Reiter, 2012). Similarly, importin binding to an NLS-like ciliary localisation sequence (CLS) is required for some proteins to accumulate inside cilia, such as the kinesin Kif17 (Garcia-Gonzalo and Reiter, 2012).

Transmembrane proteins, unlike peripheral membrane proteins, must enter ciliary membranes by moving laterally from the periciliary membrane; as diffusion barriers often separate these, it is suggested that machinery engaging CLSs in the cargo facilitates this process (Chih *et al.*, 2012; Hu *et al.*, 2010). The ciliary pore complex is mechanistically disparate from both the proximal (closest to the nucleus) axoneme and from the nuclear pore complex (Breslow *et al.*, 2013).

The most proximal accessory structures associated with the centriolar barrel are the subdistal appendages and basal foot, and the distal appendages beyond these (which mature into the transition fibres) (Reiter *et al.*, 2012).

Ninein is a component of the basal foot, which is recruited by Odf2. Together, these promote centrosomal MT docking and nucleation (Delgehyr *et al.*, 2005; Ishikawa *et al.*, 2005). Odf2 has multiple splicing variants which cause this protein to localise to a variety of points along the basal body and ciliary axoneme. One Odf2 splicing variant, Cenexin1, localises to the distal/subdistal appendages and is essential for ciliogenesis (Chang *et al.*, 2013), indicative of the necessity of these structures in building a cilium. *MKS6* protein product CC2D2A is also essential in the assembly of subdistal structures in a number of species; *Cc2d2a -/-* mouse embryonic fibroblasts lack cilia, Odf2 and (concordantly) ninein is reduced (Veleri *et al.*, 2014), implying a structural or regulatory role of this MKS protein at the subdistal structures. However, *mks-6* mutant TZ ultrastructure appears normal in *C. elegans*, indicating that disruption

of specific components, such as the MKS proteins, at the base of the cilium does not necessarily lead to total loss of the TZ (Williams *et al.*, 2011).

The transition fibres (*Figure 1.1*) are located at the distal end of the basal body and serve as the main membrane attachment point for the basal body, as a site of protein target [including target by IFT particles (Deane *et al.*, 2001) and septin, which functions in an actin-regulated diffusion barrier at the ciliary base proximally to the transition fibres (Francis *et al.*, 2011; Hu *et al.*, 2010)], and as a physical block to transport. Electron micrographs suggest that inter-fibre spaces are too small for vesicles to traverse - about 60 nm in diameter - which could fit large protein complexes, but not vesicles (Nachury *et al.*, 2010; Reiter *et al.*, 2012). Large proteins thus require active transport to enter the cilium, but not for movement around the cilium (Breslow *et al.*, 2013; Takao *et al.*, 2014).

The TZ begins distally to the transition fibres (although certain definitions include these as a TZ constituent), characterised by Y-links connecting the doublet MTs to the overlying membrane at the ciliary necklace (*Figure 1.1A*) (Reiter *et al.*, 2012). These are also structures believed to be involved in a permeability barrier or 'smart filter', restricting membrane and soluble proteins based on CLSs; *Chlamydomonas reinhardtii* and *C. elegans* mutants lacking Y-links fail to accumulate proteins correctly in the ciliary membrane and *MKS4*-encoded protein CEP290 is essential for Y-link formation in *C. reinhardtii* (Craige *et al.*, 2010; Garcia-Gonzalo *et al.*, 2011; Garcia-Gonzalo and Reiter, 2012). However, the exact biochemical nature of Y-links is unknown.

Genetic and biochemical analysis in *C. elegans*, mouse and human models have identified two major protein modules located within the TZ protein interaction network, as indicated in *Figure 1.2*. These are the NPHP module and the MKS module, predominantly comprising proteins established to contribute primarily to NPHP or MKS, respectively. MKS proteins have been indicated in yellow, for ease of analysis. Briefly, the NPHP module proteins are proposed to interact with the axonemal MTs, and MKS module proteins with the ciliary membrane. These modules are hypothesised to also interact with the Y-links at the TZ, but only CEP290 is confirmed to be a structural component of these. CEP290 also appears to be a vital protein in tethering the flagellar transition zone to the ciliary membrane (Craige *et al*., 2010; Yang *et al.*, 2015). Notably, RPGRIP1L function is crucial for the integrity of the TZ, and is thought to promote its assembly (Blacque and Sanders, 2014; Garcia-Gonzalo and Reiter,

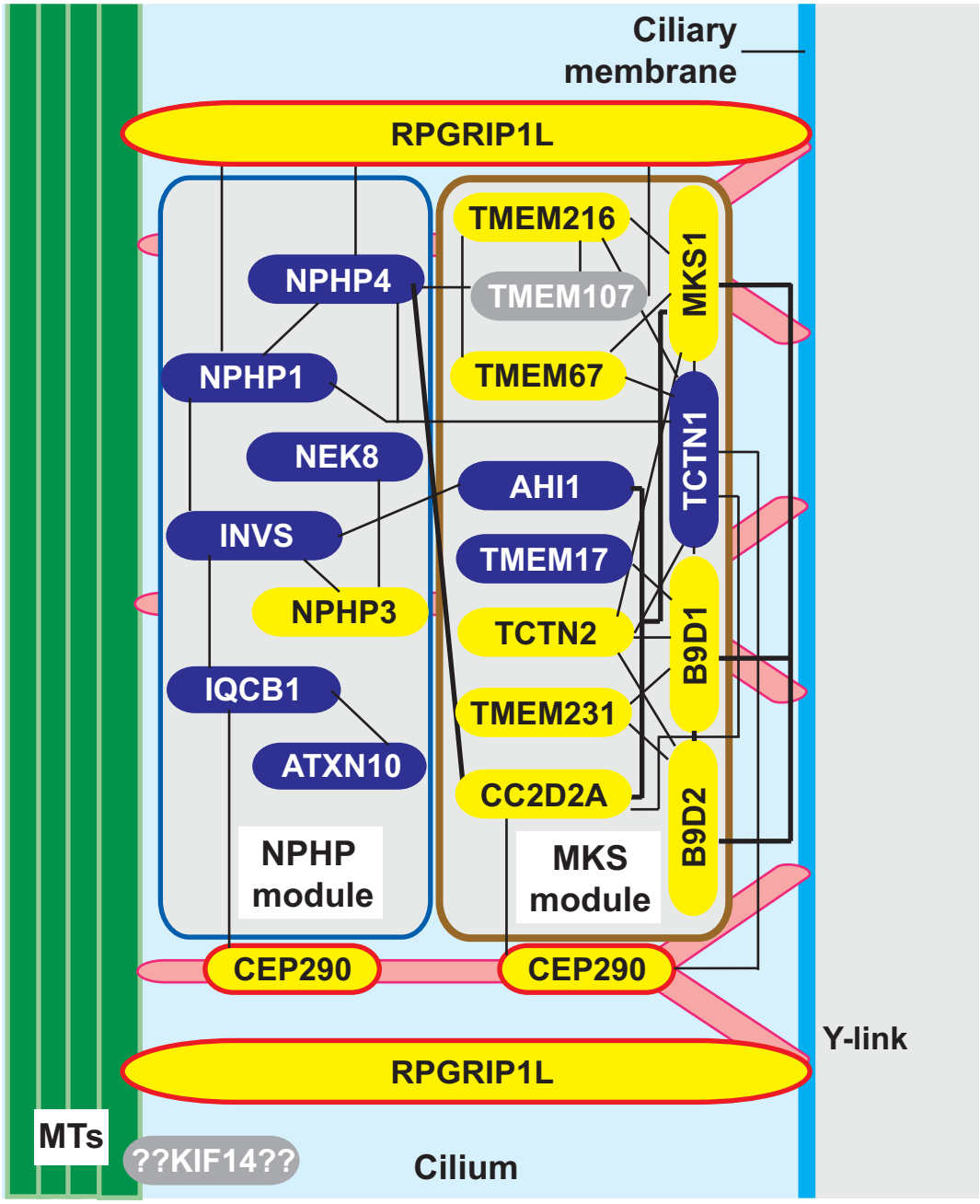

FIGURE 1.2: Proposed protein interaction network within the TZ, indicated by human gene names, and deduced through biochemical and genetic analysis in human, mouse and *C.elegans* models. The NPHP and MKS modules predominantly comprise NPHP- and Joubert syndrome-/MKS-associated proteins, respectively. Coded as follows: yellow, MKS-associated; blue, key components of the NPHP/MKS modules not associated with MKS; grey, MKS-associated but with unknown localisation/interactors; red outline, vital component for assembly/maintenance of TZ; and black lines, protein-protein interaction. The NPHP and MKS modules are proposed to interact with the MTs or staggered along the ciliary membrane, respectively. Proteins from both modules are proposed to interact with the Y-links, which may have CEP290 as a crucial component. RPGRIP1L is hypothesised to promote TZ assembly. TZ, transition zone; MT, microtubule. Sources: Blacque and Sanders, 2014; Jensen *et al.*, 2015; Garcia-Gonzalo and Reiter, 2012; OMIM and UniProt, 2015; Yee *et al.*, 2015.

2012; Jensen *et al.*, 2015; OMIM and UniProt, [accessed 2016]; Yee *et al.*, 2015). It is of note that the localisation of meckelin to the TZ is additionally supported by the presence of an X-box domain within this protein (Smith *et al.*, 2006), which is characteristic of a ciliary protein (Efimenko *et al.*, 2005).

The protein modules are proposed to be anchored together by MKS-5/RPGRIP1L. Taken together with evidence that Y-links are lost in MKS/MKSR/NPHP double mutants, these data imply that a number of these proteins may represent elements of the Y-link/ciliary necklace structures anchoring axonemal MTs to the ciliary membrane and functioning as a ciliary gate (Williams *et al.*, 2011). In support of this, bioinformatics have revealed a correlation between absence of TZ proteins and lack of Y-links, implicating the MKS proteins as structural components or regulators of Y-links (Barker *et al.*, 2014a).

The separation into modules simplifies our understanding of associated ciliopathies; these are likely disorders of larger, synergistic molecular complexes with partial functional redundancy and a common biological function. In *C. elegans*, for instance, at least one protein from each complex must be abrogated in order to display a phenotype, except in the case of RPGRIP1L (Williams *et al.*, 2011). However, in mammalian models, mutation of a single gene is sufficient (Barker *et al.*, 2014b).

TMEM216 and TMEM67 have been visualised at the basal body/TZ of the primary cilium (Abdelhamed *et al.*, 2013; Adams *et al.*, 2012; Valente *et al.*, 2010). However, aside from localising to the basal body and ciliary membrane, TMEM216 and TMEM67 also localise to the endoplasmic reticulum, Golgi and cytoplasmic vesicles (Lee *et al.*, 2012; Wang *et al.*, 2009), in addition to the actin cytoskeleton (Adams *et al.*, 2012). This could simply represent production and transport within the cell, or may be indicative of alternative roles of these proteins or different isoforms of these proteins within the cell, such as in vesicular trafficking, signal transduction and/or cytoskeletal remodelling.

In support of alternative cellular roles of ciliary proteins, several BBS proteins, including the basal body component BBS4, and OFD1 interact with proteasomal subunits (Gerdes *et al.*, 2007; Liu *et al.*, 2014). Moreover, BBS11 mutation reportedly affects the B-box domain of TRIM32, a ubiquitin ligase involved in proteasomal degradation of actin through interaction with myosin (Kudryashova *et al.*, 2005; Locke *et al.*, 2009). It has been suggested that basal

body proteasomal regulation regulates certain paracrine signalling pathways (Liu *et al.*, 2014), indicating possible extra-ciliary sources of unexplained signalling defects.

Intraflagellar transport, trafficking into the cilium and ciliogenesis

Subsequent to centrosomal docking, the ciliary axoneme extends using intraflagellar transport (IFT). IFT involves continuous, bidirectional movement of membrane-bound particles, driven by the MT motors cytoplasmic dynein and kinesin-2 associated with two subcomplexes, IFT-A and IFT-B. IFT-A is used in retrograde transport to the ciliary base and IFT-B is used in anterograde transport to the ciliary tip. IFT is also involved in ciliary maintenance, disassembly and signalling (Garcia-Gonzalo and Reiter, 2012; Ishikawa and Marshall, 2011). For instance, IFT20 is localised to the basal body and the ciliary axoneme however, this is also found at the Golgi complex. IFT20 particles are vitally involved in ciliogenesis through appropriate delivery of ciliary membrane proteins via the Golgi (Follit *et al.*, 2006), illustrating the necessity of appropriate trafficking in ciliogenesis. Loss of IFT proteins typically leads to ciliogenesis defects and, resultantly, ciliopathy phenotypes (Bhogaraju *et al.*, 2013; Bujakowska *et al.*, 2015; Lee *et al.*, 2015; Williams *et al.*, 2014).

Numerous immunofluorescence studies indicate that IFT proteins, such as IFT52 and IFT46, IFT-B protein complexes, are in two pools at the ciliary base, only one of which is involved in transport. These pools are below the TZ and at the juncture at which the ciliary membrane and periciliary membrane attach, particularly around the transition fibre attachment region (Buisson *et al.*, 2013; Deane *et al.*, 2001; Lee *et al.*, 2015; Reiter *et al.*, 2012; Sedmak and Wolfrum, 2010; Sedmak and Wolfrum, 2011; Williams *et al.*, 2011).

The IFT complex is a large, multimeric complex, with a number of components greater than 100kDa. Many of its cargoes, such as dynein, are also large complexes. These are reported to be assembled prior to entering the ciliary axoneme and are thought to be actively transported into the cilium through the “ciliary pore complex” (Wei *et al.*, 2015). IFT recruitment to basal bodies and entry of IFT particles into the flagella of *Chlamydomonas* are dependent both on correct actin organisation and myosin function, implicating the cytoskeleton in flagellum and, likely, cilium assembly (Avasthi *et al.*, 2014).

IFT particle movement within the ciliary axoneme occurs on a restricted set of MTs – fast IFT particles observed in the ciliary axoneme have frequently been demonstrated to fuse with slower ones – and IFT particles are reused upon returning to the ciliary base (Buisson *et al.*, 2013).

When the final steady state of the cilium is reached, IFT machinery, powered by molecular motors, transports cargo, such as tubulin (Craft *et al.*, 2015), up and down the axoneme. IFT particles also turn over proteins, including signalling proteins, in a compartment at the distal tip (He *et al.*, 2014; Ishikawa and Marshall, 2011; Pedersen and Rosenbaum, 2008; Rosenbaum and Witman, 2002).

Ciliary import of membrane proteins is dependent on polarised exocytosis adjacent to the basal body (Nachury *et al.*, 2010; Pazour and Bloodgood, 2008; Rosenbaum and Witman, 2002). The cilium itself has also been proposed to secrete ectosomes, vesicles containing proteolytic enzymes, and is thought to be a source of bioactive molecules (Wood *et al.*, 2013). However, the significance of ectosomes in cellular behaviour, is a relatively unexplored area of research.

Previous studies reported that six ESCRT proteins, involved in ubiquitinated protein transport, abscission of the midbody in cytokinesis and budding of vesicles from the cell surface, could be identified within the TZ proteome of *Chlamydomonas*. These data importantly imply an involvement of ESCRT proteins and membrane trafficking machinery in the function of TZ complex proteins or associated complexes (Diener *et al.*, 2015).

The role of the TZ complex proteins in ciliogenesis, inclusive of the MKS proteins, appears predominantly to be in regulating entry of appropriate proteins and lipids into the ciliary membrane through correct trafficking function of the ciliary gate (Aldahmesh *et al.*, 2014; Chih *et al.*, 2012; Garcia-Gonzalo *et al.*, 2011; Roberson *et al.*, 2015; Szymanska *et al.*, 2014). $Rab8^{GTP}$, for instance, contacts the BBSome and promotes ciliary elongation, but inhibiting $Rab8^{GTP}$ leads to typical BBS phenotypes, suggesting that BBS may result from a vesicular trafficking defect (Nachury *et al.*, 2007). This also begs the question of whether ciliary vesicular trafficking machinery is used beyond the cilium, as implied in the above evidence of IFT20 function in the cilium and at the Golgi. In additional support of this, partial knockdown of *IFT27* in *Chlamydomonas* led to cytokinesis defects and knockout led to lethality (Qin *et al.*, 2007). Similarly, in

vertebrates, IFT20, IFT88, and IFT57 form a complex in T cells, despite the fact that these cells do not build cilia (Finetti *et al.*, 2009). Here, the IFT proteins are functioning at the immunological synapse.

Forming an immunological synapse is a process considered to be analogous to ciliogenesis, similarly requiring centrosomal migration and docking at the plasma membrane, Golgi rearrangement and effective vesicular trafficking, and rearrangement of the actin and MT cytoskeletons (*Appendix 1*; Griffiths *et al.*, 2010). At the immune synapse, IFT components, such as IFT20, used in ciliogenesis are also used to effect endocytosis and exocytosis (Finetti *et al.*, 2009). Furthermore, Cdc42 and the Par proteins, previously discussed in the context of polarity determination, are also implicated in formation of this region (Ludford-Menting *et al.* 2005). The immunological synapse is thus a site of interest, particularly as centrosome docking appears to be concomitant with designating a specialised membrane in this region (Griffiths *et al.*, 2010). A compartmentalised membrane is a crucial feature for proper ciliary function, also implying that centrosome migration and docking are of particular importance when studying ciliary dysfunction.

Cellular phenotypes in animal models of MKS

Multiple examples exist of animal models of MKS mimicking the cellular features observed in patient cells, such as the aberrant basal body migration reported in the *Tmem67*$^{tm1Dgen/H1}$ knockout mouse (Abdelhamed *et al.*, 2015). However, evidence has been reported of mouse/rat models with normal docking of the basal body in *MKS1* mutants (Weatherbee *et al.*, 2009) or shortened or over-abundant cilia in *MKS1* and *-3* mutants (Tammachote *et al.*, 2009), and of *C. elegans mks-3* null mutants with no obvious ciliogenesis defects (Williams *et al.*, 2011). Furthermore, structurally normal cilia have been revealed in a *B9D1*-null zebrafish mutant, although these cilia did not correctly signal or have correct protein localisation, implying a functional role of this gene in targeting proteins to the cilium or regulating their access (Dowdle *et al.*, 2011). One study of zebrafish *tmem67* morphants and *tmem67*-null (bpck) mice revealed developmental abnormalities (including renal, skeletal and eye abnormalities) associated with ciliopathy and dysfunctional cilia, but no global loss of ciliogenesis, basal body docking or Wnt/planar cell polarity signalling, indicating

that developmental abnormalities may be attributed to elevated proliferation (Leightner *et al.*, 2013). Discrepancies have been ascribed to the use of different species as models, different types of mutation (as these may lead to phenotypes of varying severity) or the differences in tissue or cell type used (Norris and Grimes, 2012).

It is possible that MKS proteins have a role in signalling. Based on the variability of effects of MKS mutations in animal models on ciliary structure, cilium-dependent signalling and disease-associated tissue defects, it is also possible that MKS mutations simultaneously lead to a number of subcellular changes. These may include failure to build a cilium, failure of the TZ to compartmentalise, or other alterations that result in global perturbation of signal transduction pathways. In support of a hypothesised role of MKS proteins beyond signalling alone, these are known to have evolved long before vertebrate developmental signalling (Barker *et al.*, 2014a). Developmental signalling was not their earliest role, and is thus unlikely to be their only role now.

There is also evidence of extra-ciliary roles of proteins associated with ciliopathy. For instance, mutations in *Atmin*, a DNA damage protein and transcription factor, lead to shortened cilia; mutant mice also develop defects in Wnt/PCP-modulated oriented cell division (Goggolidou *et al.*, 2014b) and proteasomal degradation (Gerdes *et al.*, 2007). Furthermore, meckelin at the endoplasmic reticulum participates alongside other cytosolic machinery in the degradation of surfactant protein SP-C proprotein (Wang *et al*., 2009), indicating the potential of additional, TZ-independent roles of MKS proteins.

1.3 Cilium-dependent signalling

Vesicular trafficking initially contributes transmembrane proteins and lipids to ciliogenesis, and is subsequently used for cilium maintenance and cilium-dependent signalling (Nachury *et al.*, 2010). Cilia are only able to effect their primary function, signalling, due to a selective, biochemically-specialised and segregated membrane (Wei *et al.*, 2015).

Signalling pathways underlying ciliogenesis are not fully understood, but it is known that components of the non-canonical Wnt/planar cell polarity (PCP) pathway modulate correct localisation and posterior tilting of cilia in zebrafish

(Borovina *et al.*, 2010), *Xenopus* (Park *et al.*, 2008) and mice (Hashimoto *et al.*, 2010). These processes are linked to developmental defects, such as aberrant neural tube closure (Gray *et al.*, 2009; Park *et al.*, 2006).

MKS mutants display phenotypes indicative of alterations to developmental signalling pathways, including Hedgehog (Hh) and Wnt signalling. The role of cilia in Hh signalling is fairly well-accepted (Gerdes *et al.*, 2009), whilst their role in the canonical and non-canonical Wnt signalling pathways remains controversial (Wallingford and Mitchell, 2011).

Hedgehog signalling

In mammals, there are three Hh signalling pathways, governed by three different ligands. These act as mitogens and as morphogens by determining whether Hh pathway genes are transcribed or repressed to effect downstream function, particularly during development. The best studied of these is Sonic hedgehog (Shh), which controls the number and identity of digits (Buxton *et al.*, 2004). The necessity of a cilium in regulating this signalling pathway, as detailed below, therefore means that the loss of a cilium has obvious implications in the development of the limb bud, and can easily be linked with the polydactyly observed in ciliopathies.

Figure 1.3 illustrates how Hh signalling is transduced through the cilium. Briefly, in the absence of Hh ligand, transmembrane Patched (Ptch) receptor, prevents repressed seven transmembrane protein Smoothened (Smo) from entering the ciliary membrane. Glioma (Gli) proteins are proteolytically processed and Gli activator remains in the cilium, bound to Sufu, until it is proteasomally degraded. Simultaneously, Gli repressor enters the nucleus and prevents the transcription of Hh pathway genes (Berbari *et al.*, 2009; Nozawa *et al.*, 2013).

Upon Hh binding, however, Ptch leaves the cilium and accumulates in vesicles in the cytosol. This allows the activation of Smo, causing its ciliary accumulation, and promotes cleavage of Gli proteins. Gli activators use IFT to translocate to the nucleus, activating target gene transcription (Berbari *et al.*, 2009; Gerdes *et al.*, 2009; Nozawa *et al.*, 2013).

Hh signalling activity at the immunological synapse is another example of this behaving as a modified cilium. At the immunological synapse, Hh signalling

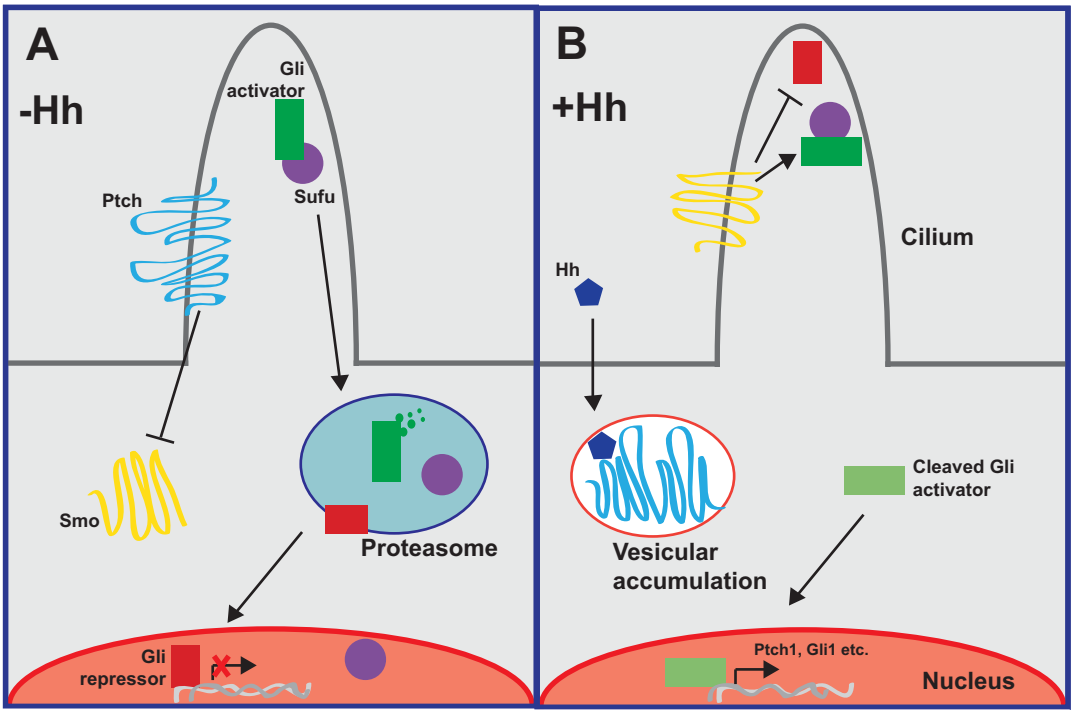

FIGURE 1.3: In vertebrates, components of the Hedgehog (Hh) pathway localise to the cilium. (A) In the absence of Hh ligand, Ptch receptor remains in the cilium and inhibits transmembrane protein Smo from accumulating on the ciliary membrane. Gli proteins are then proteolytically processed; Sufu binding prevents transcription by the activator form of Gli, whilst the repressor forms of Gli inhibit Hh target gene transcription in the nucleus. (B) Upon Hh binding, Ptch leaves the cilium, alleviating its inhibition of Smo. Activated Smo is recruited to the ciliary membrane, promoting cleavage of full-length Gli and producing Gli activators. Through intraflagellar transport, Gli activators translocate to the nucleus, activating Hh target gene expression. Adapted from Berbari *et al.*, 2009; Nozawa *et al.*, 2013.

is activated upon T-cell receptor activation, triggering Rac1 synthesis and concomitant actin remodelling, centrosome reorientation and vesicular granule release (de la Roche *et al.*, 2013)

Components of this pathway localise to and are transduced through the cilium (Haycraft *et al*., 2005; May *et al*., 2005) (*Figure 1.3*). Ciliary accumulation of Hh components is not necessary for Hh pathway activation; however, transduction at the cilium is necessary for appropriate regulation of this pathway (Fan *et al.*, 2014). A number of centrosomal and IFT proteins, in allowing appropriate transduction of this pathway, thus affect both ciliogenesis and Hh signalling; this has been demonstrated in studies of Talpid3 (Yin *et al*., 2009), OFD1 (Ferrante *et al*., 2006), Arl13b (Caspary *et al*., 2007), Kif3a and IFT172 (Huangfu and Anderson, 2005), amongst many others.

Certain MKS-related phenotypes are consistent with Hh pathway defects, such as neural tube dorsalisation, which is concordant with decreased Gli2 activity (Dowdle *et al.*, 2011). Analysis of developmental abnormalities in MKS1 loss-of-function mouse mutants demonstrated that a number of these defects (for instance, patterning of the neural tube and limb) are in response to disrupted, cilium-dependent Shh signalling. Cells in the neural tube, for instance, have a reduced response to high levels of Shh. MKS1 acts downstream of Ptch1, through the Gli proteins, to regulate spatial patterning of the neural tube and limb bud (modulating ventral and posterior signalling, respectively). However, a number of defects (such as in the liver and kidney) cannot be attributed to altered Hh signalling (Weatherbee *et al.*, 2009).

A *TMEM67* (*MKS3*) mouse model demonstrating variable neurological features associated with a loss of primary cilia also displayed diminished Shh signalling and perturbed canonical Wnt/β-catenin signalling, associated with hyperactive Dishevelled-1 (Dvl-1) at the basal body. This evidence supported an interaction between not only the Hh signalling pathway and TMEM67, but between Dvl and TMEM67 (Abdelhamed *et al.*, 2013).

Wnt signalling

The Wnt signalling pathway is involved in cell growth, polarity and fate determination, enabled in part due to divergence into three different pathways, canonical/β-catenin dependent, and two non-canonical/β-catenin-independent

pathways: planar cell polarity (PCP) and Wnt/calcium (Kikuchi *et al.*, 2009). It is also heavily implicated in the development of cystic kidney disease in a number of ciliopathies (Goggolidou *et al.*, 2014a).

Briefly, Wnt signalling, as detailed in *Figure 1.4*, initiates upon Wnt ligand binding and activating Frizzled receptors. In the canonical cascade, this leads to stabilisation and nuclear localisation of β-catenin (as opposed to its ubiquitination and proteasomal degradation), triggering activation of Wnt target genes. These target genes regulate, in particular, cell growth and differentiation (Lancaster and Gleeson, 2010; Lerner and Ohlsson, 2015; Kikuchi *et al.*, 2009). PCP signalling controls the migration and polarity of cells relative to a plane of tissue, acting through Dvl to activate small GTPases RhoA and Rac, Rho-associated kinase (ROCK) and Jun N-terminal kinase (JNK) (Lancaster and Gleeson, 2010; Lerner and Ohlsson, 2015; Kikuchi *et al.*, 2009). Additional information about the Rho GTPases is included within the next section.

Finally, the calcium-dependent Wnt pathway participates in a multitude of functions, including cell migration, cytoskeletal rearrangements, cell polarity and regulation of canonical Wnt signalling. This pathway also acts through Dvl and a small GTPase, Cdc42. Furthermore, it involves a number of other proteins such as filamin A, which interacts with meckelin (Adams *et al.*, 2012), and mitogen activated protein kinase (MAP), which is inappropriately activated by TMEM67 in polycystic kidney disease (Du *et al.*, 2013; Lerner and Ohlsson, 2015; Kikuchi et al., 2009).

Persistent β-catenin activation during development causes renal cysts (Saadi-Kheddouci *et al.*, 2001), but so does downregulation of canonical Wnt signalling (Pinson *et al.*, 2000), and loss of core PCP proteins (Cao *et al.*, 2010). This highlights how carefully these signals must be controlled, particularly for kidney homeostasis.

Wnt signalling is involved in ciliogenesis: manipulation of Dvl and axin, components of non-canonical pathways, disrupts cell migration and randomises centrosome positioning (Schlessinger *et al.*, 2007). Interestingly, the PCP effector proteins Fuzzy and Inturned are highly expressed in ciliated cells, and knockdown of these in *Xenopus* results in profound defects in ciliogenesis and (perhaps resultantly) Hh signalling (Park *et al.*, 2006). Futhermore, Fuzzy may participate in vesicle trafficking (Gray *et al.*, 2009), and Inturned is needed for actin assembly, possibly through Rho localisation, which impacts on basal body

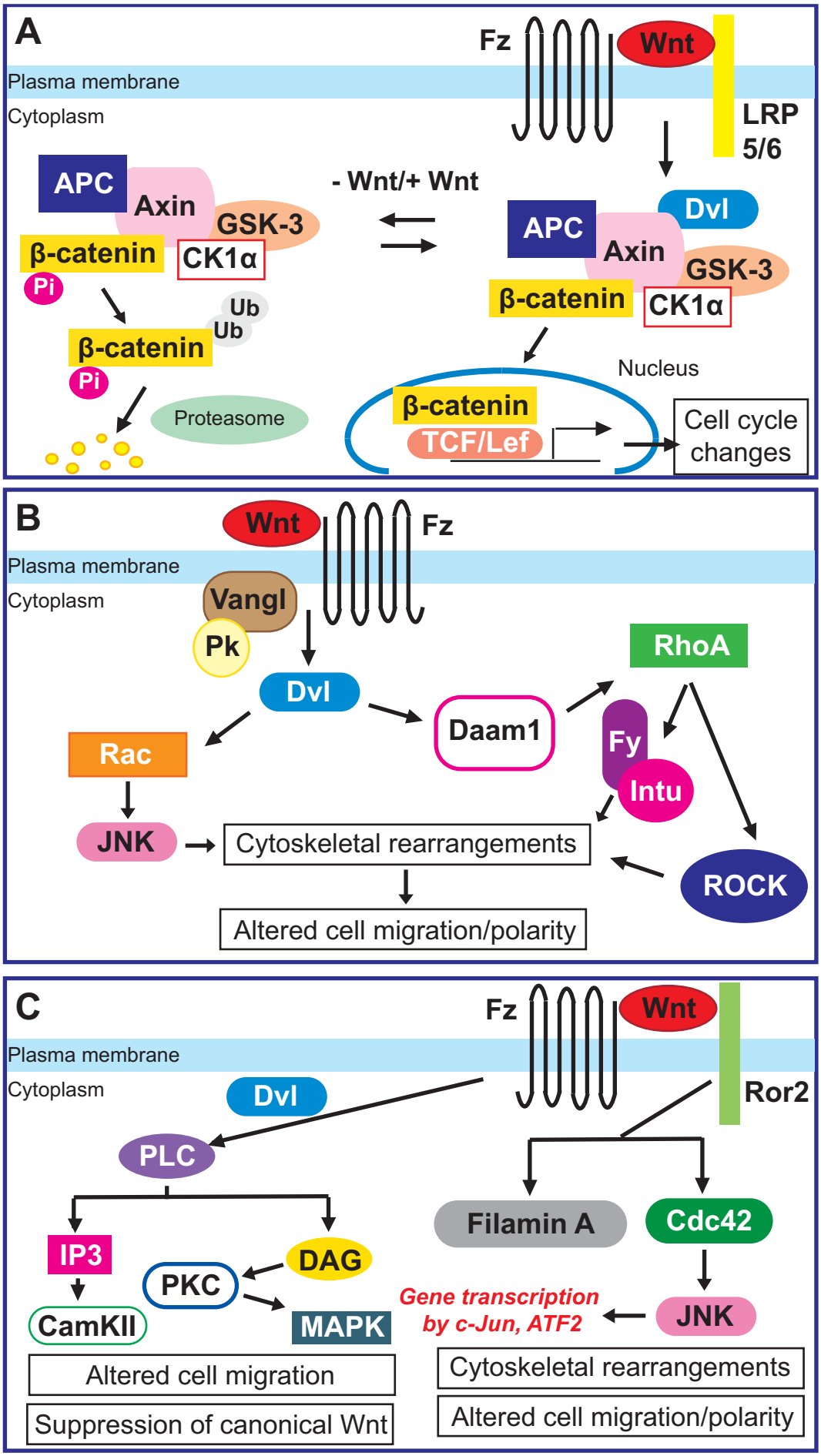
A
Fz
Wnt
Plasma membrane
Cytoplasm
LRP
5/6
APC
Axin
GSK-3
β-catenin
CK1α
Pi
- Wnt/+ Wnt
Dvl
APC
Axin
GSK-3
β-catenin
CK1α
Ub
Ub
β-catenin
Pi
Nucleus
Proteasome
β-catenin
TCF/Lef
Cell cycle
changes
B
Wnt
Fz
Plasma membrane
Cytoplasm
Vangl
Pk
Dvl
RhoA
Daam1
Fy
Intu
Rac
JNK
Cytoskeletal rearrangements
ROCK
Altered cell migration/polarity
C
Fz
Wnt
Plasma membrane
Cytoplasm
Dvl
Ror2
PLC
IP3
DAG
PKC
CamKII
MAPK
Filamin A
Cdc42
Gene transcription
by c-Jun, ATF2
JNK
Altered cell migration
Suppression of canonical Wnt
Cytoskeletal rearrangements
Altered cell migration/polarity

FIGURE 1.4: Summary diagram showing the canonical and non-canonical Wnt signalling pathways, a number of the involved components and the major roles of each. (A) Canonical Wnt signalling. When Wnt signalling is inactive, β-catenin is targeted for proteosome-mediated degradation; however, in the presence of Wnt, the "destruction complex" is inhibited. β-catenin is then stabilised, enters the nucleus and activates the transcription of Wnt target genes. (B) The non-canonical/planar cell polarity pathway. This pathway is associated with activation of small GTPases Rho and Rac, Rho kinase (ROCK) and JNK to effect cytoskeletal rearrangements. (C) The non-canonical/Ca2+ pathway. This is responsible for the Dvl-enabled activation of calcium/calmodulin-dependent kinase (CaMK) and PKC, appearing to inhibit the β-catenin pathway and altering cell migration. Wnt5a and Ror2 can, alternatively, act on filamin A or Cdc42 to regulate cell migration and polarity through cytoskeletal rearrangements. Fz, Frizzled; LRP5/6, lipoprotein receptor-related protein-5/6; APC, adenomatosis polyposis coli; GSK-3, glycogen synthase kinase-3; CK1α, casein kinase 1α; Dvl, Dishevelled; TCF/Lef, T-cell factor/lymphoid enhancing factor; Pk, Prickle; JNK, c-Jun N-terminal kinase; Daam1, Dishevelled-associated activator of morphogenesis 1; Fy, Fuzzy; Intu, Inturned; ROCK, Rho-associated kinase; PLC, phospholipase C; IP3, inositol trisphosphate; DAG, diacylglycerol; PKC, protein kinase C; MAPK, mitogen-activated protein kinase; Cdc42, cell division control protein 42 homolog; ATF2, activating transcription factor 2. Sources: Lancaster and Gleeson, 2010; Lerner and Ohlsson, 2015; Kikuchi *et al*., 2009.

docking at the apical surface (Park *et al.*, 2008). Asymmetric localisation of PCP components regulating posterior displacement of centrioles has also been reported in numerous studies (Borovina *et al.*, 2010; Guirao *et al.*, 2010; Hashimoto *et al.*, 2010). We can thus conclude that non-canonical Wnt, particularly PCP, signalling is vital for the initial stages of ciliogenesis (i.e. centriole reorientation and basal body docking).

As with the Hh pathway, several Wnt pathway components have been localised to the cilia and/or basal body (e.g. APC and β-catenin) and loss of ciliary and basal body proteins causes hyper-responsiveness to β-catenin signalling at the expense of non-canonical Wnt signalling (Corbit *et al.*, 2008; Oh and Katsanis, 2012), suggesting that the cilium might participate in Wnt signalling.

In the case of *BBS*-depleted zebrafish embryos, upregulated canonical Wnt signalling resulted from defective proteasomal targeting of β-catenin (Gerdes *et al.*, 2007). This may suggest that Wnt signalling is dependent on the cilium being fully functional, but that the Wnt defects may actually be cilium-independent and secondary, unrelated functions of the basal body/axonemal proteins playing alternative roles within the cell (Oh and Katsanis, 2012).

TMEM67 protein is essential for the phosphorylation of non-canonical Wnt receptor ROR2 upon Wnt5a stimulation, and interacts with both proteins at the ciliary TZ. In a recent study, *TMEM67*-mutant mice did not respond to Wnt5a, which is likely to inhibit Shh and canonical Wnt signalling; however, pulmonary defects, including cell polarity and epithelial branching defects, could be rescued by RhoA stimulation (Abdelhamed *et al.*, 2015).

This evidence is strongly indicative of MKS proteins having a key role in non-canonical Wnt signalling (with downstream effects on canonical Wnt and Shh signalling), whether as a receptor or another mediator of signal transduction. Whether this happens within the cilium or the cytosol, however, is unclear.

The posited role of cilia in Wnt signalling is controversial, with certain groups arguing that there is no role for cilia in Wnt signalling (Huang and Schier, 2009). Nonetheless, *MKS1, TMEM67, CEP290* and *RPGRIP1L* mutant mice do commonly demonstrate alterations to Wnt signalling, whether in the canonical and/or PCP pathways (Abdelhamed *et al.*, 2013; Lancaster *et al.*, 2011; Mahuzier *et al.*, 2012; Wheway *et al.*, 2013), suggesting that this abstruse

connection requires additional investigation. It is possible, considering the localisation of many ciliopathy proteins, such as inversin (Mahuzier *et al.*, 2012), to the basal body that the centrosome itself acts as a hub for Wnt signalling.

The Rho GTPases

The Rho GTPases are a subfamily of the Ras superfamily of small GTPases. These are molecular switches that are principally activated by Wnt/PCP signalling to control diverse signal transduction pathways, altering cell polarity, membrane transport, migration and transcription, chiefly through their effects on actin and MT dynamics (Ellenbroek and Collard, 2007; Etienne-Manneville and Hall, 2002).

These molecules switch between an “active” and “inactive” state through conformational changes associated with GTP or GDP binding, respectively. Numerous GTPase-activating proteins (GAPs) of varying specificity stimulate GTP hydrolysis to GDP using GTPases, promote GDP binding and bind effector proteins, thereby inactivating the GTPase. A similar number of guanine nucleotide exchange factors (GEFs) catalyse nucleotide exchange and mediate activation of the GTPase through a conformational change that increases the binding affinity toward effector proteins (Ellenbroek and Collard, 2007; Etienne-Manneville and Hall, 2002).

Rho GTPases can only bind effector proteins and transduce signals received from, for example, growth factor receptors, adhesion receptors, or G-protein coupled receptors, when they are in an active state. Activation is strictly spatially and temporally regulated by GAPs and GEFs and by guanine nucleotide dissociation inhibitors (GDIs). GDIs bind inactive Rho GTPases into cytoplasmic complexes and prevent their translocation to, and thus activation at, the plasma membrane (Ellenbroek and Collard, 2007). Full activation of effectors downstream of the GTPases is thought to only occur upon fulfilment of certain criteria; for instance, full activation of Pkn requires RhoA binding, lipid association and autophosphorylation events (Bishop and Hall, 2000; Mukai *et al.*, 1994).

The best-characterised members of the Rho GTPases are Cdc42 (involved in filopodium formation), Rac1 (involved in lamellipodium formation) and RhoA (involved in stress fibre and focal adhesion formation), all of which impact upon

cell migration. However, there are 22 mammalian members in total, all of which are involved in generation of actin structures (Bishop and Hall, 2000; Ridley, 2006).

There are multiple effector proteins associated with the Rho GTPases. These include the p21-activated kinases (PAKs), serine/threonine kinases able to bind active Cdc, a number of of which can bind active Rac (Hofmann *et al.*, 2004); and Rho-associated coiled-coil-containing protein kinases (ROCK), which are serine/threonine kinases that bind active RhoA and regulate actomyosin-mediated cell migration and cell-substrate adhesion (Riento and Ridley, 2003).

In further example of effectors, the actin depolymerising proteins ADF/cofilins are thought to be regulated downstream of small GTPases. Cofilin is phosphorylated at a serine near its N-terminus by LIM kinase *in vivo* and *in vitro*, it is believed, by upstream Rac activation (Arber *et al.*, 1998; Pollard *et al.*, 2000; Yang *et al.*, 1998), regulated by Pak1 and ROCK (Edwards *et al.*, 1999; Maekawa *et al.*, 1999).

Rac1 and Cdc42 are established mediators of cell polarity (Pruyne and Bretscher, 2000; Schlessinger *et al.*, 2007), hypothesised to operate through regulation of MT dynamics in the pericentrosomal region and cell apex. This activity is mediated using aPKC, Lis1 (Kirjavainen *et al.*, 2015; Sipe *et al.*, 2013) and PAR (partitioning-defective) proteins such as Par3 or Par6, which function as Cdc/Rac effector proteins and adaptor proteins, respectively (Joberty *et al.*, 2000). Through a similar mechanism, Rac1 and Cdc42 are also responsible for establishing cell shape through downstream action on the cytoskeleton, cell-cell junctions and membrane protrusion (Etienne-Manneville and Hall, 2002).

Finally, the Rho GTPases promote endocytosis and exocytosis, for instance at the immune synapse following Hh-induced T-cell activation (de la Roche *et al.*, 2013), by driving MTOC and Golgi reorientation and enabling spatially-specific release of secretory granules, or the pinocytosis facilitated by Cdc42/Rac-dependent actin protrusions (Etienne-Manneville and Hall, 2002)

Multiple ciliopathies display defects in the Rho GTPases, the actin cytoskeleton, and in functions associated with these, such as cell migration, polarity and focal adhesion development, leading me to examine the cytoskeleton and the Rho GTPases in the subsequent results chapters.

Other cilium-dependent signalling

Several other crucial developmental signalling pathways have been linked to the cilium, such as platelet-derived growth factor (PDGF; Schneider *et al.*, 2005), fibroblast growth factor (FGF; Tanaka *et al.*, 2005), receptor tyrosine kinase (Christensen *et al.*, 2012) and Notch/Delta (Ezratty *et al.*, 2011). However, investigation into the role of MKS genes in these pathways has been limited.

Ciliary involvement in developmental signalling is conserved across numerous organisms, with evidence recently emerging of cilium-modulated Hh signalling extending even to the sea urchin (Warner *et al.*, 2014) and *Drosophila* (Kuzhandaivel *et al.*, 2014); however, dependence on cilia to regulate signalling appears species-dependent (Yamamoto *et al.*, 2015). Together, these data imply that the cilium and associated proteins probably evolved with this function.

1.4 The cytoskeleton

The cytoskeleton underlies the minutiae of motility and cytoplasmic organisation in eukaryotic cells and is primarily responsible for maintenance of a stable - yet dynamic and adaptable - cell structure throughout cellular processes such as growth, division and movement. These cellular processes involve three types of filament - intermediate filaments, MTs and actin. I explore actin and MTs in this thesis, but will not cover intermediate filaments. Present understanding of the cytoskeleton often informs our knowledge of the aetiology of disease; genetic defects affecting the building or function of primary cilia, such as Meckel-Gruber syndrome, and their intersection with the cytoskeleton is the predominant focus of this thesis.

The structure of actin filaments

Actin is the major component of the thin filaments of muscle cells, and of the cytoskeletal system of non-muscle cells. It is involved in diverse cellular functions, such as effecting locomotion through the extension of pseudopods. Cellular movement is necessary in multicellular organisms during processes which include morphogenetic movement during embryonic development,

remodelling of the nervous system, chemotactic movements of immune cells and wound healing (Otterbein *et al.*, 2001; Pollard *et al.*, 2000).

Monomeric, globular actin (G-actin) assembles to form polymers of filamentous actin (F-actin) (Otterbein *et al.*, 2001). These filaments are polarised through arrangement of the globular subunits head-to-tail into a double helical polymer. Based on the arrowhead pattern formed when myosin binds actin filaments, the rapidly-growing end is referred to as the barbed end and the slowly-growing end is the pointed end (Pollard *et al.*, 2000; Pollard and Borisy, 2003; Wegner, 1982). The barbed end is preferentially used for filament growth and actin filaments are largely oriented with their barbed ends in the direction of growth (Small *et al.*, 1978), supported by experiments showing that permeabilised cells provided with fluorescent actin subunits add these to the barbed ends at the leading edge of the cell (Symons and Mitchison, 1991; Watanabe and Mitchison, 2002).

Cell migration and focal adhesions

Directional cellular movement is necessary for numerous critical processes across all domains of life; in eukaryotes, this includes a plethora of embryonic developmental systems, wound healing, tumour cell metastasis and immune responses (Mitchison and Cramer, 1996; Pollard and Borisy, 2003). For example, small, circular wounds can be healed by a contraction-based mechanism of the surrounding cells, in which an actomyosin cable lines the edge of the wound (Conrad *et al.*, 1993) and, through generation of roughly equal force across the cells bordering the wound, “purse-string” closure involving inward migration occurs (Cramer, 1999).

It is widely accepted, that animal cells use the actin cytoskeleton for crawling motility (Mitchison and Cramer, 1996), in addition to less common methods such as antigen-antibody binding (Pavalko *et al.*, 1988).

In order to migrate, cells must attain a spatial asymmetry, specifically a “leading edge” and a cell rear, in response to migratory stimuli (Lauffenburger and Horwitz, 1996). It is recognised that a cell must reorganise its actin cytoskeleton to effect lamellipodial protrusion at the leading edge, adhere, translocate the cell body and retract the tail at the rear (Cramer, 1999; Nobes and Hall, 1999)

The fibroblast cell regions (the lamellipodium, lamella, cell body and rear of the cell) all have characteristic properties which enable them to be tracked separately during cell locomotion by time-lapse microscopy. Through this, it has been determined that the lamellipodium, cell body and tail all appear to move forward roughly in the same direction, whereas the lamella appears to remain in the same place as the cell body proceeds (Cramer, 1999).

Abercrombie *et al.* (1970) first introduced the term "lamellipodium", describing "thin, sheet-like, mobile, commonly transitory projections from the cell", also noting their occurrence "particularly at and near the front end of a fibroblast." Further, it was found by Euteneuer and Schliwa (1984) that even small fragments taken from these lamellipodia engaged in persistent, translocative behaviour.

These lamellipodia lack nuclei or other organelles (Euteneuer and Schliwa, 1984), primarily being made up of actin filaments and actin-associated proteins within a cross-linked meshwork (Lauffenburger and Horwitz, 1996). This is important as it suggests that protein synthesis is not necessary for motility in the short-term.

Alternatively at the leading edge of the cell, the surface which forms the "front" of the migrating cell, are filopodia. These are thin, finger-like projections, formed of bundled actin filaments (Lauffenburger and Horwitz, 1996; Nobes and Hall, 1999). Lamellipodia and filopodia both consist of polarised F-actin, but these different conformations are achieved through use of different actin-binding proteins (Small *et al.*, 2002).

Lamellipodial protrusion is induced by Rac (Ridley *et al.*, 1992) and, through appropriate assembly or disassembly and organisation of actin filaments, cell motility is controlled by a cascade of intracellular signalling (Lauffenburger and Horwitz, 1996; Nobes and Hall, 1999). Lamellipodia are responsible for directional protrusion of the front of the cell, enabled by dynamic actin cytoskeleton re-organisation, and for the development of adhesions to attach the cell to the underlying substrate (Abercrombie, 1980; Nobes and Hall, 1999; Small *et al.*, 2002). Lamellipodia and focal adhesions are both vital during migration.

Adhesion occurs when cells are plated *in vitro*, and is considered to be the next stage in cell migration. As mentioned, the leading edge is considered to be the preferential locus where adhesions form. These persist and mature, fixed on

the substratum as the cell regions migrate over them, thereby moving centripetally, before finally detaching when they reach the cell rear (Couchman and Rees, 1979; Lauffenburger and Horwitz, 1996). These have a vital role in cell migration; mean size of focal adhesions precisely predicts cell speed, for instance (Kim and Wirtz, 2013).

Focal adhesions are organised aggregates of specialised proteins with diverse functions, including structural, signalling and mechanosensing proteins. These aggregates include proteins such as integrin, fibronectin and focal adhesion kinase. Focal adhesions are distributed over the basal surface of adherent cells, providing a structural intermediate and a signalling site between the actin cytoskeleton and the extracellular matrix (ECM) (Geiger *et al.*, 2009; Patla *et al.*, 2010; Prager-Khoutorsky *et al.*, 2011).

Transient adhesions, often called focal contacts or focal complexes, appear initially as submicron-sized vinculin-, alpha-actinin- or paxillin-positive dots, before maturing into more stable structures, called focal or fibrillar adhesions. These focal adhesions, unlike the focal contacts, are elongated structures associated with the actin filament bundles of the cytoskeleton (Bershadsky *et al.*, 1985; Wolfenson *et al.*, 2009). This elongation and maturation is enabled by the exertion of tension in specific actin filament bundles - stress fibres - extending from the rudimentary focal contacts towards the cell body (Couchman and Rees, 1979; Wolfenson *et al.*, 2009). Formation of focal adhesions is therefore affected by the rigidity of the ECM (Zamir *et al.*, 2000) as this will affect the potential tensile strength of the stress fibres.

Dysfunction of focal adhesion components is observed in a few ciliopathy models. In one example, RPGR-deficient cells demonstrated dysregulation of focal adhesion kinase, a 20% reduction in plasma membrane β1-integrin receptors, and inhibition of fibronectin-induced signalling. These cells also displayed dense actin bundles and reduced numbers of cilia (Gakovic *et al.*, 2011). Notably, multiple focal adhesion proteins, including vinculin, paxillin and focal adhesion kinase, also localise to the basal bodies of multiciliated cells, forming complexes that interact with actin. Furthermore, disruption of focal adhesion kinase leads to defects in basal body migration and docking (Antoniades *et al.*, 2014), cellular defects observed in MKS models, indicating that these complexes may have undiscovered cellular roles which may inform our knowledge of ciliopathies

Focal adhesions in the lamella eventually mature and stop growing, remaining in this region in stationary cells or ending in the posterior lamella in motile cells, before gradually disassembling (Wolfenson *et al.*, 2009). The cell body must advance over these focal adhesions in order to move. It is the subject of debate as to how this translocation occurs, however. The two current key models explain migration in terms of contraction of acto-myosin fibres, or in terms of actin polymerisation balanced with membrane tension (Fournier *et al.*, 2010).

In the presence of active myosin II, strong adhesions to the extracellular substrate form and subsequent actomyosin contraction leads to a tension between the actin filaments at the leading edge and the cell body. Tension force can then be transmitted as a strong, propulsive traction force to the cell adhesions, allowing cellular movement through use of the cytoskeletal actin filaments (Fournier *et al.*, 2010).

The role of myosin II is controversial; it has long been argued that myosin filaments interact with actin filaments, providing a contractile force to move the cell body forward by pulling the cell substrate over the focal adhesions in a similar way to skeletal muscle contraction (Abercrombie, 1980). More recently, myosin has been assigned a lesser role, and is now associated with organisation of the direction of force as opposed to directly generating motile force (Lo *et al.*, 2004). Furthermore, it was demonstrated by Lo *et al.* (2004) that myosin IIB null fibroblasts still migrate, and did so faster than control cells; however, the resultant polarity of migration was unstable, suggesting that myosin II has more of a regulatory role in cell migration.

Several studies have reported that migration involves myosin-independent forces, namely attributing traction force to actin filament assembly (Fournier *et al.*, 2010). It has been hypothesised that actin filament assembly provides a structure, which the myosin II then uses to pull the cell body and that the plasma membrane transmits this force from the front to the back of the cell (Fournier *et al.*, 2010).

Finally, retraction of the tail end of the cell is required to complete a migratory movement. Myosin-powered contraction is responsible for unsticking of the focal adhesions at the back and sides of the cell, causing the tail end to be pulled by the rest of the cell (Fournier *et al.*, 2010). In the absence of myosin, the tail end moves through actin depolymerisation (Mseka and Cramer, 2011).

Microtubule structure and organisation

Microtubules (MTs) are the other major constituent of the cytoskeleton, functioning predominantly as tracks for motor proteins carrying varied cargoes. MTs are essential for numerous cellular functions, such as motility, intracellular transport/vesicular trafficking and cell division, in addition to acting as the principal component of the axoneme in cilia and flagella (Amos and Schlieper, 2005).

These structures are tubular polymers of α- and β-tubulin heterodimers (which have 50% amino acid similarity), arranged head-to-tail in 13 staggered protofilaments to make up a ~24 nm-wide hollow cylinder. This structure can be elongated by the addition of more tubulin dimers and, like actin, these are polar structures, a feature key to their function. Tubulin heterodimers are preferentially added to the plus end, which is characterised by its exposure of β-tubulin subunits, in contrast to the minus end, which has exposed α-tubulin subunits (Amos and Schlieper, 2005; Desai and Mitchison, 1997; Evans *et al.*, 1985; Walker *et al.*, 1988; Weisenberg, 1972).

MTs run straight, which enables MT-associated motor proteins such as dynein (a plus end-directed motor) and kinesin (a minus end-directed motor) to travel for long distances, carrying cargo including vesicles or organelles. The orientation of MTs (and thus the direction of transport) is cell type-dependent; for example, nerve axons are arranged with the plus ends of longitudinally-placed MTs pointing away from the cell body, epithelia orient plus ends towards the basement membrane, and fibroblasts typically display MTs radiating from the cell centre with the plus ends at the periphery (Hirokawa, 1998).

Nucleation and organisation of MTs can occur from multiple sites, known as microtubule organising centres (MTOCs). These contain γ-tubulin, which nucleates the formation of new MTs from large complexes referred to as the γ-tubulin small complex (γ-TuSC) in nearly all eukaryotes. These γ-TuSCs form part of the γ-tubulin ring complex (γ-TuRC) in many eukaryotes, but constituents of this complex vary (Kollman *et al.*, 2011). Furthermore, these also act as a minus end cap (Keating and Borisy, 2000).

The centrosome is the main MTOC in most animal cells and, as discussed previously, becomes the basal body of primary cilia. However, many MTs have acentrosomal origins (Kollman *et al.*, 2011), including the Golgi

complex (Chabin-Brion *et al.*, 2001; Efimov *et al.*, 2007) or the outer nuclear envelope (Bugnard *et al.*, 2005). These alternative, acentrosomal origin points also contain centrosomal proteins ninein, pericentrin and γ-tubulin (Bugnard *et al.*, 2005; Mogensen *et al.*, 2000). MTs can be severed and stabilised by association with other factors, but they can also be released, then transported using molecular motors and tethered at alternate, acentrosomal sites, such as the adherens junctions (Bellett *et al.*, 2009; Keating and Borisy, 1999; Meng *et al.*, 2008).

Cytoplasmic conditions ultimately determine the source of MTs. In fibroblasts (and most other proliferating and migrating animal cells), free MT minus ends become destabilised, leading to centrosomally-focused MTs. Contrastingly, epithelial cells (and most differentiated animal and fungal cells) have stable, free MT minus ends stabilised by, for instance, ninein-containing complexes, leading to frequent acentrosomal MT foci (Bartolini and Gundersen, 2006; Keating and Borisy, 1999).

1.5 Research questions and aims

The research problem

The major obstacles currently impeding research into ciliopathies are the inability to make genotype-phenotype correlations between mutations and the spectrum of disease phenotypes – this is a convoluted problem, dependent on genetic context, the type of mutation, the subsequent protein structure, and so on – and the exact subcellular roles of the proteins involved.

The role of the “ciliopathy” proteins in building and maintaining a functional cilium is a hotly-investigated topic in ciliary research. A role of these proteins in a “ciliary gate” at the transition zone appears almost certain. However, evidence for additional extra-ciliary roles of these proteins is rapidly accumulating. These extra-ciliary roles have common themes: many of these proteins are involved in processes or protein complexes associated with the cytoskeleton.

The pertinent question for ciliopathy research is thus whether the alternate functions that these proteins appear to have are a result of the loss of a cilium, whether these proteins have a primary role beyond the cilium which

subsequently impacts on ciliogenesis and ciliary function, or whether the proteins have multiple, independent roles in the cell.

The MKS proteins have been linked to actin-mediated centriole migration and docking (Abdelhamed *et al.*, 2015; Dawe *et al.*, 2007b; Valente *et al.*, 2010), to Y-link/ciliary necklace formation (Williams *et al.*, 2011) and, likely associated with this, regulation of ciliary membrane composition (Roberson *et al.*, 2015) and Hedgehog signalling (Dowdle *et al.*, 2011).

Other associated defects are not as easily explained by ciliary loss or dysfunction, however. The role of cilia in Wnt signalling remains enigmatic, but many of the consequences of dysregulation of this pathway correlate with loss of a cilium. Ciliopathy proteins, such as TMEM67, have proven involvement in the Wnt signalling pathway – this protein is involved in Wnt5a transduction (Abdelhamed *et al.*, 2015) - and MKS mutant mice commonly show alterations to Wnt signalling pathways (Abdelhamed *et al.*, 2013; Lancaster *et al.*, 2011; Mahuzier *et al.*, 2012; Wheway *et al.*, 2013). Elucidating this obscure connection between Wnt signalling and the cilium remains of vital importance for the field, and may be resolved if the roles of these proteins can be ascertained.

Aside from a possible signalling role, emerging evidence for cilium-independent functions of MKS proteins indicate these may act in regulation of actin networks, as indicated by their interaction with filamin A (Adams *et al.*, 2012) and localisation along actin fibres (Dawe *et al.*, 2009), but evidence from research into other ciliopathies suggest these proteins may have more diverse extra-ciliary roles than these (Vertii *et al.*, 2015). These roles include, but are not limited to: vesicular trafficking; centrosome cohesion; proteasomal degradation of cytoskeletal components; cytoskeletal links; focal adhesions; polarity; and migration, which will be discussed throughout this thesis. The currently established locations of TMEM216 and TMEM67 in the cell are depicted in *Figure 1.5*. However, understanding of their function at these locations, and whether they function beyond these locations, remains limited.

Aims and hypotheses

The aim of this thesis is to elucidate the cellular roles of the MKS proteins beyond the cilium, in order to formulate a more accurate model of how these

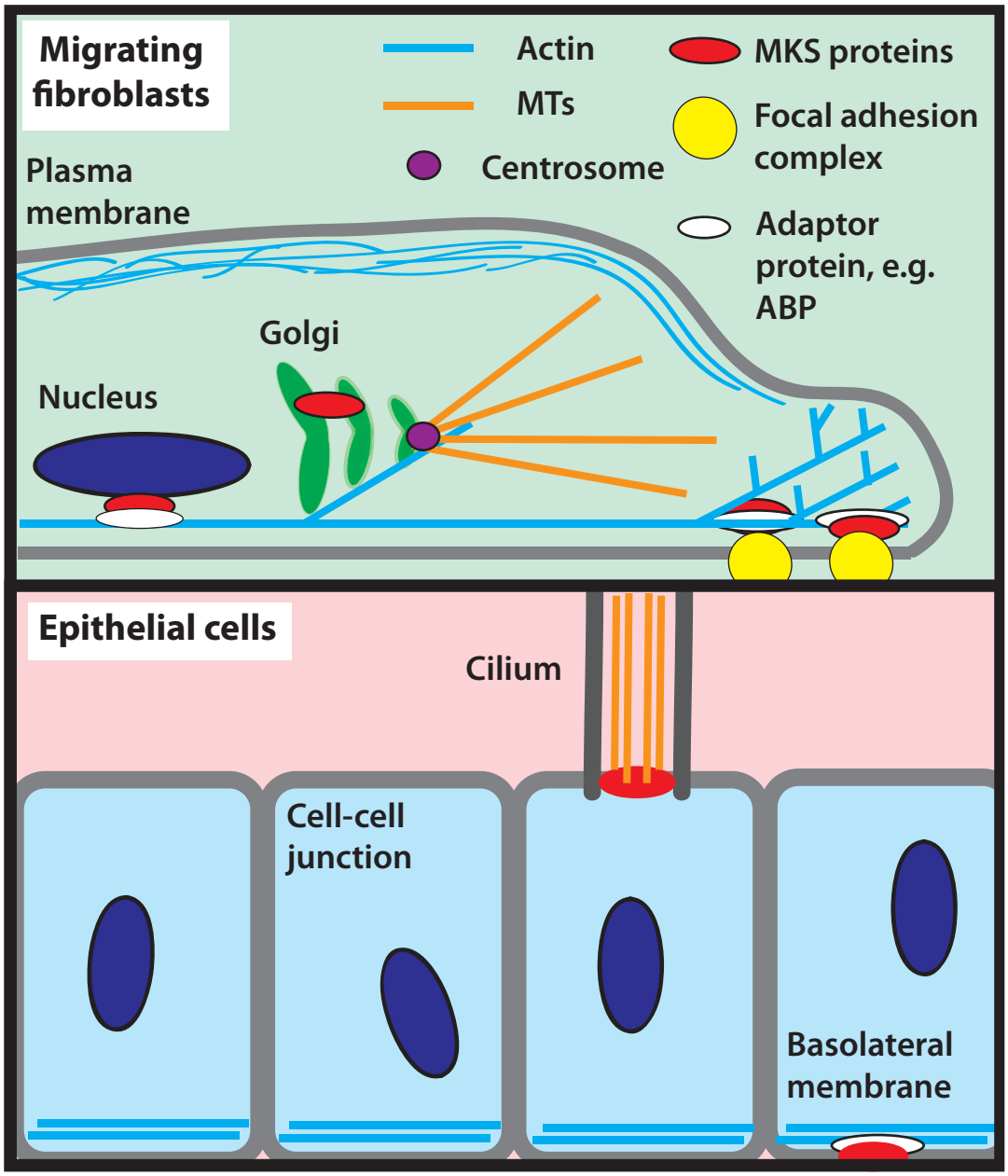

FIGURE 1.5: Model to demonstrate established MKS protein localisation. MKS proteins have been established to localise to the nuclear envelope, actin (which may or may not occur via other proteins), focal adhesion complexes and the ciliary transition zone; however, any additional sites of MKS proteins and their function at these subcellular locations have yet to be elucidated. Identification of their localisation and function is, therefore, to form the subject of this thesis.

proteins might function in the cell, with a view to advise future pursuance of appropriate therapeutic treatment (in the case of the milder diseases) or genetic counselling (in the case of the severe diseases) with regard to this spectrum of disorders.

The hypotheses tested in this thesis are as follows:

Chapter III: Actin in *MKS2* and *MKS3* patient cells changes temporally, and is structurally altered compared with control fibroblasts

Chapter IV: Abnormal Rho/ROCK pathway activity is associated with the abnormal cellular phenotypes observed in MKS patient cells

Chapter V: MTs are organised differently and are structurally altered in MKS patient cells.

Chapter VI: Defects observed in MKS patient cells occur in a specific order, not simultaneously; defects are linked to Rho pathway activity.

CHAPTER II: MATERIALS AND METHODS

2.1 Cell culture, drug treatments and transfection

hTERT immortalised *MKS3/TMEM67* [c.653G>T p.R217X]+[c.785T>C p.M261T] and *MKS2/TMEM216* c.253C>T p.R85X neonatal patient fibroblasts, as used by Valente *et al.* (2010) were obtained from Colin Johnson (Leeds Institute for Molecular Medicine) together with age-matched hTERT-immortalised controls (or wild-type) and cultured in DMEM/F-12 + GlutaMAX (Gibco) supplemented with 20% Fibroblast Growth Medium (FGM) (AMS Biotech) 10% foetal calf serum at 37°C/5% CO_2, and split at roughly 70% confluency in TrypLE Express (Gibco) to sub-passage. All cells were used for experiments at passage 11-21.

For micropattern experiments, cells were plated onto medium crossbow fibronectin micropatterns (Cytoo) according to the manufacturer's instructions.

The jasplakinolide-treatment experiment involved fibroblasts plated for 24 hours on glass coverslips before addition of 10 nM jasplakinolide in fresh medium. They were incubated, as above, for 3 days before being fixed and stained.

In acute drug treatment experiments, fibroblasts were plated onto collagen-coated coverslips for 20 minutes. A number of extracellular matrices were trialled for this, but collagen I was selected as the most appropriate as cells from wild-type and *MKS2* lines adhered fastest to this substrate. Following this, media was removed and appropriate concentrations of drug in medium (or fresh medium for the control) were applied for 40 minutes before fixing. These concentrations were: C3 transferase, 2.5µg/µL; Y27632, 5µM; H1152, 5µM; and blebbistatin, 50µM. Drug concentrations were selected based on working concentrations suggested by the suppliers, on previous studies using similar cell lines, and on an empirical determination of the effective and lethal dosages of the inhibitor; drugs were used at a concentration that did not cause >30% of the cells to die, but one at which alterations to the cytoskeleton could be seen upon microscopic examination.

In prolonged drug treatment experiments, fibroblasts were plated onto collagen-coated coverslips for 1 day, media was removed and appropriate concentrations of drug (or corresponding control) in FGM were applied for 3

days before fixing. These concentrations were: C3 transferase, 1µg/µL; Y27632, 1µM; H1152, 1 µM; and blebbistatin, 5nM.

For plasmid transfection experiments, cells were trypsinised and resuspended in 80 µL transfection medium per transfection (14.4 µL Supplement 1 and 65.6 µL Cell Line Nucleofector Solution R from Lonza Amaxa Cell Line Nucleofector Kit R), electroporated using a Lonza Nucleofector device with 1 µg of the relevant plasmid, resuspended in fresh medium and plated at appropriate density onto glass coverslips; cells were fixed and stained as normal after 4 days.

Plasmids used for transfection were wild-type, constitutively active and dominant negative Rho (pcDNA3-EGFP-RhoA-wt, Addgene Plasmid 12965, G. Bokoch; pcDNA3-EGFP-RhoA-Q63L, Addgene Plasmid 12968, G. Bokoch; and pcDNA3-EGFP-RhoA-T19N, Addgene Plasmid 12967, G. Bokoch), and Rho kinase Δ3 – a constitutively active plasmid with a C-terminal truncation, but containing the kinase domain and coiled-coil region, shown to induce actin polymerisation and focal adhesion formation (Ishizaki *et al*., 1997).

For siRNA transfection, IMCD3 cells (ATCC CRL-2123) were plated onto glass coverslips overnight. 1 µL lipofectamine (Invitrogen Lipofectamine 3000 transfection kit) was added to every 1000 µL OptiMEM (Gibco). Separately, the appropriate siRNA [100 pmol of non-targeting (*negative control*), 100 pmol each of three *MKS1* siRNAs (*positive control*) (all Invitrogen Stealth RNAi) or 100 pmol of Coronin 7 SMARTpool siRNA (Dharmacon)] was added to 50 µL OptiMEM and 1.5 µL P3000. Next, 600 µL of transfection medium was added to each siRNA tube, and these were incubated at room temperature for 5 minutes. This solution (150 µL per coverslip) was added to the centre of the IMCD3 coverslips; these were incubated (37°C/5% CO_2) for 4 days, then fixed and stained.

For nocodazole treatment of microtubules, fibroblasts were plated on coverslips for at least 24 hours, then were treated with 10 µM nocodazole (Sigma) in pre-warmed medium for 45 minutes. Cells were fixed (0 minute time point) or fresh, warm media replaced the nocodazole for 2 minutes before fixing and staining for centrosomes and microtubules.

For temporal dependency experiments, cells were simultaneously plated, then fixed every 5 minutes and stained for the relevant structures.

Temporal dependency drug treatment experiments involved treating fibroblasts with actin stabilising (jasplakinolide - CalBioChem) and disassembly (latrunculin B – provided by M. Schrader) drugs (30 minutes after plating), microtubule stabilising (taxol – provided by J. Wakefield) and disassembly (nocodazole - Sigma) drugs, or DMSO (Sigma) (5 minutes after plating) – all at 10 μM in medium, apart from DMSO, which was at 0.1%. These were then fixed and stained for actin and microtubules 1 hour after plating.

Serum-starvation involved replacing medium with serum-free medium twice over 24 hours, then fixing and staining 2 days after the second medium change.

2.2 Fixation and immunofluorescence

Glass coverslips were coated with enough collagen I to cover the coverslip, left overnight at 4°C, then washed with PBS, prior to use in all experiments lasting 2 hours and under; experiments longer than this used untreated glass coverslips. Cells were plated at appropriate density and left to adhere at 37°C/5% CO_2 prior to fixing.

To label actin, cells were fixed in 4% formaldehyde, 0.1% gluaraldehyde in cytoskeleton buffer (10mM MES pH 6.1, 138 mM KCl, 3mM MgCl, 10mM EGTA pH 7.0) with sucrose for 20 minutes, washed with PBS-0.1% Triton, then left to permeabilise in PBS-0.5% Triton for 10-15 minutes. Cells were blocked in AbDil (2% BSA in PBS-0.1% Triton) for over 15 minutes before labelling with Alexa-Fluor 594 phalloidin to stain F-actin (1:100, Invitrogen) or AlexaFluor488 deoxyribonuclease 1 (DNase 1) to stain G-actin (1:500, Invitrogen), washed off with PBS-0.1% Triton after 25-40 minutes.

Immunofluorescence was used to label the remaining subcellular structures, as follows.

For ROCK-1 and phosphomyosin labelling, cells were fixed in 4% formaldehyde in cytoskeleton buffer (10mM MES pH 6.1, 138 mM KCl, 3mM MgCl, 10mM EGTA pH 7.0) with sucrose for 20 minutes, washed with PBS-0.1% Triton, then left to permeabilise in PBS-0.5% Triton for 10-15 minutes. Cells were blocked in AbDil (2% BSA in PBS-0.1% Triton) for over 15 minutes before labelling with primary antibody for 1 hour (*Table 2.1*), washed with PBS-0.1% Triton, then treated with1:1000 Alexa-Fluor 488 goat anti-mouse or anti-rabbit for 45 minutes.

TABLE 2.1: Details of primary (upper) and secondary (lower) antibodies used in immunofluorescence

Antibody	Stains	Concentration	Source
ROCK-1 (Rabbit)	Rho-associated coiled-coil-containing protein kinase1	1:100	Chemicon (AB3885)
Phosphomyosin light chain (Mouse)	Phosphomyosin	1:200	Cell Signalling (3675S)
Myosin (Rabbit)	Myosin	1:100	AbD Serotec (6490-1004)
GM130	Cis-Golgi	1:500	BD Biosciences (610822)
γ-tubulin (Rabbit)	Centrosome	1:500	Sigma (T3559)
Acetylated α-tubulin (Mouse)	Cilia/acetylated tubulin	1:500	Sigma (T7451)
ZO-1 (Rat)	Tight zunctions	1:500	Chemicon (MAB1520)
α-tubulin (Mouse)	Microtubules	1:500	Sigma (T9026)
Pericentrin (Rabbit)	Pericentriolar material	1:500	Abcam (ab4448)
YL1/2 (Rat)	Tyrosinated tubulin	1:200	Provided by J. Salisbury
AlexaFluor 488/594 goat anti-mouse	Mouse primaries	1:1000	Invitrogen (A11001/ A11005)
AlexaFluor 488/594 goat anti-rabbit	Rabbit primaries	1:1000	Invitrogen (A11008/ A11012)
Alexa-Fluor 488 donkey anti-rat	Rat primary	1:1000	Invitrogen (A21208)

For myosin, Golgi, centrosome/PCM, cilia, microtubules tyrosinated tubulin, and tight junction staining, cells were fixed in -20°C methanol (45 seconds for pericentrin, 3 min for Golgi, 5 mins for all others), washed with PBS and blocked as above, followed by 1 hour incubation with the relevant primary antibodies (*Table 2.1*), and 45 minute incubation with secondary antibodies (*Table 2.1*).

In all experiments, the nucleus was stained using 1µg/ml 4',6-diamidino-2-phenylindole (DAPI) for 1 minute, then washed with PBS-0.1% Triton prior to mounting in Vectashield (Vector Laboratories).

2.3 Microscopy and image acquisition

Samples were visualised using a Zeiss Axio Observer Z1 inverted microscope and 40x 1.2NA or 100x 1.4 NA oil objective, controlled by AxioVision software (Carl Zeiss). Images were captured using a CoolSnap HQ2 camera (Photometrics) and processed in AxioVision and ImageJ.

For cell volume analysis, samples were viewed using a 63x 1.4NA objective on a Zeiss LSM510 confocal microscope controlled by LSM examiner software. Constant exposure settings and pinhole size were used for all samples and cells imaged were randomly selected across the coverslips. Cell height was analysed in 15 randomly-selected cells from each cell line.

2.4 Image analysis and statistical analysis

Cell area was calculated from phase contrast images (n = at least 13 cells per cell line) using MetaMorph software, then mean cell area was calculated from these. The Kruskal-Wallis test was then used to compare differences in mean area ± standard error between the cell lines.

Quantification of the progression of actin organisation was performed by identifying five stages of actin phenotypes; these were rounded, blebbing, showing protrusions, showing intracellular actin, and elongated. At each time point, 3 repeats were performed, categorising 100 cells on each coverslip. The percentage of cells showing each phenotype was plotted as a box plot, separated by cell line, displaying mean, standard deviation (SD) and range of the data at each time point and colours to indicate the phenotype.

Line scan analyses to initially compare the prominent actin bundles were performed on 1000 actin bundles from at least 100-150 micrographs of each cell line, taken at 100x magnification. MetaMorph software was used to examine pixel intensity across each actin bundle, which was then exported into a Microsoft Excel spreadsheet. Each actin bundle was manually assessed to determine the beginning and end of the bundle across a series of pixel measurements; this was performed by subtracting the background of each series of measurements (determined to be a figure just greater than the bottom two values of each series of measurements) from each pixel intensity value individually, and considering an increase of ≥1000 from the background to define an actin bundle. These defined actin bundles were next exported to GraphPad software. Actin bundle line width was calculated as the mean number of values defining an actin bundle in each cell line. Mean pixel intensity – a measure of brightness – was calculated by working out the mean intensity of each actin bundle, then averaging this in each cell line. Graphs were drawn of the mean pixel intensity and line width of each actin bundle (1000 data points per cell line), and mean pixel intensity and line width ± SD in each cell line using GraphPad software. These data were analysed for difference using a χ^2 test (as they were not normally distributed) within the same software. Subsequent line scan analyses used at least 50 lines, sourced from at least 10 cells, to gauge thickness of lines.

For fluorescence intensity measurements, MetaMorph software was used to ascertain fluorescence intensity of each channel in each of 300 cells (100 cells in 3 repeats) from all cell lines. A line was drawn around the cell perimeter and average fluorescence intensity of each channel within this perimeter was calculated using the software to attain separate mean G- and F-actin fluorescence intensity per cell. G- and F-actin fluorescence intensity of each cell line was calculated by averaging these measurements across the cell population. Mean G:F-actin ratios were calculated by totalling the G:F-actin intensity of each cell and dividing this by the number of cells (i.e., 300 cells in each cell line). Graphs of mean F-actin fluorescence intensity ± SEM, mean G-actin fluorescence intensity, and mean ratio of G-actin fluorescence intensity:F-actin fluorescence intensity were plotted using GraphPad. A two-tailed Mann-Whitney (U) test was used to determine statistical difference between the cell lines.

Normality was tested using a D'Agostino & Pearson omnibus normality test in GraphPad Prism.

In experiments determining temporal appearance of phenotypes, assessment of number of cells showing phenotypes such as prominent bundles, 0-2 microtubule foci and dispersed Golgi were counted by eye in multiple, randomly-selected fields of view. At least 100 cells were counted per coverslip, and three repeats were performed of each of these experiments.

To determine temporal difference in microtubule, actin and Golgi phenotypes, mean number of cells showing each phenotype was calculated ± SD, and a χ^2 test was used to determine difference between each patient cell line and control cells over the first hour after plating in regard to mean proportion of cells displaying each phenotype.

2.5 Reverse Transcription Polymerase Chain Reaction

Fibroblasts (5-10 x 10^5) were pelleted and total RNA extracted using the High Pure RNA Isolation kit (Roche) according to the manufacturer's instructions. RNA concentration was measured using a Biophotometer (Eppendorf). Equal RNA concentrations for each sample were reverse-transcribed using the OmniScript kit (Qiagen) according to the manufacturer's instructions and touchdown PCR (*Table 2.2*) was performed with resulting cDNA and appropriate primers (*Tables 2.3* and *2.4*), designed using Primer3, Eurofins to verify melting temperature and MAFFTT when aligning isoforms. Negative control experiments were run of each primer set by running through the whole process using 1 µL of water in place of reverse transcriptase; GAPDH primers acted as a positive control, confirming roughly equal RNA presence across all three cell lines.

Pooled products from three repeats were run on an ethidium bromide-containing 2% agarose-TAE gel at 100V for 30 minutes alongside HyperLadder I (BioLine) and products visualised using a UVP UV transilluminator.

TABLE 2.2: Touchdown PCR programme used for polymerase chain reaction.

Initial denaturation: 94°C 5 min
Then 20 cycles (30 seconds per stage):
Denaturation: 94°C
Annealing: Progressive decrease from 60°C to 50°C throughout the cycles
Extension: 72°C
Then 15 cycles:
Denaturation: 94°C 30 seconds
Annealing: 55°C 30 seconds
Extension: 72°C 1 minute
Final Extension: 72°C 5 minutes
Held at 10°C until removed and used

TABLE 2.3: Primers designed against each of the actin isoforms and DNA melting temperature

Primer name		Primer Sequence		Tm
ACTA1 L		AGAGCTACGAGCTGCCAGAC		61.4
ACTA1R		GGCATACAGGTCCTTCCTGA		59.4
ACTA2 L		TCATCACCAACTGGGACGAC		59.4
ACTA2 R		CGCCTGGATAGCCACATACA		59.4
ACTC1 L		TGTCACCACTGCTGAACGTG		59.4
ACTC1 R		CAATGAAGGAGGGCTGGAAG		59.4
ACTB L		TGAGCGCAAGTACTCCGTGT		59.4
ACTB R		TGTCACCTTCACCGTTCCAG		59.4
ACTG1 L		TGTCAGGGCTGAGTGTTCTG		59.4
ACTG1 R		AGTAACAGCCCACGGTGTTC		59.4
ACTG2 L		CCCTCTTCCAGCCTTCCTTT		59.4
ACTG2 R		GTCAGCAATGCCAGGGTACA		59.4

L- Left, R – Right. ACTA1 – Actin alpha 1,skeletal mucle. ACTA2 –Actin alpha 2, smooth muscle, aorta. ACTC1 – Actin alpha, cardiac muscle 1. ACTB – Actin, beta. ACTG1 – Actin gamma 1. ACTG2 – Actin gamma 2, smooth muscle, enteric.

TABLE 2.4: Primers designed against actin-binding proteins involved in (A) stress fibres and (B) lamellipodial structures and DNA melting temperature of each.

A

Name	Primer Sequence	Tm	Primer length (bp)	Product size
ARPC2L	GAAAACAATCACGGGGAAGA	55.3	20	158
ARPC2R	TGGAACCAAAACGGAGAATC	55.3	20	
ARPC3L	GAAAGTTTTCGACCCTCAGAATG	58.9	23	284
ARPC3R	CAAATCACCCTTGATAACCCACT	58.9	23	
CAPZA1L	CCGACTTCGATGATCGTGTGT	59.8	21	189
CAPZA1R	CAGGCGTGAACTGATCCATGT	59.8	21	
CAPZA2L	TTCAATGATGTTCGGTTACTGCT	57.1	23	149
CAPZA2R	AAGTCGCCATGTTCTGTTATCAA	57.1	23	
CFL1L	GGAGGGCAAGCCTTTGTGA	58.8	19	229
CFL1R	GCAGTTTGGGAAGGCCAGA	58.8	19	
CFL2L	ATGGTTTGGGATCTTTTTGCAC	56.5	22	177
CFL2R	GAAAAATTCCATGGTGCCAAGT	56.5	22	
CTTNL	GACCGACCCTGATTTTGTGA	57.3	20	219
CTTNR	TCCATTCGGTCTTGTTCCAC	57.3	20	
DSTNL	GCAAAGAGATCTTGGTTGGAGAT	58.9	23	275
DSTNR	GAGATCTTCTGGTCCATTTGCTT	58.9	23	
EVLL	TGCAGGATCAGCAGGTTGTG	59.4	20	277
EVLR	TGGTGCTGCTCCATCACTTG	59.4	20	
PFN1L	AGGAGGAGTCATCCCGTTTA	57.3	20	108
PFN1R	GAGCCAGAAGAAGGAAGGAA	57.3	20	
PFN2L	TATTGTGGACTTGGCTGTCTTG	58.4	22	254
PFN2R	TCCCAGATGTAACAAAGTGCAG	58.4	22	
PFN3L	ACTCGGAGCGCGATGG	56.9	16	142
PFN3R	AGATGGCCGCCAGCAG	56.9	16	
PFN4L	CCAAATCACTGGAAGGCAGT	57.3	20	112
PFN4R	ACATGCTTGGTTCCCAAGAG	57.3	20	
WASF1L	AAAGTGCCAAGAGCACCTCA	57.3	20	195
WASF1R	TGGCAAGGCAGAAAGTGAGT	57.3	20	
WASF2L	TGCTGCCCACCTTCTTTTTC	57.3	20	129
WASF2R	TTGGTTGCTTCAGGGAAAGC	57.3	20	
WASF3L	CACAAACTGCCTTCGTCAGC	59.4	20	179
WASF3R	AAGAGAAGACCCGGGACCA	58.8	19	
TMSB4XL	TGCAAAGAGGTTGGATCAAGTTT	57.1	23	138
TMSB4XR	CCAACATGCAAGTTCTTTCCTTC	58.9	23	
WASLL	ACCTCCACCACCATCAAGG	58.8	19	270
WASLR	ACCCCCAACACAGATGGAG	58.8	19	

B

Name		Primer Sequence		Tm		Product size
ACTN1 L		AGAAGCATGAGGCCTTCGAG		59.4		
ACTN1R		CCAGATTGTCCCACTGGTCA		59.4		156
ACTN2 L		GGGGTGAAACTGGTGTCCAT		59.4		
ACTN2 R		GTCCAAGGCCATCTTTCCAG		59.4		226
ACTN3 L		CATGCAGCGCAAACTAGAGG		59.4		
ACTN3 R		ATCTCCGAGAGCAGCCAGTC		61.4		234
ACTN4 L		GGAAGGGCTCCTTCTCTGGT		61.4		
ACTN4 R		CCTCTGCATCCAGCATCTTG		59.4		236
CORO1A L		CTCACAGACCACCTGGGACA		61.4		
CORO1A R		CAGGCGATGTCTAGCACAGG		61.4		177
CORO1B L		ACAGAGCCGGTGGTGGTACT		61.4		
CORO1B R		GCTCTTGTCCTTGCATGCTG		59.4		234
CORO1C L		TGCCTCTCCATCTCTCACCA		59.4		
CORO1C R		CAGCCCTTCCAAAACAGAGG		59.4		185
CORO2A L		CACGGCCTACAGGAAGGAAC		61.4		
CORO2A R		CGTACTCATGGGGCTTGTGA		59.4		163
CORO2B L		GACCAGGGTCTGATGGCTTC		61.4		
CORO2B R		GTGACCTTGGGCCACTTCTC		61.4		215
CORO6 L		ACTATACCCCCATGCGCAAC		59.4		
CORO6 R		TGCTGTTCCAGCACACACTG		59.4		219
CORO7 L		GGCAGCTGTGACTGATCTGG		61.4		
CORO7 R		ATCTTCTCCGTGTGGCCTGT		59.4		159
FSCN1 L		GCAAGTACTGGACGCTGACG		61.4		
FSCN1 R		GCTGCCCATTCTTCTTGGAG		59.4		153
FLNA L		TCACCATCGATGCAAAGGAC		57.3		
FLNA R		AGAAGGGGATCTCGTCACCA		59.4		186
FLNB L		AAGTGGGGTCTCTGGGGTTT		59.4		
FLNB R		ACGGGCTGTCCTTGATGTCT		59.4		162
PLS1 L		AAGGTGGGGAAGATGGACCT		59.4		
PLS1 R		GCAGGCACGGGTATGTGTTA		59.4		204
PLS2 L		GCACTCTCACACTGGCCTTG		61.4		
PLS2 R		TGAGGTCCAGAACAGGCAGA		59.4		204
PLS3 L		GGGAGCCAACATGAAAAAGC		57.3		
PLS3 R		CGTCATTGGCTTTCTGACCA		57.3		206
TAGLN L		AAGCGCAGGAGCATAAGAGG		59.4		
TAGLN R		GCCCTCTCCGCTCTAACTGA		61.4		155
TAGLN2 L		TGGCAGTAGCCCGAGATGAT		59.4		

TAGLN2 R		TTGCAGCTGGTTATCCGAGA		57.3		101
IQGAP1 L		GGATGGGATGAACCTCCAAA		57.3		
IQGAP1 R		GGTGATGGCAGGGATTTGTT		57.3		225
IQGAP2 L		CGAGAATACGCTGCTTGCAC		59.4		
IQGAP2 R		CGGGGCTTCTGAGTTGATTC		59.4		236
IQGAP3 L		ACCTCCTCGCCATGACTGAT		59.4		
IQGAP3 R		TGGGTTCAGGAAGCGGTAGT		59.4		185
MACF1 L		TCACGCGCCTTTCATAGAGA		57.3		
MACF1 R		TGCTAACAGCCACACCTGCT		59.4		154
MYH2 L		CCAACTTCCAGAAGCCCAAG		59.4		
MYH2 R		TTTGAGCCCCAGAGAAGAGC		59.4		195
MYH10 L		CGACACGCGGACCAGTATAA		59.4		
MYH10 R		ATCGGCTGGAAGAGAAGCTG		59.4		235
PALLD L		GTCGCTATGCAGCACTTTCG		59.4		
PALLD R		CAAGGCAATGGCTGTTTCAG		57.3		163
VIL1 L		GGGCAAGAGGAACGTGGTAG		61.4		
VIL1 R		CTGGTCTCGGATCTCCTTGG		61.4		172
CNN2 L		AGTGAGGGCCGTACAAGGAA		59.4		
CNN2 R		AGGCTGGAGAATCGCTTGAG		59.4		197
CNN3 L		GGGCGGCAAGTATATGATCC		59.4		
CNN3 R		CATCCTGGTACTCGCCATGA		59.4		154
TPM1 L		GCTGAGAAGGCAGCAGATGA		59.4		
TPM1 R		CCAGGTCGCTCTCAATGATG		59.4		184
TPM2 L		TACAAGGTTTGGGCCGAGGT		59.4		
TPM2 R		TCCAGCTTCAGCATCTGCAT		57.3		243
TPM3 L		TGCTTTTGAGACGCCAGTGT		57.3		
TPM3 R		TTGGTCCATGCCTATCAACG		57.3		153
TPM4 L		TAGAAAACCGGGCCATGAAG		57.3		
TPM4 R		TTTCAGATGCAGCCTCCAGA		57.3		249
FHOD1 L		AGCTGTCCCTGGAAGAGCAG		61.4		
FHOD1 R		GGCACCAGGTCTTTGTCCTC		61.4		208
ZYX L		CTGCGAGGGCTGTTACACTG		61.4		
ZYX R		TGTGGTAGTCGGGGACACAG		61.4		197
CRP1 L		CCTGGGATCTGACACCATCA		59.4		
CRP1 R		GGTGCCAAGATGTGTCCTCA		59.4		164
VASP L		GACCACTTCCGAGACCCAAC		61.4		
VASP R		GGAAAGGAGAAGCGGGTCTT		59.4		200

L- Left, R – Right. (A) also shows primer size; primers in (B) are all 20 bp. Full names of DNA each primer sequence is designed against are also described.

2.6 Sodium Dodecyl Sulfate Polyacrylamide Gel Electrophoresis (SDS-PAGE)

Cells grown in culture flasks for ≥4 days were trypsinised, centrifuged, and chilled lysis buffer (20mM Tris-HCl pH 7.4, 150mM NaCl, 1mM EDTA, 0.5% Triton X-100, 0.5% NP-40; 1mM PMSF and protease inhibitor cocktail added just before use) was immediately applied to the pellet. This was incubated at 4°C for 15 minutes. Lysates were sheared with a 1ml syringe and 25 gauge needle and frozen at -20°C until needed. A Bradford assay (BioRad) was used to check the protein concentration using a UV spectrophotometer (Eppendorf Biophotometer Plus), ensuring that equal total protein was loaded (about 30 µg per lane).

SDS 10% polyacrylamide gels were used to separate proteins by gel electrophoresis. Samples were denatured at 100°C for 5 minutes in 4x sample buffer (0.125M Tris pH 6.8, 2% SDS, 40% glycerol, roughly 0.015% Bromophenol Blue powder and 10% β-mercaptoethanol) prior to loading. 15 µL of sample-buffer mix per lane was run alongside Color Plus Prestained Protein Marker (BioLabs).

Two identical gels were simultaneously run. One was stained with Coomassie Blue stain to visualise the protein on the gel. The other was used for a Western blot – it was electrotransferred onto PVDF membrane in transfer buffer (48mM Tris, 39mM glycine, 0.037% SDS, 20% methanol) at 220mA at room temperature for 90 mins using 1:750 primary (rabbit anti-myosin and rabbit anti-ROCK (as before, *Table 2.1*), with rabbit anti-VDAC1/2/3 (Abcam, Cat No. ab15895, used at 1:200), a protein in mitochondrial ion channels, as a loading control) and secondary antibody (goat anti -rabbit IgG-peroxidase - Sigma, Cat. No. A3687 - used at 1:10000). ECL reaction mixture (PerkinElmer) was added and chemiluminescence visualised by exposure to X-ray film (Fujifilm).

CHAPTER III: MKS patient cells display characteristic prominent actin bundles due to filament turnover defects

3.1 Introduction

Ciliopathy research is only just beginning to explore wider subcellular issues associated with the ciliopathies, and there seems to be remarkable correlation in cellular phenotypes amongst this spectrum of disorders. For instance, similar increases in actin stress fibre prominence are observed upon alteration to genes involved in Joubert syndrome (Huang *et al.*, 2011), Bardet-Biedl syndrome (Hernandez-Hernandez *et al.*, 2013) and nephronophthisis (Veland *et al.*, 2013).

Previous studies have connected alterations to MKS proteins to morphologically-similar defects in the actin cytoskeleton. MKS1 and meckelin, the *TMEM67* (*MKS3*) protein product, interact with actin-binding isoforms of nesprin-2; this is one of a group of scaffolding proteins involved in maintenance of the actin cytoskeleton and nuclear positioning. Notably, nesprin-2 is also necessary for centrosome migration during ciliogenesis, potentially through its effects on actin (Dawe *et al.*, 2009). Furthermore, meckelin localises to basolateral actin fibres and its loss triggers remodelling of the actin cytoskeleton into prominent bundles and hyperactivation of RhoA signalling (Valente *et al.*, 2010). Mutations in *TMEM216* and *TMEM67* are both reported to cause prominent actin bundles to form (Dawe *et al.*, 2009; Valente *et al.*, 2010), possibly due to this RhoA hyperactivation.

The actin bundling and cross-linking protein Filamin A also interacts with meckelin, and loss of either protein results in similar cellular phenotypes; these include defects in basal body positioning, RhoA hyperactivation and dysregulation of the canonical Wnt pathway (Adams *et al.*, 2011). Finally, knockdown of *RPGR*, the best studied binding partner of the *MKS5* paralogue *RPGRIP1L* (Khanna *et al.*, 2009), leads to more prominent actin bundles, impaired ciliogenesis and cell-substrate attachment (Gakovic *et al.*, 2011). Taken together, these data indicate that MKS proteins have important functions in actin cytoskeletal organisation and regulation; however, their precise role and the underlying molecular mechanism involved remains unknown.

The current chapter tests the hypothesis that actin in *MKS2* and *MKS3* patient cells changes temporally and is structurally altered compared with control fibroblasts.

In the present chapter, I describe the temporal effects of mutations at the *MKS2* and *-3* loci upon actin organisation, affecting TMEM216 and meckelin, respectively. I report that actin levels are modified in patient cells, and trace this to defects in turnover of existing filaments, not in transcription or in generating new filaments.

The data reported in the current chapter replicate the previous studies demonstrating that mutations in *TMEM216* (*MKS2*) and *TMEM67* (*MKS3*) lead to structural alterations to the actin cytoskeleton, but additionally indicate that these genes affect the spatiotemporally-appropriate maintenance and turnover, not the initial generation, of actin filaments. This is the first instance of study into the temporal appearance of these defects, and of whether these develop from existing stuctures or *de novo*.

3.2 Results

Actin organisation is altered in MKS patient cells

In order to first ascertain whether any gross morphological changes exist, I plated control and MKS patient fibroblasts on glass coverslips, fixed and took phase contrast images of these cells. *MKS2* patient cells demonstrated significantly increased spreading and more variable size when compared with wild-type cells; mean area (± SEM) of these cell lines was 5,526±432 and 1,708±80 μm^2, respectively (n=13 and 14 cells, respectively; Kruskal-Wallis test, $p<0.001$). However, *MKS3* patient cells were more variable but not significantly different in size from control cells, demonstrating a mean area of 2,570±380 μm^2 (n=15 cells) (*Figure 3.1*). This suggests that there may be an underlying problem with the actin cytoskeleton, as one of the key regulators of cell shape.

In order to improve the current characterisation of actin organisational defects in MKS patient cells (Dawe *et al.*, 2009; Valente *et al.*, 2010), I plated wild-type and MKS patient fibroblasts onto crossbow-shaped micropatterned coverslips and fixed and stained them with fluorescently-labelled phalloidin to highlight filamentous actin. Micropatterned coverslips were used due to their

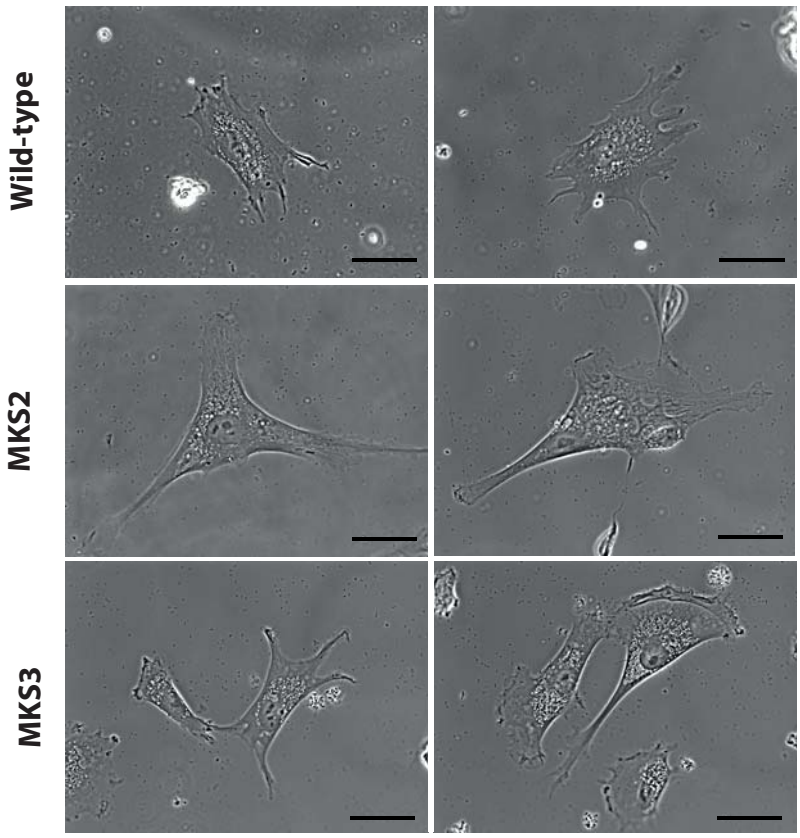

FIGURE 3.1: *MKS2* patient cells exhibit increased cell spreading
Phase contrast images showing cell morphology in wild-type, *MKS2* and *MKS3* patient cells. *MKS2* patient cells appear larger than controls, while *MKS3* cells are more variable in size. Scale bars represent 40 μm.

ability to fix cell shape, a feature which may affect actin organisation. *MKS2* patient fibroblasts formed prominent cell body actin bundles (*Figure 3.2, red arrowhead*), as previously reported (Valente *et al.*, 2010). *MKS3* patient fibroblasts generated highly ruffled lamellipodia but no prominent actin bundles, in contrast to previous results (*Figure 3.2, yellow arrowhead*) (Adams *et al.*, 2011; Dawe *et al.*, 2009). Cells had only been allowed to settle for an hour before fixing; however, in published data, these defects were reported after an undisclosed number of days. This raised the possibility that actin defects in the patient cells vary over time.

To determine how actin organisation temporally develops in MKS patient cells, I plated wild-type and MKS patient fibroblasts onto collagen I-coated coverslips, then fixed and stained cells with fluorescently-labelled phalloidin every 10 minutes for an hour, then again at 2 hours after plating. Actin organisation was described during cell spreading (over the 2 hours after plating), and during cell growth and division (over the 7 days after plating). Wild-type and *MKS3* patient cells developed actin-rich blebs, which were not apparent in *MKS2* patient cells, within 10-20 minutes of plating (*red arrowheads, Figure 3.3*); these cells then formed protrusive structures (microspikes, lamellipodia and, less commonly, filopodia). Fibroblasts carrying the *MKS2* mutation formed prominent cell body actin ~40 minutes after plating on collagen I-coated coverslips, in contrast to the less-prominent cell body actin observed in wild-type and *MKS3* patient cells (*yellow arrowheads, Figure 3.3*), following which the cell elongated. Similar prominent actin bundles develop in *MKS3* patient cells 4 days after plating (*yellow arrowheads, Figure 3.4*). These results indicate that mutations in *MKS2* and *MKS3* act differently upon the actin cytoskeletal regulatory machinery.

In order to disentangle the subtleties of these actin organisational defects, I quantified the progression of actin organisation in these cell lines. I identified five stages of actin organisation and reported the percentage of cells demonstrating each of these phenotypes every 10 minutes for the first hour after plating, then at 2 hours after plating (*Figure 3.5*). These stages were rounded (*Figure 3.5a*), blebbing (*Figure 3.5b*), showing protrusions (*Figure 3.5c*), showing intracellular actin (*Figure 3.5d*), and elongated (*Figure 3.5e*). *MKS2* and *MKS3* patient cells progressed more rapidly through the initial stages of actin organisation (*Figure 3.5a* and *b*), but progression slowed down in these

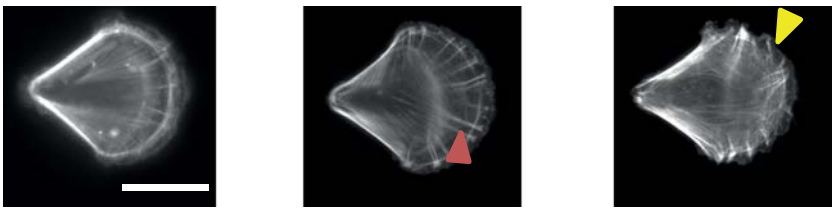

FIGURE 3.2: Actin organisation is aberrant in MKS patient cells.
Cells were grown on crossbow-shaped fibronectin-coated micropatterned coverslips and fixed and stained with fluorescently-labelled phalloidin. Note the presence of prominent actin bundles in *MKS2* patient cells (red arrowhead) and highly ruffled lamellipodia in *MKS3* patient cells (yellow arrowhead). Scale bar represents 20 µm.

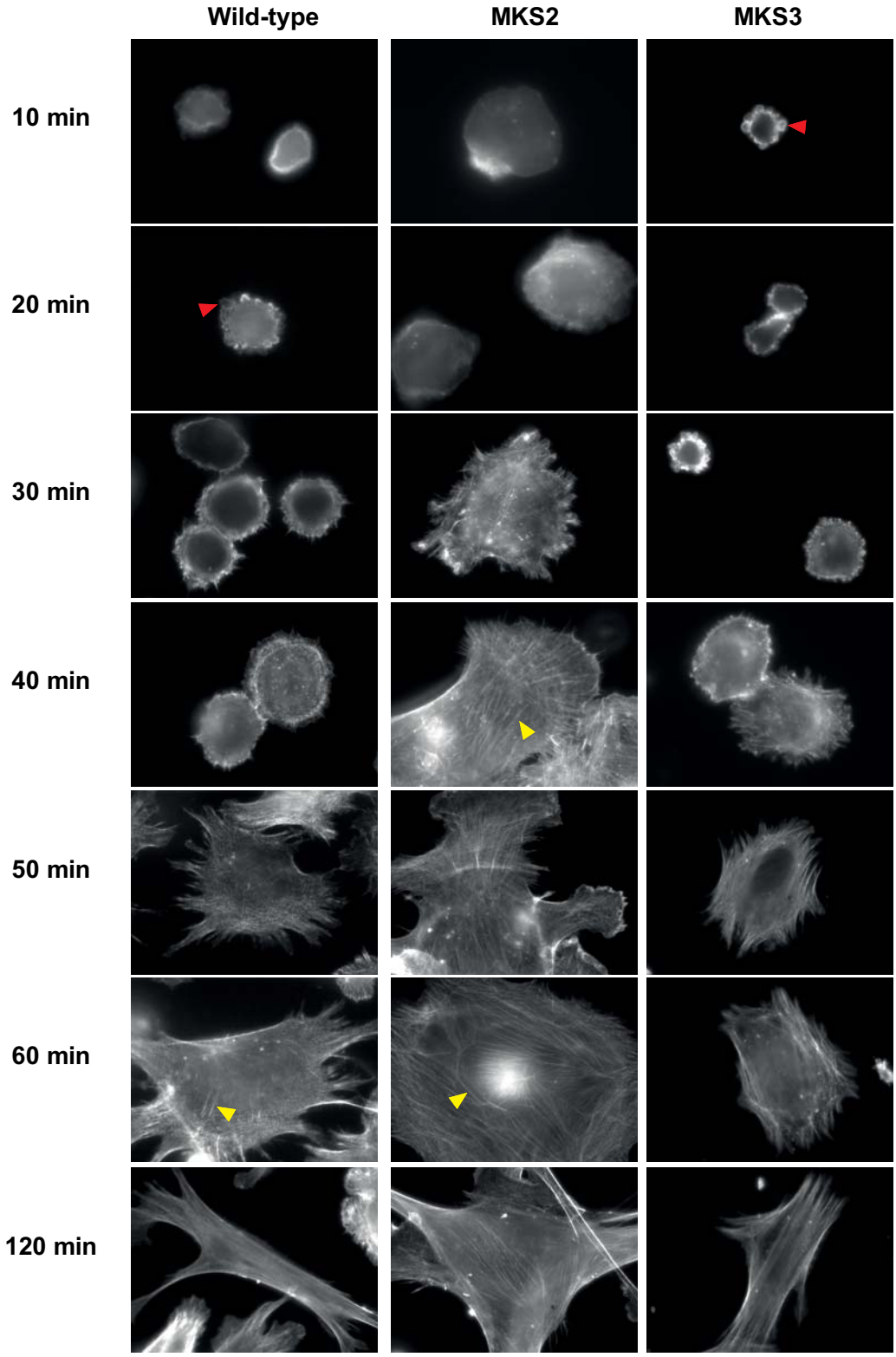

FIGURE 3.3: Aberrant actin organisation develops rapidly after plating in *MKS2* patient cells.

Fibroblasts were plated on collagen I-coated coverslips, fixed and stained with fluorescently-labelled phalloidin in order to visualise actin phenotype progression over time. Actin blebbing (red arrowheads) is followed by formation of microspikes, filopodia and lamellipodia. Intracellular actin bundles (yellow arrowheads) form, and the cell extends. Scale bar represents 20 μm.

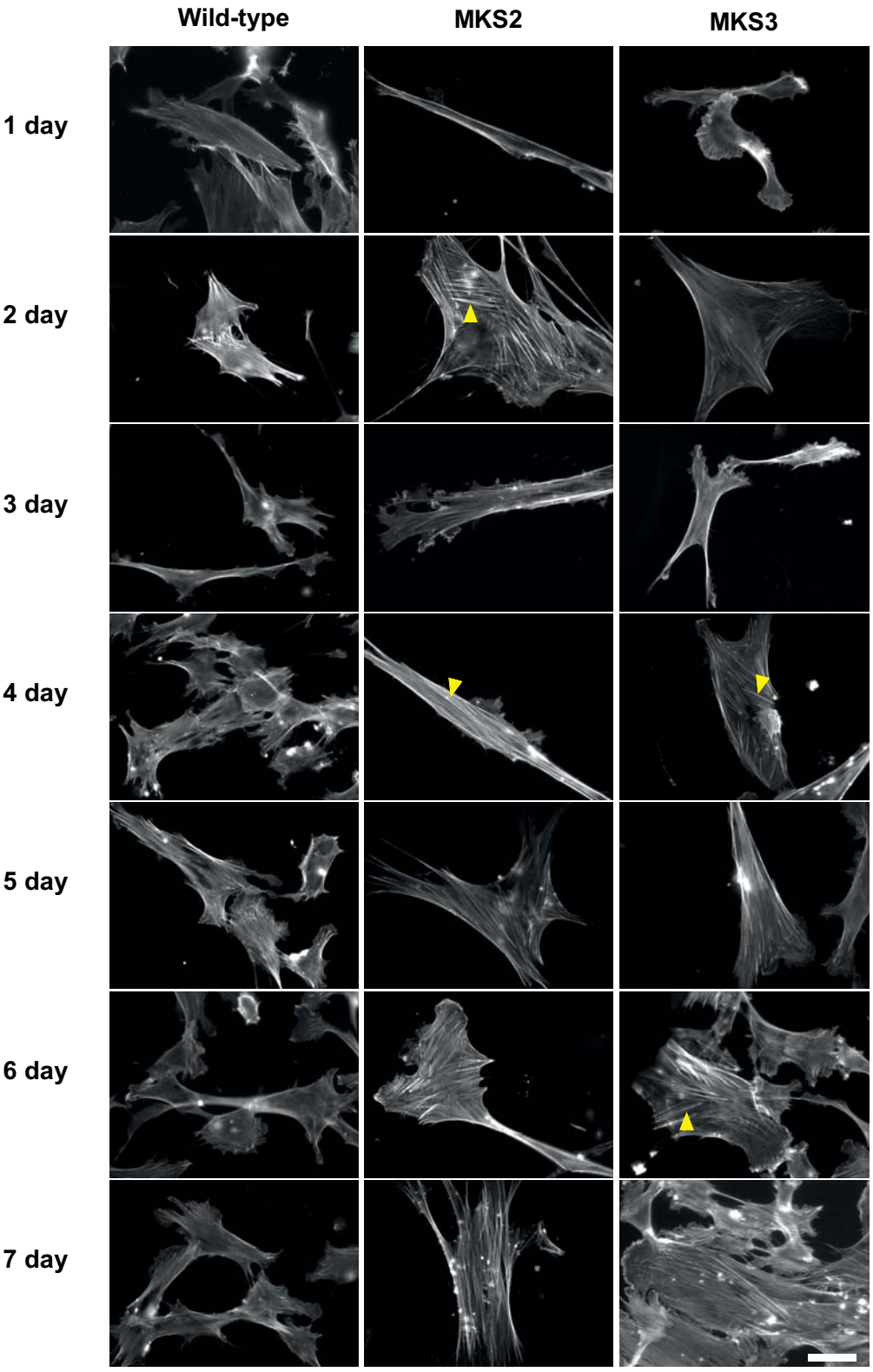

FIGURE 3.4: Prominent bundles develop in *MKS3* cells 4 days after plating. Fibroblasts were fixed and stained with fluorescently-labelled phalloidin every 24 hours after plating on coverslips, in order to visualise actin phenotype progression over time. In the first 7 days after plating, *MKS2* patient cells present prominent actin bundles; ~4 days after plating *MKS3* patient cells also begin to present prominent actin bundles. Yellow arrowheads indicate some of these prominent actin bundles in MKS patient cells. Scale bar represents 40 μm.

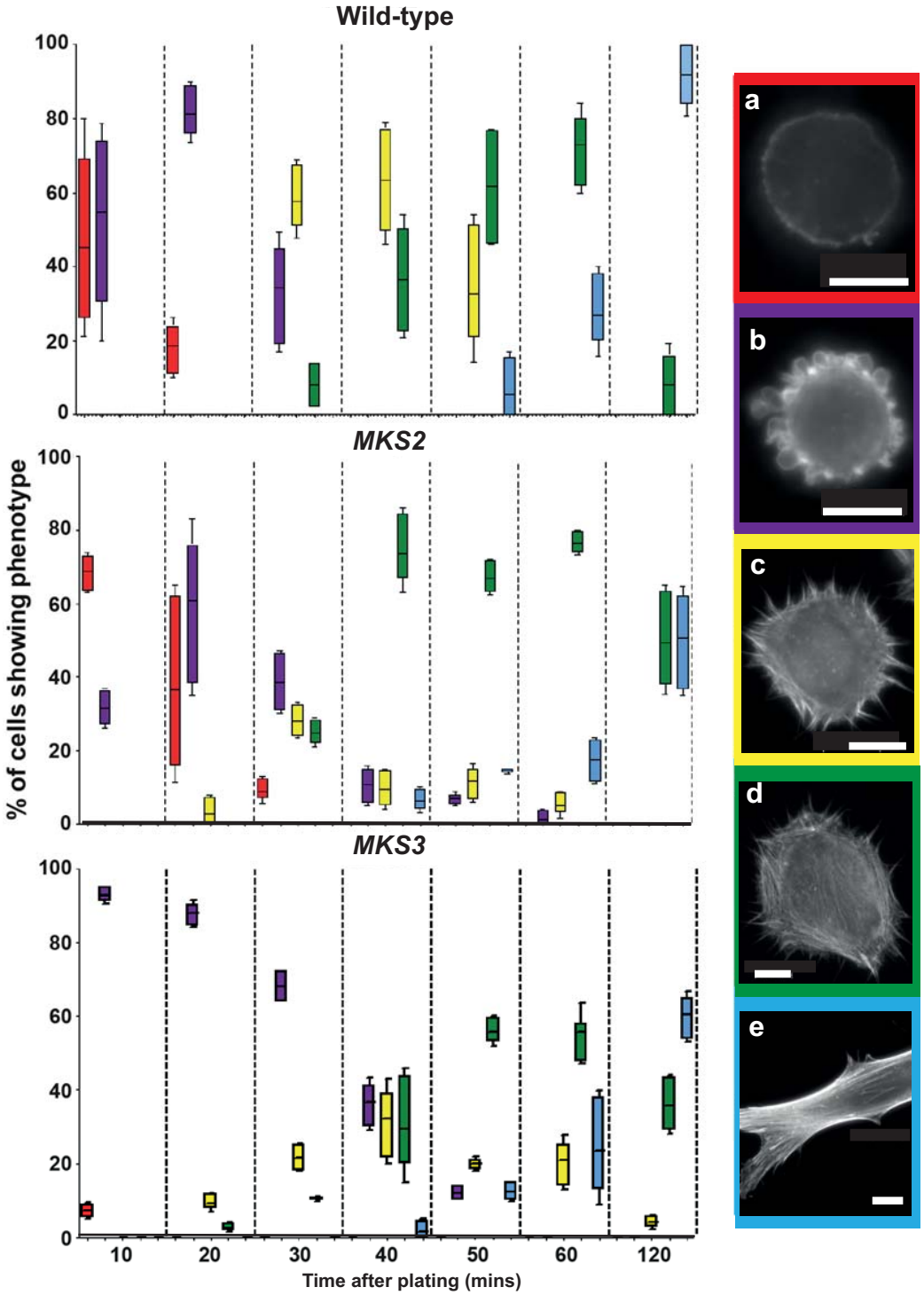

FIGURE 3.5: Aberrant actin organisation develops rapidly after plating in MKS patient cells.

Quantification of the progression of actin organisation in each cell line. Five stages of actin organisation were identified (a-e); image outline colour corresponds to bar colour in the graphs. Scale bar represents 10 μm. Graphs are plotted as mean percentage of cells with a phenotype (horizontal line on bar) ± S.D. (top and bottom of coloured bar) and range (whiskers). n=200-300 cells per time-point per cell line. *MKS2* and *MKS3* patient fibroblasts demonstrate faster progression through stages a and b than control cells, but at 60-120 minutes after plating, fewer cells are at stages c-e vs. control cells.

cell lines. At 60 and 120 minutes after plating, fewer MKS patient cells are displaying the more advanced actin organisation phenotypes (*Figure 3.5d* and *e*) when compared with wild-type cells. The absence of actin-rich blebs in *MKS2* patient cells and the rapid formation of cell body bundles but failure to progress beyond this stage may be indicative of a problem in recycling actin to or in using cytoskeletal components (such as actin-binding proteins) at the leading edge.

To verify that these prominent actin bundles in MKS patient cells differed from actin bundles in wild-type cells, I quantified pixel intensity and bundle width using line scan analyses, performed to temporally coincide with prominent bundle development (*MKS2*, 1 hour after plating; *MKS3*, 4 days after plating). At least 1,000 bundles were analysed from images of at least 100 cells per cell line, taken under identical exposures.

Actin bundles in *MKS2* and *MKS3* patient fibroblasts (*red, Figure 3.6*) had a higher mean and median pixel intensity; the prominent actin bundles in *MKS2* patient fibroblasts had a mean pixel intensity of 3,973±1498, compared with a mean pixel intensity of 2,302±1139 in wild-type cells (χ^2 test, $p<0.001$). The corresponding median values were 3,667 and 2,015, respectively. Prominent actin bundles in *MKS3* patient fibroblasts, similarly, had a mean pixel intensity of 5,898±2,633, compared with a mean intensity of 3,011±1,145 in wild-type fibroblasts ($p<0.001$). The equivalent median intensity values were 5,246 and 2,849, respectively.

Actin bundles are also thicker in MKS patient cells; *MKS2* patient cells had actin bundles with a mean width of 11±3 pixels, compared with a mean width of 6±2 in wild-type cells; the corresponding median bundle widths were 11 and 5 pixels, respectively. Actin bundles in *MKS3* patient cells had a mean width of 6±2 pixels, compared with a mean width of 4±1 pixels in wild-type cells, with equivalent median values of 6 and 4 pixels-wide, respectively. Both *MKS2* bundles and *MKS3* bundles were thus highly significantly brighter and thicker (χ^2 test, $p<0.001$) (*Figure 3.6*) than their wild-type counterparts.

I next evaluated whether the increased cell spreading observed in these cells was associated with increased cell volume, or with changes to the actin cytoskeleton. I constrained fibroblasts on micropatterned coverslips, which were then fixed and visualised after an hour. Confocal imaging was used to make XY, XZ and YZ projections of these cells in order to approximate their three-dimensional structure. From these, I was able to measure cell height when cell

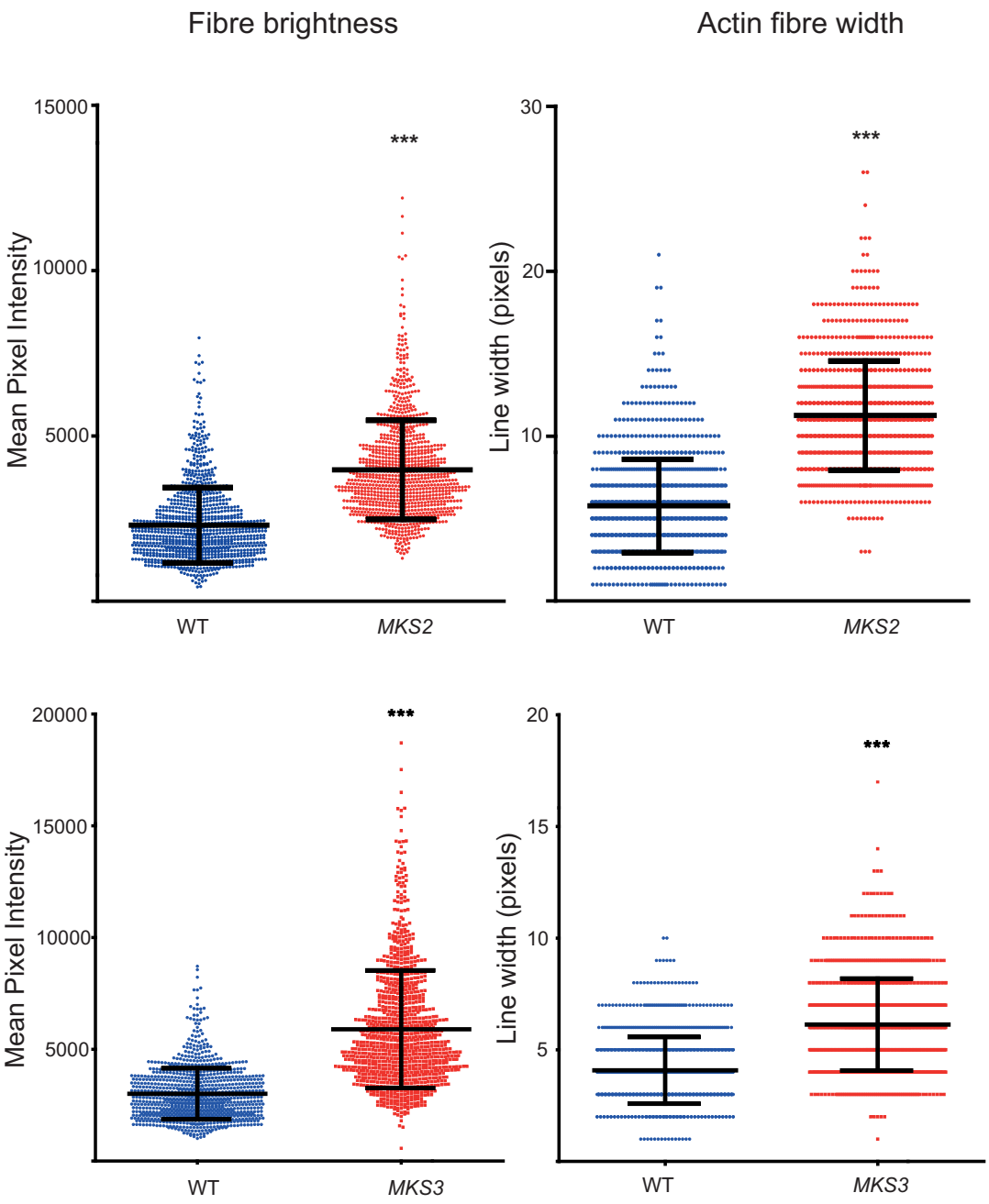

FIGURE 3.6: Actin bundles in MKS patient cells are brighter and thicker.
Line scan analyses of actin bundles in control and MKS patient fibroblasts (n=1,000 lines from at least 100 cells per cell line). Line scans were performed to temporally coincide with the appearance of prominent bundles (*MKS2*, 1 hour; *MKS3*, 4 days). Graphs show mean pixel intensity or line width of bundles ± SD, indicating *** statistical significance of $p<0.001$ (χ^2 test). Corresponding median pixel intensity for these data are as follows: WT vs. *MKS2*, 2,015 and 3,667, respectively; WT vs. *MKS3*, 2,849 and 5,246, respectively. Median bundle widths are as follows: WT vs. *MKS2*, 5 and 11 pixels, respectively; WT vs. *MKS3*, 4 and 6 pixels, respectively.

shape was restricted, enabling me to use a single measurement to deduce whether increased cell volume was responsible for the increased cell spreading observed in MKS fibroblasts (*Figure 3.7*).

Cell height was approximately equal in wild-type and MKS patient cells (8.5 μm average, n=15 cells per cell line), but that *MKS2* patient cells had increased actin blebbing protruding from their apical surface, presumably underlying membrane; these cells also contained intense G-actin staining (*green, Figure 3.7*). These results indicate that cell spreading is not due to increased cytoplasmic volume, but may be due to altered cytoskeletal properties; these abundant, non-polarised protrusions (actin bleb-like, as opposed to lamellipodia or filopodia) may be indicative of altered cortical F-actin levels. The increased G-actin intensity reported additionally led me to investigate levels of G- and F-actin in MKS patient cells.

G- and F-actin levels are perturbed in MKS patient cells

In order to examine relative G- to F-actin levels, I plated wild-type and MKS patient cells on crossbow-shaped micropatterned coverslips, then fixed and stained the cells with fluorescently-labelled DNase1 to label actin monomer and fluorescently-labelled phalloidin to label actin filaments.

The cells (n=300 cells per cell line) were imaged under identical conditions. G-:F-actin ratios were calculated per cell by dividing mean G-actin fluorescence intensity by mean F-actin fluorescence intensity, from which mean G-:F-actin ratio for the population was calculated. G- and F-actin levels significantly increased in *MKS2* patient cells [$p<0.001$ using a Mann-Whitney (U) test], and G-actin levels significantly decreased in *MKS3* patient cells [$p<0.001$, Mann-Whitney (U) test], (*Figure 3.8*). Mean G-:F-actin ratio significantly increased in *MKS2* and decreased in *MKS3* patient cells [$p<0.001$, Mann-Whitney (U) test] (*Figure 3.8*), revealing a perturbation in G-:F-actin balance.

These results imply that actin transcription, stabilisation or degradation are dysregulated in *MKS2* and *MKS3* patient cells; I therefore examined actin in within these contexts.

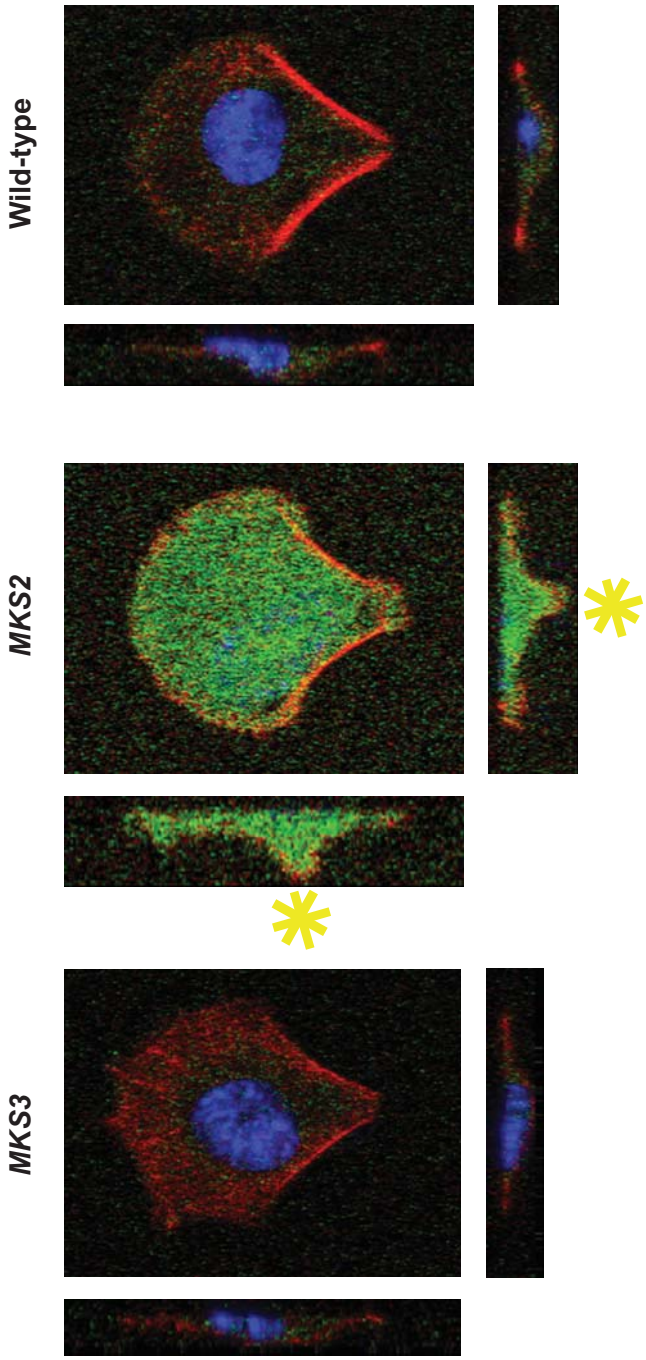

FIGURE 3.7: MKS patient cell volume is normal, but *MKS2* patient cells demonstrate more actin blebbing.

Maximum intensity projections of confocal XYZ images (coloured panels), demonstrating cell height when cell shape is constrained by growth on micropatterned coverslips. Cells were stained with fluorescently-labelled phalloidin to mark F-actin (red), DNase1 to label G-actin (green) and DAPI to label DNA (blue). Yellow asterisks indicate protrusions on the apical surface of *MKS2* cells. Note that cell height is approximately equal in all cell lines.

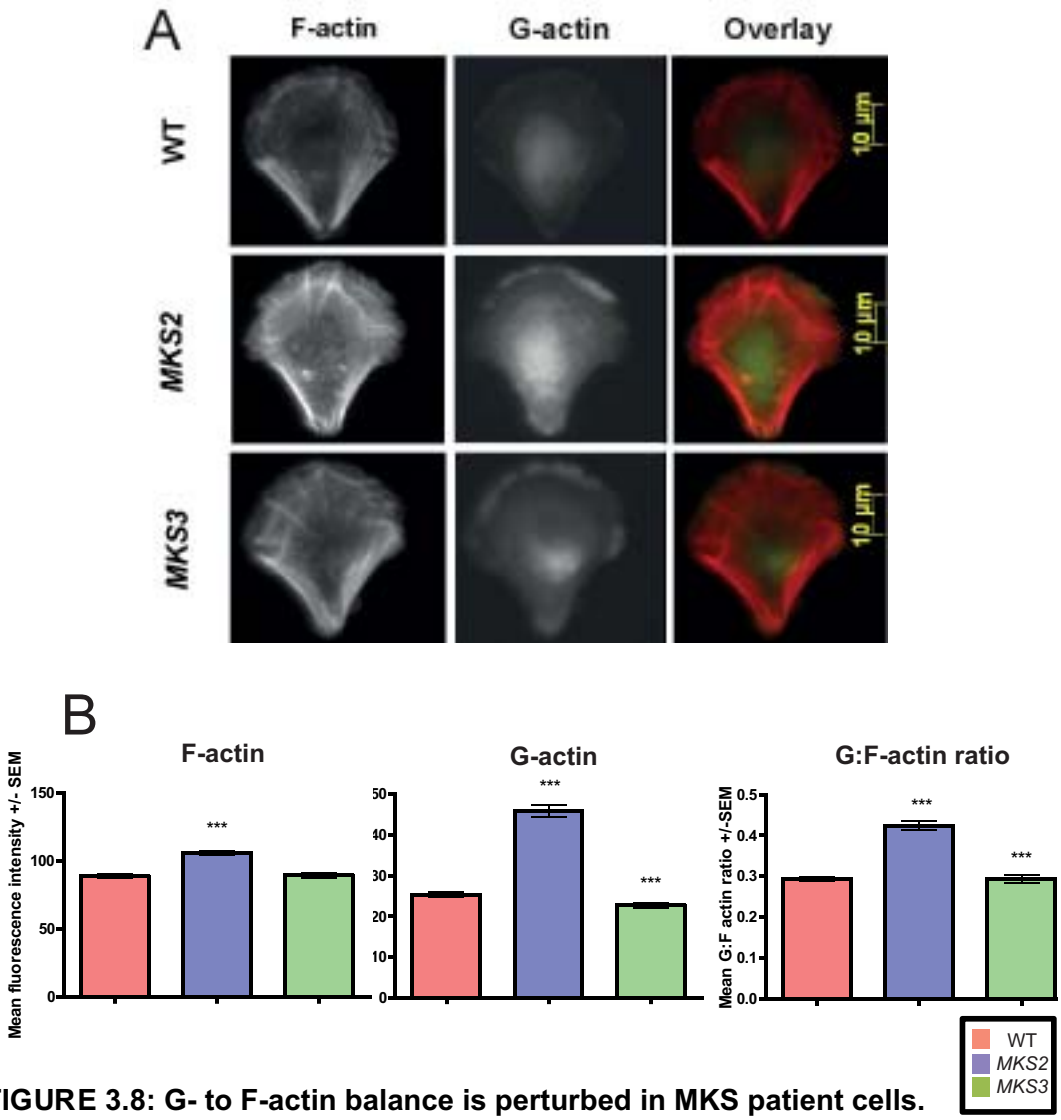

FIGURE 3.8: G- to F-actin balance is perturbed in MKS patient cells. (A) Widefield images of G- (green) and F-actin (red) labelled in fibroblasts grown on micropatterned coverslips. (B) Mean fluorescence intensity of G-actin and of F-actin were calculated for each cell individually, and a mean of the population calculated from this. G-:F-actin ratios were calculated by dividing mean fluorescence intensity of G-actin in each cell by mean fluorescence intensity of F-actin in the cell and a mean figure was calculated from the cell population. G- and F-actin levels and mean G-:F-actin ratio were significantly increased in *MKS2* patient cells, whilst G-actin levels and mean G-:F-actin ratio were significantly decreased in *MKS3* patient cells.

Actin filament turnover is dysregulated in MKS patient cells

To investigate whether actin levels are altered at a transcriptional level, I assessed comparative levels of actin mRNA. I used RT-PCR and primers specific to each known actin isoform to compare the three cell lines, showing that actin mRNA levels did not appear to differ between MKS patient cell lines when compared with wild-type cells (*Figure 3.9*). Whilst this technique is only semi-quantitative, these data indicate that actin defects likely occur post-transcriptionally in MKS patient cells.

I next aimed to establish whether aberrant actin organisation occurs through spatially- or temporally-inappropriate formation of prominent bundles using the G-actin pool, or turnover (remodelling or stabilisation) of existing actin filaments. I treated cells with 10nM jasplakinolide for 3 days, stabilising existing filaments and preventing turnover into new actin structures in a concentration and time-dependent manner (Cramer, 1999), then fixed and highlighted actin with fluorescently-labelled phalloidin. The prominent actin bundles present in untreated cells (*yellow arrowheads, Figure 3.10*) no longer formed in any of the MKS patient cells following jasplakinoide treatment (n>100 cells across 3 repeats); however, actin filaments were still apparent in the cell body of wild-type and MKS patient cells (*Figure 3.10*), suggesting that these structures develop from existing filaments and indicating a defect in filament turnover.

3.3 Discussion

I have demonstrated that the previously reported defects (Adams *et al.*, 2011; Dawe *et al.*, 2009; Valente *et al.*, 2010) in actin organisation displayed in fibroblasts carrying a mutation in *TMEM216* (*MKS2*) or *TMEM67* (*MKS3*) occur in a temporally-distinct manner, indicating that these mutations influence cytoskeletal machinery in different ways. I confirmed that the prominent actin bundles of MKS patient cells are morphologically-distinct from wild-type actin bundles, and revealed that they may be connected to an imbalance in G-:F-actin levels in these cells.

Altered G- and F-actin levels may be either causative or symptomatic of the prominent actin bundles observed in *MKS2* and *-3* patient fibroblasts; increased amounts of G-actin and increased numbers of actin filaments in these cells may

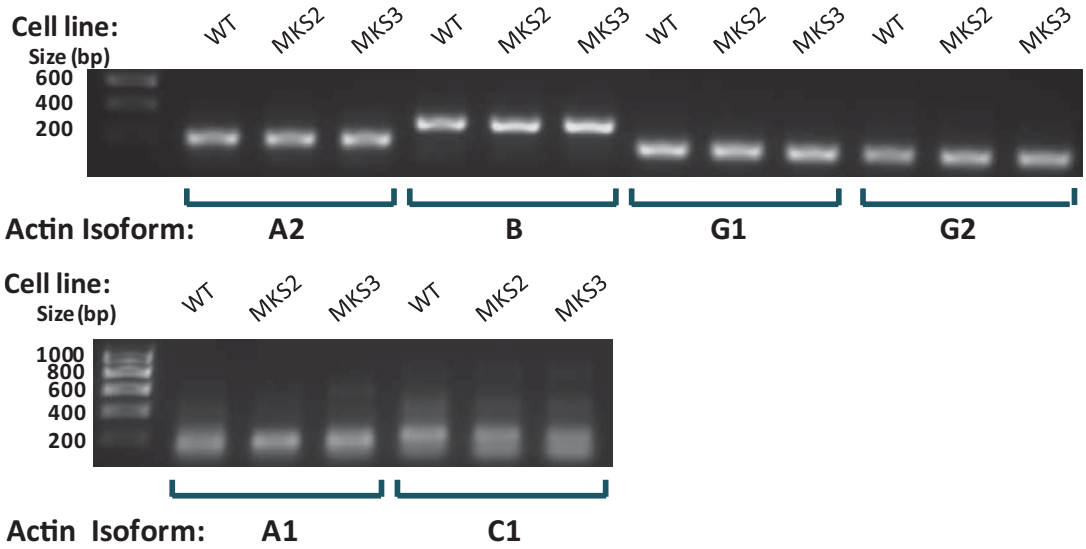

FIGURE 3.9: Actin mRNA levels remain unaltered in MKS patient cells. RT-PCR was performed using RNA extracted from each cell line and primers specific to 6 actin isoforms, revealing no difference in mRNA levels of any actin isoform.

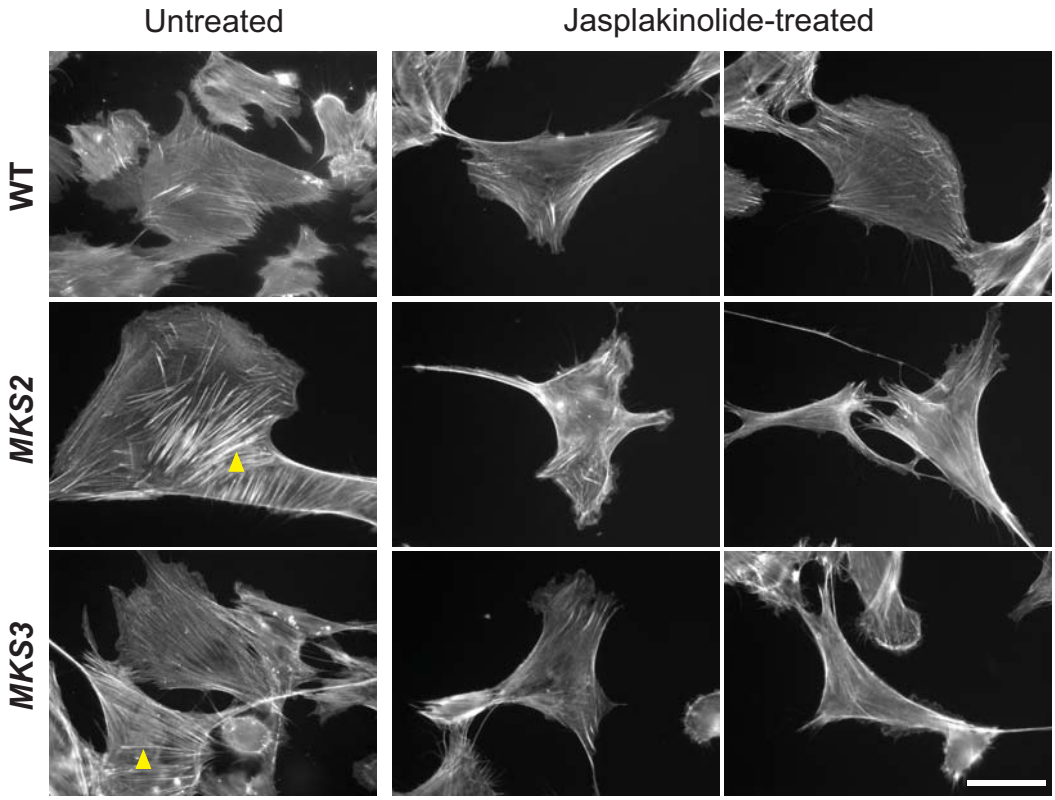

FIGURE 3.10: Jasplakinolide treatment induces prominent actin bundle disassembly in MKS patient cells.

Fibroblasts were plated for 24 hours, then treated with 10 nM jasplakinolide for 3 days, fixed and stained with fluorescently-labelled phalloidin to label actin structures. Drug-treated cells continued to form actin structures in all cell lines, but not stress fibres and not the prominent actin bundles of the MKS patient cells (indicated by yellow arrowheads). Scale bar represents 40 μm.

induce more filament nucleation (*de novo* or from existing filaments, respectively). However, greater F-actin levels are likely reflective of the presence of these prominent actin bundles. The demonstrably increased G-actin levels in *MKS2* patient fibroblasts may be due to concomitant disassembly of a proportion of these prominent bundles as they are being built, and decreased G-actin levels in *MKS3* patient fibroblasts may be indicative of increased monomer incorporation into filaments.

Establishing why and how these prominent actin bundles are inappropriately built is an important avenue of investigation as it may provide clues to the roles of MKS proteins in cells, and thus the molecular aetiology of Meckel-Gruber Syndrome and of the other ciliopathies.

Actin defects associated with the *MKS2* and *MKS3* loci

Actin has not been thoroughly investigated in cells with mutations at the *MKS2* and *-3* loci. Only one study has examined the effects of *MKS2* mutations on the actin cytoskeleton (Valente *et al.*, 2010) and, only 2 prior studies have examined the effects of *MKS3* mutations (Adams *et al.*, 2011; Dawe *et al.*, 2009). Two of these previous studies (Dawe *et al.*, 2009; Valente *et al.*, 2010) used patient cell lines with the same mutations as those of the current project and these reported the same prominent actin bundles. The other of these studies used an *MKS3* siRNA knockdown in IMCD3 cells and demonstrated loss of basal and basolateral actin when compared with scrambled siRNA-treated cells (Adams *et al.*, 2011), strongly implicating these proteins in an actin organisational or regulatory function.

Meckelin, the *MKS3* protein product interacts with actin-binding isoforms of nuclear envelope protein nesprin-2 (Dawe *et al.*, 2009), and with actin cross-linking protein filamin A (Adams *et al.*, 2011). The latter of these interactions appears, in addition to preventing aberrant actin structures from forming, to maintain normal RhoA activity (Adams *et al.*, 2011). Furthermore, hyperactivation of RhoA and Dishevelled, non-canonical/PCP Wnt signalling pathway components has been demonstrated in the current *MKS2* and *MKS3* patient cells, in *Tmem216* siRNA-knockdown IMCD3 cells, and in HEK293 cells transfected with meckelin deletion constructs (Adams *et al.*, 2011; Dawe *et al.*, 2009; Valente *et al.*, 2010).

RhoA signalling is established to effect stress fibre formation (Bishop and Hall, 2000; Ridley, 2006) and filamin A is an actin cross-linking protein that is used during migration (Janmey *et al.*, 1990), and the prominent actin bundles could feasibly be stress fibres or cross-linked bundles. Furthermore, an aberrant interaction of nesprin-2 with actin filaments and with the nuclear envelope may be affecting the actin structures formed in these cells. It is also of note that Rho-generated stress fibres (Cowan and Hyman, 2007), filamin A cross-linked F-actin (Li *et al.*, 1999) and the nuclear positioning effected by nesprin-2 (Chang *et al.*, 2015) are all structures that influence cell migration, a process which has been revealed in unpublished work by our group to be disrupted in these patient cells (Barker and Dawe, unpublished). Together these data imply that Dvl/RhoA signalling and/or actin-binding proteins may be responsible for the prominent actin bundles generated in these cells.

Actin defects in other ciliopathies

Emerging evidence has reported mutations to a number of “ciliary” genes resulting in actin defects. Aberrant actin organisation (Gakovic *et al.*, 2011; Hernandez-Hernandez *et al.*, 2013; Ravanelli and Klingensmith, 2011; Werner *et al.*, 2013; Yin *et al.*, 2009), dynamics (Cao *et al.*, 2012; Kim *et al.*, 2010) or actin-related functions, particularly in cell migration [such as cell spreading, cell shape (Pitaval *et al.*, 2010), or membrane retraction (Gilden *et al.*, 2012)] all appear as common features of ciliopathy mutants. However, beyond the aforementioned *MKS2* and *MKS3* associations, the actin cytoskeleton has not been widely investigated in MKS.

A number of ciliary proteins, such as Bbs proteins, localise to filamentous actin – for instance, in the actin-based stereocilia of hair cells (May-Simera *et al.*, 2015) – and to actin-rich focal adhesions where they modulate the actin cytoskeleton (Hernandez-Hernandez *et al.*, 2013), which may be indicative of a cilium-independent, actin regulatory role of other ciliary proteins, including the MKS proteins.

A hypothetical influence of the ciliopathy genes in actin remodelling is supported by evidence that *TRIM32*, a gene encoding an E3 ubiquitin ligase involved in the ubiquitination of actin, is also a BBS gene, revealing

proteasomal degradation of actin as a key feature of this ciliopathy (Chiang *et al.*, 2006).

Furthermore, when BBS genes *Bbs4, Bbs6,* and *Bbs8* are disrupted, abnormal stress fibre aggregates form (Hernandez-Hernandez *et al.*, 2013). These structures are not like the prominent bundles that I observe in regard to their length, but also have measurably increased thickness. However, like those seen in the Dawe (2009), Valente (2010) and Adams (2011) studies, these also appear to be Rho pathway-dependent; in the absence of Bbs proteins, RhoA-GTP levels were highly upregulated, but subsequent RhoA inhibitor treatment rescued BBS-associated phenotypes, such as cilia length and number, and actin cytoskeleton integrity. These findings imply that the Bbs proteins regulate ciliary length and the actin cytoskeleton through alteration of RhoA signalling (Hernandez-Hernandez *et al.*, 2013). Importantly, this study also indicates that drug treatment can reverse a number of cellular features of BBS, supporting the possibility of associated therapeutic development. Furthermore, the potential of reversal of cellular phenotypes with such drugs stimulated the subsequent chapter investigating the Rho-dependency of these actin defects.

Inversin, the ciliary protein integral to nephronophthisis, has also been associated with the actin cytoskeleton – *inv*$^{-/-}$ MEFs demonstrate compromised migration, cytoskeletal rearrangements (such as distorted lamellipodia and extensive filopodia formation) (Veland *et al.*, 2013; Werner *et al.*, 2013). Notably, however, these altered lamellipodia and supernumerary filopodia are not like the actin structures observed in the current MKS patient cells. Nonetheless, inversin-null MEFs also demonstrate elevated canonical Wnt signalling – like the mouse model of MKS3 (Abdelhamed *et al.*, 2013) – and dramatically altered activity and localisation of non-canonical/PCP Wnt signalling pathway components (Veland *et al.*, 2013; Werner *et al.*, 2013), like the MKS patient cells (Dawe *et al.*, 2009; Valente *et al.*, 2010). This indicates that the ciliopathies could still be affecting similar pathways, and further supporting a link between ciliary components and RhoA activity or regulation.

Molecular mechanisms behind aberrant actin phenotypes

To commence investigation into a molecular explanation for the actin phenotype, I revealed that the prominent actin bundles occurred post-

transcriptionally, and from existing filaments. These features remain unreported in prior research into the aberrant actin structures observed in other ciliopathies.

The implication of the current data, in addition to the above discussed similarities with the other ciliopathies, was that the aetiology of the MKS actin defects may be within a branch of the Wnt signalling pathways.

Canonical Wnt signalling affects transcription, as opposed to having a direct effect on actin and, given the short time frame of defect generation, this was unlikely to be the cause. Contrastingly, the non-canonical Wnt/PCP pathway signals, in part, via the Rho GTPases - including Rho, Rac and Cdc42 - to effect changes to the actin cytoskeleton and control cell polarity. Loss of components of this pathway are known to lead to cystogenesis (Cao *et al.*, 2010; Werner *et al.*, 2013), either through defective proliferation or polarisation, making such signalling in the ciliopathies of interest.

Various branches of the Wnt/PCP pathway are involved in actin cytoskeletal organisation and developmental phenotypes (renal cyst formation, and convergent extension and neural crest migration defects). Furthermore, a number of components of Wnt/PCP signalling pathways have been commonly associated with the other ciliopathies [particularly BBS (Gerdes *et al.*, 2007; Hernandez-Hernandez *et al.*, 2013; Ross *et al.*, 2005) and NPHP (Simons *et al.*, 2005; Veland *et al.*, 2013)], meaning that investigation into a subset of these pathways were an obvious topic of investigation.

RhoA appears to be upregulated in the current MKS patient cells (Dawe *et al.*, 2009; Valente *et al.*, 2010), so I next aimed to manipulate the Rho GTPases in these cells to examine their role in generating the prominent actin bundles. Chapter IV therefore addresses the hypothesis that abnormal ROCK pathway activity is responsible for actin structures observed in MKS patient cells.

CHAPTER IV: Cellular phenotypes in MKS patient cells are ROCK-dependent

4.1 Introduction

Investigation into the influence of signalling pathways in ciliopathies has accrued variable amounts of evidence, dependent on the signalling pathway in question. Research into Hedgehog (Hh) signalling in vertebrate cells supports a definite role of ciliogenesis upstream of Hh pathway defects – if a cilium is not correctly built, Hh signalling cannot occur within it (Corbit *et al.*, 2005; Eggenschwiler and Anderson, 2007; Huangfu *et al*., 2003). Investigation into the multiple branches of Wnt signalling in relation to cilia, however, is far more confusing and often appears contradictory. This investigation is an important topic of research; understanding the molecular aetiology of the ciliopathies – such as the signalling pathways which appear to be acting upstream of developmental defects – would not only allow us to deduce other possible downstream effects of these diseases, but would enable us to devise appropriate therapeutic targets.

Wnt signalling is not reportedly transduced through the cilium (Huang and Schier, 2009; Leightner *et al*., 2013), but loss or dysfunction of proteins involved in cilia or ciliogenesis often have downstream consequences reminiscent, particularly, defects in the Wnt/PCP signalling pathway. Equally, alterations to Wnt signalling often mimic cellular features associated with ciliopathies (Cui *et al*., 2013; Hernandez-Hernandez *et al*., 2013; Park *et al*., 2006; Veland *et al*., 2013). For example, mice deficient in Wdpcp, a transition zone protein, exhibit cellular defects such as an altered actin cytoskeleton, including decreased membrane ruffling. Furthermore, these mutant mice demonstrate concomitant developmental defects, including aberrant convergent extension cell movement, and cardiac outflow tract and cochlea defects. These are phenotypes typically associated with Wnt/PCP perturbation and, in fact, these mice also display differences in canonical and Wnt/PCP pathway components at an mRNA level (Cui *et al*., 2013).

Through the Rho GTPases, Wnt/PCP signalling is well-established as a modulator of actin dynamics (Etienne-Manneville and Hall, 2002), but evidence is increasingly finding Rho pathway activation upstream of aberrant actin

structure formation in the ciliopathies. The integrity of the actin cytoskeleton and ciliary length are both defective in *Bbs4*-deficient cells, which could be rescued by Rho inhibitor treatment (Hernandez-Hernandez *et al*., 2013), suggesting Rho-dependency of these phenotypes.

RhoA is reportedly upregulated in the current MKS patient cells (Dawe *et al*., 2009; Valente *et al*., 2010), and transition zone proteins are known to form multi-protein complexes; it is therefore possible that TMEM216 and meckelin also participate, directly or as part of a complex, in a similar, modulatory role within this pathway.

I therefore aimed to determine whether aberrant Rho/Rho kinase (ROCK) signalling influences the abnormal cellular phenotypes observed in MKS patient cells. To this end, I investigated the involvement of the ROCK/myosin II pathway in forming prominent actin bundles of *MKS2* and *MKS3* patient cells, and in other atypical structures – such as dispersed Golgi – that I revealed in these cells in the present chapter. These data indicate that ROCK is likely to act upstream of a number of cellular defects reported in *MKS2* and *MKS3* patient cells.

4.2 Results

Rho kinase/myosin II signalling is required for actin abnormalities in MKS patient cells

To test whether the prominent actin bundles observed in *MKS2* patient fibroblasts are generated in a Rho signalling pathway-dependent manner, I plated MKS patient cells for 20 minutes, i.e. just prior to prominent actin bundle formation (Chapter III), then treated them with no drug (untreated control; *Figure 4.1A*), or inhibitors of Rho (2.5 µg/µL; *Figure 4.1B*), Rho-kinase (ROCK) (5 µM for both; *Figure 4.1C* and *D*) or myosin II (50 µM; *Figure 4.1E*) for 40 minutes, then visualised actin using fluorescently-labelled phalloidin to determine the effect of these drugs on actin organisation (n=3 experiments). Drug concentrations were selected as detailed in Chapter II. Two different ROCK inhibitors – both with equal ROCK1 and ROCK2 affinity – were used to enhance the validity of these results.

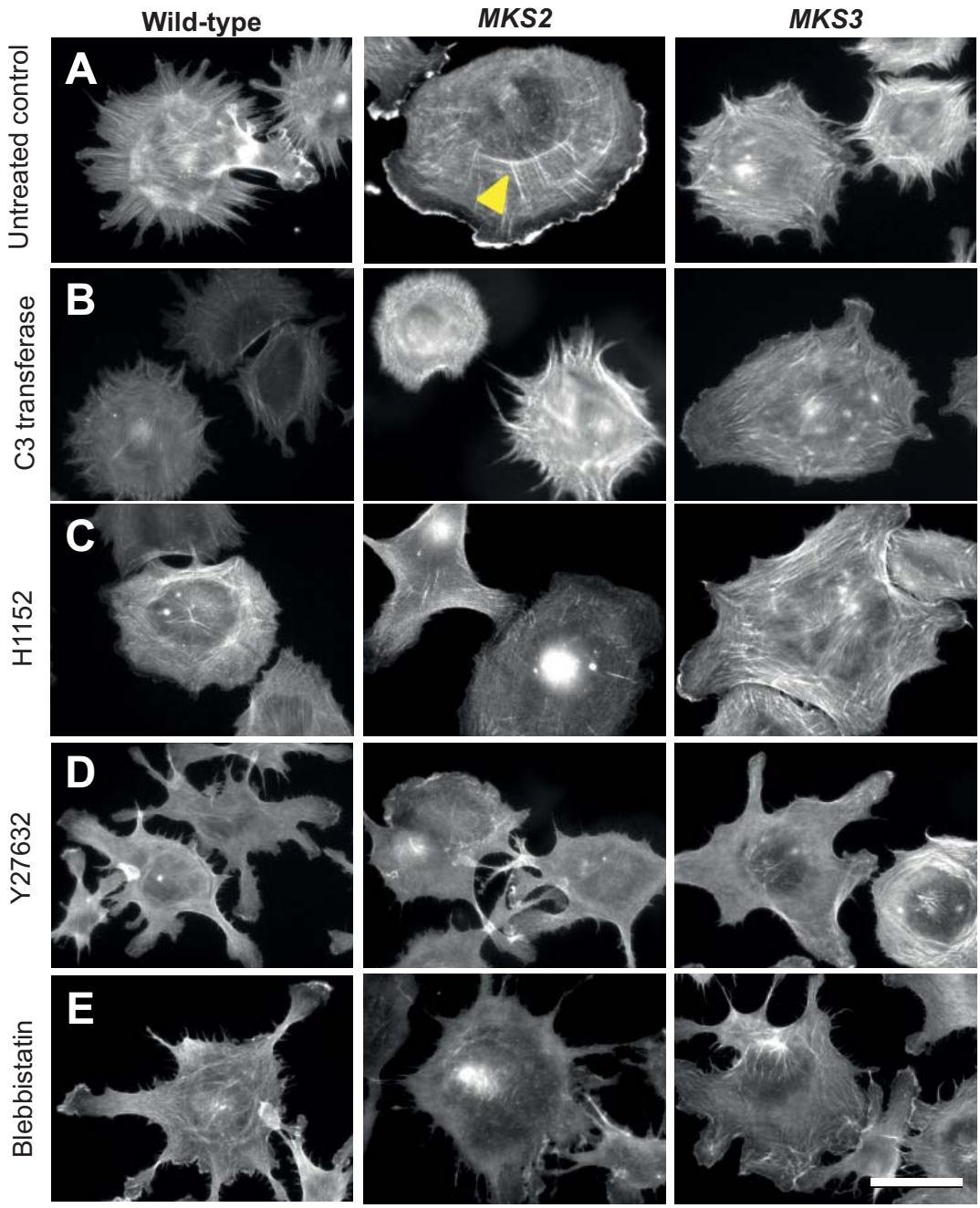

FIGURE 4.1: Prominent bundles do not form in *MKS2* patient cells following acute treatment with ROCK-pathway inhibitors.

Fibroblasts were plated for 20 minutes, drug-treated with compounds to inhibit Rho (B), Rho-kinase (C, D), or myosin II (E) for 40 minutes, then fixed with fluorescently-labelled phalloidin to reveal F-actin organisation. Prominent bundles in *MKS2* patient cells (yellow arrowheads) in control conditions (A) disassemble upon Rho pathway inhibitor treatment (B-E). Scale bar = 20 μm.

I revealed that treatment with any of these Rho/ROCK/myosin pathway inhibitors prevented the prominent bundle formation typically observed in *MKS2* patient cells; *Figure 4.1A* illustrates the prominent bundles normally present in *MKS2* patient cells, but not the other cell lines (*yellow arrow*). However, *Figure 4.1B-E* demonstrates that neither prominent bundles nor notable cell body actin structures are apparent in any cell line following drug treatment. Fibroblasts in all lines do, however, adopt an altered morphology following Rho pathway inhibitor treatment: there are more actin-based extensions with no obvious polarity. Generation of prominent actin bundles is therefore likely to be ROCK/myosin II pathway-dependent. However, the marked response of these cells to experimental perturbation of the Rho signalling pathway indicates that this aberrant actin organisation is not caused by insensitivity to Rho activation and a subsequent failure to generate negative feedback in these cells.

To determine whether the prominent actin bundles in *MKS3* patient cells are also Rho pathway-dependent, I plated control and *MKS3* patient cells for 3 days. This time period was selected as this was a day prior to prominent bundle formation in these cells, as demonstrated in Chapter III. I then either changed the medium (untreated control; *Figure 4.2A*) or drug-treated the cells for 1 day with inhibitors of Rho (1 µg/µL, *Figure 4.2B*), ROCK (5 µM, *Figure 4.2C, D*) or myosin II (10 µM, *Figure 4.2E*), then visualised the filamentous actin cytoskeleton with fluorescently-labelled phalloidin (n=3 experiments).

Prominent bundles did not form in *MKS3* patient cells upon prolonged treatment (*Figure 4.2B-E*), as they did in untreated *MKS3* cells (*Figure 4.2A*). These data suggest that actin defect generation, and possibly persistence, may be associated with the Rho pathway hyperactivity demonstrated in these cells (Dawe *et al.*, 2009; Valente *et al.*, 2010).

To establish whether the prominent bundles observed in MKS patient cells could be mimicked in control cells, the control cells were transfected with a RhoA GFP-tagged construct which was either normal or had a mutation (Q63L) to induce constitutive activation. Cells were fixed after 4 days, reflective of time taken for prominent bundles to develop in *MKS3* patient cells, and actin was visualised at this time point. Constitutive activation of Rho induced control cells to display thicker prominent actin bundles (n=3 experiments; *Figure 4.3*). Prominent bundles following constitutive Rho activation had a mean thickness of 9.75 pixels; compared with the normal 5.767 pixel-thick bundles, these were

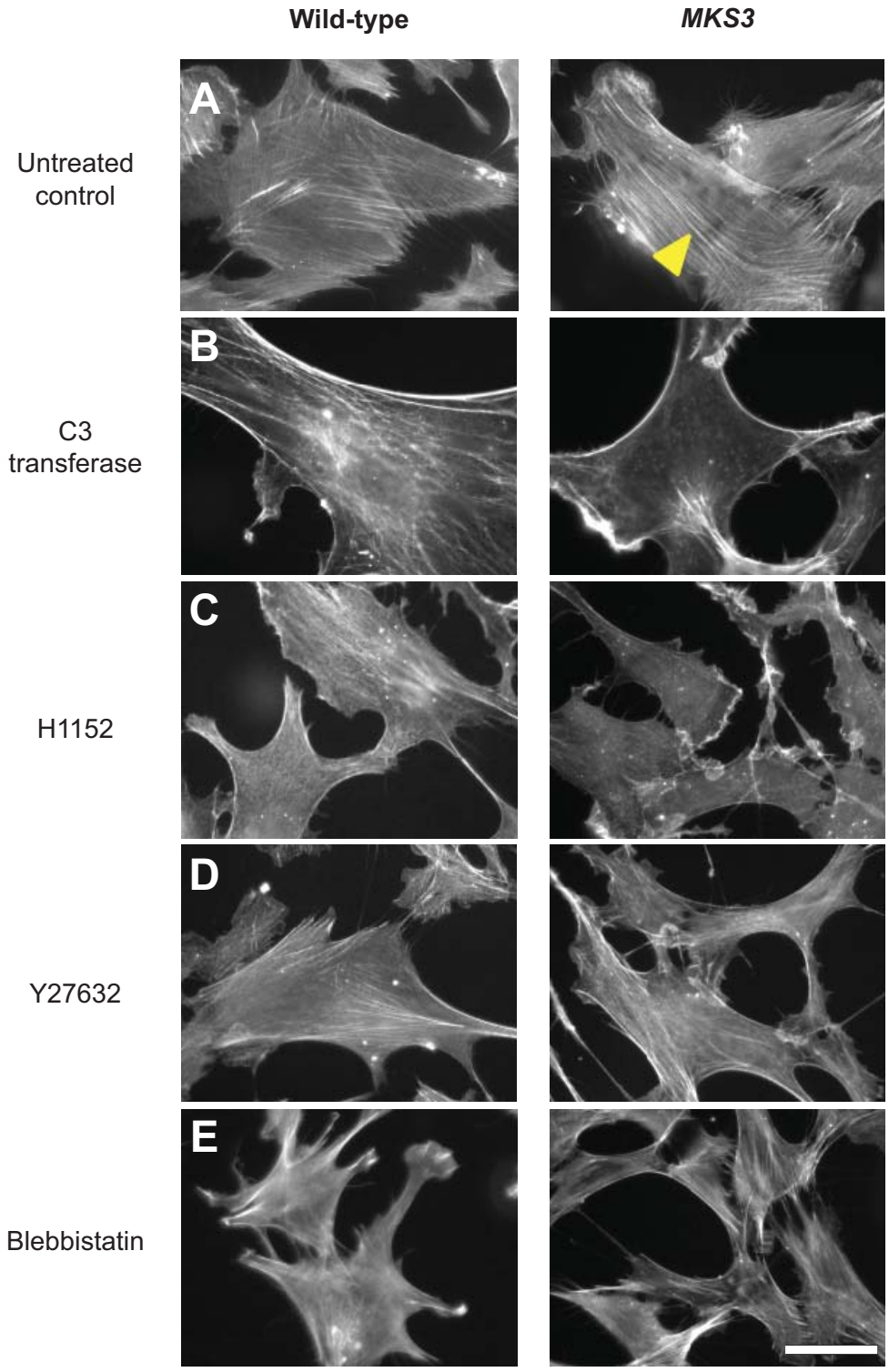

FIGURE 4.2: Prominent bundles do not form following prolonged treatment with ROCK-pathway inhibitors.

Fibroblasts were plated for 1 day, drug-treated with compounds to inhibit Rho (B), Rho-kinase (C, D), or myosin II (E) for 3 days, then fixed with fluorescently-labelled phalloidin to reveal F-actin organisation. Prominent bundles in *MKS3* patient cells (yellow arrowhead) under control conditions (A) disassemble upon Rho pathway inhibitor treatment. Rho inhibition (B) led to an increase in cortical actin in wild-type and *MKS3* cells. Scale bar represents 20 μm.

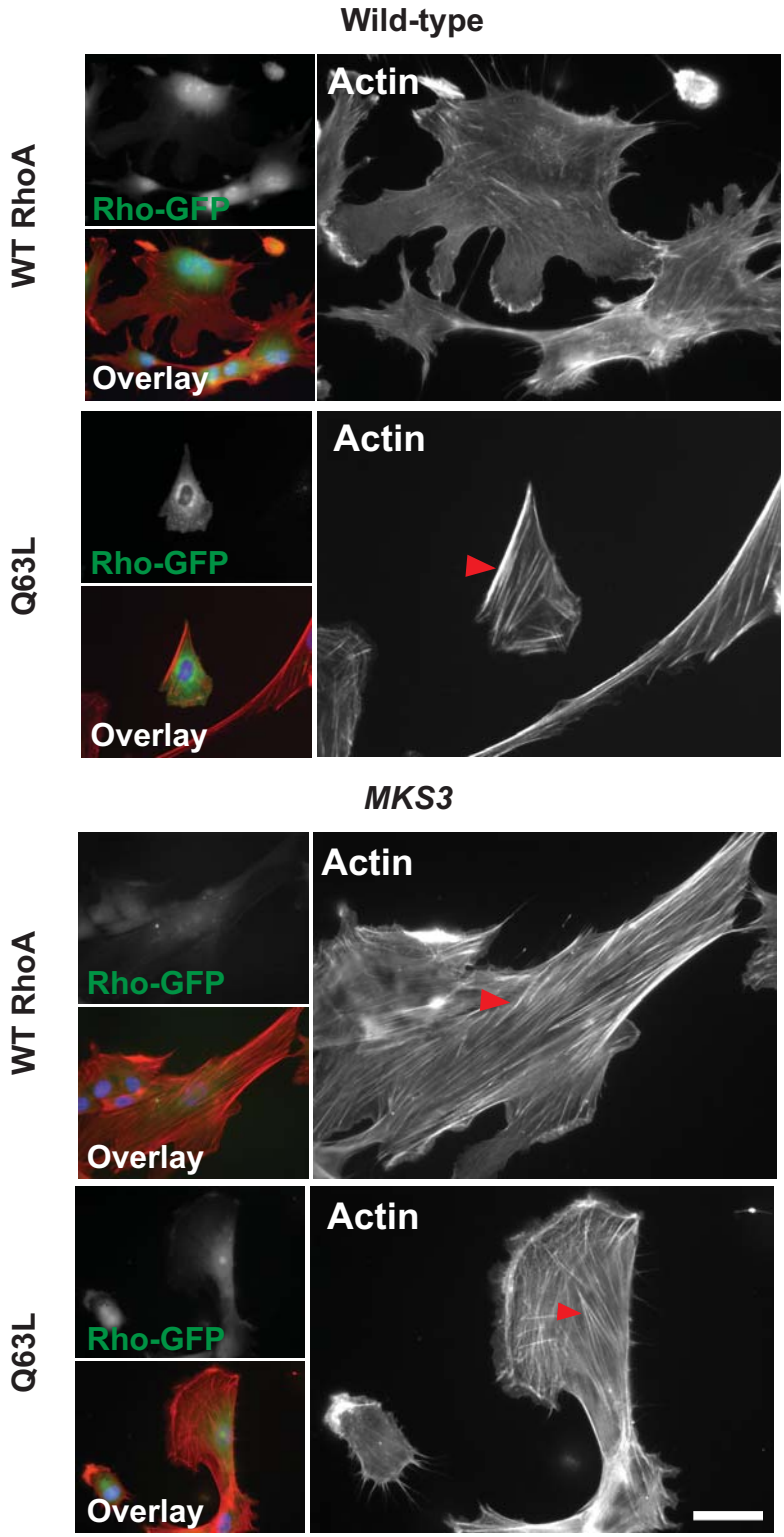

FIGURE 4.3: Transfection with constitutively-active Rho leads to thicker actin bundles in wild-type fibroblasts, but not *MKS3* patient fibroblasts.
Fibroblasts were electroporated with a GFP-tagged RhoA construct or constitutively active RhoA construct (Q63L) and, after 4 days, fixed and stained with fluorescently-labelled phalloidin. Q63L RhoA caused wild-type cells to present more prominent bundles, but had no effect on *MKS3* patient cells. In overlay images, red corresponds to actin, green to Rho-GFP and blue to DAPI (nucleus). Scale bar represents 40 μm.

significantly thicker (n=20 bundles measured from each; χ^2 test; $p<0.01$); however, Q63L RhoA transfection caused no significant alteration to *MKS3* actin bundle thickness, in which 6.129 pixel-thick bundles became 7.6 pixel-thick bundles (n=20 bundles; χ^2 test; $p>0.05$). *MKS2* patient cells did not typically survive this transfection, so equivalent results are not shown. This result supports a hypothesis that the actin defects are caused by hyperactivation of the RhoA pathway, and suggests that MKS patient cells demonstrate relatively uncontrolled RhoA activity.

To ascertain whether RhoA signalling could be inactivated in MKS patient cells, and whether this would ameliorate the actin phenotype, I transfected control and MKS patient cells with a dominant negative RhoA construct (T19N) in order to inactivate RhoA, then examined actin in after 4 days (n=3 experiments).

RhoA inactivation prevented all but small intracellular actin bundles from developing in MKS patient cells, and prevented the cell spreading observed in untreated cells (*Figure 4.4*). This implies that the prominent actin bundles and the cell spreading of MKS patient cells develop due to RhoA activation.

To determine whether the actin defects observed were also associated with ROCK activation downstream of this, as opposed to through other signalling pathways, cells were transfected with a constitutively active Rho-kinase [ROCKΔ3 - a plasmid with a C-terminal truncation, but containing the kinase domain and coiled-coil region (Ishizaki *et al*., 1997)], and actin was visualised.

ROCKΔ3 transfection significantly increased the thickness of actin bundles in control cells from 5.767 pixels to 11.84 pixels (χ^2 test; $p<0.01$), but had no effect in *MKS2* (11.25 pixels to 9.63 pixels; χ^2 test; $p>0.05$) or *MKS3* patient cells (6.129 pixels to 9.25 pixels; χ^2 test; $p>0.05$) (n=20 bundles examined from each cell line; *Figure 4.5*). ROCKΔ3 had no statistically significant effect (χ^2 test; $p>0.05$) on the proportion of cells displaying prominent bundles in control or MKS patient cell populations (n=3 experiments). This supports a conclusion that Rho/ROCK dysregulation in MKS patient cells is responsible for the formation and/or maintenance of the prominent actin bundles observed.

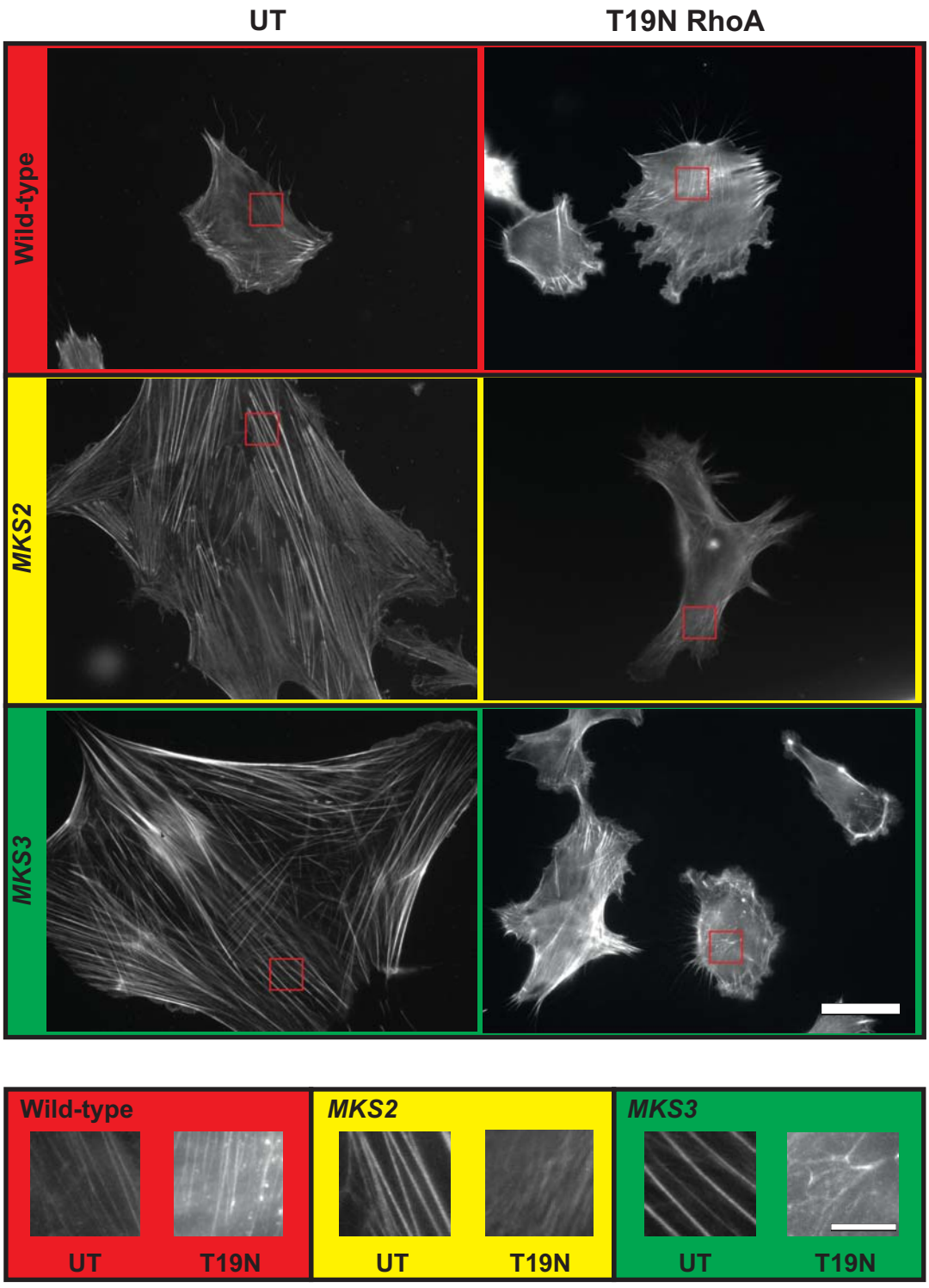

FIGURE 4.4: Transfection with dominant-negative Rho abolishes prominent bundle formation in MKS patient cells.

Fibroblasts were electroporated with a GFP-tagged dominant negative RhoA construct (T19N) or plated without treatment (UT), and fixed and stained with fluorescently-labelled phalloidin after 4 days. T19N RhoA prevented development of the prominent bundles of untreated MKS cells, and ameliorated the cell spreading typically observed in these cells. Scale bar represents 40 μm on the large images, and 10 μm on the small images.

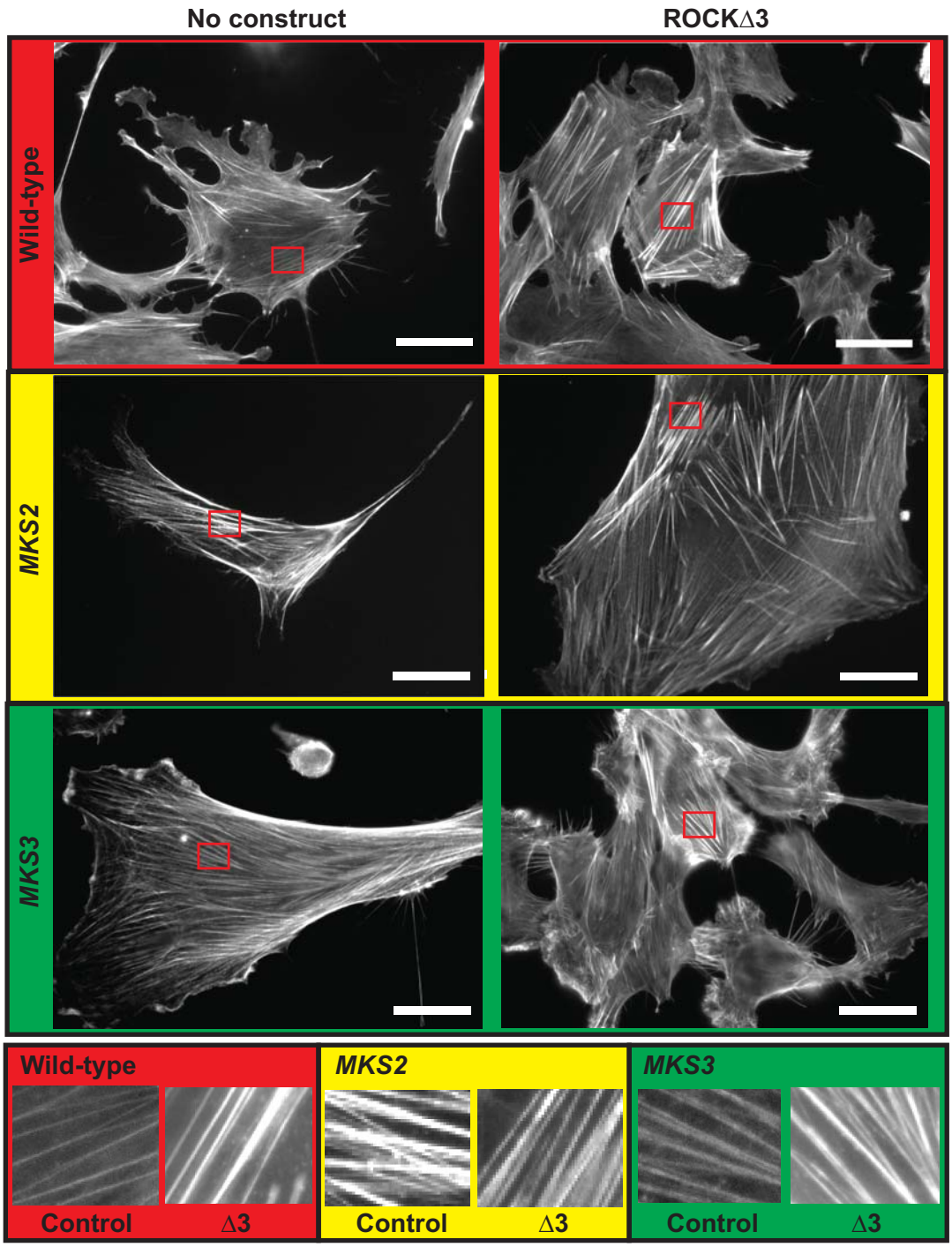

Average % cells showing prominent actin bundles

40%	35% n.s.	49%	38% n.s.	29%	16% n.s.

FIGURE 4.5: ROCKΔ3 transfection increases the prominence of actin bundles in wild-type cells, but not MKS patient cells.

Fibroblasts were electroporated with ROCKΔ3 construct or no construct, plated for 4 days, fixed and stained for actin with fluorescently-labelled phalloidin. Bundle thickness (upper panels), increased in control populations but not in MKS patient cell lines, but percentage of cells demonstrating prominent actin bundles did not change (table). Lower panels show magnified actin bundles. Scale bars represent 40 μm.

ROCK and myosin behaviour are altered in MKS patient cells

To test whether the localisation of ROCK or myosin was also affected in MKS patient cells, I plated these and control cells for 4 days. Immunofluorescence was then used to examine localisation of these proteins (n=3 experiments). ROCK localisation was perinuclear/ nuclear across all cell lines (*Figure 4.6*). Myosin localisation was not observably altered in *MKS3* patient fibroblasts, but displayed fibrillar patterning in *MKS2* patient cells, presumably along the prominent actin bundles (*Figure 4.6A*).

To resolve whether the prominent bundles were decorated with active myosin, indicative of contractility, phosphomyosin was also visualised in these cell lines 4 days after plating. Actin and phosophomyosin frequently co-localised (*Figure 4.6B*), suggesting that these prominent bundles are likely to be contractile actin structures [such as stress fibres or graded polarity bundles (Cramer *et al*., 1997)], which would also support ROCK-dependency of their development.

As RhoA is known to be hyperactivated in MKS patient cells (Adams *et al*., 2011; Dawe *et al*., 2009; Valente *et al*., 2010), and I postulate that the actin defects are Rho/ROCK pathway-dependent, I examined ROCK-1 and myosin levels in whole cell lysates of control and *MKS3* patient cells via Western blot (n=3 experiments).

As a semi-quantitative method, levels of these proteins could not be very accurately determined, but myosin levels appeared unaltered in *MKS3* patient cells, but ROCK-1 levels appeared to be increased in *MKS3* patient cells (*Figure 4.7*).

An increase in ROCK levels is likely concomitant with the observed increase in *MKS2* and *MKS3* patient cells of RhoA activity (Dawe *et al*., 2009; Valente *et al*., 2010), which occurs upstream of ROCK, as this pathway is known to modulate actin cytoskeletal changes (Kikuchi *et al*., 2009). It is, thus, probable that *MKS2* and *-3* mutations are causing these actin defects through hyperactivation of the Rho/ROCK signalling pathway.

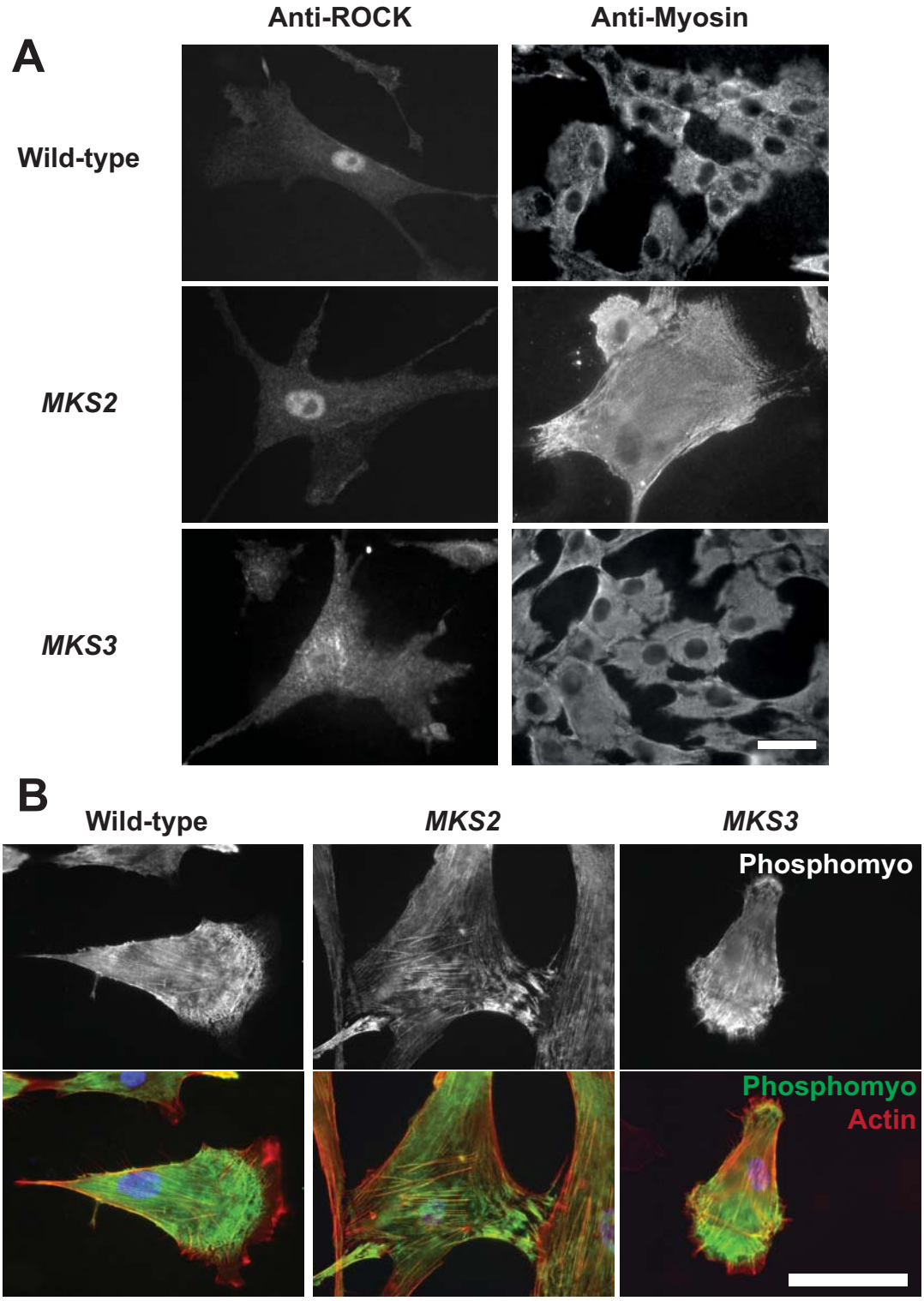

FIGURE 4.6: Myosin localisation differs in *MKS2*, but is unaltered in *MKS3*; ROCK localisation is unaltered in MKS patient fibroblasts; and phosphomyosin localises to MKS2 prominent actin bundles.

Fibroblasts were plated, fixed and stained to visualise myosin, ROCK, actin and phosphomyosin. There were no differences in ROCK localisation in MKS patient cells, but *MKS2* patient cells demonstrate fibrillar patterning of myosin (A). Phosphomyosin staining localises to prominent actin bundles in *MKS2* (B). Scale bar represents 40 μm. *(Phosphomyosin experiment performed and visualised by Amy Barker).*

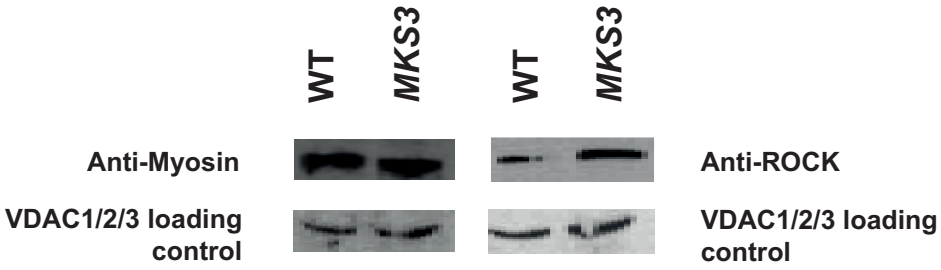

FIGURE 4.7: ROCK-1 levels are increased in *MKS3* patient cells, but myosin levels are not altered.

Western blotting indicated that more ROCK-1 may be expressed in *MKS3* patient fibroblasts, but there was no difference in myosin levels between control and *MKS3* patient cells.

Actin defects are accompanied by modified actin binding protein transcription and Golgi defects

The mechanism by which Rho and ROCK amplify actin bundle formation in MKS cells is unknown, but I posited that this may be linked to alterations to actin-binding protein (ABP) behaviour. Myosin, as such an ABP, may be responsible. Although the level of myosin protein in MKS patient cells appears not to be altered, TMEM216 and meckelin may induce myosin to effect an enhanced function through increased activation; this hypothesis is supported by the phosphomyosin observed associated with MKS prominent actin bundles (*Figure 4.6*).

To determine whether other likely candidate ABP behaviours were modified, such as those involved in actin bundling function or lamellipodial ruffling, I examined 55 ABPs at the transcript level. These ABPs were selected based on their involvement in stress fibre and lamellipodium formation, and levels of these were evaluated, alongside the positive and negative controls GAPDH, and RNase-free water in place of reverse transcriptase, respectively. These ABP RNA transcript levels were examined in control and MKS patient cells using RT-PCR with primers specific to these ABPs. These RT-PCR reactions were repeated 3 times, and agarose gels reported in *Figure 4.8* represent typical results.

Amongst all of the ABPs investigated, profilin 3 and coronin 7 were the only proteins to be altered at a transcript level (red and yellow stars respectively, *Figure 4.8*). Both were downregulated in MKS patient cells, and profilin 3 was predominantly found as an isoform with a higher molecular weight in *MKS3* cells (*Figure 4.8*). Profilin 3 is a relatively unknown protein, but is proposed to interact with mDia3 and phosphoinositides (Behnen *et al*., 2009). It is hypothesised that profilin 3 is principally expressed in the kidney and testis, which is functionally relevant to the present study. However, in polycystic kidney disease cases, this transcript is found to be elevated, contrasting with our results (Hu *et al*., 2001). As very little is known about this protein, and as no siRNA or antibodies are available which are specific to this transcript/protein, this result was not pursued any further.

Coronin 7 is a protein known to function in maintenance of Golgi morphology and membrane trafficking (Rybakin *et al*., 2006; Rybakin *et al*.,

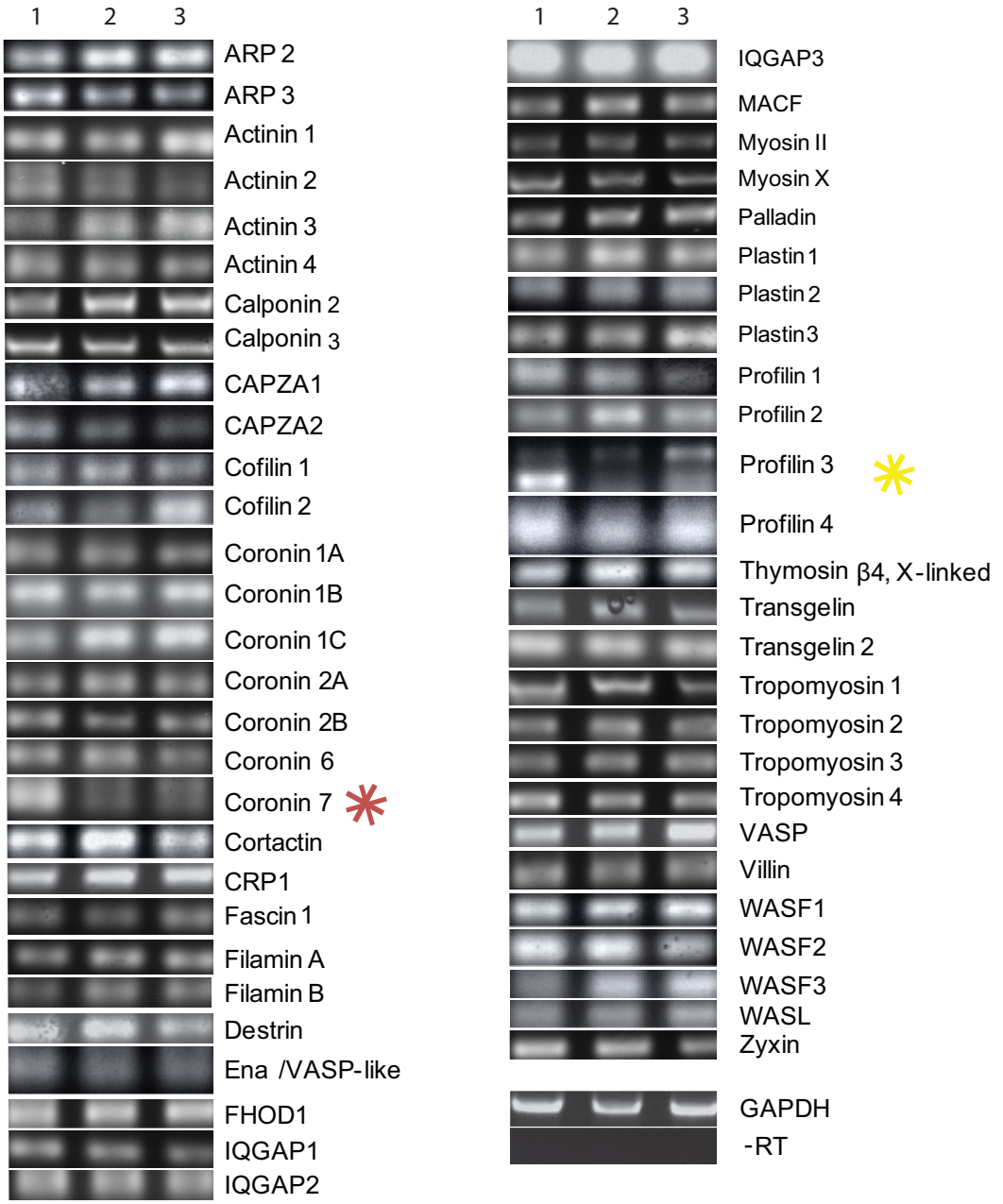

FIGURE 4.8: Coronin 7 and profilin 3 transcript are altered in MKS patient fibroblasts.

RT-PCR was performed using RNA from each cell line and primers specific to a number of actin-binding proteins. Gels pictured are representative of 3 repeats. Note that coronin 7 transcript (red asterisk) and profilin 3 transcript (yellow asterisk) are different in patient cells compared with wild-type cells. GAPDH acts as a loading control, and the '-RT' represents the negative control of GAPDH containing no reverse transcriptase during reverse transcription. Cell lines are wild-type (1), *MKS2* (2) and *MKS3* (3).

2004), and in protecting actin filaments from depolymerisation (Shina *et al*., 2010). For these reasons, I next inspected Golgi morphology and localisation in MKS patient cells using anti-GM130 to visualise the cis-Golgi and anti-γ-tubulin to visualise the centrosome (n=3 experiments).

An hour after plating, the Golgi was perinuclear in control and *MKS3* patient cells, but dispersed in *MKS2* patient cells, although the Golgi was still partially associated with the centrosome in these cells (*Figure 4.9*). This dispersal was then mimicked at 4 days in *MKS3* patient cells, but not in control cells (*Figure 4.9*). As these results are concordant with the vesicular trafficking defects observed in other ciliopathy models [such as BBS (Blacque *et al*., 2004; Nachury *et al*., 2007)], this indicates that ciliary proteins may be involved in other subcellular structures besides the cytoskeleton, or that Golgi defects may occur downstream of cytoskeletal or ciliary defects.

In order to elucidate the role of ROCK in Golgi dispersal – or, indeed, whether it has any responsibility for this phenotype – I examined Golgi dispersal, using anti-GM130 to highlight cis-Golgi and anti-γ-tubulin to highlight the centrosome, in MKS patient cells upon transfection with ROCKΔ3 (n=3 experiments).

Following constitutive ROCK activation, the proportion of cells demonstrating dispersed Golgi (white arrowheads, *Figure 4.10*) significantly increased in wild-type cells (χ^2 test; $p<0.001$), but not in MKS patient cells (χ^2 test; $p>0.05$ in both cell lines). This provides additional evidence of ROCK dysregulation in these cells although, notably, fewer *MKS3* patient cells revealed Golgi dispersal (table, *Figure 4.10*). These data indicate that ROCK activation may not be at its maximum in these cells, but may be less regulated than in control fibroblasts.

4.3 Discussion

In the current series of experiments, I evaluated the involvement of Rho and its downstream effectors in the development of prominent actin bundles in MKS patient cells. I revealed that these actin bundles are likely generated, and possibly maintained, by dysregulation of Rho kinase signalling. I also observed morphological modifications to the Golgi apparatus in these cells, which may also be associated with inappropriate ROCK pathway activation.

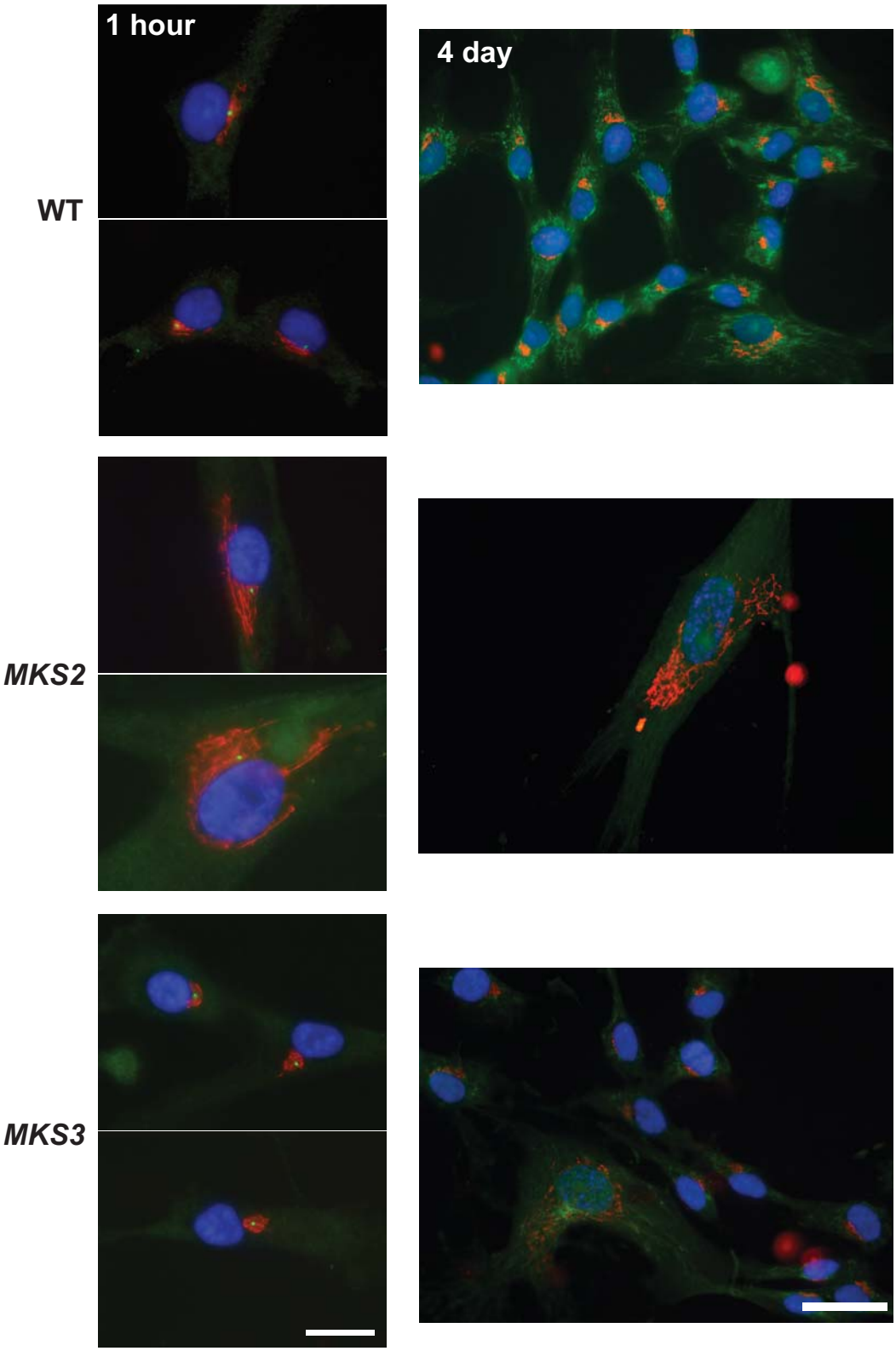

FIGURE 4.9: Golgi organisation is altered in *MKS2* patient fibroblasts within an hour after plating.

Immunofluorescence using anti-GM130 (red) to visualise cis-Golgi, and γ-tubulin to visualise the centrosome (1 hour, green) or fluorescently-labelled DNase 1 (4 day, green), fixed an hour or 4 days after plating. *MKS2* patient cells reveal dispersed Golgi at 1 hour, and *MKS3* patient cells at 4 days. DAPI (blue) was used to indicate the nucleus. Scale bar represents 20 μm (1 hour) or 40 μm (4 day).

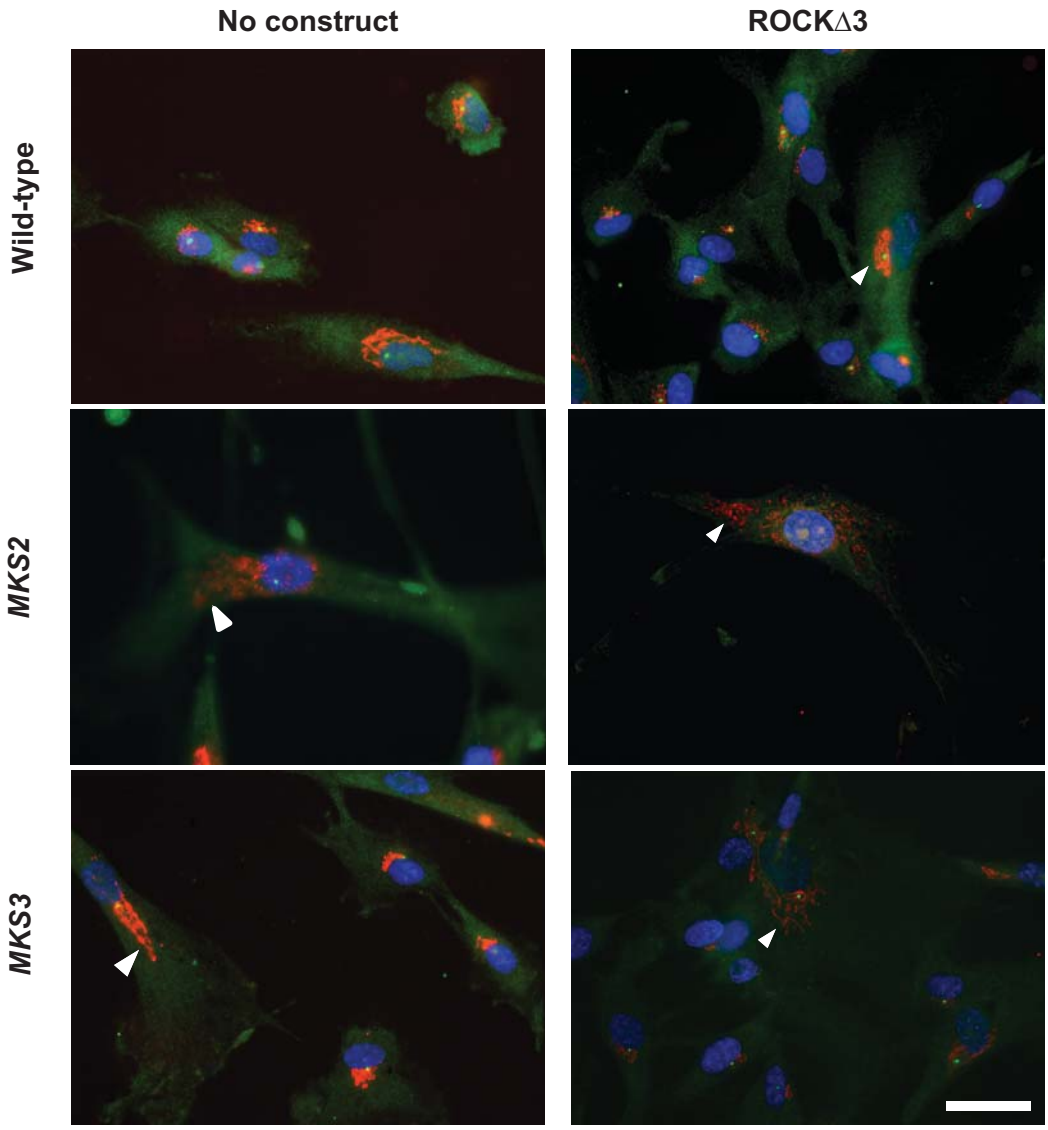

% cells showing dispersed Golgi

	Control	Δ3
Wild-type	4%	30%
MKS2	44%	47%
MKS3	13%	9%

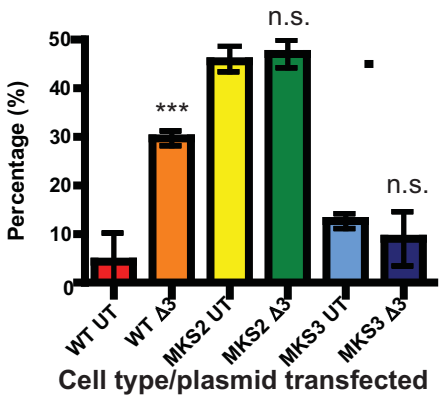

FIGURE 4.10: ROCKΔ3 transfection causes Golgi to disperse in more wild-type cells, but does not affect Golgi dispersal in MKS patient cells.
Fibroblasts were electroporated with ROCKΔ3 construct or no construct, plated for 4 days, fixed and cis-Golgi (red - anti-GM130), centrosomes (green - γ tubulin) and nuclei (DAPI - blue) were visualised. The number of cells demonstrating dispersed Golgi (white arrowheads) increased in control populations but not in MKS patient cell lines (table, graph - mean ±SD). ***P<0.001; N.S., not significant, P>0.05. Scale bars represent 40 μm.

This was the first research to reveal alterations to coronin 7 transcription, and to the Golgi apparatus in this disease (although, unfortunately, antibodies are not available against coronin 7, so protein localisation and levels could not be determined). This was also amongst the first evidence of Rho/ROCK signalling prompting cellular defects in cells with alterations to MKS proteins, as opposed to these occurring as a consequence of cilium loss. These results are important as they indicate that the MKS proteins may directly or indirectly interact with the Rho signalling pathway, and this may happen upstream of the failure to build a cilium. These data provide valuable clues as to the function of these, and possibly other ciliopathy proteins.

How does Rho signalling trigger ciliopathies?

My results have illustrated a model in which hyperactive Rho induces prominent actin bundle formation over 40 minutes and, simultaneously, the Golgi disperses in *MKS2* patient cells; this is likely before the basal body would dock, or a cilium would be generated in cilium-forming cells. The present results therefore suggest that Rho GTPase-induced cytoskeletal remodelling may preclude effectual vesicular trafficking and, either subsequently or concurrently, basal body migration and docking.

Previous models have posited a system in which Dvl (a generalised Wnt pathway transduction component) and Rho mediate actin network-regulated basal body docking. This is proposed to occur at an appropriate location, established through an existing anteroposterior axis and, subsequently, Dvl and Rho establish ciliary planar polarity. This hypothesis is based on the observation that the direction of ciliary beating is refined following basal body docking and axonemal extension, in a positive feedback loop (Boisvieux-Ulrich *et al.*, 1990; Mitchell *et al.*, 2007).

Initial cell polarity could be set by any number of factors, including PCP effectors (which may include “ciliary” proteins); appointing initial polarity would be followed or accompanied by directional protein trafficking, basal body migration and docking, and axonemal extension and, according to this model, polarity would be subsequently refined and maintained by ciliary signal transduction.

The above evidence suggests that MKS proteins likely function during or prior to basal body docking. It would be most parsimonious to presume that these proteins act early following plating, and thereby exert a number of downstream effects; for instance, by altering the activity of Rho signalling pathways. Rho GTPases are known to affect polarity establishment (Gao *et al*., 2011; Kirjavainen *et al.*, 2015), polarised membrane trafficking (Park *et al*., 2008), basal body docking (Pan *et al*., 2007; Park *et al*., 2008), axonemal extension (Hernandez-Hernandez *et al*., 2013), actin cytoskeleton rearrangements (Etienne-Manneville and Hall, 2002), centrosome amplification and splitting (Chevrier *et al*., 2002; Ling *et al*., 2015), and cell migration (Veland *et al*., 2013), and defects are observed in all of these processes in MKS patient cells, supporting an interaction with Rho signalling.

Furthermore, a number of the ciliopathies have diverse alterations to the actin cytoskeleton, indicating an involvement of Rho GTPase cross-talk; these include distorted lamellipodia and extensive filopodia in (the NPHP-causative) inversin-null mutants (Veland *et al*., 2013; Werner *et al*., 2013) and prominent actin stress fibres in Joubert syndrome (Huang *et al.*, 2011), NPHP (Veland *et al.*, 2013) and BBS (Hernandez-Hernandez *et al.*, 2013). If these defects are, in fact, caused primarily by alterations to Rho signalling, compounds to regulate these pathways could have markedly effective therapeutic potential.

Polarity determination in MKS

It should be noted that multiple signalling pathways converge on Rho/ROCK signalling; these include transforming growth factor (TGF)β (Zhang, 2009) and vascular endothelial growth factor (VEGF; van der Meel *et al.*, 2011). However, there is evidence to suggest that these defects occur in the Wnt/PCP signalling pathway, as discussed in Chapter I and the subsequent sections. The signalling upstream of the Rho/ROCK defects is not investigated in the current thesis, but should be evaluated in future experiments, for instance, by examination of the effects of inhibitors of the candidate upstream pathways upon the cellular defects.

A number of Wnt/PCP pathway components influence cell polarity and directional protein trafficking – processes important to ciliogenesis – and in the effective polarised protrusion and consequential migration required for

convergent extension in vertebrates (Heisenberg *et al*., 2000; Wallingford *et al*., 2000; Wang *et al*., 2006). The present results regarding morphological alterations to the Golgi beg the question of whether directional protein trafficking, a function of cell polarity, has also been perturbed. Is loss of polarity, directional protein trafficking, ROCK pathway dysregulation, or another factor the primary defect? As disruption to PCP results in neural tube closure defects (Jessen *et al*., 2002) comparable those seen in ciliopathies (Badano *et al*., 2006b), this pathway may be a pertinent subsequent avenue of investigation.

We have found defects in polarised migration in MKS patient cells (Barker *et al.*, unpublished data), which is a phenotype also observed in inversin mutants (Veland *et al*., 2013). Inversin is a ciliary protein and the gene product mutated in NPHP2, a form of nephronophthisis; it also functions as a molecular switch between Wnt signalling pathways during renal development in zebrafish and convergent extension movements in gastrulating *Xenopus laevis* embryos (Simons *et al*., 2005).

In establishing cell polarity, a global directional cue is required to orient a field of cells. Wnt is thought to function as such a polarity cue in vertebrates, using a signalling gradient. For instance, in mouse and chick limb bud, Wnt5a gradients are translated into directional information using variable phosphorylation of Vangl2 (a Wnt/PCP pathway component) in a Wnt-receptor complex. The most highly phosphorylated Vangl2, corresponding to highest *Wnt5a* expression, is located at the most distal processes and the least phosphorylated at the proximal processes (Gao *et al*., 2011), causing asymmetric limb outgrowth. Vangl2 is also enriched at the basal body (Ross *et al*., 2005). Wnt11 released from the neural tube, similarly, acts through the Wnt/PCP pathway as a necessary directional cue for myocytes, enabling muscle fibre organisation in the chick embryo (Gros *et al*., 2009).

The mechanistic link between PCP signalling and the cilia is not precisely known, although some components localise to the cilium and are required for ciliogenesis (e.g. Fuzzy localises to cilia in multiciliated cells (Gray *et al.*, 2009)).

Wdpcp, a PCP effector, has recently been demonstrated to be required in ciliogenesis in addition to its role in noncanonical Wnt/PCP signalling; Wdpcp-deficient mice showed actin cytoskeletal defects (namely reduced membrane ruffling), smaller focal adhesions, and the disruption in cell polarity and directed cell migration typically associated with ciliopathies. Wdpcp-deficient cells were

not able to recruit necessary ciliary proteins (such as Mks1 and Sept2) to the transition zone, disrupting ciliogenesis (Cui *et al*., 2013). The authors suggest a separable role of Wdpcp in ciliogenesis and in actin dynamics, but it is more probable that one engenders the other. In light of the present results, I propose that ROCK pathway-induced actin cytoskeletal changes precede ciliogenesis defects.

Protein trafficking in MKS

Wnt/PCP effectors, such as Fuzzy and Inturned, are vital to membrane trafficking; this includes exocytosis in secretory cells (probably during tethering or fusion), trafficking to basal bodies and to the apical tips of cilia (Gray *et al*., 2009), and is key in ciliogenesis. Ciliopathy phenotypes such as polydactyly occur in the absence of these factors, which likely results from the absence of a cilium (and thus dysregulated Hedgehog signalling) and impaired secretion (Gray *et al*., 2009). Relatedly, Cdc42, an effector of Ca^{2+}-dependent non-canonical Wnt signalling, is used for fusion of the exocyst to form a ciliary vesicle at the base of the primary cilium in order to enable ciliogenesis (Zuo *et al*., 2011); perturbation of this process would clearly have detrimental defects on ciliary membrane extension.

I have demonstrated in the current chapter that the structure of the Golgi apparatus is perturbed in MKS patient cells in a similar fashion to constitutively active ROCK-induced Golgi dispersal in control cells. Such an effect on the Golgi is unsurprising as previous evidence indicates that Rho signalling is essential for Golgi biogenesis (Quassollo *et al*., 2015), and Rho signalling is known to be dysregulated in these cells. Furthermore, nesprin-2 interacts with meckelin to mediate actin cytoskeletal changes (Dawe *et al*., 2009), but this nuclear envelope protein is also an essential determinant of Golgi organisation and cell polarisation (Schneider *et al*., 2011); it may be that failure of meckelin to interact with nesprin-2 prompts Golgi dispersal. However, no conclusions may be drawn about Golgi function in these cells from the present results alone.

It is possible that the Rho hyperactivity induced by MKS protein mutations also provokes vesicular trafficking defects; ciliogenesis and Golgi organisation, which both require appropriate protein trafficking, may be perturbed directly by dysregulation of Rho signalling. However, these trafficking defects may,

alternatively, occur through an intermediary action, such as alteration to the organisation or function of the cytoskeleton.

Rho in vesicular trafficking during ciliogenesis

Vesicular trafficking is crucial for ciliogenesis; molecules to be transported into the cilium must first be transported to the basal body, signals transduced through the cilium must be transported via intraflagellar transport and, to initiate ciliogenesis, the basal body associates with membrane-bound vesicles in order to dock at the apical plasma membrane. Association of the basal body with membrane-bound vesicles is dependent on Rho GTPase activation (specifically at the basal body), and is Inturned- and Dvl-mediated (Park *et al*., 2008).

Immune synapses are a focal point of endocytosis and exocytosis, directed by centrosomal docking, and are believed to represent a “frustrated cilium” (de la Roche *et al*., 2013; Griffiths *et al*., 2010). Notably, Dvl regulates distribution of presynaptic markers and function of the immune synapse (Ahmad-Annuar *et al*., 2006), implying that Dvl may have a similar function to facilitate vesicular trafficking to, from and within the cilium, potentially in basal body docking.

Failure of the basal body to dock is an established PCP defect in *Mks*-knockdown and the current patient cells (Adams *et al*., 2011; Dawe *et al*., 2007; Mahuzier *et al*., 2012) and is associated, crucially, with the marked actin cytoskeletal remodelling observed in MKS patient cells (Dawe *et al*., 2009; Pan *et al*., 2007; Valente *et al*., 2010). However, these are not the only examples in which PCP-dependent actin remodelling has been demonstrated as essential for basal body docking during ciliogenesis. For instance, Foxj1 is a vital transcription factor responsible for increasing RhoA activation during ciliogenesis, causing apical actin network development, and thus promoting basal body docking (Pan *et al*., 2007), illustrating the necessity of both PCP signal transduction and actin remodelling during the initial stages of ciliogenesis. This provides support for a hypothesised role of the MKS proteins in Rho signal pathway transduction or regulation.

However, it is necessary to note that cell shape affects actin network contractility and resultant basal body positioning and ciliogenesis. When compared with cells with a greater area (as these patient cells possess), spatially-confined cells develop contractile actin on their ventral surface,

protrusive actin structures on their dorsal surface; furthermore, cilia, which tend to be longer, are more frequently generated. It should also be noted that cells with a greater area also are more likely to develop contractile cortical actin bundles (Pitaval *et a*l., 2010).

Appropriate ROCK activity is required for centriole migration and docking at the apical surface; however, elongated cells display cilia protruding from ventral basal bodies following ROCK inhibition, suggesting that cell contractility and Rho signalling independently act upon basal body docking and axoneme extension (Pitaval *et al*., 2010).

Not only does the centrosome fail to dock in multiple ciliopathies, but many of these exhibit other centrosomal defects, including centrosomal amplification. A previous study of MKS models, including *MKS1* and *-3* patient cells and shRNA knockdown of *Mks1* and *Mks3* in IMCD3 cells reported cilia and centrosome over-duplication (Tammachote *et al*., 2009). Centrosome amplification is known to be ROCK-dependent (Ling et al., 2015), and inhibition of p160ROCK (ROCK1) causes centrosomes to split and microtubule-dependent docking defects (Chevrier et al., 2002), so this is a subset of phenotypes of interest to us.

Finally, multiple phenotypes correlating with this proposed role of MKS proteins upstream of other cellular defects are observed in other ciliopathies. BBS proteins interact with Wnt signalling pathways (canonical and noncanonical) (Corbit *et al*., 2008; Hernandez-Hernandez *et al*., 2013), are found at the cilium and participate in ciliogenesis (Kim *et al*., 2004; Nachury *et al*., 2007), interact with multiple facets of the actin cytoskeleton (Hernandez-Hernandez *et al*., 2013; May-Simera *et al*., 2015), and facilitate membrane delivery to the primary cilium (Kim *et al*., 2004; Nachury *et al*., 2007). The ways in which these protein complexes and behaviours work together in normal cells, and in ciliopathies, remain to be elucidated, but a Rho pathway-effected series of cellular phenotypes, such as ciliogenesis and cytoskeletal defects, is plausible considering the present results and previous ciliopathy research.

Alternate roles of MKS proteins

The present chapter aimed to address the hypothesis that aberrant Rho/Rho kinase (ROCK) signalling is responsible for the abnormal cellular

phenotypes observed in MKS patient cells. The current results indicate that Rho signalling is associated with the actin and Golgi defects observed in these cells, whether directly or through other downstream effects. The most likely alternative roles for MKS proteins besides directly regulating Rho/ROCK signalling are in centrosome cohesion, and in tethering the cytoskeleton to membranes.

Rho/ROCK signalling does not require cilia, but may be dependent on basal body integrity (Huang and Schier, 2009); in a model in which MKS proteins had a centrosome cohesion role, Rho signalling might be affected by the perturbation to basal body structure caused by their mutation. Other cellular defects, such as prominent actin bundle development, may then result from this Rho perturbation.

MKS proteins may alternatively be a cytoskeleton-membrane tether; BBS4, another ciliopathy protein, is required for the anchoring of microtubules at the centrosome (Kim *et al.*, 2004), leaving the possibility that the “ciliopathy” proteins function in a complex in a cytoskeletal organisation capacity. The microtubule cytoskeleton is an unexplored but potentially key feature of these cells, so I next examined the organisation and post-translational modification of microtubules and their attachment to centrosomes in MKS patient cells.

CHAPTER V: MKS patient cells show defects in microtubule organisation

5.1 Introduction

The microtubule (MT) cytoskeleton has diverse transport roles within cells, from protein trafficking to chromosome segregation, regulating cell shape, polarity and cell division. These functions, similarly to the actin cytoskeleton, are achieved through rapid reorganisation of MTs, necessitating the use of binding proteins. However, in the MTs, post-translational modifications are additionally used to impart changes in stability (Li and Gundersen, 2008). As a key structural component of the ciliary and flagellar axoneme (Borisy and Taylor, 1967; Kozminski *et al.*, 1995; Kozminski *et al*., 1993) – first described as "longitudinal filaments" within the 9+2 axoneme in 1954 (Fawcett), and subsequently identified as having tubulin subunits in sperm flagella (Mohri, 1968; Shelanski and Taylor, 1967) - and of multiple vital cellular functions, MTs are an important focus of ciliopathy study.

Research into MT structure, organisation and function in the field of ciliopathies has predominantly concerned interactions of the ciliary axoneme with the centrosome (as the basal body), a structure involved in MT minus end nucleation and tethering (Bialas *et al*., 2009; Delous *et al*., 2007; Drivas *et al*., 2013; Valente *et al*., 2006).

Limited research has investigated the properties of cytoplasmic MTs amongst ciliopathies. A previous study revealed that depletion of a BBSome subunit, BBIP10, leads to split centrosomes and to defects in MT polymerisation and acetylation that may be abrogated by inhibiting the BBIP10-interactor HDAC6, the histone deacetylase (Loktev *et al*., 2008). Furthermore, BBS4 is required for MTs to anchor to pericentriolar material; truncated versions of this protein cause defective targeting and anchoring of pericentriolar proteins and MT disorganisation (Kim *et al*., 2004).

Similarly, emerging evidence suggests that overexpression of Arl13b – mutations in which cause Joubert syndrome – impairs α-tubulin acetylation, implicating Arl13b in cilium length regulation through its effects on MT dynamics (Pintado *et al*., Cilia 2014 Conference (unpublished)). There has been very little previous study into the properties and regulation of MTs in the

ciliopathies in general, and none in MKS, meaning that this is a novel field of ciliopathy research.

Previous studies (Dawe *et al.*, 2009; Valente *et al.*, 2010) have revealed actin defects in the present MKS patient cells, but currently no such information regarding the MT cytoskeleton exists. The MT and actin cytoskeleton are well-established to interact in numerous ways, including via proteins such as MACF at stress fibres (Leung *et al.*, 1999) and formins at the cell cortex (Heil-Chapdelaine *et al.*, 1999). Together with the emerging evidence reporting alterations to microtubule stability in other ciliopathies, it was therefore pertinent to next examine the properties of the cytoplasmic MT cytoskeleton in MKS patient cells. I therefore aimed to address the hypotheses that, in MKS patient cells, MTs are organised differently, and that they are structurally altered.

5.2 Results

Microtubules emanate from multiple, non-centrosomal foci

I examined the microtubule cytoskeleton in MKS patient cells by fixing these and visualising α-tubulin. Microtubules in MKS patient fibroblasts appeared less radially organised, and to emanate from more than one focus more frequently than in wild-type cells (*Figure 5.1*). This was particularly pronounced in *MKS2* patient cells, so I investigated this phenotype in more depth in these cells.

At higher magnification, it was apparent that single foci from which microtubules emanate were never observed in *MKS2* patient cells [<1% compared to ~90% in control cells, n=300 cells across 3 experiments (red arrowhead, *Figure 5.2*)]; instead MTs radiate from no obvious source (*Figure 5.2,* demonstrating representative focal planes) or multiple sites (*Figure 5.3*) in *MKS2* patient cells. This suggests that MTs in *MKS2* patient cells are emanating from non-centrosomal sources or from multiple centrosomal sites of nucleation, or that MTs are tethering at multiple locations throughout the cells. These data led me to question the nature of the foci that microtubules were emanating from.

To test whether MTs were radiating from multiple spots of centriolar material (whether multiple centrosomes, or multiple centrosomal fragments), or from acentriolar sources, I fixed and co-stained these MTs and pericentrin to

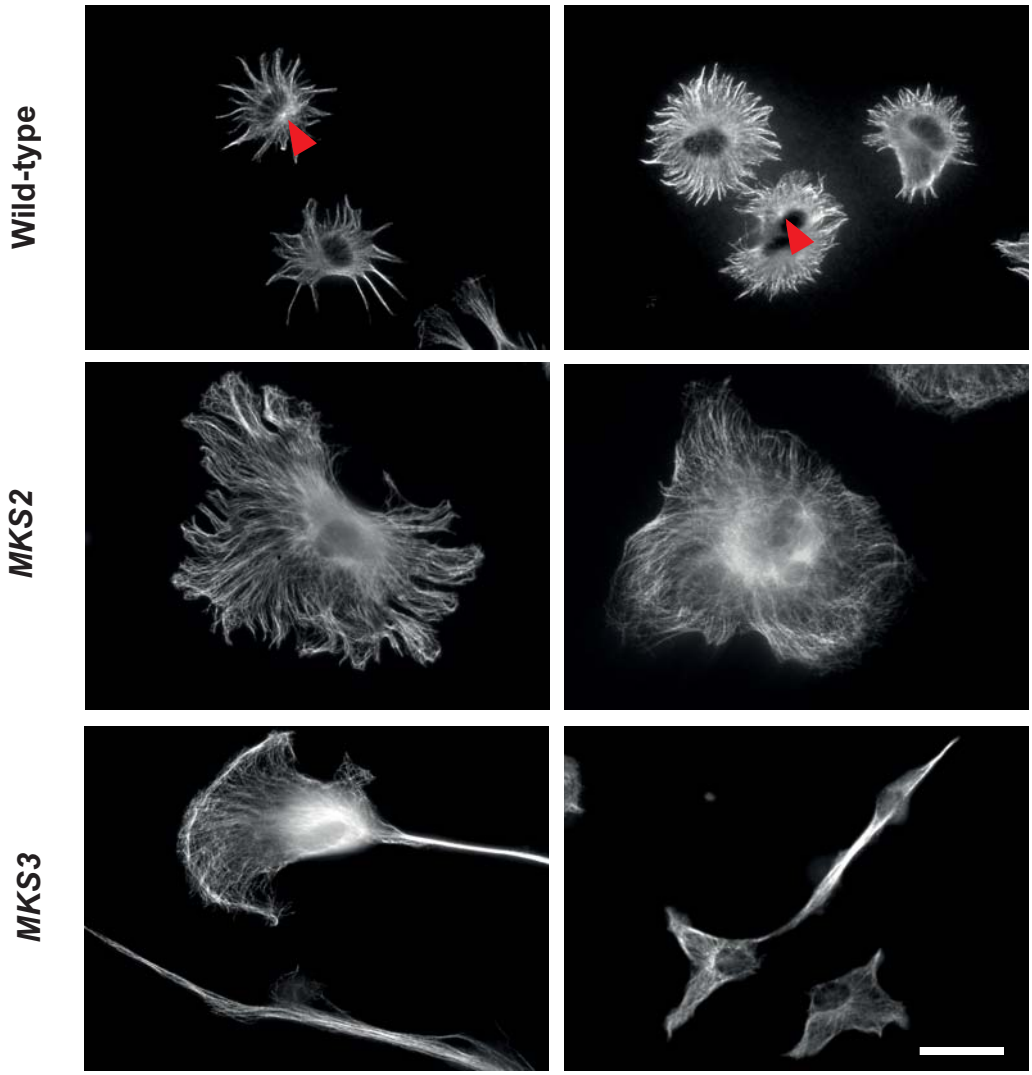

FIGURE 5.1: MKS patient cells exhibit a different microtubule organisation. Microtubules were visualised using anti-α-tubulin. These appear radially organised and emanate from a single, brighter focus (indicated with red arrows) more frequently in control than in MKS patient cells. Scale bar represents 40 μm.

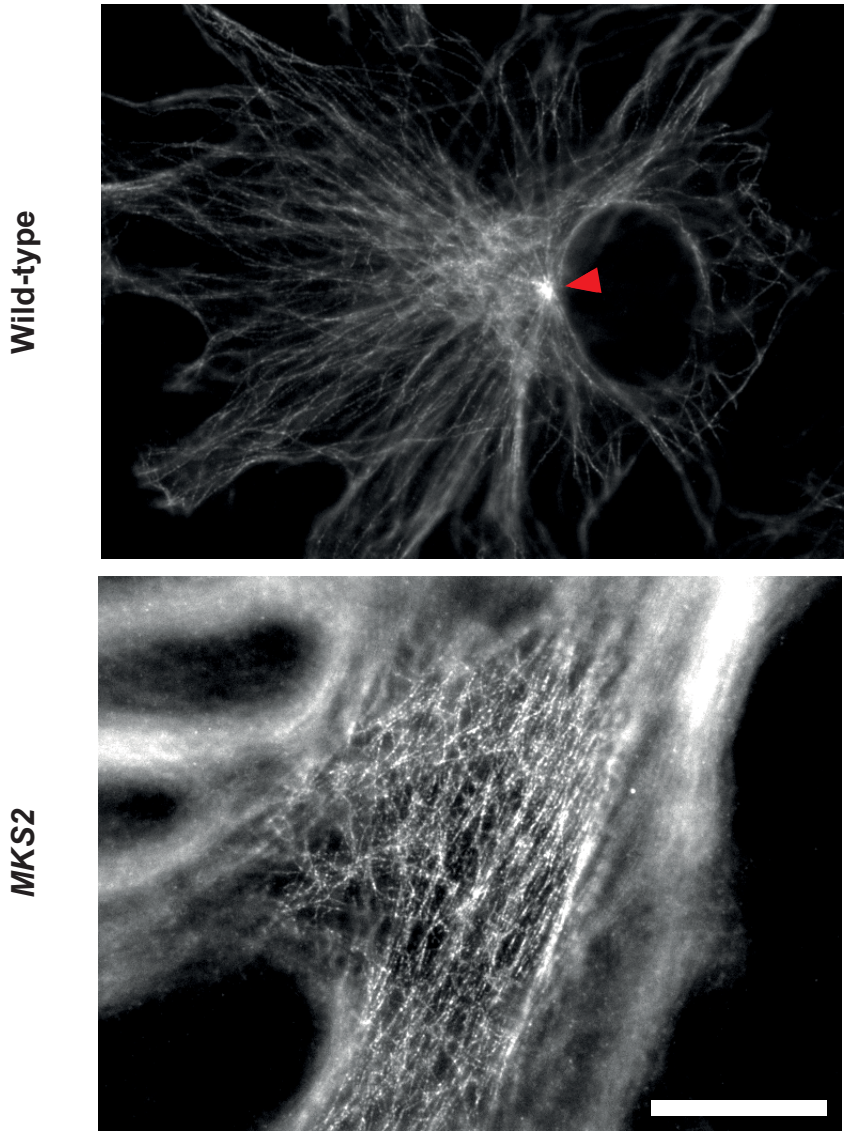

FIGURE 5.2: Single MT foci are not observed in *MKS2* patient cells.
Microtubules were visualised using anti-α-tubulin. These emanate from a single focus in wild-type cells (red arrowhead), but multiple sites (not shown) or no obvious site in *MKS2* patient cells. Images used are single-plane, single-channel images that are representative of microtubules on all planes throughout these cells. Scale bar represents 20 μm.

visualise the pericentiolar material (PCM). The MTs in control cells radiate out from a single region of pericentrin staining (*Figure 5.3*), but MTs in *MKS2* patient cells emanate from multiple regions, a number of which may be associated with pericentrin and a number of which are not (yellow arrowheads, *Figure 5.3*), implying that at least a proportion of the microtubules are nucleated or tethered at non-centrosomal sites. These results caused me to examine the degree to which MT minus ends associate with this pericentriolar material.

I investigated at the MT-PCM association in greater detail by examining MT minus ends and pericentrin in multiple regions of the cell at high magnification. Wild-type cells demonstrated a markedly close association of MT ends with clearly-defined PCM (*Figure 5.4*); however, PCM (*Figure 5.4*, Sections A) was on a completely different focal plane to MTs (*Figure 5.4*, Sections B) in *MKS2* patient cells (at least 1.5 μm apart; n= 20 cells per cell line). This suggests that the MT minus ends are not nucleated at or not stably tethered to centriolar material, possibly due to centrosomal splitting implied by the multiple pericentrin spots (*Figure 5.3*).

Tyrosination and acetylation of microtubules are altered in MKS patient fibroblasts

New MTs are established to be tyrosinated (Barra *et al*., 1974; Bre *et al*., 1987; Gundersen and Bulinski, 1986; Gundersen *et al*., 1984). Therefore, to test whether the multiple MT foci in MKS patient cells represent newly-formed MTs, or whether older, more stable MTs are being remodelled differently in these cells, I next looked at MT tyrosination and acetylation patterns.

I demonstrated that tyrosinated MTs typically do not emanate from a single focus in MKS patient cells (*Figure 5.5*), but they do in control cells (red arrowheads indicating bright spots of tyrosination, *Figure 5.5*); instead, tyrosination appears to disperse fairly equally along MTs in MKS patient cells, with no obvious MT minus ends being visualised. This implies erroneous behaviour of new MTs, specifically during assembly; this indicates that at least a subset of MTs are being incorrectly nucleated or tethered.

I next investigated whether stable microtubules appear different in MKS patient fibroblasts as this may reveal defects in maintenance, turnover and anchoring of MTs. This was achieved by visualising acetylated MTs, a marker of

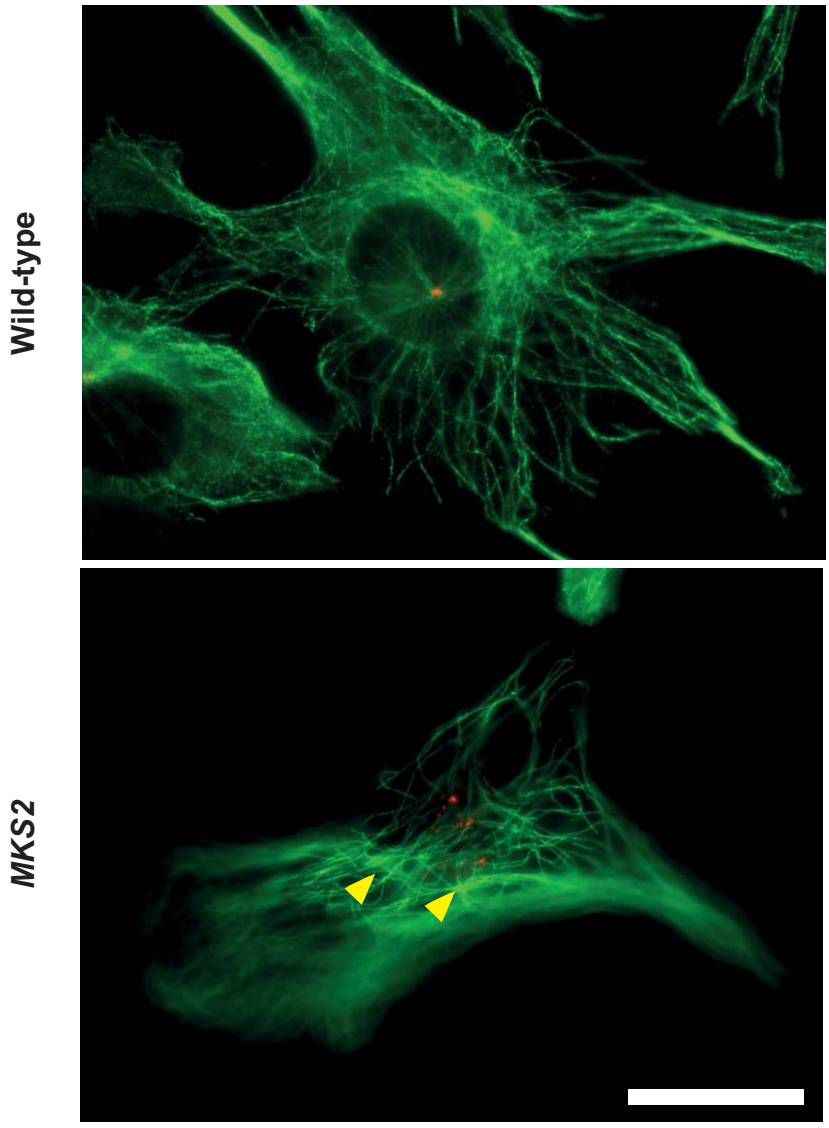

FIGURE 5.3: Multiple pericentrin-rich foci, and multiple MT foci at numerous sites are observed.

Microtubules were visualised using anti-α-tubulin (green), and PCM visualised using anti-pericentrin (red). Microtubules emanate from a single pericentrin spot in wild-type cells, but from multiple pericentrin spots or from no apparent PCM (yellow arrowhead) in *MKS2* patient cells. Scale bar represents 20 μm.

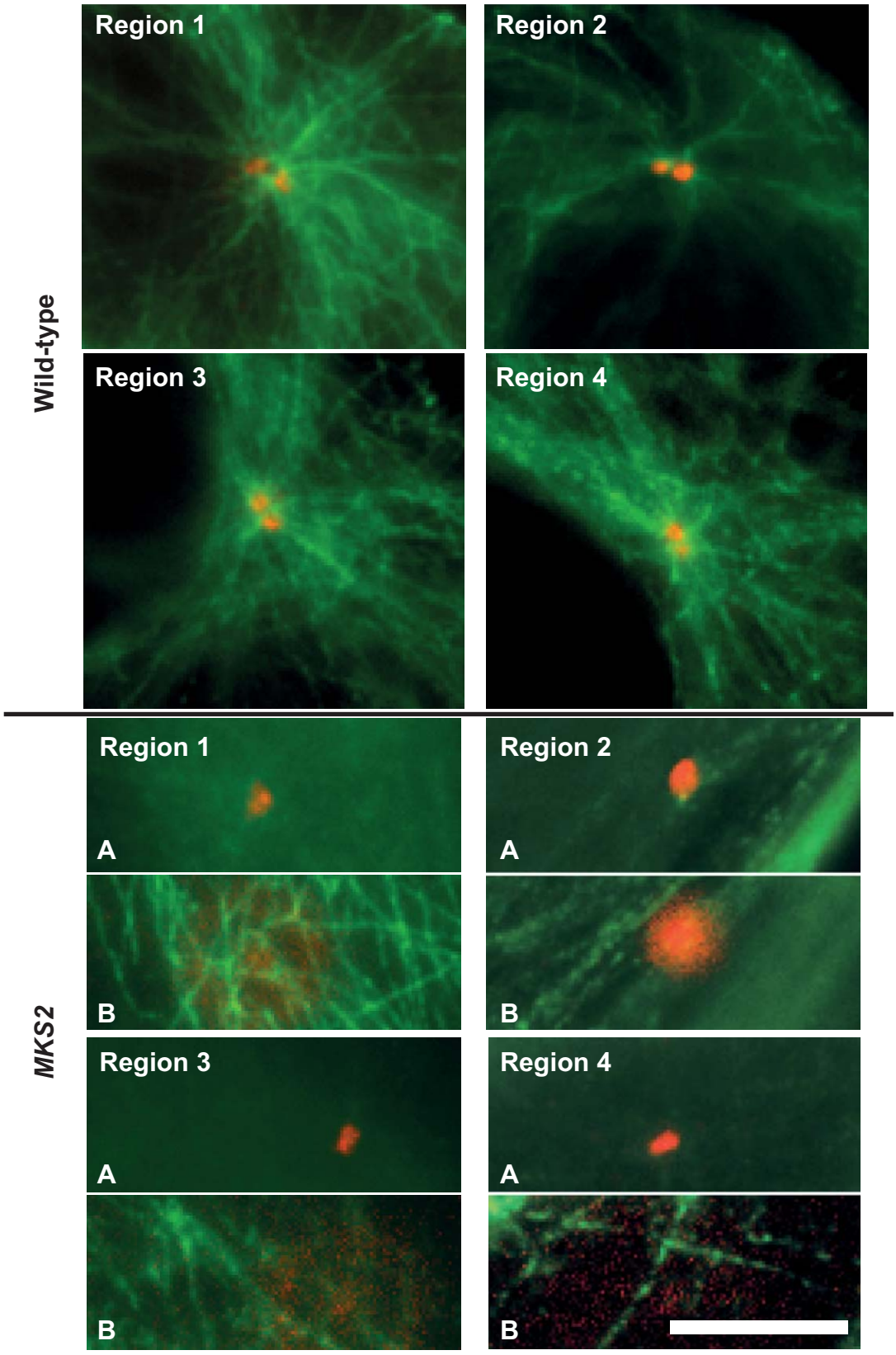

FIGURE 5.4: Microtubule ends are not markedly associated with centriolar material in *MKS2* patient cells.

Microtubules were visualised using anti-α-tubulin (green), and PCM visualised using anti-pericentrin (red). Two images were captured of each region in *MKS2* patient cells - one of the centrosome (A), and one of the focal plane of the MTs (B). A and B images were always >1.5μm apart. Scale bar represents 10 μm.

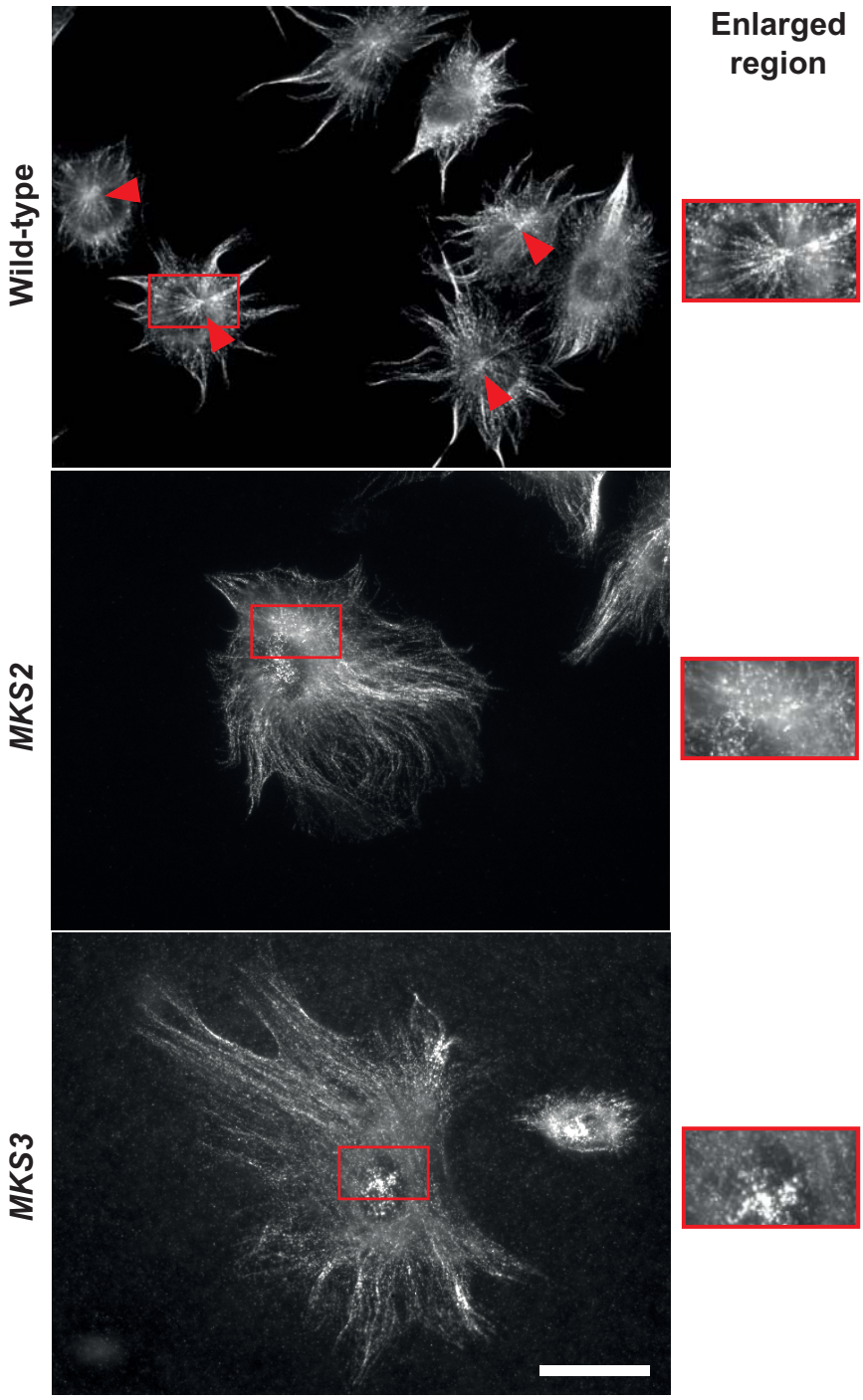

FIGURE 5.5: Tyrosinated microtubules do not emanate from a single focus in MKS patient cells.

Tyrosinated MTs were visualised using anti-YL1/2. Tyrosinated MTs emanate from single foci less commonly in MKS patient cells than wild-type cells (demonstrated at higher magnification in enlarged regions). Scale bar represents 40 μm.

stable MTs, using anti-acetylated tubulin. I revealed that acetylated tubulin staining was spread further across the cytoplasm in MKS patient cells (*Figure 5.6*), suggesting that stable microtubules extend further across these cells. This could indicate a defect in microtubule maintenance or turnover.

It was thus of interest to examine the nucleation of MTs, to determine the stage at which MTs display aberrant organisation. Following a 45 minute nocodazole treatment, I observed MT regrowth two minutes after washout and revealed that MTs are present at non-centrosomal sites in MKS patient cells (*2 min, Figure 5.7*, yellow arrowheads), in addition to radiating from γ-tubulin-rich regions. However, in control cells, MTs are solely seen associated with these presumed centrosomes (*2 min, Figure 5.7*). MTs, whether centrosomal or acentrosomal, were not observed before this washout stage (*0 min, Figure 5.7*). This implies firstly that defects in MT organisation are observed almost immediately, and secondly confirms errors in nucleation, stabilisation or tethering of these structures at a centrosome. Importantly, these data indicate that MT organisational changes in MKS patient cells cannot solely be attributed to loss of centrosome integrity, as the centrosome appears intact in these cells.

5.3 Discussion

In the present series of experiments, I endeavoured to ascertain whether MKS patient fibroblasts exhibit defects to the MT cytoskeleton, as there is evidence of changes to MT anchoring associated with BBS (Kim *et al*., 2004) and to MT acetylation associated with Joubert syndrome (Pintado *et al*., Cilia 2014 Conference (unpublished)).

I observed a disorganised MT cytoskeleton in MKS patient cells, revealing errors in localisation of MT ends to a single centrosome or to centriolar material in *MKS2* fibroblasts. Instead, MTs appear to emanate from multiple foci of unknown molecular constitution in *MKS2* patient cells. These cells demonstrated multiple spots of pericentrin, but MTs were observed on a separate focal plane to these. These data indicated that MTs do not have minus ends embedded in a centriole in these patient cells; the disorganised MT cytoskeleton was concluded to have non-centrosomal origins.

This is a novel area of research – no studies to date report upon the MT cytoskeleton in MKS and a limited number of studies report defects to the

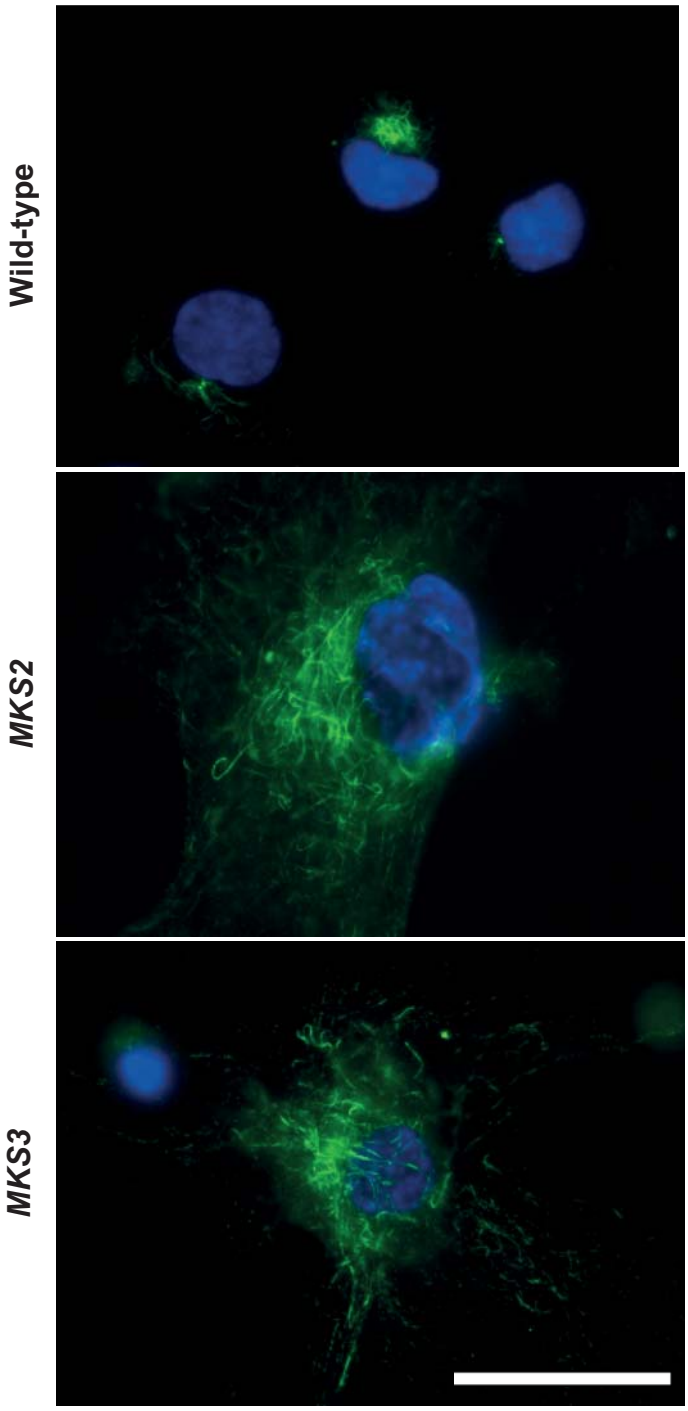

FIGURE 5.6: Acetylated MTs are dispersed in MKS patient cells.
Acetylated MTs were visualised using anti-acetylated tubulin (green), shown alongside nuclear staining (DAPI, blue). Acetylated MTs are spread further through the cytoplasm in MKS patient cells than wild-type cells. Scale bar represents 40 μm.

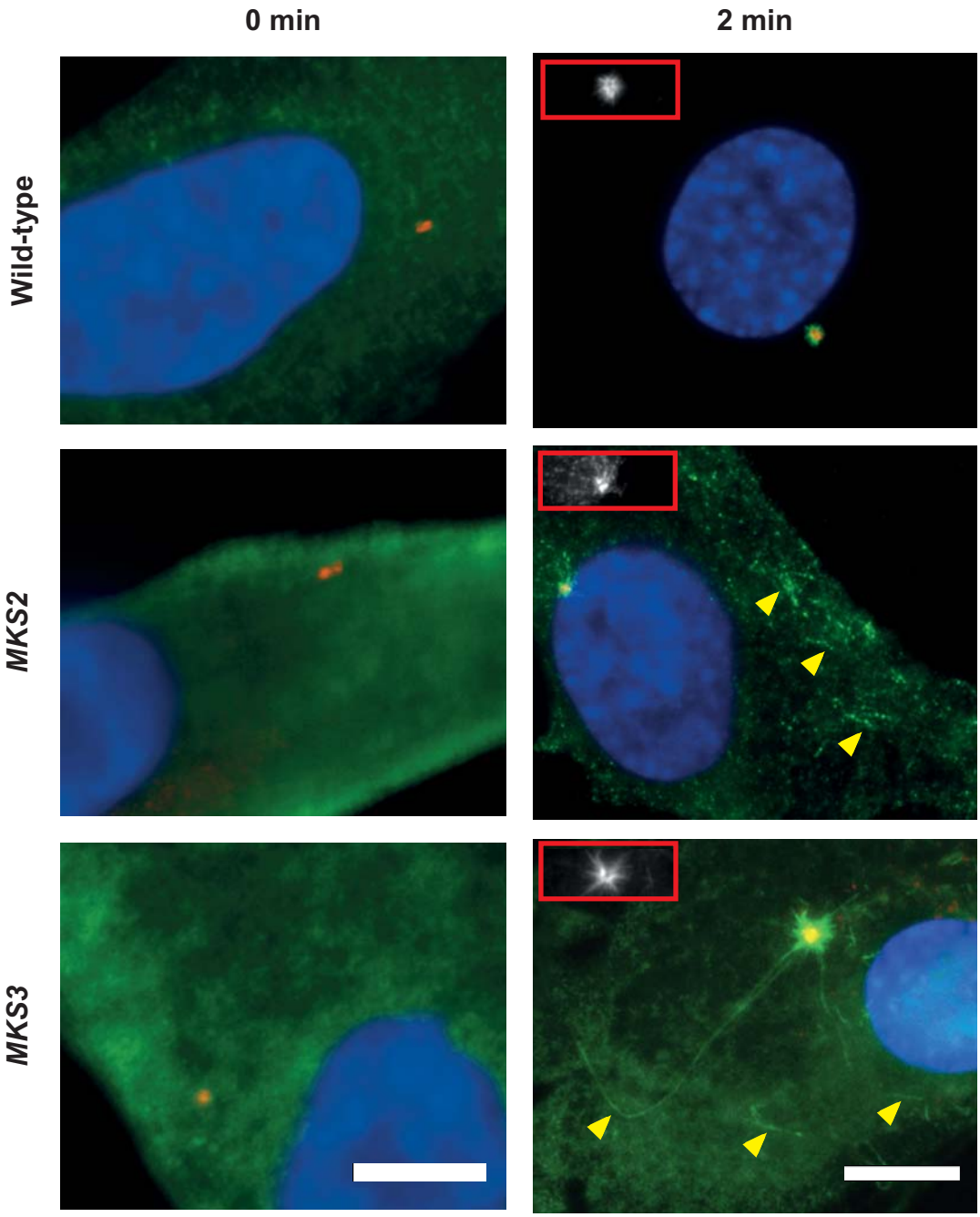

FIGURE 5.7: MTs are present at acentrosomal sites following nocodazole treatment of MKS patient cells.

Microtubules were visualised using anti-α-tubulin. MTs emanate from the centrosome (γ-tubulin, red; and inset, red box) in MKS patient cells and control cells 2 mins after washout of nocodazole, but are also observed growing at acentrosomal sites (yellow arrowheads) in MKS patient cells. MTs are not observed in any cell line following this nocodazole treatment. Nuclei were visualised using DAPI (blue). Scale bar represents 10 μm.

cytoplasmic MTs in ciliopathies (Kim *et al*., 2004; Loktev *et al*., 2008), with fewer still beginning to report post-translational modifications to MTs (Loktev *et al*., 2008; Pintado *et al*., Cilia 2014 Conference (unpublished)).

I observed differences in the tyrosination and acetylation of cytoplasmic MTs in MKS patient cells. Tyrosinated MTs commonly emanated from more than one focus, and acetylated microtubules were spread throughout the cell to a greater degree. Firstly, the dispersed localisation of tyrosination, a marker of newly assembled MTs, implies that MTs are polymerising at more than one location. This was supported by my observation that MTs were present at multiple locations following nocodazole washout. However, these cells also revealed MTs radiating from a single presumed centrosome and, from this, I cannot exclude the possibility of MTs being nucleated and stabilised at multiple locations throughout the cell. Based on the demonstrable absence of γ-tubulin spots and of MT ends at pericentrin spots after this stage, it is more probable that MTs are nucleated here and subsequently become untethered (and potentially tethered elsewhere), or that they break and disperse throughout the cell.

The prevalence of stable, acetylated microtubules throughout the cytoplasm indicates no difficulty of MKS patient cells in nucleating and stabilising microtubules. Instead, it appears that MTs are built and stabilised and are inappropriately positioned; this could be due to hyperstabilisation of microtubules, or tethering of microtubules at multiple subcellular locations. To conclude, it appears that MTs are nucleated at the centrosome and at other acentrosomal sites, they break or untether, then inappropriately stabilise throughout the MKS patient cells.

This is an important discovery, firstly as MTs effect crucial cellular roles and, secondly, as other subcellular defects (such as in the Golgi and in ciliogenesis) may be caused by or associated with these MT/centrosome phenotypes. As MT defects have not previously been examined in MKS, such an association has yet to be investigated, but MT defects may underlie other subcellular defects associated with MKS, and possibly even other ciliopathies.

Microtubule asymmetry and reorganisation

The organisation and structure of the MT cytoskeleton is extremely important for its function. In order to support polarised functions, such as cell migration and vesicular trafficking, the MT network must be asymmetric. During cell motility, protrusive actin structures may form in the absence of MTs, but MTs are required to enable their polarised distribution (Vinogradova *et al*., 2009).

MTs typically radiate from a centrosomal MT organising centre (MTOC), with their plus ends at the cell edges. Mesenchymal motile cells such as fibroblasts extend their MT array primarily in the direction of movement, presumably to direct vesicular trafficking and actin polymerisation here; similarly, neurons display distinct MT asymmetry corresponding to their necessary vesicular transport functions (Vinogradova *et al*., 2009).

By contrast, in the epidermis basal cell MTs emanate from an apical centrosome, and suprabasal cell MTs nucleate at cell-cell junctions. Upon differentiation of the epithelium, MTs are often (but not always) dissociated from the centrosome, which does not lose its ability to nucleate. This allows MTs to be arranged in an apical web and longitudinal bundles, with minus ends spread over the apical region and plus ends at the basal region (Bacallao *et al*., 1989; Lechler and Fuchs, 2007).

The centrosome typically nucleates radially symmetric MTs at the cell centre (Holy *et al*., 1997; Salaycik *et al*., 2005), which are then distributed by a number of possible mechanisms if a cell is to create asymmetry.

Alterations to microtubules to generate asymmetry

One such mechanism is spatial regulation of MT stabilisation and catastrophe. MTs constantly undergo periods of catastrophe and rescue (Kirschner and Mitchison, 1986), which can be performed selectively by the cell to generate an asymmetric MT network. Various cellular activities make this possible, one being enrichment of MTs in posttranslationally modified tubulin, such as detyrosinated tubulin, to create more stable MTs in distinct regions (Gundersen and Bulinski, 1988; Salaycik *et al*., 2005). Focal adhesions - used to attach to the extracellular substrate during cell migration and spreading -

conversely, act as a common site of catastrophe, with particular frequency at the cell rear (Efimov and Kaverina, 2009; Efimov *et al*., 2008).

As mentioned, hyperstabilisation of MTs may be responsible for their disorganisation in MKS patient cells. Hyperstabilisation may be caused by ineffective depolymerisation (e.g. at focal adhesions) or by spatially inappropriate posttranslational modification of the MTs; if the cell does not effectively polarise, the latter is especially likely as MTs may be ubiquitously stabilised regardless of location.

A study of the BBSome subunit BBIP10 revealed a requirement for this protein but no other tested BBS protein (BBS1, BBS12 or PCM-1) in MT acetylation (Loktev *et al*., 2008). This previous study concluded that BBIP10 is required to stabilise MTs *in vivo*, and that the decreased acetylation and density of microtubules observed upon BBIP10 depletion result from global MT destabilisation. This study also demonstrated multiple foci of pericentrin and γ-tubulin staining when BBIP10 is absent, resembling the phenotypes I observe in MKS patient cells. These split centrioles were, importantly, able to nucleate but not to anchor MTs (Loktev *et al*., 2008). The MT dynamics observed in BBIP10-depleted cells correlates with the MKS patient cell phenotypes, i.e. MTs appear to be nucleated but not anchored at split centrioles, and this is an important study as these data indicate partial loss of function of the centrosomes in these cells. However, depletion of BBIP10 hindered stabilisation and, separably, acetylation of MTs (Loktev *et al*., 2008), but the opposite appears to be true of MKS cells.

A related mechanism of asymmetric MT array generation is through use of MT-binding proteins, such as MAPs, +TIPs, and motors, to move or modify MTs in the array. The current hypothesis in the field is that posttranslational modifications of tubulin mark subsets of MTs to affect downstream recruitment and behaviours of these effector proteins (Verhey and Gaertig, 2007). It appears that posttranslational modification can have a stabilising effect, and that stabilisation can also result in posttranslational modification (e.g. acetylation and detyrosination), but that these can also occur independently (Wloga and Gaertig, 2010).

For example, katanin, a microtubule-severing protein required for motile cilia biogenesis, acts as a negative regulator of posttranslational modifications in the cell body (Sharma *et al*., 2007). Polyglutamylation of MTs affects the

binding of MAP1A and MAP1B, however; these are proteins thought to be involved in MT assembly through tubulin conformational changes (Bonnet *et al*., 2001). Tubulin detyrosination impedes association of some +TIPs, plus-end tracking proteins, with MTs (Verhey and Gaertig, 2007). Tubulin detyrosination and acetylation are also known to decrease binding and motility of kinesin-1 (Reed *et al*., 2006), and tubulin acetylation positively regulates dynein binding capacity (Dompierre *et al*., 2007), plus- and minus-end motors (respectively) involved in the majority of MT functions.

With regard to my results, the increased acetylation and more widespread tyrosination may therefore impact upon the behaviour of MT-binding proteins such as these. For instance, dysregulated motor protein behaviour may result from these posttranslational modifications. This could alter extensive cellular behaviours such as migration, during which kinesin and dynein function in nuclear positioning (Scheffler *et al*., 2015; Tsai *et al*., 2010), substrate adhesion (Krylyshkina *et al*., 2002), secretion of matrix proteases (Bachmann and Straube, 2015), and delivery of mRNA encoding β-actin and Arp2/3 complex components to the leading edge, promoting protrusion (Mingle *et al*., 2005; Oleynikov and Singer, 1998). These are a few of a plethora of other necessary roles of MT motor proteins alone, not mentioning other MT-interacting proteins, indicating how impactful these posttranslational MT alterations could be.

Microtubule-binding proteins, such as kinesins, have been thoroughly investigated in the ciliopathies during intraflagellar transport (IFT), affecting features including cilium length, for instance (Cole *et al*., 1998; Rosenbaum and Witman, 2002). Indeed, proteins perturbed in ciliopathy, such as BBSome subunits, are constituents of the mammalian IFT particle (Williams *et al*., 2014). Furthermore, there are numerous links between mutations in IFT components and ciliopathy, particularly skeletal ciliopathies; for instance, Jeune syndrome and and Mainzer-Saldino syndrome can both be caused by defects in IFT172, an IFT-B component (Halbritter *et al*., 2013). MAP4 has also been associated with ciliary and Golgi architecture. In a series of experiments, Zahnleiter *et al*. (2015) reported that patient cells with *MAP4* mutations demonstrate cellular phenotypes reminiscent of those observed in MKS patient cells, such as supernumerary centrosomal spots, decreased percentage of ciliated cells (and shorter cilia), and dispersed Golgi. These data imply a focal role of aberrant MT-

associated functions during the manifestation of these diseases, but are yet to elucidate the scope or exact nature of their role.

In addition to modulating actin cytoskeletal function, the Rho GTPases also influence posttranslational modification and stability of MTs, particularly during polarisation. ROCK modulates MT acetylation by phosphorylating tubulin polymerization promoting protein 1 (TPPP1/p25), which inhibits histone deacetylase 6 (HDAC6), an important enzyme in MT acetylation; this process is also essential to cell migration, as revealed in a wound closure assay (Schofield *et al*., 2012). Furthermore, Rho and its downstream effector mDia are required to selectively generate detyrosinated MTs at a wound edge (Cook *et al*., 1998; Palazzo *et al*., 2001a), affecting MT stability here to enable polarised migration. MT tip proteins enhance cortical capture of MTs using Rho-controlled selective stabilisation at a wound edge. This has been demonstrated to occur through direct interaction of cortical proteins with MTs and through indirect bridging using actin filaments (Gundersen *et al*., 2004).

With this evidence in mind, it is apparent that dysregulation of Rho/ROCK signalling could be a factor underlying the aberrant posttranslational MT modifications observed in MKS patient cells. As these changes to MT structure and organisation may be responsible for migration, polarity and a number of other cellular defects in MKS, it is possible that Rho/ROCK signalling alterations may precede MT defects and may therefore indirectly effect all concomitant cellular defects.

Alternative mechanisms for generating MT asymmetry

Another mechanism for generating asymmetry is to nucleate MTs at or reassign MTs to a γ-tubulin-rich non-centrosomal site, such as the Golgi (which, with the centrosome, reorients to the leading edge) (Efimov *et al.*, 2007; Rivero *et al*., 2009), or an apical membrane (Bellett *et al*., 2009; Meng *et al*., 2008; Mogensen *et al*., 2000).

Golgi dispersal can be caused by MT depolymerisation or inhibition of dynein function; centrosomal MTs are responsible for pericentrosomal location of the Golgi, whereas Golgi-nucleated MTs maintain Golgi ribbon integrity (Rios, 2014). It is therefore possible that an altered MT nucleation site or loss of

centrosomal anchorage cause Golgi dispersal in MKS patient cells through disorganisation of centrosomal MTs.

Golgi-derived MTs also function in vesicular trafficking, providing tracks toward the cell front, and cell polarity (Zhu and Kaverina, 2013). Cells lacking Golgi-derived MTs migrate more slowly in wound-healing assay, probably due to dysfunctional protein trafficking to the leading edge (Hurtado *et al.*, 2011), illustrating the importance of correctly nucleated MTs in directional migration. It would therefore be logical that, in MKS patient cells, cytoskeletal defects induce Golgi defects, with a number of downstream consequences associated with vesicular trafficking.

As in centrosome-nucleated MTs, dynein is used to anchor Golgi-nucleated MTs (Rivero *et al*., 2009); however, unlike centrosome-nucleated MTs, which are radially organised, the Golgi preferentially orients MTs towards the leading edge of motile cells to generate asymmetry (Efimov *et al*., 2007).

In polarised cells such as epithelia, MTs are rearranged from a radial, centrosomal array into a non-centrosomal array (Bacallao *et al*., 1989). This occurs by centrosomal nucleation of MTs, followed by reassignment of MTOC function, which occurs by movement of nucleators such as γ-tubulin (Feldman and Priess, 2012) and MT minus-end anchoring proteins such as ninein (Mogensen *et al*., 2000) to the apical membrane. Subsequently, MT plus-ends are captured at the adherens junctions and link to cortical dynein to provide the mechanical force needed for release and translocation of MTs from centrosomes to apical sites (Bellett *et al*., 2009; Meng *et al*., 2008). It has been proposed that generation of non-centrosomal apico-basal MT arrays in polarised epithelia is predominantly through this MT plus- and minus-end capture, as opposed to nucleation at these locations (Bellett *et al*., 2009).

Removal of MT anchoring protein CAMSAP3 in HeLa cells, a minus-end binding protein that stabilises non-centrosomal MTs, leads to an increase in centrosomal MTs, which are more detyrosinated than the non-centrosomal MTs. In a previous study, depletion of this protein led to upregulation of RhoA, and associated actin stress fibre formation due to increased RhoGEF activity, which is normally inhibited by MT binding. These data also revealed that non-centrosomal MTs capture GEF-H1 better than detyrosinated, centrosomal MTs (Nagae *et al*., 2013). This was a critical finding as this indicates that different populations of MTs have different interactions with signalling molecules, such

as Rho pathway components, meaning that maintaining the correct balance has important implications for other cellular structures, and for cellular behaviours. This is important when considering the MKS cellular phenotypes; posttranslational differences to the MTs may occur upstream of ROCK pathway hyperactivation, and thereby actin defects and potentially Golgi defects, or of other signalling pathway dysregulation.

Nucleation and anchoring of MTs at alternate sites and the de-anchoring of centrosomal MTs also observed following *BBS4* silencing (Kim *et al*., 2004) may be associated with a number of ciliopathy defects. For instance, these may be associated with Golgi dispersal as centrosomally-nucleated MTs maintain Golgi morphology (Rios, 2014), with directional cell migration and with centriole migration defects during ciliogenesis as Golgi-nucleated MTs are required for both (Rios, 2014), and with Rho-mediated actin stress fibre formation. From my results, I cannot definitively link Rho activity to posttranslational MT modifications or to the increased number of MT foci observed in MKS patient cells, but these data provide additional evidence that these may be connected.

Non-centrosomal arrays of MTs are more typically seen in differentiated cell types (Bartolini and Gundersen, 2006), perhaps indicating that the MKS patient cells may be displaying numerous epithelial-like phenotypes. Relatedly, the MT array can be asymmetrically repositioned by subcellular migration of the centrosome; MTs anchored to the actin cortex provide the pulling force required for this (Tang and Marshall, 2012).

Centrosomal repositioning occurs during cell division, migration, immune synapse formation and ciliogenesis (Tang and Marshall, 2012). It is known that *Mks1* and *-3* siRNA knockdown and mutation of *TMEM216* in the current patient fibroblasts block centriole migration during ciliogenesis (Dawe *et al*., 2007; Valente *et al.*, 2010) and centrosome orientation during cell migration (unpublished data), The disorganised MT cytoskeleton in MKS patient cells may therefore be due to misplacement of the centrosomal array of MTs, possibly linked to the aberrant actin structures observed in these cells. Noncanonical/PCP Wnt signalling through Cdc42/aPKC is responsible for centrosome reorientation and the resultant establishment of MT polarity in fibroblasts and HeLa cells (Kodani *et al*., 2009; Palazzo *et al.*, 2001b; Schlessinger *et al*., 2007), processes which are perturbed in MKS cells. The present and previous data support failure of the centrosome to correctly polarise

as a primary defect in these cells; however, if this were the primary role of MKS proteins, it would be hard to explain the altered posttranslational modifications and apparent increased number of foci in the MTs of these cells.

It is far more probable that a Rho signalling defect in MKS precedes failure of the centrosome to reorient and, whether dependently or independently of this, MT and actin structural and organisational defects. Whether or not Rho dysregulation is responsible, appropriately regulated actin and MT networks are required to implement directional migration (Magdalena *et al*., 2003) and these are both aberrant in MKS patient cells, meaning that either or both may be responsible for migration defects.

In investigating my hypotheses that MKS patient cells have differently organised and structurally altered MTs, I have demonstrated altered sites of MT emanation and changes to posttranslational modifications of these, which are likely linked. It is unlikely that MKS proteins have independent roles in MT, actin and Golgi organisation and Rho signalling in cells; it is more probable that a primary defect instigates structural or morphological changes to the cell, or signalling cascades, which cause the other defects. I therefore aimed to temporally determine the primary cellular defect with the aim of better disentangling the molecular aetiology of MKS phenotypes.

CHAPTER VI: Microtubule defects temporally precede, but do not cause, the other cellular defects

6.1 Introduction

The microtubule (MT) and actin cytoskeleton are established to interact in a range of functions, such as mitosis and directional cell migration (Waterman-Storer and Salmon, 1999), during ciliogenesis (Lemullois *et al*., 1988; Park *et al*., 2006), and in Golgi positioning and function (Gad *et al*., 2012; Shen *et al*., 2012). It is therefore not illogical to suppose that the observed phenotypic defects (i.e. prominent actin bundles, changes to MT foci, Golgi dispersal) may be associated with each other, or to a primary defect upstream of these.

Multiple molecular components are known to be behind MT-actin interaction, with Rho pathway components governing a large proportion; for instance, microtubule-actin crosslinking factor (MACF) binds actin and stabilises MTs (Leung *et al*., 1999), and has been shown to participate in Wnt/β-catenin signal transduction (Chen *et al*., 2006). MACF1b localises to the Golgi (Lin *et al*., 2005), reflecting a role in regulating the actin and MT cytoskeletons here, and of these in regulating Golgi function (Kakinuma *et al*., 2004).

A number of other Rho pathway effectors, such as mDia1, are known to be MT-actin interactors. This is a formin homology protein which aligns MTs parallel to F-actin bundles (Ishizaki *et al*., 2001), possibly to facilitate cellular processes such as cell migration. WHAMM, similarly, is coordinated by RhoD and its effectors in Arp2/3- and filamin A-dependent cytoskeletal dynamics, effecting such functions as cell adhesion and cell migration (Gad *et al*., 2012). Defects or dysregulation of such integrators of signalling, cytoskeleton and the Golgi – which may be the primary function of MKS proteins - is the most parsimonious explanation for the defects observed.

The Golgi is a site of MT nucleation (Efimov *et al*., 2007), and both actin and MTs are used to position the Golgi and enable its function (Egea *et al*., 2013). Multiple MT-actin interactors operate at the Golgi, such as WHAMM (Campellone *et al*., 2008; Shen *et al*., 2012), functionally integrating all three subcellular structures. As these are all defective structures in MKS patient cells, cytoskeleton-Golgi interactors are of obvious interest.

Determining the temporal occurrence of the cytoskeletal and Golgi defects may help us to elucidate the primary defect that is causative of the other defects. I thus aimed to resolve the temporal order in which the phenotypic defects occur, testing the hypothesis that these defects occur in a specific order, not simultaneously. Furthermore, I aimed to determine whether a connection exists between the MT defects and the Rho signalling pathway, as with the association of Rho with the actin defects.

6.2 Results

Microtubule organisational defects are the first to occur in MKS patient cells

To examine whether the defects that I have characterised in actin organisation (Chapter III), MT post-translational modifications and organisation (Chapter V) and Golgi organisation (Chapter IV) occurred simultaneously or whether they could be temporally separated, I plated wild-type and MKS patient fibroblasts on collagen I-coated coverslips and fixed at 5 minute intervals, using immunofluorescence to visualise MT organisation (*Figure 6.1*), tyrosinated MT organisation (*Figure 6.2*), acetylated MT organisation (*Figure 6.3*), and Golgi complex organisation (*Figure 6.4*).

I found that MT defects are apparent 20 minutes after plating (*Figure 6.1*). Within this time, MTs develop multiple, unidentifiable foci of emanation in *MKS2* patient cells, which contrast with the single foci often observed in control and *MKS3* patient cells (*red arrowheads, Figure 6.1*). Within the first 20 minutes of plating, cells of all cell lines typically display few visible MTs, and thus MT foci are rare (*Figure 6.1, 10-20 minutes*). Following this stage, bright spots of α-tubulin mark what is presumed to be individual MT foci, a concentrated mass of minus ends of MTs (*red arrowheads, Figure 6.1*). These foci cannot be resolved as easily in *MKS2* patient cells. At 60 minutes after plating, single foci of MTs remain common in WT and *MKS3* patient cells (*red arrowheads, Figure 6.1*), but no apparent single MT focus is observed in almost any *MKS2* fibroblasts (*MKS2 20-60 minutes, Figure 6.1*).

The same pattern was also true of tyrosinated MTs – within 20 minutes, these emanate from single foci (*red arrowheads*, *Figure 6.2*) more commonly in

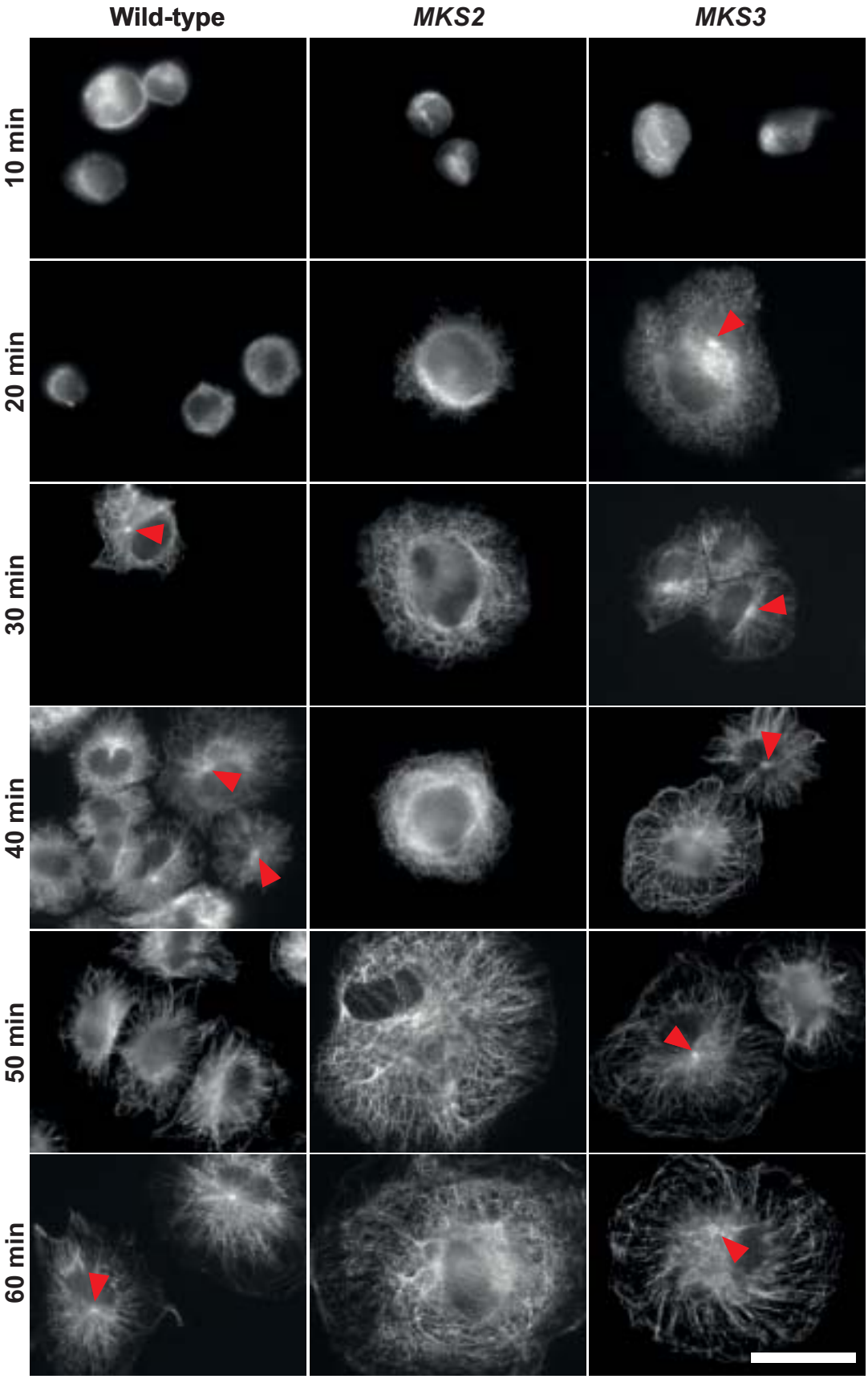

FIGURE 6.1: MKS patient cells develop MT defects within 20 mins.
MTs visualised using anti-α-tubulin. MTs emanating from single foci are marked with red arrowheads. Within 20 minutes, MTs emanate from unidentifiable foci more commonly in *MKS2* patient cells. Scale bar represents 40 μm.

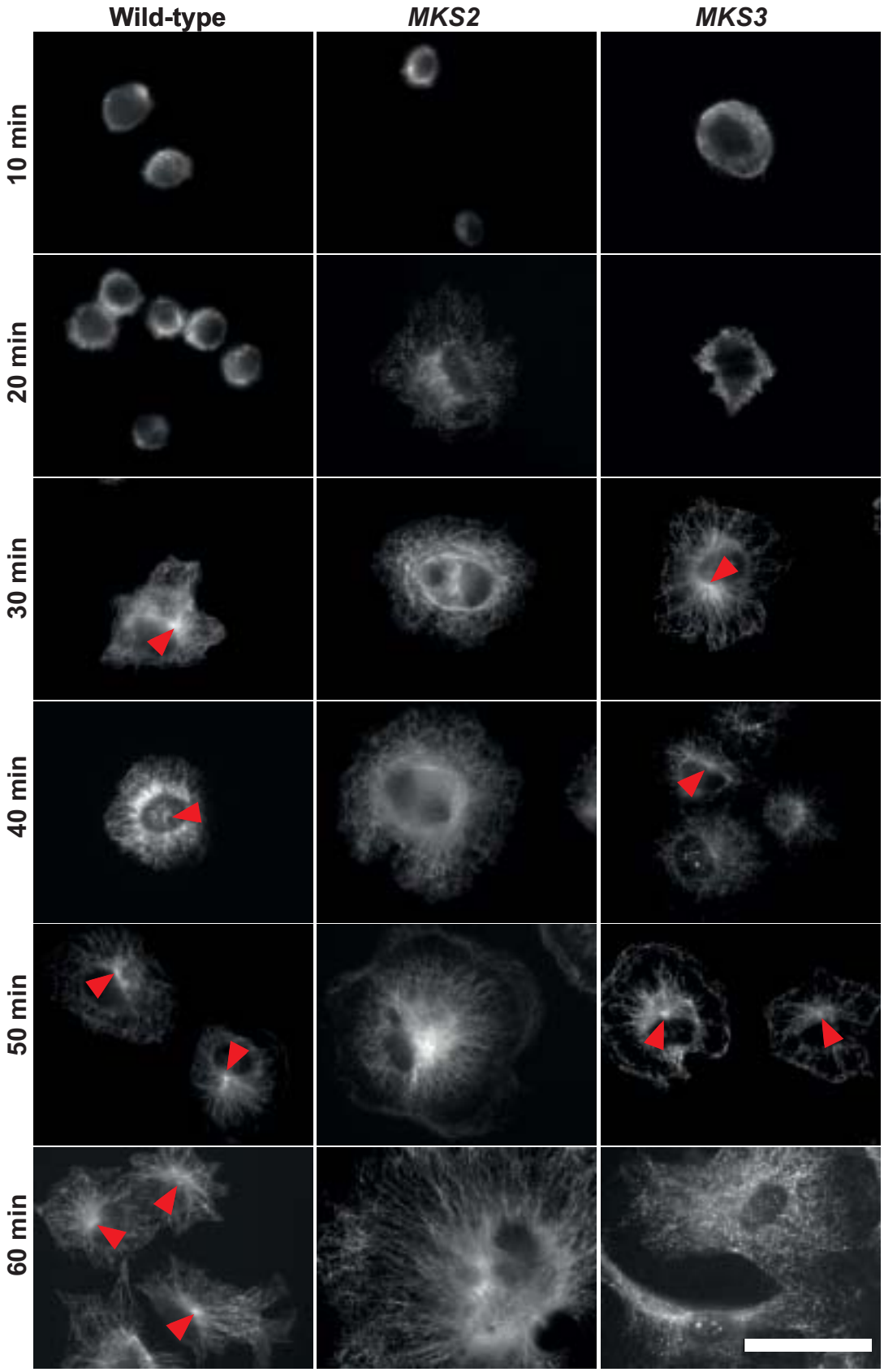

FIGURE 6.2: MKS patient cells develop differently-patterned tyrosination of MTs less than 20 mins after plating.

Tyrosinated MTs visualised using anti-YL1/2. Single foci are indicated with red arrowheads. Tyrosinated MTs emanate from an unidentifiable number of foci in *MKS2* patient cells within 20 mins after plating. Scale bar represents 40 µm.

control and *MKS3* patient cells than in *MKS2* patient cells. In *MKS2* patient cells, MTs frequently have no clear single origin from 20-30 minutes until 60 minutes following plating – they emanate, instead, from a more widespread, cytoplasmic region of immunofluorescence (*Figure 6.2*).

To further resolve the differences between control and MKS patient cells, I next quantified the percentage of cells demonstrating each of these phenotypic defects. Control and MKS patient cells simultaneously generate MTs (*0 foci, Figure 6.3*) and simultaneously tyrosinate MTs (*0 foci, Figure 6.4*). Differences were reported at individual time points between control and *MKS3* patient cells in the number of cells with MTs emanating from 1 or 2+ foci. Overall, however, there is no significant difference between control and *MKS3* cell lines in the number of MT foci during the first hour after plating ($p>0.05$, χ^2). However, the proportion of cells revealing MTs (*Figure 6.3*) and tyrosinated MTs (*Figure 6.4*) emanating from multiple foci is significantly increased ($p<0.001$, χ^2) in *MKS2* patient cells at all time points (*blue bars*, *Figure 6.3* and *6.4*), demonstrating this as one of the earliest cellular defects.

Acetylated microtubules are initially dispersed across the entire cytoplasm in control and MKS patient fibroblasts (*20 minutes, Figure 6.5*), but condense to a small, perinuclear region in wild-type cells around 30-40 minutes after plating (*40 minutes, Figure 6.5*). This acetylated MT condensation occurs 50-60 minutes after plating in *MKS2* patient cells, but acetylated tubulin appears to remain spread through the cytoplasm to a greater degree in these cells than in WT cells (*60 minutes, Figure 6.5*).

The Golgi complex remained perinuclear in control and *MKS3* patient cells over the 60 minute time course, but dispersal throughout the cytoplasm – in which sections appeared to “bud” away (*red arrowheads, 50 minutes, Figure 6.6*) or extend throughout the cytoplasm (*red arrowheads, 60 minutes, Figure 6.6*) - was observed from 40 minutes after plating in *MKS2* patient fibroblasts (*Figure 6.6*).

Quantification of the percentage of cells demonstrating acetylated tubulin centralisation indicates that this process begins to occur 15-20 minutes after plating in wild-type cells (*dotted line, Figure 6.7*), but not until later in *MKS2* patient cells. In *MKS2* patient cells, this process appears to begin 30 minutes after plating, but the rate of centralisation across these cells only increases rapidly from 40 minutes after plating (*continuous red line*, *Figure 6.7*).

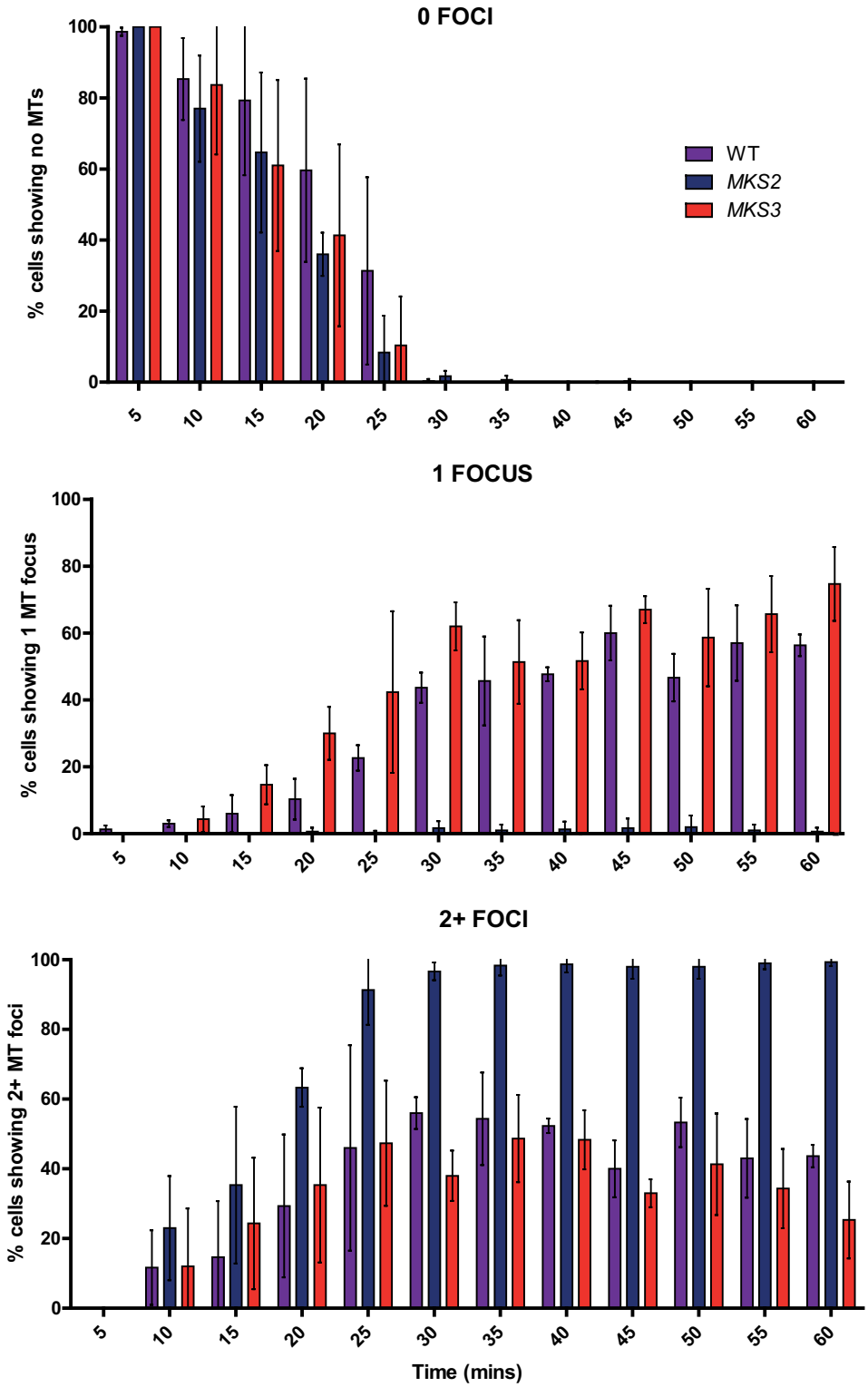

FIGURE 6.3: *MKS2* patient cells demonstrate an increased number of MT foci
Graphs report mean percentage of cells demonstrating the displayed number of foci +/- SD. MTs show no site of emanation initially, but gradually MTs emanate from a single or multiple sites in roughly equal numbers between wild-type and *MKS3* patient cells, and multiple sites in *MKS2* patient cells significantly more frequently ($p<0.001$, $\chi 2$).

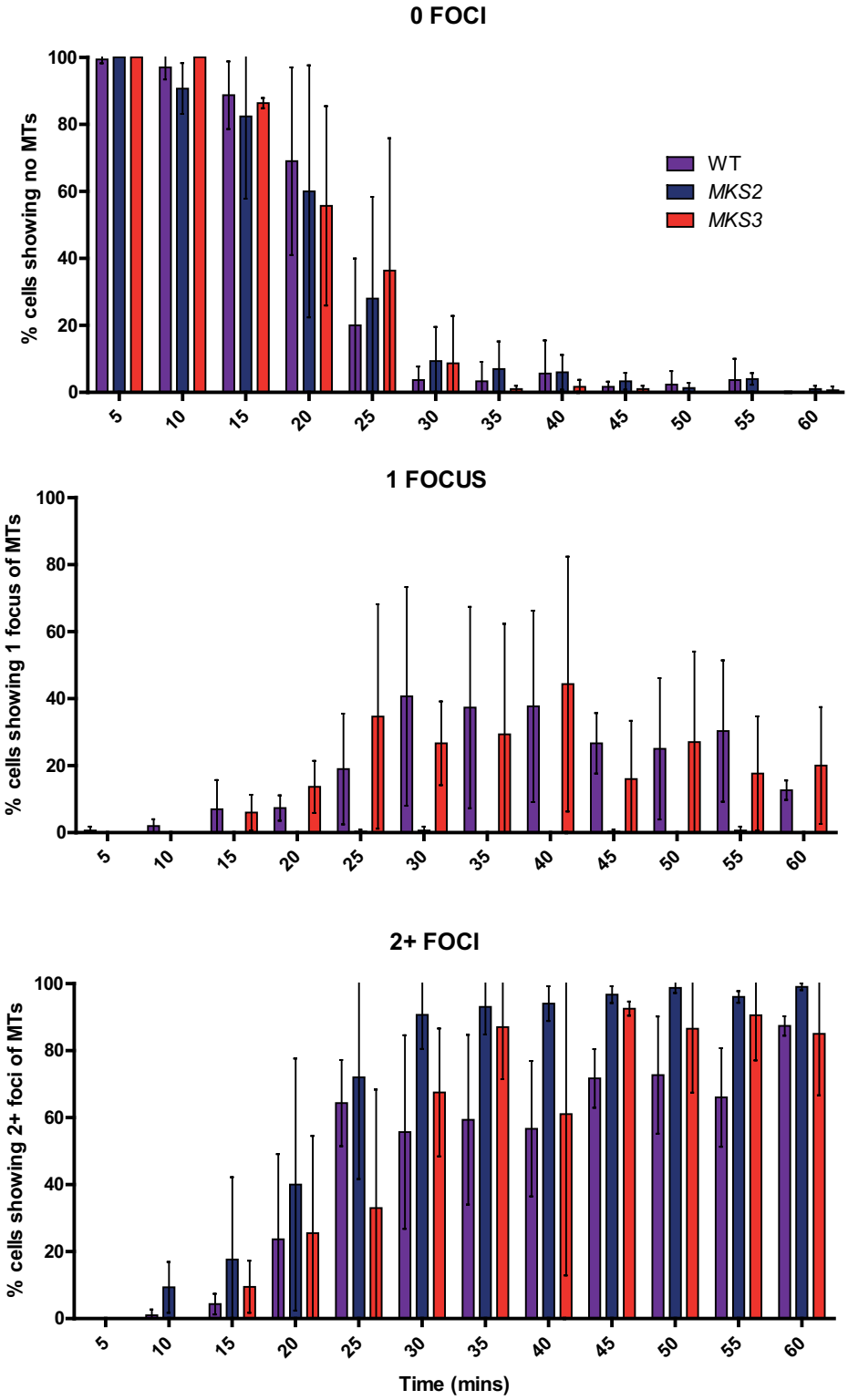

FIGURE 6.4: Tyrosinated MTs appear to emanate from an increased number of foci in *MKS2* patient cells.

Graphs report the mean percentage of cells demonstrating the displayed number of foci +/- SD. Tyrosinated MTs show no site of emanation initially, but gradually MTs positive for anti-YL1/2 binding emanate from a single or multiple sites in roughly equal numbers between wild-type and *MKS3* patient cells, and multiple sites in *MKS2* patient cells significantly more frequently ($p<0.001$, $\chi 2$).

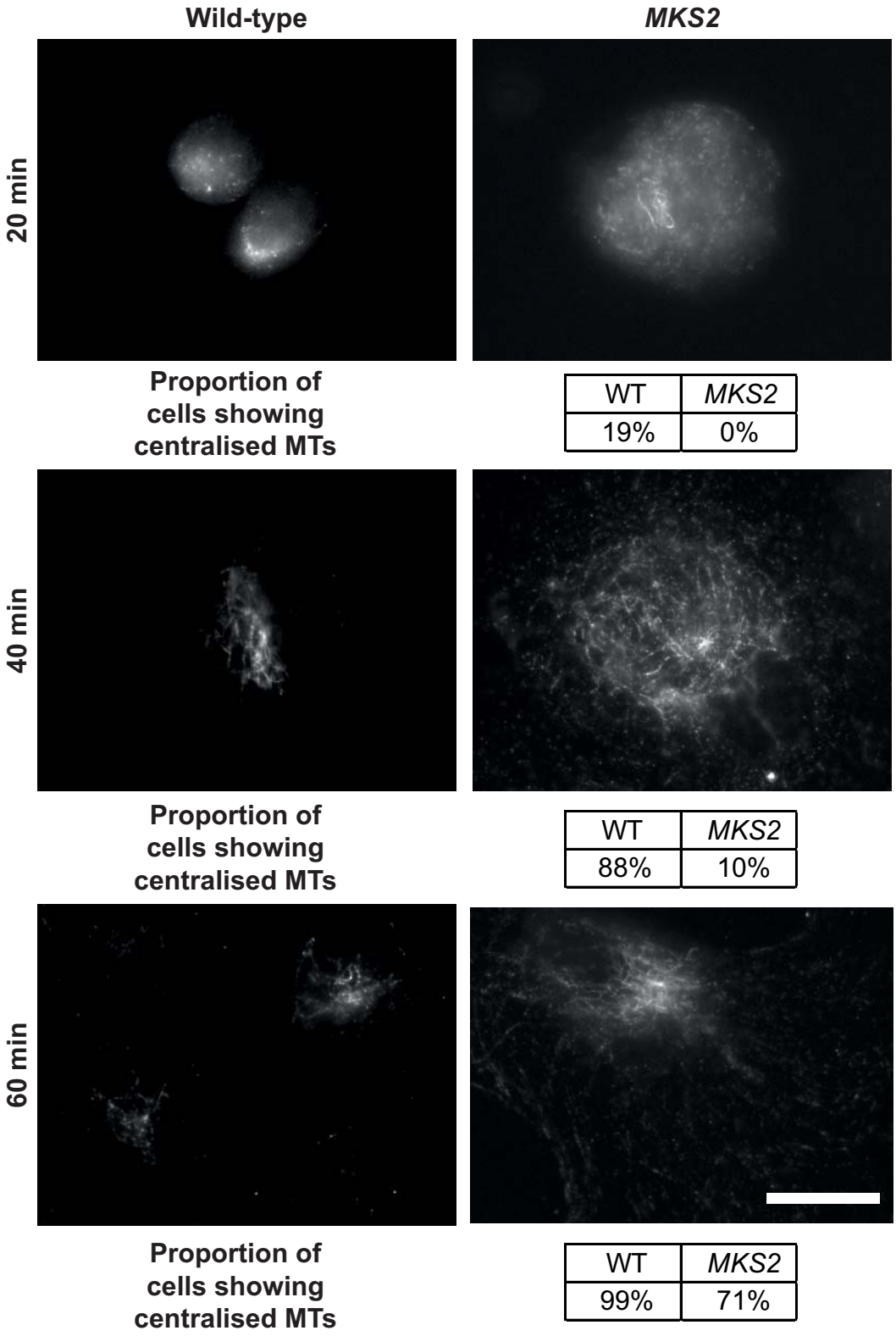

FIGURE 6.5: MT acetylation remains dispersed for longer in *MKS2* cells. Acetylated MTs visualised using anti-acetylated tubulin and representative images are displayed, along with the percentage of cells demonstrating centralised MTs at these time points. Acetylated MT dispersal persists for 50 minutes in *MKS2* patient cells, but condenses 30-40 minutes after plating in control cells and, to a lesser extent, in *MKS3* patient cells. Scale bar represents 20 μm.

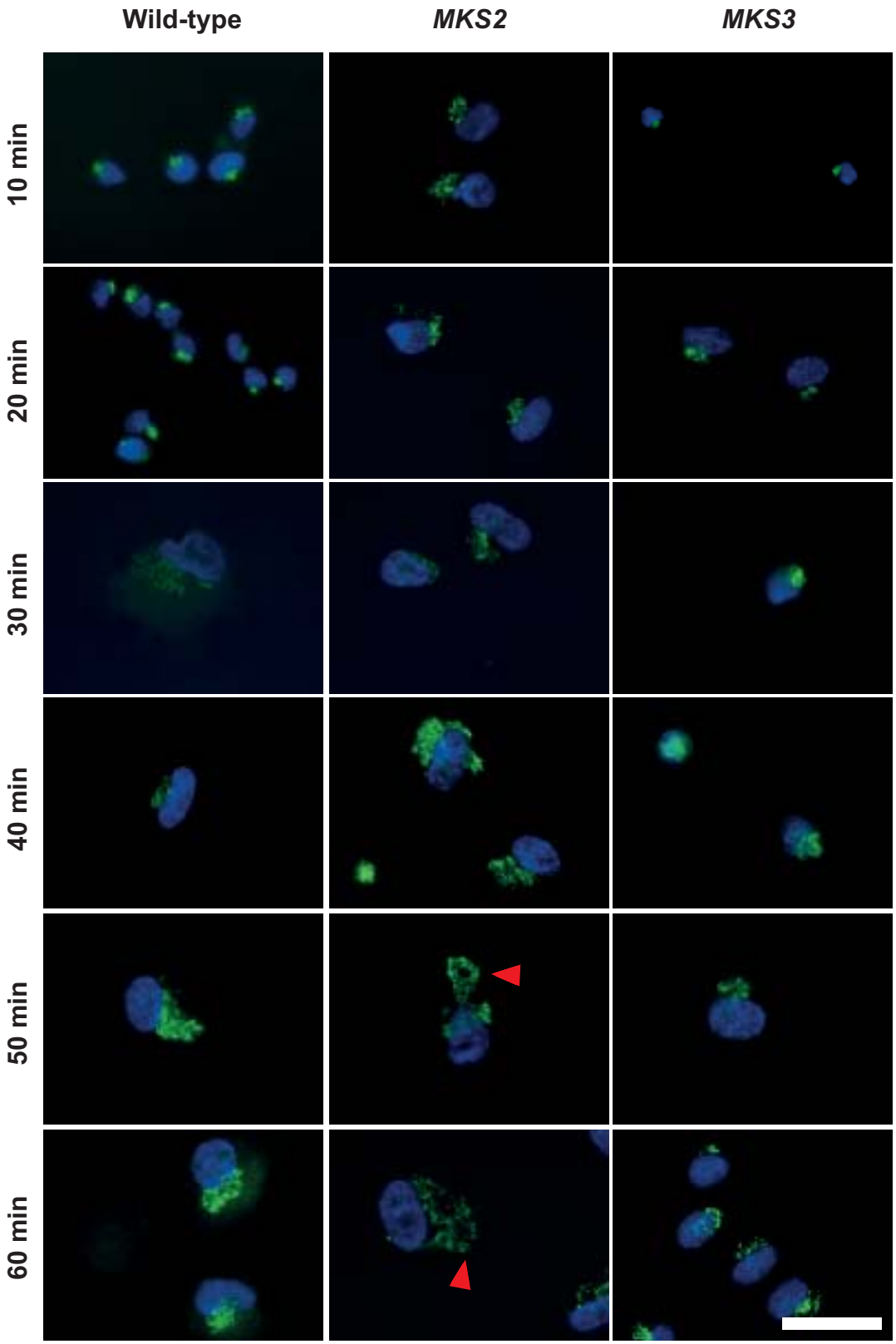

FIGURE 6.6: *MKS2* patient cells reveal Golgi dispersal 40-50 mins after plating.

Golgi was visualised using anti-GM130 (green), and the nucleus using DAPI (blue). Golgi disperses in *MKS2* patient cells (red arrowheads), but not in control or *MKS3* patient cells, starting 40 mins after plating. Scale bar represents 40 μm.

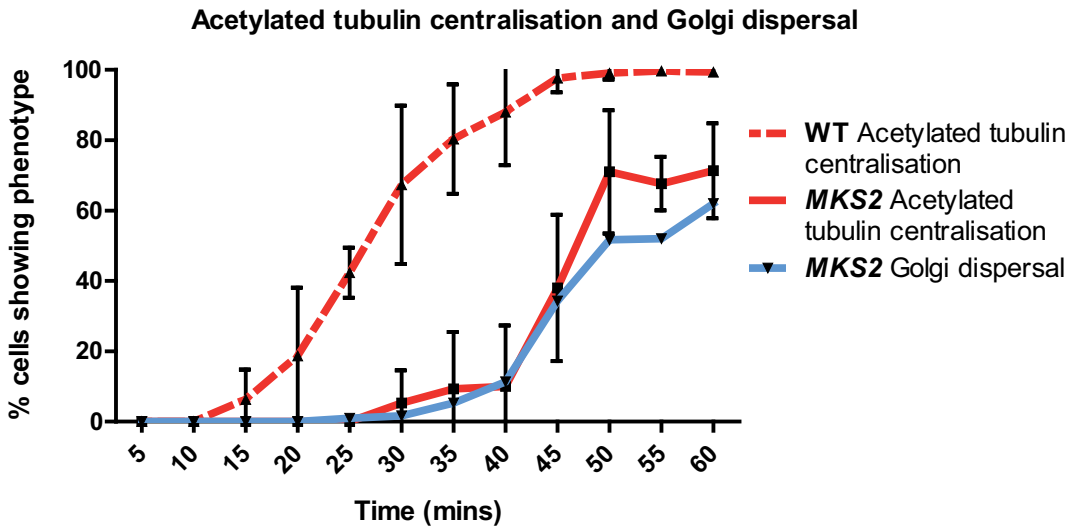

FIGURE 6.7: Acetylated tubulin centralises later and to a lesser extent in *MKS2* patient cells, concurrently with Golgi dispersal.

Graphs report the mean percentage of cells with the relevant phenotype +/- SD. The proportion of cells demonstrating centralisation of acetylated tubulin staining in the first hour after plating is highly significantly different between control and *MKS2* patient cells ($p<0.001$, $\chi 2$). At an identical time point to centralisation of acetylated tubulin staining, the Golgi complex disperses in *MKS2* patient cells.

Centralisation of acetylated tubulin appears to occur concurrently with Golgi dispersal in *MKS2* patient cells (*blue line, Figure 6.7*), suggesting that these defects may be directly or indirectly connected.

In Chapter III, I demonstrated that the actin defects occur around 40 minutes after plating in *MKS2* patient cells. The present results therefore indicate that the MT defects are the first to occur - differences arise before 20 minutes for all MTs and tyrosinated microtubules, followed by altered behaviour of the Golgi, acetylated microtubules and actin defects (simultaneously).

These data, together with the data from Chapter V, imply that *TMEM216* mutations (in *MKS2* patient cells) first cause MT defects; this may be due to aberrant centrosomal nucleation or anchoring of minus ends, or through inappropriate breakage or tethering of MTs. Subsequently, this appears to have an effect on MT stability, as indicated by the prolonged dispersal of acetylated tubulin staining throughout the cytoplasm. How MT defects interacted with Rho hyperactivity, or with the actin and Golgi defects (which temporally coincided with changes to acetylated tubulin localisation), however, was unclear from these data alone. Importantly, these defects occur before a cilium would normally develop, which would be observed over a period of hours, as opposed to minutes (Seeley and Nachury, 2010). These data are therefore indicative of intrinsic defects to cytoskeletal development.

TMEM67 mutations (in *MKS3* patient fibroblasts) did not reveal any of these cellular defects within the first hour of plating, but in Chapters III to V, I found that these defects are mimicked in these cells. I did not determine a temporal order of appearance of actin, MT and Golgi defects in *MKS3* cells (other than determining that these all occur around 3-4 days following plating), but would presume that these followed a similar temporal order. However, the length of time taken for these defects to arise means that it is possible that these occur downstream of ciliary dysfunction.

Rho pathway components affect microtubule behaviour

I next aimed to test whether the MT foci are altered by manipulation of ROCK pathway components, which are implicated in the prominent actin bundle formation in Chapter IV, and in previous work (Dawe *et al*., 2009; Valente *et al*., 2010). I transfected control and *MKS2* patient cells with constitutively active and

dominant negative Rho, and with constitutively active (△3) ROCK and examined α-tubulin (as a MT marker) and γ-tubulin (as a centrosomal marker). *MKS3* patient fibroblasts were not examined as I had not resolved when changes to MT foci appear in these cells

I demonstrated that transfection with constitutively active Rho (Q63L), dominant negative Rho (T19N) (*Figure 6.*8) and constitutively active ROCK (*Figure 6.*9) lead to MTs emanating from single centrosomal foci in >75% of *MKS2* patient cells (n= 300 cells across 3 repeats of each experiment). This is not observed in any *MKS2* patient cells in the absence of these constructs. These data imply that, similarly to the actin defects, dysregulation of Rho pathway signalling may also be connected to the MT defects in MKS patient cells.

Microtubule defects and actin defects occur independently in MKS patient cells

To ascertain whether the MT defects influence actin defects (and vice versa), I treated wild-type and MKS patient fibroblasts either with taxol (to stabilise microtubules) and nocodazole (to disassemble microtubules) – both 5 minutes after plating (i.e. preceding microtubule defect occurrence) – and examined actin filaments an hour after plating. In another experiment, I treated cells with jasplakinolide (to stabilise actin filaments) or latrunculin B (to prevent actin assembly) – both 30 minutes after plating (i.e. preceding actin defect occurrence) - and visualised microtubules, fixing at an hour after plating, as cytoskeletal defects have occurred by this point in *MKS2* patient cells (n= 3 experiments under each drug treatment).

Treating cells with nocodazole or taxol had no effect on the formation of cell body actin, but prevented the formation of *MKS2*-associated prominent actin bundles (*Figure 6.10*). This indicates that MKS-associated actin phenotypes likely occur downstream of the MT defects seen in *MKS2* patient cells – disruption of MT organisation rescues normal actin bundle formation.

Treatment with jasplakinolide and latrunculin B had equivalent effects on the MT cytoskeleton of all three fibroblast lines. Jasplakinolide caused MTs to elongate and tubulin staining to condense around the cell centre, with no identifiable focus of emanation in any cell line (*Figure 6.11*). Latrunculin B,

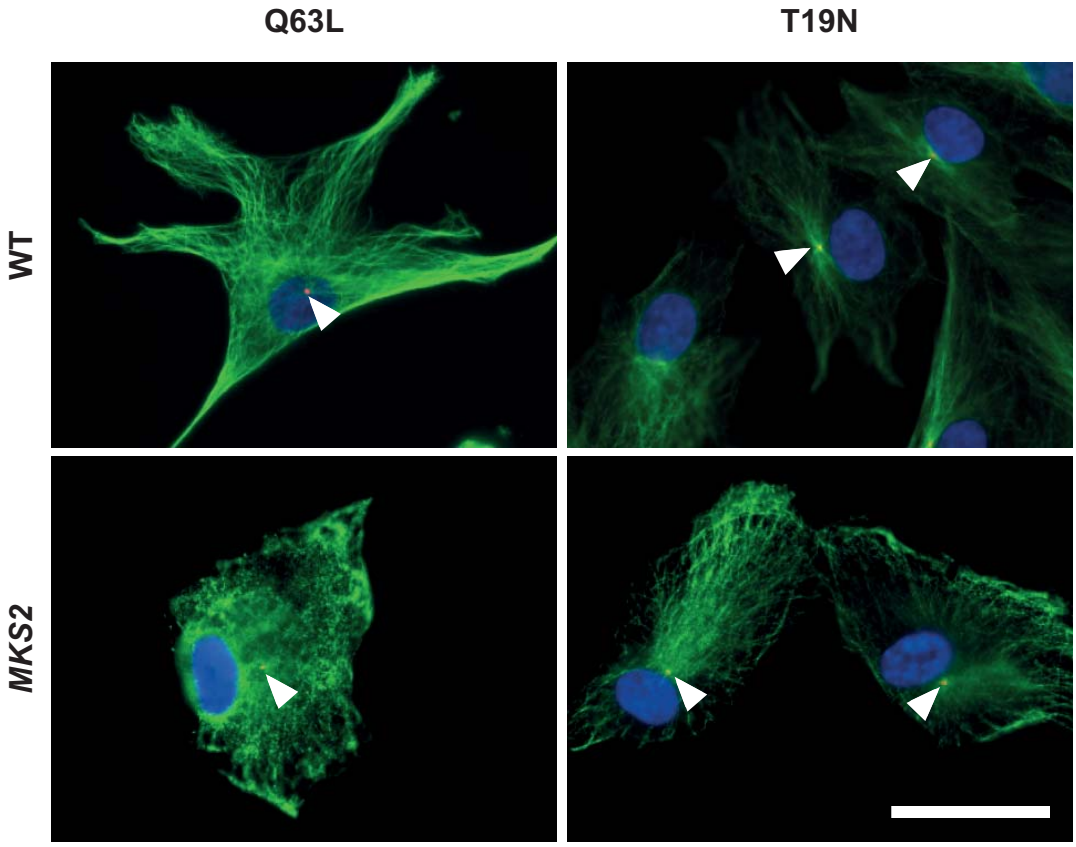

FIGURE 6.8: Dominant negative and constitutively active Rho decrease the number of MT foci in *MKS2* patient cells.

MTs visualised using anti-α-tubulin (green), centrosomes visualised using anti-γ-tubulin (red and white arrowheads) and nucleus visualised using DAPI (blue). Electroporation with Q63L (constitutively active) and T19N (dominant negative) Rho generates MTs emanating from single foci more frequently in *MKS2* patient cells, but electroporation with these constructs has no effect on control cells. Scale bar represents 40 μm.

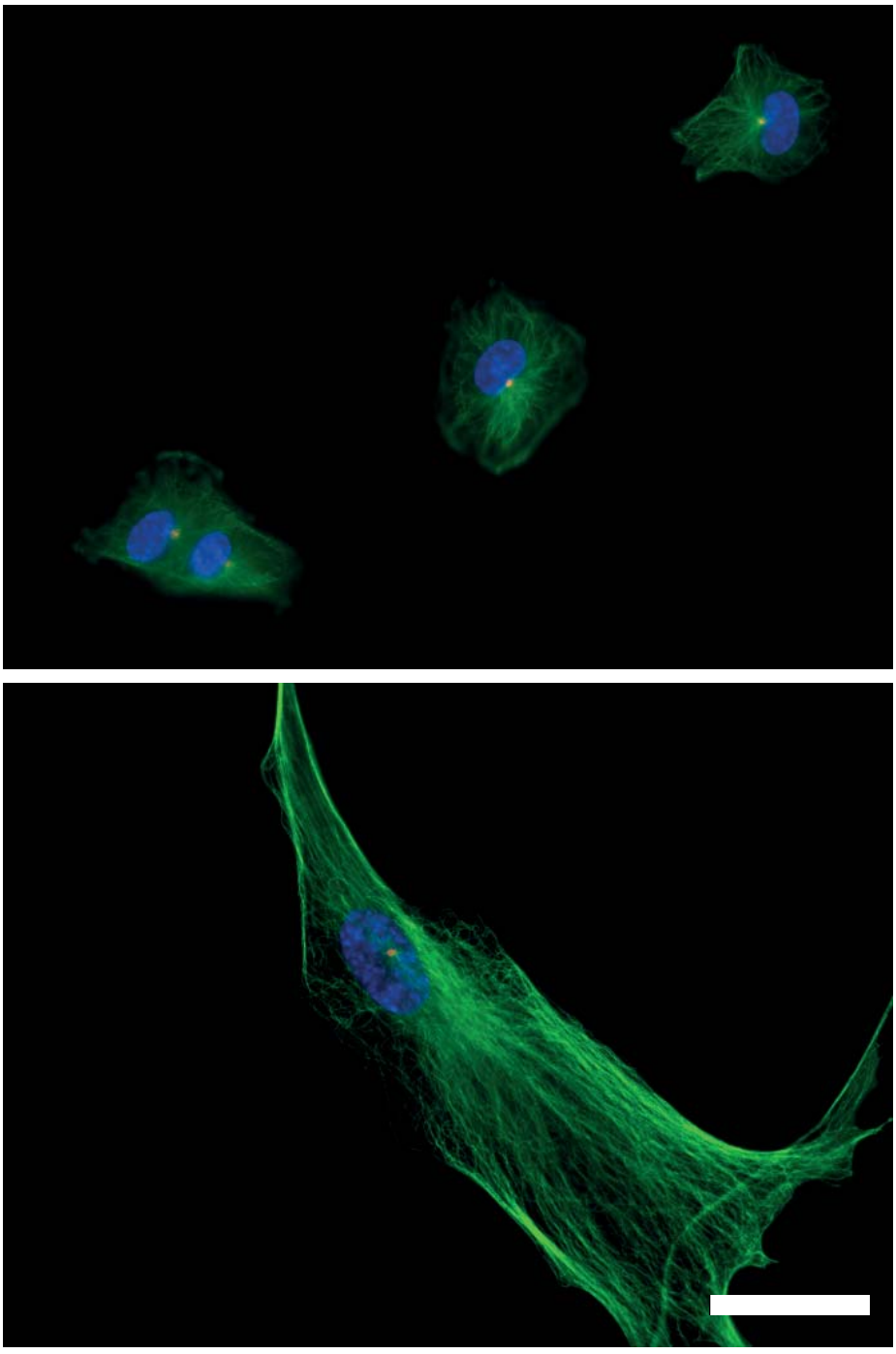

FIGURE 6.9: Constitutively active ROCK affects the number of MT foci in *MKS2* patient cells.

MTs visualised using anti-α-tubulin (green), centrosomes visualised using anti-γ-tubulin (red) and nucleus visualised using DAPI (blue). MTs emanated from single foci in *MKS2* patient cells more frequently following transfection with constitutively active ROCK. Scale bar represents 40 μm.

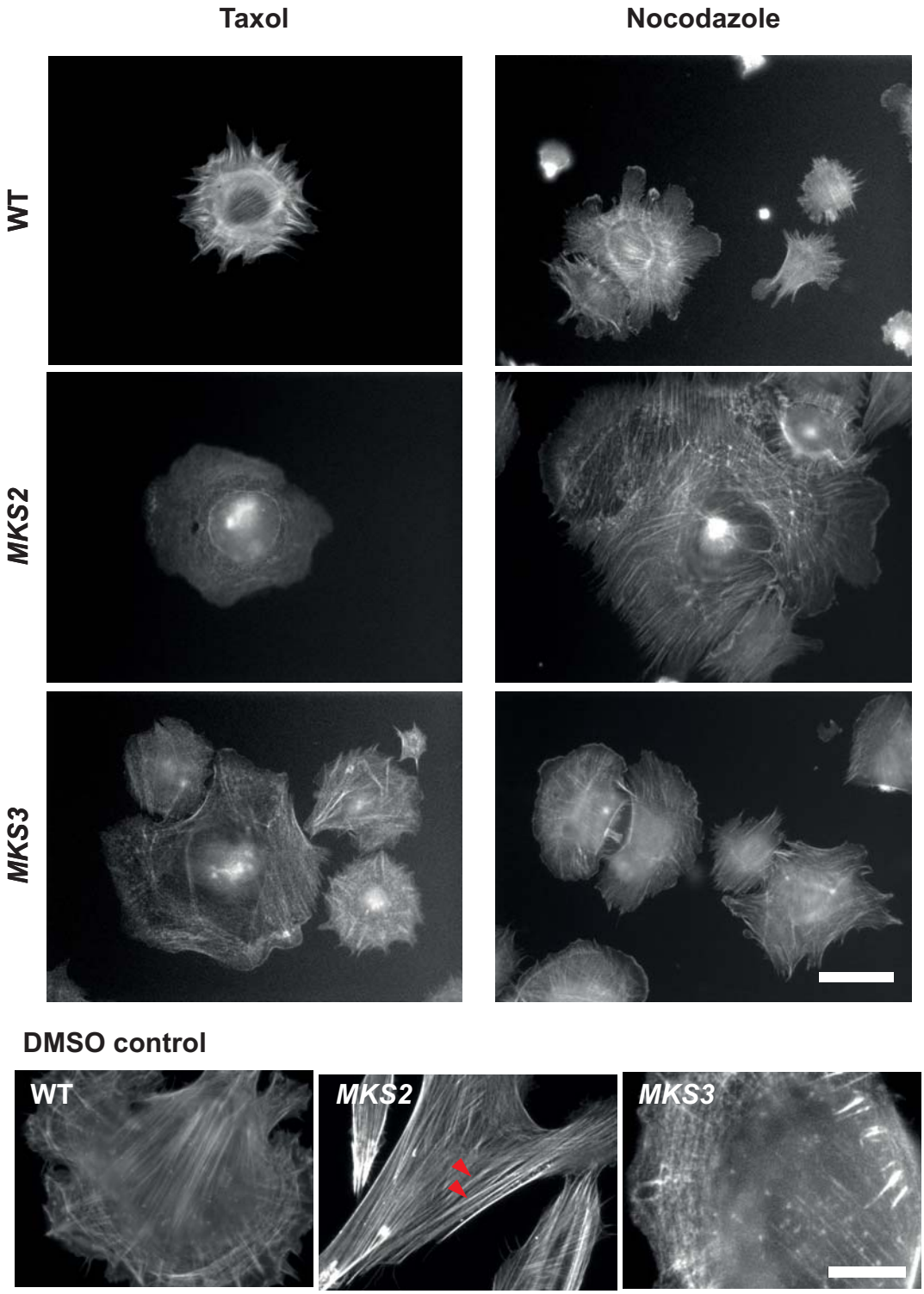

FIGURE 6.10: MT disassembly and stabilising drug treatments cause MKS-associated prominent actin bundles to disassemble, but have no effect on normal intracellular actin structures.

Cells were plated for 5 mins, drug-treated with taxol to stabilise microtubules or nocodazole to disassemble microtubules, then actin was fixed and visualised using fluorescently-labelled phalloidin 1 hour after plating. Taxol and nocodazole both cause the *MKS2* prominent actin filaments observed following DMSO control treatment (red arrowheads) to disassemble, but other actin structures remain intact. Scale bar represents 40 μm or 20 μm for DMSO control.

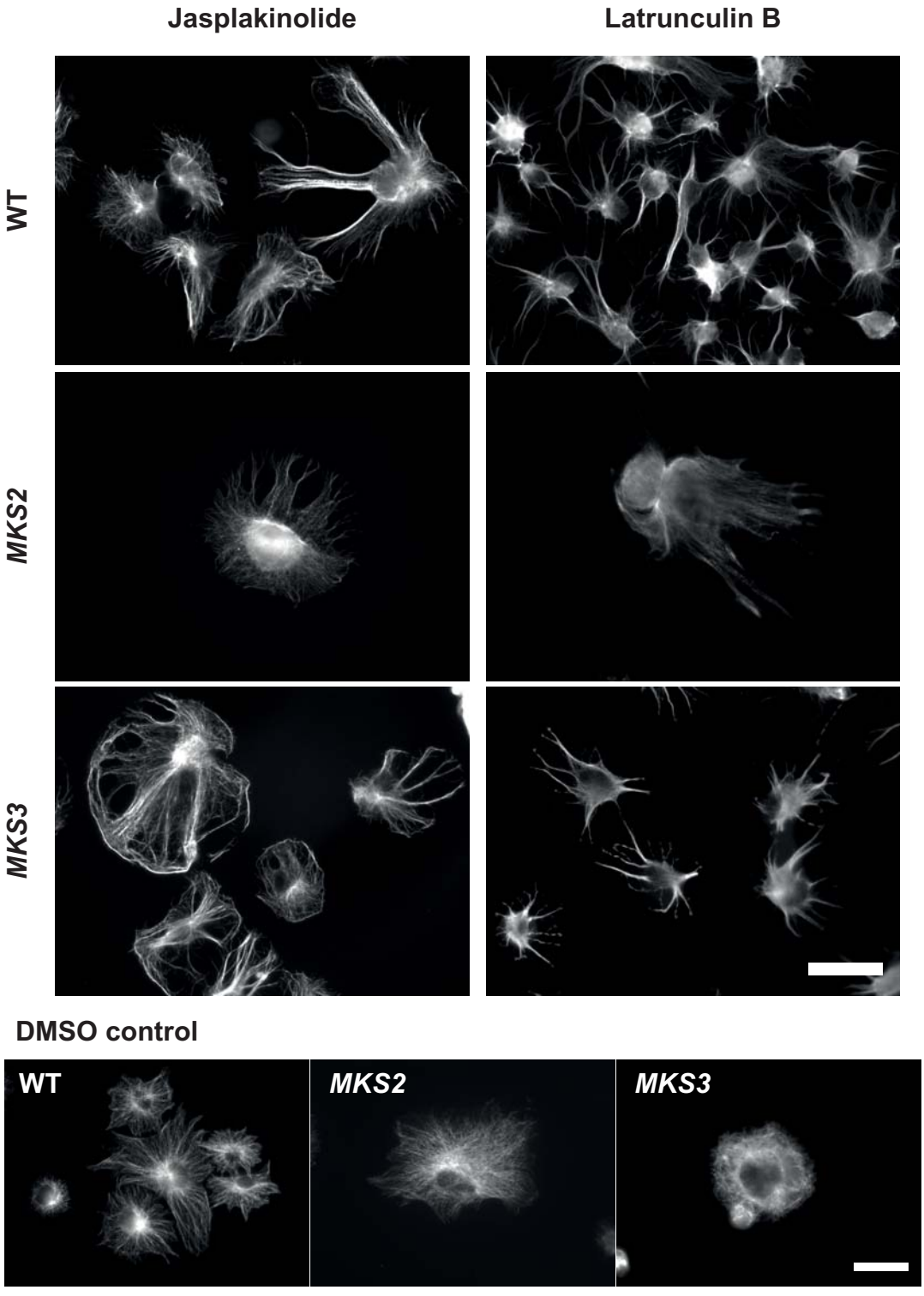

FIGURE 6.11: Actin drug treatments alter MT organisation similarly in all cell lines.

Cells were plated for 30 minutes prior to addition of jasplakinolide (to stabilise actin filaments) or latrunculin B (to prevent actin assembly), then fixed 1 hour after plating, using immunofluorescence to visualise microtubules (anti-α-tubulin). Compared with the DMSO control, both drugs caused disruption to the MT cytoskeleton. However, *MKS2* patient cells appeared different to control cells following either drug treatment. Scale bars represent 40 μm.

similarly, caused rounding of the cell body and elongated protrusive MT structures to form in all cell lines, with no identifiable focus of MT emanation (*Figure 6.11*). Neither of these drug treatments appeared to alter the number of MT foci present in *MKS2* any more than in the other cell lines; actin-dependent cell shape changes are likely behind this, so I can come to no conclusions as to the dependency of the MT defects on the actin defects.

Defects are expected to occur independently of ciliogenesis

It could be argued that many of these defects are merely a downstream consequence of ciliogenesis failure. To test this, I plated wild-type cells in either the serum-containing medium used throughout all of the experiments or serum-free medium. A low proportion of cells were ciliated under serum-containing conditions when compared to serum-free conditions (between 6-10% of 300 cells examined across 3 experiments) (*Figure 6.12*). This indicates that, even if MKS patient cells are attempting ciliogenesis, very few would be doing so under experimental conditions.

6.3 Discussion

In the present chapter, I aimed to question the temporal relationships between the actin, MT and Golgi defects in MKS patient cells in order to elucidate a primary cause, or at least an order of phenotypes to infer a causal relationship.

I found that defects in the MTs are the first to occur. These defects took as little as 10 minutes to become established, in the case of tyrosinated and total tubulin, in which MTs were observed emanating from multiple or no obvious foci in *MKS2* patient cells. Actin defects and Golgi defects then occurred around 30-40 minutes following plating and appeared to temporally coincide with the condensation of acetylated microtubules to the cell centre, i.e. the stabilisation of microtubules at the cell centre. These three phenotypes appear concomitant, but I cannot conclude from the current data whether alterations to actin, MTs, or a source upstream of these, are responsible for the Golgi defects.

The number of MT foci appear reduced to a single focus in *MKS2* patient cells upon ROCK signalling pathway activation or inactivation, implicating

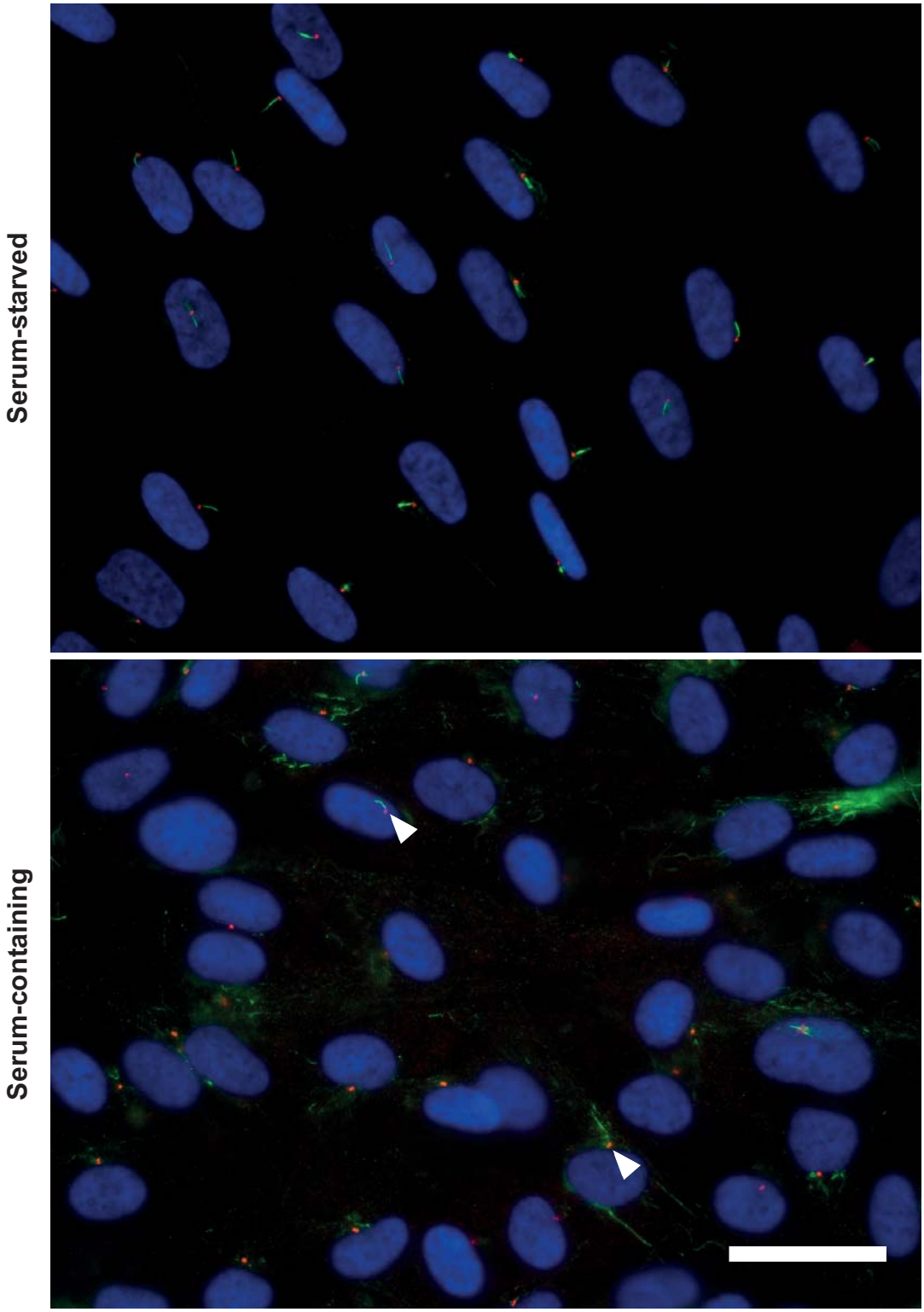

FIGURE 6.12: A low percentage of wild-type cells are ciliated under experimental conditions when compared with serum starvation conditions. Cilia visualised using anti-acetylated-tubulin (green), centrosomes visualised using anti-γ-tubulin (red) and nucleus visualised using DAPI (blue). Cilia in serum-containing conditions indicated with white arrowheads. Few cilia are present in control cells in serum-containing, experimental conditions. Scale bars represent 40 μm.

dysregulation of this pathway as a causative agent of the increase in number of MT foci in MKS. When paired with the likely ties with the actin defects, these data strongly implicate Rho signalling in generating MKS phenotypes. Reinforcing this, the MT and actin defects were found to occur independently of each other.

Besides being the first instance of MT defects being reported in MKS, these results are, furthermore, the first to connect the previously described dysregulation of Rho signalling (Adams *et al*., 2011; Dawe *et al*., 2009; Valente *et al*., 2010) to this phenotype, and to identify changes to the actin and MT cytoskeleton as temporally separable phenotypes in this disease. This is important as it enables us to begin to construct an order of defects, providing clues as to the primary role of MKS proteins.

Microtubule-actin interactors have important cellular functions

To effect capricious cellular function, such as motility, the cytoskeleton must remain adaptable; for this, correctly organised and structurally functional MTs and actin must interact. A variety of structures and proteins enable their cooperation, such as focal adhesions, motor proteins (e.g. myosin and kinesin), MT-actin crosslinking factor (MACF) and formins. Based on the results reported in this thesis, MKS proteins TMEM216 and TMEM67 may function in a similar role, or may be constituents of such structures or proteins.

Focal adhesions, actin-linked structures involved in cell locomotion through extracellular matrix attachment, are built and become contractile in a Rho-regulated process, also serving as sites of signal transduction (Burridge and Chrzanowska-Wodnicka, 1996). MTs also interact with these structures in order to establish cell polarity, which has a dual role. Firstly, focal adhesions stabilise the MT (Kaverina *et al*., 1998), which explains how MTs specifically stabilise at the leading edge; secondly, MTs deliver localised doses of relaxing signals to the focal contact to stimulate disassembly as the focal adhesion moves rearward with respect to the moving cell (Kaverina *et al*., 1999). By this method, MTs are able to modulate the behaviour of the actin cytoskeleton.

Focal contact formation and maturation is controlled by a complex interplay of the effects of Rho GTPases on cell contractility and MT stability (Ng *et al*., 2014). Alterations are reported in focal adhesion structure or function in a

number of ciliopathies, indicating that such MT-actin crosstalk may be a topic of interest for subsequent study in the ciliopathies. RPGR-deficient cells, a model with reduced number of cilia, demonstrate focal adhesion kinase dysregulation and impaired attachment to fibronectin (Gakovic *et al*., 2011). Similarly, inversin/nephrocystin-2-null MEFs have diffuse focal adhesion distribution and impaired directional cell migration (Veland *et al*., 2013). Furthermore, *Bbs4-, 6-* and *8*-deficient cells demonstrate overabundant focal adhesions, which are associated with increased levels of active RhoA (Hernandez-Hernandez *et al*., 2013). Finally, a number of nephrocystins are known to constitute part of the focal adhesion kinase complex (Simms *et al*., 2009). It is of note that we also observe alterations to focal adhesion morphology in MKS patient cells on certain substrates (Meadows and Dawe, unpublished). These alterations may occur up- or downstream of alterations to actomyosin contractility and/or alterations to MT organisation and stability in these cells, which remains to be determined.

Evidence indicates that motor proteins may be crucial to MT-actin interactions; for instance, myosin IIB and V (the actin-based motors) localise to MTs (Kelley *et al*., 1996; Waterman-Storer and Salmon, 1999). Myosin IIB is of particular interest as it localises to MT ends in the leading lamellipodia of migrating cells (Kelley *et al*., 1996), which may be associated with the altered MT foci in MKS patient cells; here it is thought that myosin IIB provides retrograde flow of actin or vesicles along MTs from the leading edge (Kelley *et al*., 1996; Waterman-Storer and Salmon, 1999). Myosin IIB is also required for centriole migration during ciliogenesis (Hong *et al.*, 2015) and coordinates actin dynamics and MT acetylation to effect biogenesis of the primary cilium (Rao *et al.*, 2014). When actin assembly is blocked in migrating cells, MTs extend into the lamellipodium without undergoing catastrophe, reinforcing their functional connection (Waterman-Storer and Salmon, 1999). Furthermore, kinesin, the MT plus end-directed motor protein, localises to stress fibres upon MT depolymerisation (Okuhara *et al*., 1989). Association between these cytoskeletal components is complex, and is crucial for appropriate cellular movement.

In Chapter IV, I reported differences in myosin and phosphomyosin localisation in *MKS2* patient fibroblasts. If MKS proteins function in myosin-dependent actin-MT interactions, this provides a possible explanation as to why

MT minus end placement is altered. However, it is more probable that altered myosin and phosphomyosin localisation is a downstream consequence of forming prominent actin bundles.

MACF co-localises with actin stress fibres and ruffles, and with detyrosinated MTs, stabilising them and tethering them to actin (Leung *et al*., 1999). MACF1, alongside ELMO (engulfment and motility) proteins, is also implicated in the formation and persistence of Rac-induced actin protrusions, essential structures for directed cell migration, through its interaction with actin and with MTs (Margaron *et al*., 2013). MACF1-deficient keratinocytes fail to efficiently migrate due to the transience of the polarised membrane; MTs at the plasma membrane in these cells do not undergo typical pause and catastrophe, nor tethering to the actin cytoskeleton. This occurred downstream of mDia activation and was also paired with failure of the MTOC and Golgi to reorient (Kodama *et al*., 2003), reminiscent of MKS phenotypes. Such a correlation is indicative of how intertwined these cellular features are, and illustrating the complexity of deducing the underlying function of MKS proteins.

Formins are another example of MT-actin interactors that may be of interest to study in the context of MKS proteins. These nucleate actin filament formation from the barbed end, and the best studied of which are Rho GTPase effectors mDia1, -2, and -3 (Goode and Eck, 2007). Formins such as mDia1 and -2 are, independently of their actin-based functions, tasked with stabilisation of MTs oriented towards the leading edge (Bartolini *et al*., 2008; Ishizaki *et al*., 2001; Palazzo *et al*., 2001), regulating integrin signalling here (Palazzo *et al*., 2004). These are posited to contribute to cell polarity through their involvement in vesicular trafficking and/or effects on the cytoskeleton at the cell front (Bartolini *et al*., 2008; Lin *et al*., 2002).

Two formins, DIA1 (human mDia1 orthologue) and FMNL1, are required for MTOC reorientation in T cells (Gomez *et al*., 2007), a process perturbed in MKS. This MTOC reorientation is Cdc42- and Rac1-dependent (Gomez *et al*., 2007; Stowers *et al*., 1995), and requires appropriate MT dynamics (Li and Gundersen, 2008), providing support for a Rho-associated cause of this phenotype in MKS.

Inverted formins (INF) -1 and -2 are of particular interest to us as they display a number of features associated with MKS. INF1 associates with MTs and, when its expression is induced in fibroblasts, prompts actin stress fibre

formation, the acetylation of MTs (features observed in MKS patient fibroblasts), and MT-actin coalignment (Young *et al*., 2008). INF2 associates with Cdc42 and Rac1, regulates vesicular transport and mediates the detyrosination of MTs that is necessary for MTOC reorientation, all independently of its actin polymerisation and depolymerisation activities (Andres-Delgado *et al*., 2010; Madrid *et al*., 2010). Furthermore, MT acetylation capacity has been reported to be a function of the FH2 domain, meaning this is likely a general function of formins (Thurston *et al*., 2012).

Formins are effectors and modulators of Rho GTPase signalling; when Rho GTPases bind their N-terminal Rho GTPase-binding domain, autoinhibition of the diaphanous-related formins is alleviated, allowing the FH2 domain to nucleate actin filament polymerisation, but the activated formin can recruit Rho GTPase components. For instance, it is thought that RhoA activates FH1/FH2 domain-containing protein 1 (FHOD1) through ROCK, following which FHOD1 is hypothesised to associate with Rac to inhibit lamellipodium generation (Gasteier *et al*., 2003; Young and Copeland, 2010). In addition to actin stress fibre production, RhoA may induce MT stabilisation (Cook *et al*., 1998); this would promote MT growth towards the leading edge, stimulating Rac1 activity, and thus additional actin protrusions to form.

The actin structure generated upon formin activation (and thus the cellular function) is dependent on a number of factors, such as the associated GTPase, the formin activated and the cellular context (Young and Copeland, 2010). For example, RhoB induces mDia1 or -2-instigated endosome association with actin filaments, which impedes their motility (Fernandez-Borja *et al*., 2005; Wallar *et al*., 2007).

These previous data indicate a role of these actin-MT interactors in posttranslational modification of MTs, and their involvement with Rho signal transduction. These data reveal formins as potential proteins of interest in study of the aetiology of MKS. It is possible that MKS proteins have a similar role to formins, or possibly even interact, whether directly or indirectly, with formins. Multiple MT-actin interactors function in stress fibre and actin ruffle formation, MT stabilisation, canonical and non-canonical Wnt signalling, MTOC reorientation, cell polarity and directed cell migration. These are all features with reported defects in MKS and the other ciliopathies, meaning that MKS proteins

having a role in MT-actin interaction may prove the most parsimonious explanation for all of these observed defects.

This hypothesis is supported in study of other ciliopathies; polycystic kidney disease protein PKD2 interacts with mDia1 (Rundle *et al*., 2004). However, this has not yet been demonstrated in MKS, and is not a topic of active study as evidence of cytoskeletal involvement in ciliopathy is a novel area of research. This role of MKS proteins could, however, also explain failures in ciliogenesis; MTs are the major axonemal component and involved in ciliary vesicle trafficking (Sorokin, 1962; Sorokin, 1968; Sotelo and Trujillo-Cenoz, 1958). Furthermore, centriole migration is actin- and MT-dependent (Boisvieux-Ulrich *et al*., 1987; Boisvieux-Ulrich *et al*., 1990; Burakov *et al*., 2003), so dysfunction of a component involved in cytoskeletal interaction could have widespread effects.

Microtubule-actin interactors at the Golgi

A number of the aforementioned MT-actin interactors, in addition to a plethora of other proteins, have a functional role at the Golgi complex. If MKS mutations do represent an alteration to these, this may explain the Golgi dispersal occurring subsequently to the MT defects, and in conjunction with the actin defects.

MACF1 is one such protein: it interacts with p230 to achieve transport of GPI-anchored proteins from the TGN to the plasma membrane, along the MT and actin cytoskeleton (Kakinuma *et al*., 2004). MACF1 exists in multiple isoforms; MACF1b is predominantly localised to the Golgi, where it maintains Golgi structure; siRNA against MACF1 induced Golgi dispersal (Lin *et al*., 2005) similar to that seen in MKS patient cells.

WHAMM is a protein with similar function; this is Golgi-associated, with MT-binding and Arp2/3-mediated actin nucleation capabilities that occur independently of each other. Vesicles are recruited by WHAMM and remodelled into tubules, with WHAMM proposed to act as a physical link to the MTs (orchestrating membrane tubulation) and actin (promoting tubule elongation) (Campellone *et al*., 2008; Shen *et al*., 2012). RhoD is also implicated here, binding WHAMM to effect changes in cell attachment and actin dynamics, and thus cell migration (Gad *et al*., 2012). RhoD also localises to early endosomes

and the Golgi and – as the binding partner of WHAMM – is similarly vital to anterograde vesicular trafficking from the ER to the plasma membrane (Blom *et al*., 2015). We cannot resolve the exact details of the Golgi dispersal observed in MKS, but these data indicate that the MKS proteins may, therefore, have additional, undiscovered functions that are analogous to those of such MT-actin binding proteins.

It should be noted that, although MTOC and Golgi positioning events are evidently connected by their links to the cytoskeleton and Rho signalling (e.g. ROCK inhibition accelerates cell migration but inhibits MTOC and Golgi positioning), they are separately controlled. Disruption of MTs inhibits MTOC polarity, whereas Golgi polarisation is actin- and ABP-dependent (specifically upon Arp2/3, WASP and the FH2 domain of mDia1), but not vice versa (Magdalena *et al*., 2003), concomitant with my observation of independent MT and actin defects. Additionally, Rho stimulation of MT stability is independent of actin stress fibre formation (Cook *et al*., 1998), all supporting a conclusion that MKS proteins operate upstream of cytoskeletal defects.

A role of MKS proteins in tethering the cytoskeleton to membranes is a reasonable hypothesis. If these were acting as membrane-cytoskeleton tethers, responsible for the dynamics of both, perturbation would result in a number of the changes observed in the cell, such as alteration of post-translational modifications to and site(s) of nucleation of the MT cytoskeleton, actin stress fibre development, aberrant ciliogenesis and, downstream of these, Golgi dispersal.

Evidence in support of this hypothesised role of ciliopathy proteins is beginning to accumulate. CEP290 is thought to be a key Y-link constituent, binding the ciliary membrane and MTs (Craige *et al.*, 2010; Drivas *et al*., 2013); TMEM67, associated with filamin A, binds along basolateral actin fibres (Adams *et al*., 2011); and numerous other MKS proteins are known to associate with post-Golgi vesicles along MTs, in addition to localising to many other membranous structures (Collado-Hilly *et al*., Cilia 2014 Conference (unpublished); Lee *et al*., 2012).

Rho pathway involvement in MT-actin interaction

RhoA and Rac1 induce generation of various actin structures, and certain phases of MT dynamic instability can effect activation of these proteins. For instance, RhoG-activated MT growth in fibroblasts (but not the presence of MT polymer alone) causes Rac1 activation, leading to actin polymerisation and actin protrusive structure formation at the leading edge (Gauthier-Rouviere *et al*., 1998; Waterman-Storer and Salmon, 1999).

Taken with my phenotypic observations and the data suggesting RhoA hyperactivation in the current patient cells, it is reasonable to alternatively posit a role of MKS proteins upstream of cytoskeletal defects and of Rho signal transduction. It may be that inappropriate activation of certain Rho signalling pathways causes these phenotypes; RhoD, for instance, is a WHAMM binding partner (Gad *et al*., 2012), together playing a key role in actin and MT functions, e.g. adhesion and migration.

Currently there is no data implicating ciliopathy proteins either as a tether, or functioning upstream of Rho to cause these phenotypes, but the data from my study, combined with the literature, provide insight as to how either of these may be the primary function of MKS proteins.

CHAPTER VII: GENERAL DISCUSSION

7.1 The roles of MKS proteins

Within this thesis I have attempted to establish the extra-ciliary roles of the MKS proteins, in order to deduce a model for how these proteins might function in a cell.

I have shown an involvement of MKS proteins in the regulation and organisation of the actin and microtubule (MT) cytoskeleton, in addition to affecting the structure of the Golgi apparatus. In agreement with my hypotheses, I revealed that alterations to the cytoskeleton, including prominent actin bundle formation, occur in a temporally-dependent manner, which was a novel finding. Furthermore, I described novel evidence of changes to the number of MT foci and defective post-translational modifications to the MT cytoskeleton (which coincided with Golgi dispersal) in MKS patient cells. In addition, I found that these defects appeared to occur downstream of ROCK pathway dysregulation. I have, therefore, demonstrated unreported extra-ciliary functions of the MKS proteins and begun an investigation into the signalling pathways underlying these functions.

From these data, and based upon evidence from current ciliopathy research, I therefore postulate three possible roles for MKS proteins within the cell, as follows.

MKS proteins are centrosome cohesion molecules

It is possible that the MKS proteins maintain centrosome integrity. I revealed that *MKS2* patient cells displayed numerous foci of pericentrin staining, but that the disorganised MTs of these cells observed to emanate from multiple foci did not appear to emanate from these pericentrin-containing points. If *MKS2* mutations lead to dissolution of the centrosome, loss of centrosome integrity may be the factor precluding MT emanation from a single centrosome.

This would lead to MT disorganisation. A fragmented centrosome could cause mechanical breakage of the MTs, leading to multiple MT networks across the cell, an observed phenotype. Such activity would make the MT network more dynamic in these cells as the number of MT ends would increase, which

allows more rapid polymerisation and catastrophe (Keating and Borisy, 1999; Yu *et al.*, 1994). However, the acetylated tubulin staining, a marker of stabilised tubulin, indicated the converse to be true – tubulin appeared to be stabilised throughout the cell.

Alternatively, increased tethering of MT plus- or minus-ends at these regions of dispersed fragmented pericentriolar material may occur, increasing the stability of the MTs. It may be that PCM components are mislocalised, i.e. not forming an intact centrosome by surrounding the centrioles, and spread through the cell in MKS. These would be observed as acentrosomal sites of MT origin. This hypothesis is supported by observations of acetylated tubulin dispersal and multiple acentrosomal foci in the *MKS2* patient cells. This scenario is possible; ninein, a PCM component, is frequently observed stabilising free MT minus ends in epithelial cells, resulting in numerous acentrosomal foci (Bartolini and Gundersen, 2006; Mogensen *et al.*, 2000). Furthermore, handover of MTOC function to acentrosomal sites is a common feature in epithelial polarisation, which features Par protein-dependent movement of nucleators, such as PCM components, away from the centrosome to an apical surface (Feldman and Priess, 2012).

In additional support, a previous study using live imaging of MTs demonstrated that split centrioles in cells depleted of BBIP10, a subunit of the BBSome (a ciliary structure, components of which are often associated with BBS), could nucleate but not anchor MTs (Loktev *et al.*, 2008). Similarly, *BBS4* silencing induced PCM1 mislocalisation and associated deanchoring of centrosomal MTs (Kim *et al.*, 2004), supporting the possibility of tethering as a role of centrosomal components such as MKS protein complexes.

However, the nocodazole washout demonstrated that MTs nucleate at multiple subcellular locations in *MKS2* patient cell. This means that aberrant nucleation – MTs nucleating from, not tethering at, acentrosomal sites or pericentriolar components besides pericentrin - appears to be the most probable cause of centrosome-dependent MT disorganisation in *MKS2* patient cells. Furthermore, it is of note that this defect occurs on such short time-scales that this is highly unlikely to be cilium-dependent. Nonetheless, it is possible that, subsequent to centrosome splitting, increased MT breakage and tethering may follow aberrant nucleation.

Similar defects in centrosome integrity or number have been observed in conjunction with a number of ciliopathies, including MKS models. A study of kidney tissue and cells from *MKS1* and *MKS3* patients, in addition to shRNA knockdown of *Mks1* and *Mks3* in IMCD3 cells, reported over-duplication of centrosomes and cilia in these. This implicates MKS1 and MKS3 in centrosome duplication although, notably, this paper defined multiple centrosomes based on γ-tubulin staining, without confirming these were intact or functional (Tammachote *et al.*, 2009); it is therefore possible that these cells also demonstrated split centrosomes. Importantly, the current results also imply that multiple 'centrosomal' nexuses may be functional in nucleating or tethering MTs in *MKS2* patient cells.

Nek5, a kinase involved in primary cilium functioning, has previously been reported to promote centrosome integrity through pericentriolar material recruitment, and to enhance the MT nucleation involved during mitotic centrosome separation (Prosser *et al.*, 2015), further coupling centrosome cohesion behaviour, the cilium and MT dynamics.

Depletion of BBS8 and BBIP10 in human RPE cells leads to increased centrosome splitting, which appears remarkably similar to the pericentrin staining that I observed in *MKS2* cells. BBS8 depletion, additionally, caused a reduction in pericentin levels, but cells were still able to generate cilia (Loktev *et al.*, 2008).

BBIP10 depletion also led to a BBSome-independent reduction in MT polymerisation and stabilisation, as demonstrated by a reduction in cytoplasmic MT density and, indirectly, also in acetylation. BBIP10 overexpression concordantly increased MT acetylation, despite no direct interaction with MTs; this was proposed to occur through BBIP10 inhibition of HDAC6 (Loktev *et al.*, 2008). SAS-1, a protein related to C2CD3 (which is affected in OFD syndrome), is critical in maintaining centriole integrity and can also bind and stabilise MTs, as indicated by acetylated tubulin staining, in *C. elegans* (von Tobel *et al.*, 2014).

This has implications for my data; we can establish from the above evidence that constituents of the centrosome responsible for its integrity can also nucleate and tether MTs elsewhere in the cell, and can implement the stabilisation of MTs. If MKS proteins have similar roles, whether individually or as a complex, mutations may cause not only loss of centriole integrity, but also

errors in anchoring and stabilising MTs. It also provokes question as to the activity of enzymes that may be interacting with MKS proteins – could an interacting enzyme be responsible for MT dynamics and/or post-translational modification?

Erroneous centrosome amplification is observed in polycystic kidney disease mouse models. Polycystin-1 (*Pkd1*) knockouts abrogate centrosome amplification (Battini *et al.*, 2008), and polycystin-2 (*Pkd2*) overexpression in a mouse transgenic line results in supernumerary centrosomes due to centrosome overduplication (Burtey *et al.*, 2008), although it is unlikely that this would be caused by similar pathways to centrosomal splitting.

Interestingly, SIRT2, a nicotinamide adenine dinucleotide-dependent deacetylase that mediates deacetylation of α-tubulin, is upregulated in *Pkd1* mutant and knockdown cells; overexpression of SIRT2 in IMCD3 cells leads to aberrant centrosome amplification, and depletion prevents centrosome amplification associated with polycystin-1 loss (Zhou *et al.*, 2014). This potentially provides an aetiological link from the increased numbers of "centrosomal protein" foci to enzyme-mediated changes in MT stability.

MAP4, a MT-associated protein that bundles and stabilises MTs (Olson *et al.*, 1995) and binds septin-2 within the ciliary axoneme, regulating ciliary length (Ghossoub *et al.*, 2013), is mutated in a few uncommon ciliopathic diseases characterised by short stature and microcephaly. The mutations in these diseases were also associated with centrosome amplifications, MT-dependent dispersal of the Golgi apparatus and shortened cilia (Zahnleiter *et al.*, 2015). These cellular phenotypes, particularly aberrant MT stability and concomitant Golgi dispersal, resemble the temporal correlation I reported between acetylated tubulin restriction to the cell centre and Golgi dispersal, making this result of interest.

A hypothetical role of MKS proteins in centrosome integrity is therefore supported by the current and previous data. Loss of these, or a functionally-similar centriolar protein or enzyme, may increase the centriole number or, alternatively, may tear apart current centrosomes. The latter seems more likely in the context of the current results as the pericentrin spots seem to display too much variation in size to constitute entire centrosomes. MKS proteins may fulfil such a cohesive function. Downstream of this, loss of such a protein would

affect MT stability, ciliogenesis and, potentially, Golgi organisation, structure and function.

MKS proteins tether the cytoskeleton to membranes

Another possibility is that MKS proteins act as cytoskeleton-membrane linkers. This is supported by evidence that *MKS1*-silenced *Paramecium* cells demonstrate detachment of the cortical cytoskeleton from the plasma membrane (Campillo *et al.*, 2012). Moreover, as transmembrane proteins, TMEM216 and meckelin predictably localise to membranous structures, such as the Golgi apparatus, including the vesicles surrounding the ciliary base, ciliary membrane, nuclear envelope, cell-cell junctions and apical membrane in polarised cells; however, they also bind along basolateral actin fibres, with filamin A, the actin crosslinking protein, and with post-Golgi vesicles along MTs (Adams *et al.*, 2011; Collado-Hilly *et al.*, Cilia 2014 Conference (unpublished); Dawe *et al.*, 2009; Lee *et al.*, 2012). These proteins are not the only ciliary proteins that localise to the cytoskeleton; Bbs8 and Ift20, for instance, localise to both F-actin and MTs (May-Simera *et al.*, 2015). However, it is not known whether these proteins interact with the cytoskeleton independently or as a complex.

Unpublished work has recently demonstrated that RNAi of MKS1 leads to defective vesicular transport, plasma membrane distension, epithelial differentiation and impairment of ciliary sensory function. Crucially, this also leads to disruption of the actin cytoskeleton, particularly at cell-cell and cell-matrix adhesion sites, implicating MKS1 as an intermediate protein linking the actin cytoskeleton and membranes [Collado-Hilly *et al.*, Cilia 2014 Conference (unpublished)].

In my experiments, I demonstrated multiple cytoskeletal defects in MKS patient cells, and these appeared to be connected to a previously undescribed Golgi defect. Indeed, coronin 7, an actin-Golgi interactor with roles in promoting actin polymerisation and post-Golgi trafficking (Rybakin *et al.*, 2008; Rybakin *et al.*, 2004; Yuan *et al.*, 2014) was transcriptionally downregulated. This indicates that aberrant coronin 7 transcription occurs alongside MKS mutations, and may be associated with the Golgi morphology defects observed. It is also possible that this occurs upstream of vesicular trafficking defects to cause aberrant

ciliogenesis; however, additional study is required to investigate the effects and the causes of alterations to coronin 7 transcription.

Indeed, defects in vesicular trafficking of TMEM138 and of *MKS4*-encoded CEP290, which would typically occur along TMEM216-linked post-Golgi vesicles associated with MTs, and concomitant shortened cilia, have been reported following *TMEM216* knockdown in fibroblasts (Lee *et al.*, 2012). This indicates that TMEM216 or MKS complexes may effect their function in post-Golgi transport to the ciliary base by linking membranous structures to the cytoskeleton during directional protein transport. Moreover, this also supports the possibility that these defects precede cilium-associated defects, as failures in Golgi transport of ciliary components would interfere with ciliogenesis.

Vesicular transport is necessary not only during ciliogenesis, but also during cell migration, which is also disrupted in MKS patient cells. It is also of note that vesicular trafficking defects have a central role in BBS (Blacque *et al.*, 2004; Nachury *et al.*, 2007), although much research has investigated vesicular trafficking solely in regard to IFT. It is possible that these protein complexes function beyond the cilium, including during vesicular trafficking.

Numerous MT-actin interactors function at the Golgi, such as MACF1, which is responsible for protein transport from the TGN along the MT and actin cytoskeleton to the cell periphery (Kakinuma *et al.*, 2004), co-localising with stress fibres and stabilising MTs (Leung *et al.*, 1999). MKS proteins could feasibly have a similar function.

This hypothesis – MKS proteins as a cytoskeleton-membrane tether – makes sense with regard to a key role of MKS proteins in the base of the cilium or ciliary membrane. TMEM216 and meckelin co-localise at, and have a necessary function at the transition zone (Dawe *et al.*, 2007b; Valente *et al.*, 2010), and in ciliogenesis. Reduction of meckelin, for instance, causes the basal body orientation to be lost, in which the actin cytoskeleton is heavily implicated (Abdelhamed *et al.*, 2015; Boisvieux-Ulrich *et al.*, 1987; Boisvieux-Ulrich *et al.*, 1990; Dawe *et al.*, 2007a; Dawe *et al.*, 2007b; Lemullois *et al.*, 1987; Picariello *et al.*, 2014). Further to this, CEP290 has been implicated as a key structural component of the Y-links (Craige *et al.*, 2010; Drivas *et al.*, 2013), binding both the ciliary membrane and MTs (Drivas *et al.*, 2013). However, the other MKS module proteins are thought to have a less essential, more regulatory role in the transition zone complex; these are hypothesised to

cooperate to bind the ciliary membrane to axonemal MTs, and knockout of both an MKS module and NPHP module component are required for Y-link disruption in *C. elegans* [Blacque *et al.*, Cilia 2014 conference (unpublished)]. This may, therefore, not be the most crucial role of TMEM216 and meckelin.

MKS protein function at cell-cell junctions, the apical membrane of polarised cells and the nuclear envelope in linking to cytoskeletal components would also be logical in the context of the observed phenotypes. These are sites of MT capture prior to their organisation (Bellett *et al.*, 2009; Lechler and Fuchs, 2007; Meng *et al.*, 2008) or downstream function, such as centrosome reorientation (Salpingidou *et al*., 2007), and sites of actin polymerisation or contractility, such as in nuclear movement (Starr and Fridolfsson, 2010), protrusion formation, and focal adhesions, all of which have observed defects (in published and unpublished work). Notably, recent unpublished work from our group (Meadows and Dawe) has established that meckelin is a novel focal adhesion component. These reports of TMEM216 and meckelin localising to cytoskeleton- and membrane-associated sites throughout the cells provides the most marked evidence for the hypothesis of MKS proteins as cytoskeleton-membrane linker proteins or protein complexes.

However, it is yet to be revealed how, as a cytoskeleton-membrane linker, MKS proteins would cause changes to MT stability, number of MT foci or the apparent centrosome fragmentation, which is perhaps generated by alternate membranous sites of MT nucleation and tethering, or why the numerous observed cellular phenotypes would appear to be ROCK-dependent.

MKS proteins are signalling molecules upstream of ROCK

Accumulating evidence indicates that the ciliopathy proteins have key functions within the non-canonical Wnt/PCP pathway, whether acting from the cilium or otherwise; indeed, numerous developmental phenotypes may be attributed to dysregulated Wnt signalling (both canonical and non-canonical), particularly renal cysts (Pinson *et al.*, 2000; Saadi-Kheddouci *et al.*, 2001). However, it is hard to explain mouse models of *MKS1, TMEM67, CEP290,* and *RPGRIP1L* that do not show alterations to Wnt signalling within the context of this theory (Abdelhamed *et al.*, 2013; Lancaster *et al.*, 2011; Mahuzier *et al.*, 2012; Wheway *et al.*, 2013).

Throughout this thesis, I have demonstrated a number of cellular phenotypes which appear Rho/ROCK pathway-dependent, inclusive of the previously-observed prominent actin bundles, which are abrogated in the presence of pathway inhibitors and upon the introduction of dominant negative Rho, and mimicked by introduction of constitutively active members of this pathway.

This is accompanied by evidence suggesting that the increased number of MT foci observed in *MKS2* patient cells can be attenuated by manipulation of this pathway, suggesting that dysregulation of the ROCK pathway in these cells may be responsible for a number of cellular phenotypes. Furthermore, constitutively active ROCK induces Golgi dispersal in wild-type cells analogous to that seen in MKS patient cells, but has no effect in MKS cells, implying that the cellular results induced by active ROCK have already been maximally effected. These findings, that Rho inhibitory drugs can reverse many of the cellular defects, are important evidence in addressing my aim to advise future therapeutics for the milder ciliopathies.

Mutations in *MKS2* and loss of meckelin have both been reported to cause RhoA and Dishevelled hyperactivation, seemingly causing prominent actin bundles to develop (Valente *et al.*, 2010). I can confirm from my results that, downstream of this, ROCK levels are increased in *MKS3* patient cells, indicating that the pathway is hyperactivated. Myosin levels appeared unchanged, but localisation appeared to change; phosphomyosin and myosin were presumably localising to the actin bundles.

As supporting evidence of a role of these proteins in, more broadly, Wnt/PCP signal transduction pathways, meckelin is known to interact with Dishevelled at the basal body where Rpgrip1l, the *MKS5* protein product, stabilises it (Mahuzier *et al.*, 2012). *Rpgrip1l, tmem67* and *mks1* morphant zebrafish all display convergent extension defects (Leightner *et al*., 2013; Leitch *et al*., 2008; Mahuzier *et al*., 2012) and impaired laterality (Mahuzier *et al*., 2012), which is typically associated with Wnt/PCP signalling dysregulation. Furthermore, meckelin phosphorylates ROR2, thereby acting as a non-canonical Wnt5a receptor, mediating downstream canonical and Shh pathway inhibition and RhoA activation, and playing a crucial role in all three signalling cascades (Abdelhamed *et al.*, 2015; Abdelhamed *et al.*, 2013). ROR2 is reported to form a complex with Vangl2, another PCP component, upon

stimulation with Wnt5a (Gao *et al.*, 2011). Mutations in genes encoding Wnt5a, ROR2 and Vangl2 have been linked to spina bifida and limb bud development (Gao *et al.*, 2011), indicating that the transduction of Wnt5a signalling via ROR2 may underlie a number of the developmental defects associated with MKS.

It is currently impossible to resolve whether the defects associated with MKS occur due to dysregulation of Wnt/PCP and/or canonical Wnt signalling, or have another role that impacts Rho components downstream of this. Cystic MKS3 phenotypes have been attributed to elevated proliferation resulting from canonical Wnt dysregulation in restricted regions (Leightner *et al.*, 2013); it may be that this is the case, and that the relative importance of Wnt5a pathway transduction is tissue-specific. It is of note that different mutations in *TMEM67* induce different severity of canonical and non-canonical Wnt pathway dysregulation (Abdelhamed *et al.*, 2013). This evidence may resolve why certain mouse models demonstrate no obvious alterations to Wnt signalling – in certain tissues, upon incurring specific mutations, meckelin may not have an essential signal transduction role. Meckelin does, however, appear to be crucial in a signal transduction role in at least a number of instances.

In alternative explanation, it is established that inversin, an NPHP-causative gene, acts as a molecular switch between the Wnt signalling pathways through its actions on Dishevelled in different cellular contexts; its upregulation constrains canonical Wnt signalling by the proteasomal targeting of Dishevelled and promotes PCP signalling, and its inhibition attenuates this downregulation of canonical signalling (Simons *et al.*, 2005). Concomitantly, inversin-null MEFs demonstrate elevated β-catenin and reduced Rho GTPase activity (Veland *et al.*, 2013). *Mks1* null MEFs also show high levels of canonical Wnt/β-catenin signalling (and heightened proliferation not reported in other ciliopathies), indicating there may be a negative regulatory role of MKS proteins in canonical Wnt signalling (Wheway *et al*., 2013). Notably, loss of TMEM216 increases Dishevelled phosphorylation, modulating hyper-responsiveness of Rho signalling pathways (Valente *et al*., 2010). It is therefore possible that these MKS proteins have a similar role to inversin, as a molecular switch, or are involved in this process as part of a complex, such as those at the transition zone. In support of this hypothesis, *nphp-3*, an MKS7-causative gene (in addition to a number of other NPHP genes) genetically interacts with

nphp-2/inversin, in addition to having an essential role in convergent extension movements (Bergmann *et al.*, 2008; Zhou *et al.*, 2010).

Concordantly with this concept, these are not the only ciliopathy proteins proposed to function in Wnt signalling; *BBS* genes interact with *Vangl2* (Ross *et al.*, 2005), *bbs1, -4* and *-6* interact with *wnt11* and *wnt5b*, suppression of which leads to β-catenin stabilisation (Gerdes *et al.*, 2007), and RhoA is highly upregulated in the absence of BBS4, -6 and -8 proteins (Hernandez-Hernandez *et al.*, 2013). This indicates that a number of the transition zone-associated proteins participate in various branches of Wnt signalling. However, it should be noted that Jouberin (a ciliopathy protein encoded for by *Ahi1*) facilitates β-catenin nuclear translocation to upregulate canonical Wnt signalling but, through spatial constraint of Jouberin and β-catenin, this function is partially repressed by the cilium (Lancaster *et al*., 2011), i.e. the cilium may act as a reservoir to maintain Wnt signalling within a reduced range.

The Wnt signalling pathway also impacts on ciliogenesis. Wnt/PCP components have multiple essential functions during ciliogenesis; for instance, PCP effectors such as Dvl and Inturned regulate basal body docking and orientation, governing Rho-mediated actin reorganisation and vesicular trafficking (Park *et al.*, 2008), and Fuz is central to membrane trafficking during ciliogenesis (Gray *et al.*, 2009). It is also postulated that presence of a cilium constrains canonical Wnt signalling (Corbit *et al.*, 2008) but the importance of an intact, functional cilium (as opposed to just the basal body), and of “ciliary” proteins, within this process is unknown.

If MKS proteins (particularly meckelin), or an MKS protein complex, were to participate in Wnt/PCP (specifically Rho/ROCK) signal transduction, this could explain a number of phenotypes observed. This could even occur from a location within the basal body. In example, p160ROCK, a Rho pathway component, maintains centriole integrity as an intercentriolar linker (Chevrier *et al.*, 2002), and MKS/NPHP protein complexes may act analogously to this, as is discussed within the next section.

Alterations to Rho/ROCK signalling can explain a number of the observed phenotypes. For instance, Rho maintains MT stability in the trailing edge of migrating cells and is involved in stable MT generation at the leading edge (Cook *et al.*, 1998; Salaycik *et al.*, 2005); also, ROCK phosphorylation of TPPP1 increases HDAC6 activity, thereby reducing acetylation and impacting

upon cell migration (Schofield *et al.*, 2012). Hyperactivated Rho could thus result in ubiquitous cytoplasmic MT stabilisation and migratory defects. Changes in MT stability and actin structures would understandably also have dramatic effects on centriole migration, and on Golgi organisation and trafficking.

If MKS proteins function as Rho pathway effectors solely at the cilium, changes to nucleation and tethering of MTs and centrosome splitting are harder to explain. Furthermore, MKS proteins evolved prior to developmental signalling – Wnt and Hh signalling are restricted predominantly to metazoan organisms, but TZ complex proteins are reported throughout eukaryotes – implying that this was not the initial function of TZ complex proteins, and thus is unlikely to be their sole function now (Barker *et al.*, 2014).

Resultantly, I postulate that MKS proteins act within a complex, that this complex has more than one role, and that these proteins act synergistically to enable these structural and functional roles.

7.2 Is there more than one role of MKS proteins?

Although less parsimonious than a single role, evidence indicates that there are multiple roles of MKS proteins, likely as part of a complex that is analogous to the focal adhesions, which have both a structural and signalling role. I propose that this complex is formed at different locations throughout the cell, possibly with variable components to enable different binding partners at each location of action.

This is supported by evidence of MKS proteins having interaction partners outside of the TZ complexes, including filamin A on basolateral actin cables (Adams *et al.*, 2011), nesprin 2 at the nuclear envelope (Dawe *et al.*, 2009) and RanGAP, a GTPase activating Ran, a GTP-binding protein involved in nuclear transport (Picariello *et al.*, 2014). An MKS/ciliopathy protein complex may have the same or different roles at different locations, which may be dependent on the isoforms used; unpublished work from our group suggests that multiple isoforms of *MKS3* transcript exist, which may explain variability of effects in mouse models.

The model I hypothesise is displayed in *Figure 7.1*. I propose that the MKS protein module, whether in conjunction with the NPHP module and BBSome, or

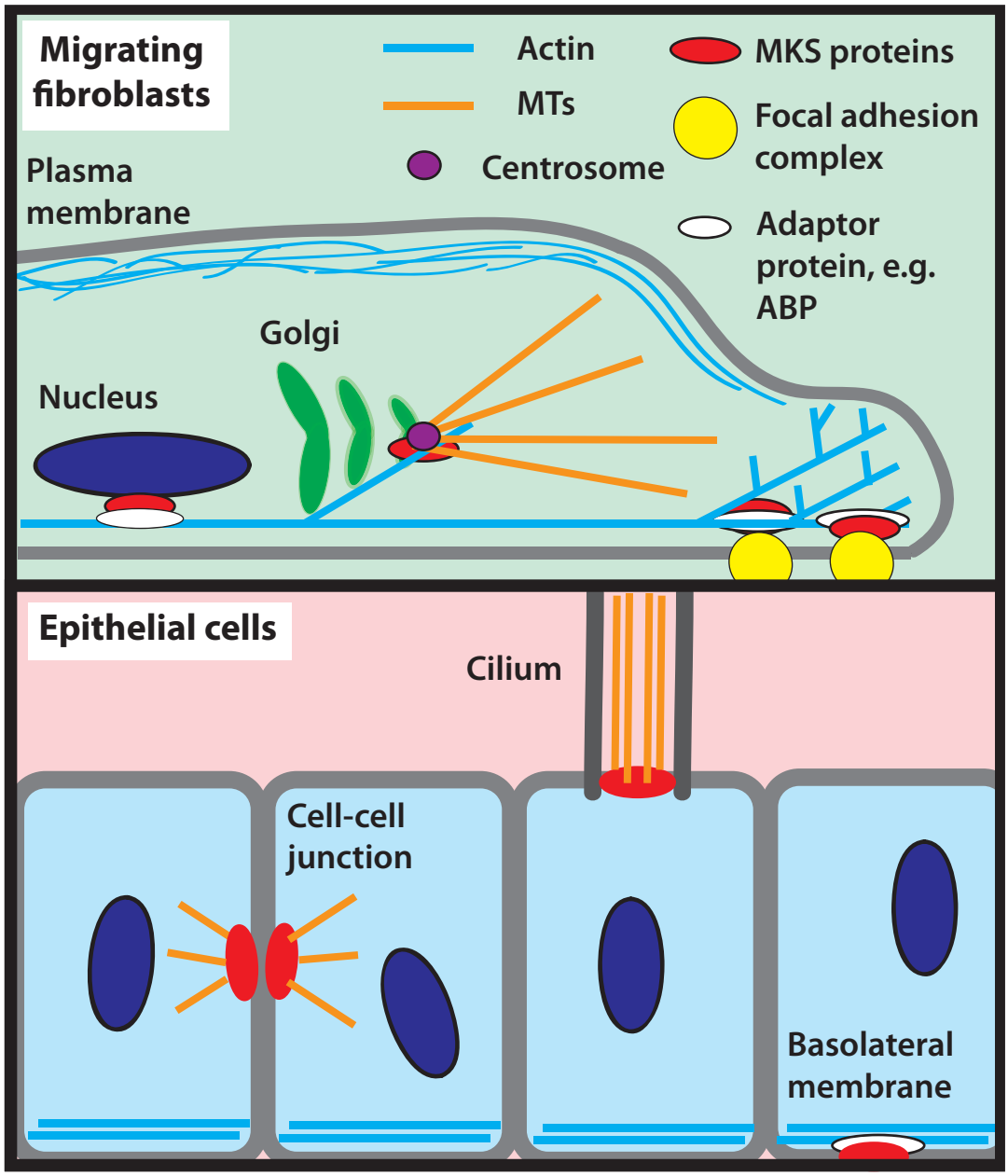

FIGURE 7.1: Model to show MKS proteins acting in a complex as Rho effectors and cytoskeleton-membrane linkers.
MKS proteins interact with nuclear envelope proteins, actin-binding proteins (white objects), the Golgi apparatus, focal adhesion complexes, cell-cell junctions, and the ciliary transition zone. I postulate that MKS protein complexes act as Rho effectors at these locations, simultaneously interacting with other complexes (such as focal adhesion complex proteins, or centrosomal proteins) to maintain the integrity of these structures. Further, I propose that these actions affect cytoskeletal dynamics, having downstream consequences on actin networks, microtubule stability, and membranous structures. Consequently, MKS mutation has observed effects on cell migration, polarity, cell spreading, vesicular trafficking and ciliogenesis.

without, functions in both a structural capacity, and as a Rho pathway effector at multiple membranous locations throughout the cell.

From the evidence presented in this thesis, I have suggested an increase in the subcellular locations of these complexes from those indicated at the end of the introduction (*Figure 1.5*) to additional MT-associated locations, including the centrosome and cell-cell junctions. Furthermore, I also propose a structural and Rho signal transduction role of these complexes at these locations.

I propose that this complex affects local cytoskeletal dynamics via indirect binding to actin fibres, using influential intermediates such as crosslinking protein filamin A. Furthermore, I suggest that through enzymatic action or another protein intermediate, this complex acts upon MT nucleators and/or tethers (e.g. through modulation of p160ROCK activation at the centrosome, or maintaining PCM integrity) to recruit and stabilise or destabilise MTs. Finally, I postulate that this complex has a necessary structural role, maintaining the integrity of a functioning transition zone. I suggest that loss of polarity, centrosome positioning, Golgi dispersal, and defects in vesicular trafficking observed in conjunction with ciliopathy occur downstream of ROCK-dependent cytoskeletal changes and loss of centrosome/basal body integrity.

Evidence would indicate that such activity may occur at the focal adhesions, for instance; MKS proteins localise here, where they are probably situated on the plasma membrane (Meadows and Dawe, unpublished), and likely induce Rho-associated actin changes during locomotion.

A dual signalling and structural role is plausible. Knockdown of RPGR, a protein causative of retinal dystrophy – a ciliopathy – leads to more prominent actin filaments and reduction in β1-integrin receptors at the cell surface, in addition to basal dysregulation of a number of signalling pathways, including Akt, Erk1/2, focal adhesion kinase and Src (Gakovic *et al.*, 2011). Focal adhesion components, including FAK, paxillin and vinculin, also associate with basal bodies to anchor them to the actin cytoskeleton (Antoniades *et al.*, 2014). It would follow that an association between signalling and basal body components could potentially occur at additional subcellular locations beyond the focal adhesions, interacting with the cytoskeleton at these locations.

Coronin 7 transcript downregulation may occur downstream of Rho pathway hyperactivation and contribute to vesicular trafficking defects. No evidence presently exists as to how coronin 7 is regulated, but nuclear expression of its

C. elegans equivalent, Pod1, is regulated by ROCK (Plotkin and Mudunuri, 2008). As ROCK appears upregulated in MKS patient cells, this appears an obvious underlying cause of transcriptional changes to coronin 7, although this remains to be determined. siRNA against Pod1 also inhibits gene expression of fibronectin, an extracellular matrix component, and secretion of MMP inhibitors, enzymes involved in degrading ECM (Plotkin and Mudunuri, 2008). As we observe reduced ECM presence in the MKS patient cells (Meadows and Dawe, unpublished), it is possible that coronin 7 regulates ECM production, downstream of ROCK hyperactivation.

It is probable that TMEM216 and meckelin have distinct roles within this proposed MKS protein complex, as implied by the different effects when these are mutated or knocked down in cells. *MKS2* has more marked, immediate effects on cell behaviour; this may indicate a more crucial role of TMEM216 than meckelin, either in the structure or function of an MKS protein complex, or independently of this protein complex. However, we are only beginning to resolve the precise function of the transition zone complexes as entities, and it would be harder still to estimate the roles of the MKS proteins independently of each other.

7.3 What does this mean for other ciliopathies?

A dual structural and signalling role of other ciliopathy complexes, such as the NPHP complex and the BBSome – functioning either with or without the MKS protein complex – would explain why multiple ciliopathies have defects in the same cellular processes. Joubert syndrome, Bardet Biedl Syndrome and nephronophthisis, amongst multiple other ciliopathies are allelic with MKS (Arts *et al.*, 2007; Baala *et al.*, 2007; Brancati *et al.*, 2009; Delous *et al.*, 2007; den Hollander *et al.*, 2006; Doherty *et al.*, 2010; Edvardson *et al.*, 2010; Gorden *et al.*, 2008; Leitch *et al.*, 2008; Noor *et al.*, 2008; Otto *et al.*, 2009; Sayer *et al.*, 2006; Srour *et al.*, 2012; Valente *et al.*, 2010; Valente *et al.*, 2006), and can have an epistatic effect on other ciliopathy loci (Leitch *et al.*, 2008); considering this, it is highly likely that disruption of one component would affect the activity of others.

Disruption of ciliopathy complexes with such a role could easily explain all of the reported cellular defects associated with ciliopathy, including aberrant

ciliogenesis and centriole movement and integrity, changes to cytoskeletal organisation and stability, altered focal adhesions, vesicular trafficking defects and dysregulated Wnt and Hh signalling.

As an effector of the Wnt/PCP pathway (whether far upstream or just of Rho/ROCK) and a cytoskeleton-membrane tether, ciliopathy protein complex components could effect changes to the actin and MT cytoskeleton through both Rho GTPase signal transduction [affecting the stability and associated function of both (Bishop and Hall, 2000; Ellenbroek and Collard, 2007; Ridley, 2006)] and through cytoskeletal recruitment and anchoring at specific membranous locations, such as the leading edge (e.g. at focal adhesions) of a migrating cell, the Golgi, ciliary vesicles associated with a centriole or the ciliary membrane.

Simultaneous structural and signalling behaviour is observed in other centrosomal proteins, such as Talpid3, defects in which cause Hedgehog signalling defects. These proteins generate cytoskeletal reorganisation which mechanistically precedes a number of ciliogenesis defects, such as actin-mediated basal body positioning and axonemal extension (Stephen *et al*., 2013; Yin *et al*., 2009). Subsequent defects observed in Hh signalling are therefore likely to be cilium-dependent (Davey *et al*., 2007; Davey *et al*., 2006).

Other ciliopathy proteins, such as Kif7, also appear to perform such an impactful role. Kif7 co-precipitates with NPHP1 (Dafinger *et al.*, 2011), and it localises to the cilium tip, where it regulates growth and catastrophe of the axonemal MT plus ends. Kif7 is also a known regulator of the Hh pathway, creating a cilium tip compartment in which Gli activity can be regulated (He *et al*., 2014). Lending support for this hypothesis, Kif7 also localises to multiple other subcellular sites beyond the cilium and is involved in maintaining structural integrity of the centrosome and the Golgi (Dafinger *et al.*, 2011).

Failure of ciliopathy protein complexes to perform either a structural or signalling role would have drastic consequences on the cell which correspond to those observed in patient cells, such as defects in migration speed and directionality (Barker and Dawe, unpublished). These may occur downstream of alterations to Rho/ROCK signal transduction, as similar defects to polarised migration are observed in inversin mutants. As mentioned, inversin is the gene product of *NPHP2* and a protein thought to act as a molecular switch between Wnt signalling pathways (Veland *et al.*, 2013), a function also described of

BBS4 (Gerdes *et al*., 2007). However, *inv*-null mutants also display cytoskeletal rearrangements (Werner *et al*., 2013) and altered focal adhesion distribution (Veland *et al*., 2013), which may the primary cause of defective migration.

Concluding that these complexes may have a structural and signalling role beyond the cilium is not a radical conclusion as IFT proteins, such as IFT20, IFT57 and IFT88 (Finetti *et al.*, 2009), are already known to be used in trafficking throughout the cell; additionally, IFT88 has recently been revealed to influence MT organisation, cell migration and polarity, irrespective of cilia (Boehlke *et al.*, 2015). Furthermore, inhibition of Rab8 activity (part of the vesicular trafficking machinery) leads to BBS-like phenotypes (Nachury *et al.*, 2007).

In addressing my primary aim, to discover the extra-ciliary roles of the MKS proteins TMEM216 and TMEM67, I have revealed that many of these roles appear to be cilium-independent. This is hard to conclusively prove, due to an absence of an appropriate cilium-free model; however, the rapid development of a number of these defects and the low rates of ciliogenesis under the serum-containing conditions used throughout these experiments indicate that the observed defects are not likely to result from the absence of a cilium. It is of further note that a recent RNAi screen of ciliary proteins in non-ciliated *Drosophila* cells uncovered a cilium-independent function of a number of these proteins in canonical Wnt signalling, supporting the present hypothesis (Balmer *et al.*, 2015). This is important for future treatment of the problem; if the ciliogenesis defect is the primary defect in the ciliopathies, it is most worthwhile to address this avenue of research. However, if another of these defects occurs upstream of this and the others, this becomes an obvious therapeutic target. Ciliogenesis failure does not explain the hepatic anomalies in MKS, a key pathogenic feature of this and a number of the other ciliopathies, as these precede ciliogenesis (Clotman *et al.*, 2008), so it is worthwhile investigating the extra-ciliary roles of the “ciliopathy” proteins to determine the most effective therapeutic targets.

7.4 Conclusions & future perspectives

It is possible for an MKS complex functioning as a Rho effector and a structural, cytoskeleton-membrane linker to be active at all of the locations that

MKS is observed in, including the focal adhesions (performing vital actions during motility), the Golgi apparatus (functioning in cytoskeleton-dependent vesicular trafficking, also impacting on ciliogenesis), cell-cell junctions (mediating MT capture), the nucleus (controlling positioning through modulation of cytoskeletal dynamics) and, of course, the transition zone (*Figure 7.1*).

At the transition zone, their best-studied role, MKS proteins are likely important regulators of ciliary membrane composition, thereby controlling Shh signalling. However, they may also interact with and influence canonical and non-canonical Wnt signalling components, such as Dvl and Inturned. However, in contrast to the prevailing view in the ciliopathy field, I believe that a diffusion barrier at the transition zone is not the primary role of MKS proteins, validated by my use of serum in my experiments, in contrast to much of the current research – control cells do not typically form many cilia under these conditions. Together, these data imply that MKS proteins perform the roles described in this thesis independently of ciliary signalling defects.

The prominence of the other ciliary proteins, such as BBS proteins, in many of these examples implies that MKS proteins would not function alone in these roles and that these “ciliopathy protein” complexes may cooperate to form structures tasked with signal transduction at multiple subcellular locations. This thesis therefore advances knowledge about the roles of MKS proteins, but may also inform research into the wider spectrum of ciliopathies, if the proteins involved do, in fact, interact to perform similar functions. This research topic therefore has vital implications in the genetic diagnosis and prognosis of this diverse group of disorders.

Future research should establish the nature of these complexes at other subcellular locations – are the same isoforms of all the proteins used throughout the cell? Do the molecular constituents of the ciliopathy protein complexes vary across subcellular locations? Which proteins are vital to the the balance and components of Wnt/PCP and canonical Wnt signalling throughout the cell? How much redundancy is there in the transition zone complex proteins at other locations? If we can ascertain the biochemical composition and activity of these ciliopathy complexes throughout the cell, therapeutic potential may be possible.

REFERENCES

Abdelhamed, Z. A., Natarajan, S., Wheway, G., Inglehearn, C. F., Toomes, C., Johnson, C. A. and Jagger, D. J. (2015). The Meckel-Gruber syndrome protein TMEM67 controls basal body positioning and epithelial branching morphogenesis in mice via the non-canonical Wnt pathway. *Disease Models & Mechanisms* **8**, 527-41.

Abdelhamed, Z. A., Wheway, G., Szymanska, K., Natarajan, S., Toomes, C., Inglehearn, C. and Johnson, C. A. (2013). Variable expressivity of ciliopathy neurological phenotypes that encompass Meckel-Gruber syndrome and Joubert syndrome is caused by complex de-regulated ciliogenesis, Shh and Wnt signalling defects. *Human Molecular Genetics* **22**, 1358-72.

Abercrombie, M. (1980). The Croonian Lecture, 1978: The Crawling Movement of Metazoan Cells. *Proceedings of the Royal Society London B* **207**, 129-147.

Abercrombie, M. H., J.E.M. and Pegrum, S.M. (1970). The Locomotion of Fibroblasts in Culture: II. "Ruffling". *Experimental Cell Research* **60**.

Adams, M., Simms, R. J., Abdelhamed, Z., Dawe, H. R., Szymanska, K., Logan, C. V., Wheway, G., Pitt, E., Gull, K., Knowles, M. A. *et al.* (2012). A meckelin-filamin A interaction mediates ciliogenesis. *Human Molecular Genetics* **21**, 1272-86.

Ahmad-Annuar, A., Ciani, L., Simeonidis, I., Herreros, J., Fredj, N. B., Rosso, S. B., Hall, A., Brickley, S. and Salinas, P. C. (2006). Signaling across the synapse: a role for Wnt and Dishevelled in presynaptic assembly and neurotransmitter release. *Journal of Cell Biology* **174**, 127-39.

Al Jord, A., Lemaitre, A. I., Delgehyr, N., Faucourt, M., Spassky, N. and Meunier, A. (2014). Centriole amplification by mother and daughter centrioles differs in multiciliated cells. *Nature* **516**, 104-7.

Aldahmesh, M. A., Li, Y., Alhashem, A., Anazi, S., Alkuraya, H., Hashem, M., Awaji, A. A., Sogaty, S., Alkharashi, A., Alzahrani, S. *et al.* (2014). IFT27, encoding a small GTPase component of IFT particles, is mutated in a consanguineous family with Bardet-Biedl syndrome. *Human Molecular Genetics* **23**, 3307-15.

Alexiev, B. A., Lin, X., Sun, C. C. and Brenner, D. S. (2006). Meckel-Gruber syndrome: pathologic manifestations, minimal diagnostic criteria, and

differential diagnosis. *Archives of Pathology & Laboratory Medicine* **130**, 1236-8.

Amos, L. A. and Schlieper, D. (2005). MTs and MAPs. *Advances in Protein Chemistry* **71**, 257-98.

Anderson, R. G. (1972). The three-dimensional structure of the basal body from the rhesus monkey oviduct. *Journal of Cell Biology* **54**, 246-65.

Andrés-Delgado, L., Anton, O. M., Madrid, R., Byrne, J. A. and Alonso, M. A. (2010). Formin INF2 regulates MAL-mediated transport of Lck to the plasma membrane of human T lymphocytes. *Blood* **116**, 5919-29.

Antoniades, I., Stylianou, P. and Skourides, P. A. (2014). Making the connection: ciliary adhesion complexes anchor basal bodies to the actin cytoskeleton. *Developmental Cell* **28**, 70-80.

Arber, S., Barbayannis, F. A., Hanser, H., Schneider, C., Stanyon, C. A., Bernard, O. and Caroni, P. (1998). Regulation of actin dynamics through phosphorylation of cofilin by LIM-kinase. *Nature* **393**, 805-9.

Arts, H. H., Doherty, D., van Beersum, S. E., Parisi, M. A., Letteboer, S. J., Gorden, N. T., Peters, T. A., Marker, T., Voesenek, K., Kartono, A. *et al.* (2007). Mutations in the gene encoding the basal body protein RPGRIP1L, a nephrocystin-4 interactor, cause Joubert syndrome. *Nature Genetics* **39**, 882-8.

Avasthi, P., Onishi, M., Karpiak, J., Yamamoto, R., Mackinder, L., Jonikas, M. C., Sale, W. S., Shoichet, B., Pringle, J. R. and Marshall, W. F. (2014). Actin is required for IFT regulation in Chlamydomonas reinhardtii. *Current Biology* **24**, 2025-32.

Baala, L., Romano, S., Khaddour, R., Saunier, S., Smith, U. M., Audollent, S., Ozilou, C., Faivre, L., Laurent, N., Foliguet, B. *et al.* (2007). The Meckel-Gruber syndrome gene, MKS3, is mutated in Joubert syndrome. *American Journal of Human Genetics* **80**, 186-94.

Babu, D. and Roy, S. (2013). Left-right asymmetry: cilia stir up new surprises in the node. *Open Biology* **3**, 130052.

Bacallao, R., Antony, C., Dotti, C., Karsenti, E., Stelzer, E. H. and Simons, K. (1989). The subcellular organization of Madin-Darby canine kidney cells during the formation of a polarized epithelium. *Journal of Cell Biology* **109**, 2817-32.

Bachmann, A. and Straube, A. (2015). Kinesins in cell migration. *Biochemical Society Transactions* **43**, 79-83.

Bachmann-Gagescu, R., Dempsey, J. C., Phelps, I. G., O'Roak, B. J., Knutzen, D. M., Rue, T. C., Ishak, G. E., Isabella, C. R., Gorden, N., Adkins, J. *et al.* (2015). Joubert syndrome: a model for untangling recessive disorders with extreme genetic heterogeneity. *Journal of Medical Genetics* **52**, 514-22.

Bachmann-Gagescu, R., Dona, M., Hetterschijt, L., Tonnaer, E., Peters, T., de Vrieze, E., Mans, D. A., van Beersum, S. E., Phelps, I. G., Arts, H. H. *et al.* (2015). The Ciliopathy Protein CC2D2A Associates with NINL and Functions in RAB8-MICAL3-Regulated Vesicle Trafficking. *PLoS Genetics* **11**, e1005575.

Badano, J. L., Kim, J. C., Hoskins, B. E., Lewis, R. A., Ansley, S. J., Cutler, D. J., Castellan, C., Beales, P. L., Leroux, M. R. and Katsanis, N. (2003). Heterozygous mutations in BBS1, BBS2 and BBS6 have a potential epistatic effect on Bardet-Biedl patients with two mutations at a second BBS locus. *Human Molecular Genetics* **12**, 1651-9.

Badano, J. L., Leitch, C. C., Ansley, S. J., May-Simera, H., Lawson, S., Lewis, R. A., Beales, P. L., Dietz, H. C., Fisher, S. and Katsanis, N. (2006a). Dissection of epistasis in oligogenic Bardet-Biedl syndrome. *Nature* **439**, 326-30.

Badano, J. L., Mitsuma, N., Beales, P. L. and Katsanis, N. (2006b). The ciliopathies: an emerging class of human genetic disorders. *Annual Review of Genomics and Human Genetics* **7**, 125-48.

Balmer, S., Dussert, A., Collu, G. M., Benitez, E., Iomini, C. and Mlodzik, M. (2015). Components of Intraflagellar Transport Complex A Function Independently of the Cilium to Regulate Canonical Wnt Signaling in *Drosophila*. *Developmental Cell* **34**, 705-18.

Barisic, I., Boban, L., Loane, M., Garne, E., Wellesley, D., Calzolari, E., Dolk, H., Addor, M. C., Bergman, J. E., Braz, P. *et al.* (2015). Meckel-Gruber Syndrome: a population-based study on prevalence, prenatal diagnosis, clinical features, and survival in Europe. *European Journal of Human Genetics* **23**, 746-52.

Barker, A. R., Renzaglia, K. S., Fry, K. and Dawe, H. R. (2014a). Bioinformatic analysis of ciliary transition zone proteins reveals insights into the evolution of ciliopathy networks. *BMC Genomics* **15**, 531.

Barker, A. R., Thomas, R. and Dawe, H. R. (2014b). Meckel-Gruber syndrome and the role of primary cilia in kidney, skeleton, and central nervous system development. *Organogenesis* **10**, 96-107.

Barra, H. S., Arce, C. A., Rodriguez, J. A. and Caputto, R. (1974). Some common properties of the protein that incorporates tyrosine as a single unit and the microtubule proteins. *Biochemical and Biophysical Research Communications* **60**, 1384-90.

Bartolini, F. and Gundersen, G. G. (2006). Generation of noncentrosomal microtubule arrays. *Journal of Cell Science* **119**, 4155-63.

Bartolini, F., Moseley, J. B., Schmoranzer, J., Cassimeris, L., Goode, B. L. and Gundersen, G. G. (2008). The formin mDia2 stabilizes microtubules independently of its actin nucleation activity. *Journal of Cell Biology* **181**, 523-36.

Battini, L., Macip, S., Fedorova, E., Dikman, S., Somlo, S., Montagna, C. and Gusella, G. L. (2008). Loss of polycystin-1 causes centrosome amplification and genomic instability. *Human Molecular Genetics* **17**, 2819-33.

Beales, P. L., Badano, J. L., Ross, A. J., Ansley, S. J., Hoskins, B. E., Kirsten, B., Mein, C. A., Froguel, P., Scambler, P. J., Lewis, R. A. *et al.* (2003). Genetic interaction of BBS1 mutations with alleles at other BBS loci can result in non-Mendelian Bardet-Biedl syndrome. *American Journal of Human Genetics* **72**, 1187-99.

Behnen, M., Murk, K., Kursula, P., Cappallo-Obermann, H., Rothkegel, M., Kierszenbaum, A. L. and Kirchhoff, C. (2009). Testis-expressed profilins 3 and 4 show distinct functional characteristics and localize in the acroplaxome-manchette complex in spermatids. *BMC Cell Biology* **10**, 34.

Bellett, G., Carter, J. M., Keynton, J., Goldspink, D., James, C., Moss, D. K. and Mogensen, M. M. (2009). Microtubule plus-end and minus-end capture at adherens junctions is involved in the assembly of apico-basal arrays in polarised epithelial cells. *Cell Motility and the Cytoskeleton* **66**, 893-908.

Berbari, N. F., O'Connor, A. K., Haycraft, C. J. and Yoder, B. K. (2009). The primary cilium as a complex signaling center. *Current Biology* **19**, R526-35.

Bergmann, C., Fliegauf, M., Brüchle, N. O., Frank, V., Olbrich, H., Kirschner, J., Schermer, B., Schmedding, I., Kispert, A., Kränzlin, B. *et al.* (2008). Loss of nephrocystin-3 function can cause embryonic lethality, Meckel-

Gruber-like syndrome, situs inversus, and renal-hepatic-pancreatic dysplasia. *American Journal of Human Genetics* **82**, 959-70.

Bershadsky, A. D., Tint, I. S., Neyfakh, A. A., Jr. and Vasiliev, J. M. (1985). Focal contacts of normal and RSV-transformed quail cells. Hypothesis of the transformation-induced deficient maturation of focal contacts. *Experimental Cell Research* **158**, 433-44.

Bhogaraju, S., Cajanek, L., Fort, C., Blisnick, T., Weber, K., Taschner, M., Mizuno, N., Lamla, S., Bastin, P., Nigg, E. A. *et al.* (2013). Molecular basis of tubulin transport within the cilium by IFT74 and IFT81. *Science* **341**, 1009-12.

Bialas, N. J., Inglis, P. N., Li, C., Robinson, J. F., Parker, J. D., Healey, M. P., Davis, E. E., Inglis, C. D., Toivonen, T., Cottell, D. C. *et al.* (2009). Functional interactions between the ciliopathy-associated Meckel syndrome 1 (MKS1) protein and two novel MKS1-related (MKSR) proteins. *Journal of Cell Science* **122**, 611-24.

Bishop, A. L. and Hall, A. (2000). Rho GTPases and their effector proteins. *Biochemistry Journal* **348 Pt 2**, 241-55.

Blacque, O. E. and Sanders, A. A. (2014). Compartments within a compartment: what *C. elegans* can tell us about ciliary subdomain composition, biogenesis, function, and disease. *Organogenesis* **10**, 126-37.

Blacque, O. E., Reardon, M. J., Li, C., McCarthy, J., Mahjoub, M. R., Ansley, S. J., Badano, J. L., Mah, A. K., Beales, P. L., Davidson, W. S. *et al.* (2004). Loss of *C. elegans* BBS-7 and BBS-8 protein function results in cilia defects and compromised intraflagellar transport. *Genes & Development* **18**, 1630-42.

Blacque, O. E., Van Dam, J., Bruel, A.-L., Slaats, G., Szymanska, K., Kennedy, J., Gaff, K., Johnson, C. A., Giles, R., Rivere, J.-B. *et al.* (Cilia 2014 conference (unpublished)). TMEM107 is a ciliopathy protein that recruits ciliopathy TMEMs to anchored ring-like domains of the *C. elegans* ciliary transition zone membrane.

Blom, M., Reis, K., Nehru, V., Blom, H., Gad, A. K. and Aspenstrom, P. (2015). RhoD is a Golgi component with a role in anterograde protein transport from the ER to the plasma membrane. *Experimental Cell Research* **333**, 208-19.

Boehlke, C., Janusch, H., Hamann, C., Powelske, C., Mergen, M., Herbst, H., Kotsis, F., Nitschke, R. and Kuehn, E. W. (2015). A Cilia Independent Role of Ift88/Polaris during Cell Migration. *PLoS One* **10**, e0140378.

Boisvieux-Ulrich, E., Laine, M. C. and Sandoz, D. (1987). In vitro effects of benzodiazepines on ciliogenesis in the quail oviduct. *Cell Motility and the Cytoskeleton* **8**, 333-44.

Boisvieux-Ulrich, E., Laine, M. C. and Sandoz, D. (1990). Cytochalasin D inhibits basal body migration and ciliary elongation in quail oviduct epithelium. *Cell and Tissue Research* **259**, 443-54.

Bonnet, C., Boucher, D., Lazereg, S., Pedrotti, B., Islam, K., Denoulet, P. and Larcher, J. C. (2001). Differential binding regulation of microtubule-associated proteins MAP1A, MAP1B, and MAP2 by tubulin polyglutamylation. *Journal of Biological Chemistry* **276**, 12839-48.

Borisy, G. G. and Taylor, E. W. (1967). The mechanism of action of colchicine. Binding of colchincine-3H to cellular protein. *Journal of Cell Biology* **34**, 525-33.

Borovina, A., Superina, S., Voskas, D. and Ciruna, B. (2010). Vangl2 directs the posterior tilting and asymmetric localization of motile primary cilia. *Nature Cell Biology* **12**, 407-12.

Brancati, F., Iannicelli, M., Travaglini, L., Mazzotta, A., Bertini, E., Boltshauser, E., D'Arrigo, S., Emma, F., Fazzi, E., Gallizzi, R. *et al.* (2009). MKS3/TMEM67 mutations are a major cause of COACH Syndrome, a Joubert Syndrome related disorder with liver involvement. *Human Mutation* **30**, E432-42.

Bre, M. H., Kreis, T. E. and Karsenti, E. (1987). Control of microtubule nucleation and stability in Madin-Darby canine kidney cells: the occurrence of noncentrosomal, stable detyrosinated microtubules. *Journal of Cell Biology* **105**, 1283-96.

Breslow, D. K., Koslover, E. F., Seydel, F., Spakowitz, A. J. and Nachury, M. V. (2013). An in vitro assay for entry into cilia reveals unique properties of the soluble diffusion barrier. *Journal of Cell Biology* **203**, 129-47.

Brody, S. L., Yan, X. H., Wuerffel, M. K., Song, S. K. and Shapiro, S. D. (2000). Ciliogenesis and left-right axis defects in forkhead factor HFH-4-null mice. *American Journal of Respiratory Cell and Molecular Biology* **23**, 45-51.

Brugmann, S. A., Cordero, D. R. and Helms, J. A. (2010). Craniofacial ciliopathies: A new classification for craniofacial disorders. *American Journal of Medical Genetics A* **152a**, 2995-3006.

Bugnard, E., Zaal, K. J. and Ralston, E. (2005). Reorganization of microtubule nucleation during muscle differentiation. *Cell Motility and the Cytoskeleton* **60**, 1-13.

Buisson, J., Chenouard, N., Lagache, T., Blisnick, T., Olivo-Marin, J. C. and Bastin, P. (2013). Intraflagellar transport proteins cycle between the flagellum and its base. *Journal of Cell Science* **126**, 327-38.

Bujakowska, K. M., Zhang, Q., Siemiatkowska, A. M., Liu, Q., Place, E., Falk, M. J., Consugar, M., Lancelot, M. E., Antonio, A., Lonjou, C. *et al.* (2015). Mutations in IFT172 cause isolated retinal degeneration and Bardet-Biedl syndrome. *Human Molecular Genetics* **24**, 230-42.

Burakov, A., Nadezhdina, E., Slepchenko, B. and Rodionov, V. (2003). Centrosome positioning in interphase cells. *Journal of Cell Biology* **162**, 963-9.

Burke, M. C., Li, F. Q., Cyge, B., Arashiro, T., Brechbuhl, H. M., Chen, X., Siller, S. S., Weiss, M. A., O'Connell, C. B., Love, D. *et al.* (2014). Chibby promotes ciliary vesicle formation and basal body docking during airway cell differentiation. *Journal of Cell Biology* **207**, 123-37.

Burridge, K. and Chrzanowska-Wodnicka, M. (1996). Focal adhesions, contractility, and signaling. *Annual Review of Cell and Developmental Biology* **12**, 463-518.

Burtey, S., Riera, M., Ribe, E., Pennenkamp, P., Rance, R., Luciani, J., Dworniczak, B., Mattei, M. G. and Fontes, M. (2008). Centrosome overduplication and mitotic instability in PKD2 transgenic lines. *Cell Biology International* **32**, 1193-8.

Buxton, P., Davey, M. G., Paton, I. R., Morrice, D. R., Francis-West, P. H., Burt, D. W. and Tickle, C. (2004). Craniofacial development in the *talpid3* chicken mutant. *Differentiation* **72**, 348-62.

Cajanek, L. and Nigg, E. A. (2014). Cep164 triggers ciliogenesis by recruiting Tau tubulin kinase 2 to the mother centriole. *Proceedings of the National Academy of Sciences of the United States of America* **111**, E2841-50.

Campellone, K. G., Webb, N. J., Znameroski, E. A. and Welch, M. D. (2008). WHAMM is an Arp2/3 complex activator that binds microtubules and functions in ER to Golgi transport. *Cell* **134**, 148-61.

Campillo, C., Jerber, J., Fisch, C., Simoes-Betbeder, M., Dupuis-Williams, P., Nassoy, P. and Sykes, C. (2012). Mechanics of membrane-cytoskeleton attachment in *Paramecium*. *New Journal of Physics* **14**, 125016.

Cao, J., Shen, Y., Zhu, L., Xu, Y., Zhou, Y., Wu, Z., Li, Y., Yan, X. and Zhu, X. (2012). miR-129-3p controls cilia assembly by regulating CP110 and actin dynamics. *Nature Cell Biology* **14**, 697-706.

Cao, Y., Park, A. and Sun, Z. (2010). Intraflagellar transport proteins are essential for cilia formation and for planar cell polarity. *Journal of the American Society of Nephrology* **21**, 1326-33.

Carvalho, R., Wang, W. and Pereira, G. (Cilia 2014 conference (unpublished)). Control of initial steps of ciliogenesis by protein kinases.

Caspary, T., Larkins, C. E. and Anderson, K. V. (2007). The graded response to Sonic Hedgehog depends on cilia architecture. *Developmental Cell* **12**, 767-78.

Cau, J. and Hall, A. (2005). Cdc42 controls the polarity of the actin and microtubule cytoskeletons through two distinct signal transduction pathways. *Journal of Cell Science* **118**, 2579-87.

Chabin-Brion, K., Marceiller, J., Perez, F., Settegrana, C., Drechou, A., Durand, G. and Pous, C. (2001). The Golgi complex is a microtubule-organizing organelle. *Molecular Biology of the Cell* **12**, 2047-60.

Chang, B., Khanna, H., Hawes, N., Jimeno, D., He, S., Lillo, C., Parapuram, S. K., Cheng, H., Scott, A., Hurd, R. E. *et al.* (2006). In-frame deletion in a novel centrosomal/ciliary protein CEP290/NPHP6 perturbs its interaction with RPGR and results in early-onset retinal degeneration in the rd16 mouse. *Human Molecular Genetics* **15**, 1847-57.

Chang, J., Seo, S. G., Lee, K. H., Nagashima, K., Bang, J. K., Kim, B. Y., Erikson, R. L., Lee, K. W., Lee, H. J., Park, J. E. *et al.* (2013). Essential role of Cenexin1, but not Odf2, in ciliogenesis. *Cell Cycle* **12**, 655-62.

Chang, W., Antoku, S., Östlund, C., Worman, H. J. and Gundersen, G. G. (2015). Linker of nucleoskeleton and cytoskeleton (LINC) complex mediated actin-dependent nuclear positioning orients centrosomes in migrating myoblasts. *Nucleus* **6**, 77-88.

Chapman, M. J. (1998). One hundred years of centrioles: the Henneguy-Lenhossek theory, meeting report. *International Microbiology* **1**, 233-6.

Chen, C. P. (2007). Meckel syndrome: genetics, perinatal findings, and differential diagnosis. *Taiwanese Journal of Obstetrics and Gynecology* **46**, 9-14.

Chen, H. J., Lin, C. M., Lin, C. S., Perez-Olle, R., Leung, C. L. and Liem, R. K. (2006). The role of microtubule actin cross-linking factor 1 (MACF1) in the Wnt signaling pathway. *Genes & Development* **20**, 1933-45.

Chen, J., Laclef, C., Moncayo, A., Snedecor, E. R., Yang, N., Li, L., Takemaru, K., Paus, R., Schneider-Maunoury, S. and Clark, R. A. (2015). The ciliopathy gene Rpgrip1l is essential for hair follicle development. *Journal of Investigative Dermatology* **135**, 701-9.

Chevrier, V., Piel, M., Collomb, N., Saoudi, Y., Frank, R., Paintrand, M., Narumiya, S., Bornens, M. and Job, D. (2002). The Rho-associated protein kinase p160ROCK is required for centrosome positioning. *Journal of Cell Biology* **157**, 807-17.

Chiang, A. P., Beck, J. S., Yen, H. J., Tayeh, M. K., Scheetz, T. E., Swiderski, R. E., Nishimura, D. Y., Braun, T. A., Kim, K. Y., Huang, J. *et al.* (2006). Homozygosity mapping with SNP arrays identifies TRIM32, an E3 ubiquitin ligase, as a Bardet-Biedl syndrome gene (BBS11). *Proceedings of the National Academy of Sciences of the United States of America* **103**, 6287-92.

Chih, B., Liu, P., Chinn, Y., Chalouni, C., Komuves, L. G., Hass, P. E., Sandoval, W. and Peterson, A. S. (2012). A ciliopathy complex at the transition zone protects the cilia as a privileged membrane domain. *Nature Cell Biology* **14**, 61-72.

Choi, S. Y., Chacon-Heszele, M. F., Huang, L., McKenna, S., Wilson, F. P., Zuo, X. and Lipschutz, J. H. (2013). Cdc42 deficiency causes ciliary abnormalities and cystic kidneys. *Journal of the American Society of Nephrology* **24**, 1435-50.

Christensen, S. T., Clement, C. A., Satir, P. and Pedersen, L. B. (2012). Primary cilia and coordination of receptor tyrosine kinase (RTK) signalling. *Journal of Pathology* **226**, 172-84.

Clotman, F., Libbrecht, L., Killingsworth, M. C., Loo, C. C., Roskams, T. and Lemaigre, F. P. (2008). Lack of cilia and differentiation defects in the liver of human foetuses with the Meckel syndrome. *Liver International* **28**, 377-84.

Collado-Hilly, M., Fisch, C., Desforges, B., Jerber, J., Combettes, L., Campillo, C. and Dupuis-Williams, P. (Cilia 2014 Conference (unpublished)). Evidence for a role of the ciliopathy protein MKS1 in cell polarity.

Cole, D. G., Diener, D. R., Himelblau, A. L., Beech, P. L., Fuster, J. C. and Rosenbaum, J. L. (1998). Chlamydomonas kinesin-II-dependent intraflagellar transport (IFT): IFT particles contain proteins required for ciliary assembly in *Caenorhabditis elegans* sensory neurons. *Journal of Cell Biology* **141**, 993-1008.

Collier, S. and Gubb, D. (1997). Drosophila tissue polarity requires the cell-autonomous activity of the fuzzy gene, which encodes a novel transmembrane protein. *Development* **124**, 4029-37.

Conrad, P. A., Giuliano, K. A., Fisher, G., Collins, K., Matsudaira, P. T. and Taylor, D. L. (1993). Relative distribution of actin, myosin I, and myosin II during the wound healing response of fibroblasts. *Journal of Cell Biology* **120**, 1381-1391.

Consugar, M. B., Kubly, V. J., Lager, D. J., Hommerding, C. J., Wong, W. C., Bakker, E., Gattone, V. H., Torres, V. E., Breuning, M. H. and Harris, P.C. (2007). Molecular diagnostics of Meckel-Gruber syndrome highlights phenotypic differences between MKS1 and MKS3. *Human Genetics* **121**, 591-9.

Cook, S. A., Collin, G. B., Bronson, R. T., Naggert, J. K., Liu, D. P., Akeson, E. C. and Davisson, M. T. (2009). A mouse model for Meckel syndrome type 3. *Journal of the American Society of Nephrology* **20**, 753-64.

Cook, T. A., Nagasaki, T. and Gundersen, G. G. (1998). Rho guanosine triphosphatase mediates the selective stabilization of microtubules induced by lysophosphatidic acid. *Journal of Cell Biology* **141**, 175-85.

Coppieters, F., Lefever, S., Leroy, B. P. and De Baere, E. (2010). CEP290, a gene with many faces: mutation overview and presentation of CEP290base. *Human Mutation* **31**, 1097-108.

Corbit, K. C., Aanstad, P., Singla, V., Norman, A. R., Stainier, D. Y. and Reiter, J. F. (2005). Vertebrate Smoothened functions at the primary cilium. *Nature* **437**, 1018-21.

Corbit, K. C., Shyer, A. E., Dowdle, W. E., Gaulden, J., Singla, V., Chen, M. H., Chuang, P. T. and Reiter, J. F. (2008). Kif3a constrains beta-catenin-dependent Wnt signalling through dual ciliary and non-ciliary mechanisms. *Nature Cell Biology* **10**, 70-6.

Couchman, J. R. and Rees, D. A. (1979). The behaviour of fibroblasts migrating from chick heart explants: changes in adhesion, locomotion and growth, and in the distribution of actomyosin and fibronectin. *Journal of Cell Science* **39**, 149-65.

Cowan C. R. and Hyman A. A. (2007). Acto-myosin reorganization and PAR polarity in *C. elegans. Development* **134**, 1035-43.

Craft, J. M., Harris, J. A., Hyman, S., Kner, P. and Lechtreck, K. F. (2015). Tubulin transport by IFT is upregulated during ciliary growth by a cilium-autonomous mechanism. *Journal of Cell Biology* **208**, 223-37.

Craige, B., Tsao, C. C., Diener, D. R., Hou, Y., Lechtreck, K. F., Rosenbaum, J. L. and Witman, G. B. (2010). CEP290 tethers flagellar transition zone MTs to the membrane and regulates flagellar protein content. *Journal of Cell Biology* **190**, 927-40.

Cramer, L. P. (1999). Organization and polarity of actin filament networks in cells: implications for the mechanism of myosin-based cell motility. *Biochemical Society Symposium* **65**, 173-205.

Cramer, L. P., Siebert, M. and Mitchison, T. J. (1997). Identification of novel graded polarity actin filament bundles in locomoting heart fibroblasts: implications for the generation of motile force. *Journal of Cell Biology* **136**, 1287-305.

Cruz, C., Ribes, V., Kutejova, E., Cayuso, J., Lawson, V., Norris, D., Stevens, J., Davey, M., Blight, K., Bangs, F. *et al.* (2010). Foxj1 regulates floor plate cilia architecture and modifies the response of cells to sonic hedgehog signalling. *Development* **137**, 4271-82.

Cui, C., Chatterjee, B., Lozito, T. P., Zhang, Z., Francis, R. J., Yagi, H., Swanhart, L. M., Sanker, S., Francis, D., Yu, Q. *et al.* (2013). Wdpcp, a PCP protein required for ciliogenesis, regulates directional cell migration and cell polarity by direct modulation of the actin cytoskeleton. *PLoS Biology* **11**, e1001720.

Dafinger, C., Liebau, M. C., Elsayed, S. M., Hellenbroich, Y., Boltshauser, E., Korenke, G. C., Fabretti, F., Janecke, A. R., Ebermann, I., Nurnberg, G. *et al.* (2011). Mutations in KIF7 link Joubert syndrome with Sonic Hedgehog signaling and MT dynamics. *Journal of Clinical Investigation* **121**, 2662-7.

Davey, M. G., James, J., Paton, I. R., Burt, D. W. and Tickle, C. (2007). Analysis of talpid3 and wild-type chicken embryos reveals roles for Hedgehog signalling in development of the limb bud vasculature. *Developmental Biology* **301**, 155-65.

Davey, M. G., Paton, I. R., Yin, Y., Schmidt, M., Bangs, F. K., Morrice, D. R., Smith, T. G., Buxton, P., Stamataki, D., Tanaka, M. *et al.* (2006). The chicken talpid3 gene encodes a novel protein essential for Hedgehog signaling. *Genes & Development* **20**, 1365-77.

Dawe, H. R., Adams, M., Wheway, G., Szymanska, K., Logan, C. V., Noegel, A. A., Gull, K. and Johnson, C. A. (2009). Nesprin-2 interacts with meckelin and mediates ciliogenesis via remodelling of the actin cytoskeleton. *Journal of Cell Science* **122**, 2716-26.

Dawe, H. R., Farr, H. and Gull, K. (2007a). Centriole/basal body morphogenesis and migration during ciliogenesis in animal cells. *Journal of Cell Science* **120**, 7-15.

Dawe, H. R., Smith, U. M., Cullinane, A. R., Gerrelli, D., Cox, P., Badano, J. L., Blair-Reid, S., Sriram, N., Katsanis, N., Attie-Bitach, T. *et al.* (2007b). The Meckel-Gruber Syndrome proteins MKS1 and meckelin interact and are required for primary cilium formation. *Human Molecular Genetics* **16**, 173-86.

de la Roche, M., Ritter, A. T., Angus, K. L., Dinsmore, C., Earnshaw, C. H., Reiter, J. F. and Griffiths, G. M. (2013). Hedgehog signaling controls T cell killing at the immunological synapse. *Science* **342**, 1247-50.

Deane, J. A., Cole, D. G., Seeley, E. S., Diener, D. R. and Rosenbaum, J. L. (2001). Localization of intraflagellar transport protein IFT52 identifies basal body transitional fibers as the docking site for IFT particles. *Current Biology* **11**, 1586-90.

Delgehyr, N., Sillibourne, J. and Bornens, M. (2005). Microtubule nucleation and anchoring at the centrosome are independent processes linked by ninein function. *Journal of Cell Science* **118**, 1565-75.

Delous, M., Baala, L., Salomon, R., Laclef, C., Vierkotten, J., Tory, K., Golzio, C., Lacoste, T., Besse, L., Ozilou, C. *et al.* (2007). The ciliary gene RPGRIP1L is mutated in cerebello-oculo-renal syndrome (Joubert syndrome type B) and Meckel syndrome. *Nature Genetics* **39**, 875-81.

den Hollander, A. I., Koenekoop, R. K., Yzer, S., Lopez, I., Arends, M. L., Voesenek, K. E., Zonneveld, M. N., Strom, T. M., Meitinger, T., Brunner, H. G. *et al.* (2006). Mutations in the CEP290 (NPHP6) gene are a frequent cause of Leber congenital amaurosis. *American Journal of Human Genetics* **79**, 556-61.

Desai, A. and Mitchison, T. J. (1997). Microtubule polymerization dynamics. *Annual Review of Cell and Developmental Biology* **13**, 83-117.

Diener, D. R., Lupetti, P. and Rosenbaum, J. L. (2015). Proteomic analysis of isolated ciliary transition zones reveals the presence of ESCRT proteins. *Current Biology* **25**, 379-84.

Dixon-Salazar, T. J., Silhavy, J. L., Udpa, N., Schroth, J., Bielas, S., Schaffer, A. E., Olvera, J., Bafna, V., Zaki, M. S., Abdel-Salam, G. H. *et al.* (2012). Exome sequencing can improve diagnosis and alter patient management. *Science Translational Medicine* **13**, 138ra78.

Doherty, D., Parisi, M. A., Finn, L. S., Gunay-Aygun, M., Al-Mateen, M., Bates, D., Clericuzio, C., Demir, H., Dorschner, M., van Essen, A. J. *et al.* (2010). Mutations in 3 genes (MKS3, CC2D2A and RPGRIP1L) cause COACH syndrome (Joubert syndrome with congenital hepatic fibrosis). *Journal of Medical Genetics* **47**, 8-21.

Dompierre, J. P., Godin, J. D., Charrin, B. C., Cordelieres, F. P., King, S. J., Humbert, S. and Saudou, F. (2007). Histone deacetylase 6 inhibition compensates for the transport deficit in Huntington's disease by increasing tubulin acetylation. *The Journal of Neuroscience* **27**, 3571-83.

Dowdle, W. E., Robinson, J. F., Kneist, A., Sirerol-Piquer, M. S., Frints, S. G., Corbit, K. C., Zaghloul, N. A., van Lijnschoten, G., Mulders, L., Verver, D. E. *et al.* (2011). Disruption of a ciliary B9 protein complex causes Meckel syndrome. *American Journal of Human Genetics* **89**, 94-110.

Drivas, T. G., Holzbaur, E. L. and Bennett, J. (2013). Disruption of CEP290 microtubule/membrane-binding domains causes retinal degeneration. *Journal of Clinical Investigation* **123**, 4525-39.

Du, E., Li, H., Jin, S., Hu, X., Qiu, M. and Han, R. (2013). Evidence that TMEM67 causes polycystic kidney disease through activation of JNK/ERK-dependent pathways. *Cell Biology International* **37**, 694-702.

Dujardin, D. L., Barnhart, L. E., Stehman, S. A., Gomes, E. R., Gundersen, G. G. and Vallee, R. B. (2003). A role for cytoplasmic dynein and LIS1 in directed cell movement. *Journal of Cell Biology* **163**, 1205-11.

Edvardson, S., Shaag, A., Zenvirt, S., Erlich, Y., Hannon, G. J., Shanske, A. L., Gomori, J. M., Ekstein, J. and Elpeleg, O. (2010). Joubert syndrome 2 (JBTS2) in Ashkenazi Jews is associated with a TMEM216 mutation. *American Journal of Human Genetics* **86**, 93-7.

Edwards, D. C., Sanders, L. C., Bokoch, G. M. and Gill, G. N. (1999). Activation of LIM-kinase by Pak1 couples Rac/Cdc42 GTPase signalling to actin cytoskeletal dynamics. *Nature Cell Biology* **1**, 253-9.

Efimenko, E., Bubb, K., Mak, H. Y., Holzman, T., Leroux, M. R., Ruvkun, G., Thomas, J. H. and Swoboda, P. (2005). Analysis of xbx genes in *C. elegans*. *Development* **132**, 1923-34.

Efimov, A. and Kaverina, I. (2009). Significance of microtubule catastrophes at focal adhesion sites. *Cell Adhesion & Migration* **3**, 285-7.

Efimov, A., Kharitonov, A., Efimova, N., Loncarek, J., Miller, P. M., Andreyeva, N., Gleeson, P., Galjart, N., Maia, A. R., McLeod, I. X. *et al.* (2007). Asymmetric CLASP-dependent nucleation of noncentrosomal MTs at the trans-Golgi network. *Developmental Cell* **12**, 917-30.

Efimov, A., Schiefermeier, N., Grigoriev, I., Ohi, R., Brown, M. C., Turner, C. E., Small, J. V. and Kaverina, I. (2008). Paxillin-dependent stimulation of microtubule catastrophes at focal adhesion sites. *Journal of Cell Science* **121**, 196-204.

Egea, G., Serra-Peinado, C., Salcedo-Sicilia, L. and Gutierrez-Martinez, E. (2013). Actin acting at the Golgi. *Histochemistry and Cell Biology*.

Eggenschwiler, J. T. and Anderson, K. V. (2007). Cilia and developmental signaling. *Annual Review of Cell and Developmental Biology* **23**, 345-73.

Ellenbroek, S. I. and Collard, J. G. (2007). Rho GTPases: functions and association with cancer. *Clinical and Experimental Metastasis* **24**, 657-72.

Etienne-Manneville, S. and Hall, A. (2001). Integrin-mediated activation of Cdc42 controls cell polarity in migrating astrocytes through PKCzeta. *Cell* **106**, 489-98.

Etienne-Manneville, S. and Hall, A. (2002). Rho GTPases in cell biology. *Nature* **420**, 629-35.

Euteneuer, U. and Schliwa, M. (1984). Persistent, directional motility of cells and cytoplasmic fragments in the absence of MTs. *Nature* **310**, 58-61.

Evans, L., Mitchison, T. and Kirschner, M. (1985). Influence of the centrosome on the structure of nucleated MTs. *Journal of Cell Biology* **100**, 1185-91.

Ezratty, E. J., Stokes, N., Chai, S., Shah, A. S., Williams, S. E. and Fuchs, E. (2011). A role for the primary cilium in Notch signaling and epidermal differentiation during skin development. *Cell* **145**, 1129-41.

Fan, C. W., Chen, B., Franco, I., Lu, J., Shi, H., Wei, S., Wang, C., Wu, X., Tang, W., Roth, M. G. *et al.* (2014). The Hedgehog pathway effector smoothened exhibits signaling competency in the absence of ciliary accumulation. *Chemistry & Biology* **21**, 1680-9.

Fan, Y., Esmail, M. A., Ansley, S. J., Blacque, O. E., Boroevich, K., Ross, A. J., Moore, S. J., Badano, J. L., May-Simera, H., Compton, D. S. *et al.* (2004). Mutations in a member of the Ras superfamily of small GTP-binding proteins causes Bardet-Biedl syndrome. *Nature Genetics* **36**, 989-93.

Fawcett, D. W. (1954). The study of epithelial cilia and sperm flagella with the electron microscope. *Laryngoscope* **64**, 557-67.

Fernandez-Borja, M., Janssen, L., Verwoerd, D., Hordijk, P. and Neefjes, J. (2005). RhoB regulates endosome transport by promoting actin assembly on endosomal membranes through Dia1. *Journal of Cell Science* **118**, 2661-70.

Ferrante, M. I., Zullo, A., Barra, A., Bimonte, S., Messaddeq, N., Studer, M., Dolle, P. and Franco, B. (2006). Oral-facial-digital type I protein is required for primary cilia formation and left-right axis specification. *Nature Genetics* **38**, 112-7.

Feldman, J. L. and Priess, J. R. (2012). A role for the centrosome and PAR-3 in the hand-off of MTOC function during epithelial polarization. *Current Biology* **22**, 575-82.

Filges, I., Nosova, E., Bruder, E., Tercanli, S., Townsend, K., Gibson, W. T., Röthlisberger, B., Heinimann, K., Hall, J. G., Gregory-Evans, C. Y. *et al.* (2014). Exome sequencing identifies mutations in KIF14 as a novel cause of an autosomal recessive lethal fetal ciliopathy phenotype. *Clinical Genetics* **86**, 220-8.

Finetti, F., Paccani, S. R., Riparbelli, M. G., Giacomello, E., Perinetti, G., Pazour, G. J., Rosenbaum, J. L. and Baldari, C. T. (2009). Intraflagellar transport is required for polarized recycling of the TCR/CD3 complex to the immune synapse. *Nature Cell Biology* **11**, 1332-9.

Follit, J. A., Tuft, R. A., Fogarty, K. E. and Pazour, G. J. (2006). The intraflagellar transport protein IFT20 is associated with the Golgi complex and is required for cilia assembly. *Molecular Biology of the Cell* **17**, 3781-92.

Fournier, M. F., Sauser, R., Ambrosi, D., Meister, J. J. and Verkhovsky, A. B. (2010). Force transmission in migrating cells. *Journal of Cell Biology* **188**, 287-97.

Francis, S. S., Sfakianos, J., Lo, B. and Mellman, I. (2011). A hierarchy of signals regulates entry of membrane proteins into the ciliary membrane domain in epithelial cells. *Journal of Cell Biology* **193**, 219-33.

Frank, V., den Hollander, A. I., Bruchle, N. O., Zonneveld, M. N., Nurnberg, G., Becker, C., Du Bois, G., Kendziorra, H., Roosing, S., Senderek, J. *et al.* (2008). Mutations of the CEP290 gene encoding a centrosomal protein cause Meckel-Gruber syndrome. *Human Mutation* **29**, 45-52.

Gad, A. K., Nehru, V., Ruusala, A. and Aspenstrom, P. (2012). RhoD regulates cytoskeletal dynamics via the actin nucleation-promoting factor WASp homologue associated with actin Golgi membranes and microtubules. *Molecular Biology of the Cell* **23**, 4807-19.

Gakovic, M., Shu, X., Kasioulis, I., Carpanini, S., Moraga, I. and Wright, A. F. (2011). The role of RPGR in cilia formation and actin stability. *Human Molecular Genetics* **20**, 4840-50.

Gao, B., Song, H., Bishop, K., Elliot, G., Garrett, L., English, M. A., Andre, P., Robinson, J., Sood, R., Minami, Y. *et al.* (2011). Wnt signaling gradients establish planar cell polarity by inducing Vangl2 phosphorylation through Ror2. *Developmental Cell* **20**, 163-76.

Garcia-Gonzalo, F. R., Corbit, K. C., Sirerol-Piquer, M. S., Ramaswami, G., Otto, E. A., Noriega, T. R., Seol, A. D., Robinson, J. F., Bennett, C. L., Josifova, D. J. *et al.* (2011). A transition zone complex regulates mammalian ciliogenesis and ciliary membrane composition. *Nature Genetics* **43**, 776-84.

Garcia-Gonzalo, F. R. and Reiter, J. F. (2012). Scoring a backstage pass: mechanisms of ciliogenesis and ciliary access. *Journal of Cell Biology* **197**, 697-709.

Gasteier, J. E., Madrid, R., Krautkramer, E., Schroder, S., Muranyi, W., Benichou, S. and Fackler, O. T. (2003). Activation of the Rac-binding partner FHOD1 induces actin stress fibers via a ROCK-dependent mechanism. *Journal of Biological Chemistry* **278**, 38902-12.

Gattone, V. H. 2nd, Tourkow, B. A., Trambaugh, C. M., Yu, A. C., Whelan, S., Phillips, C. L., Harris, P. C. and Peterson, R. G. (2004). Development of multiorgan pathology in the wpk rat model of polycystic kidney disease. *The Anatomical Record. Part A, Discoveries in Molecular, Cellular and Evolutionary Biology* **277**, 384-95.

Gauthier-Rouviere, C., Vignal, E., Meriane, M., Roux, P., Montcourier, P. and Fort, P. (1998). RhoG GTPase controls a pathway that independently activates Rac1 and Cdc42Hs. *Molecular Biology of the Cell* **9**, 1379-94.

Geiger, B., Spatz, J. P. and Bershadsky, A. D. (2009). Environmental sensing through focal adhesions. *Nature Reviews Molecular Cell Biology* **10**, 21-33.

Gerdes, J. M., Davis, E. E. and Katsanis, N. (2009). The vertebrate primary cilium in development, homeostasis, and disease. *Cell* **137**, 32-45.

Gerdes, J. M., Liu, Y., Zaghloul, N. A., Leitch, C. C., Lawson, S. S., Kato, M., Beachy, P. A., Beales, P. L., DeMartino, G. N., Fisher, S. *et al.* (2007). Disruption of the basal body compromises proteasomal function and perturbs intracellular Wnt response. *Nature Genetics* **39**, 1350-60.

Ghossoub, R., Hu, Q., Failler, M., Rouyez, M. C., Spitzbarth, B., Mostowy, S., Wolfrum, U., Saunier, S., Cossart, P., Jamesnelson, W. et al. (2013). Septins 2, 7 and 9 and MAP4 colocalize along the axoneme in the primary cilium and control ciliary length. *Journal of Cell Science* **126**, 2583-94.

Gilden, J. K., Peck, S., Chen, Y. C. and Krummel, M. F. (2012). The septin cytoskeleton facilitates membrane retraction during motility and blebbing. *Journal of Cell Biology* **196**, 103-14.

Goggolidou, P. (2014a). Wnt and planar cell polarity signaling in cystic renal disease. *Organogenesis* **10**, 86-95.

Goggolidou, P., Hadjirin, N. F., Bak, A., Papakrivopoulou, E., Hilton, H., Norris, D. P. and Dean, C. H. (2014b). Atmin mediates kidney morphogenesis by modulating Wnt signaling. *Human Molecular Genetics* **23**, 5303-16.

Goldstein B. and Macara I. G. (2007). The PAR proteins: fundamental players in animal cell polarization. *Developmental Cell* **13**, 609-22.

Gomes, E. R., Jani, S. and Gundersen, G. G. (2005). Nuclear movement regulated by Cdc42, MRCK, myosin, and actin flow establishes MTOC polarization in migrating cells. *Cell* **121**, 451-63.

Gomez, T. S., Kumar, K., Medeiros, R. B., Shimizu, Y., Leibson, P. J. and Billadeau, D. D. (2007). Formins regulate the actin-related protein 2/3 complex-independent polarization of the centrosome to the immunological synapse. *Immunity* **26**, 177-90.

Gomperts, B. N., Gong-Cooper, X. and Hackett, B. P. (2004). Foxj1 regulates basal body anchoring to the cytoskeleton of ciliated pulmonary epithelial cells. *Journal of Cell Science* **117**, 1329-37.

Goode, B. L. and Eck, M. J. (2007). Mechanism and function of formins in the control of actin assembly. *Annual Review of Biochemistry* **76**, 593-627.

Gorden, N. T., Arts, H. H., Parisi, M. A., Coene, K. L., Letteboer, S. J., van Beersum, S. E., Mans, D. A., Hikida, A., Eckert, M., Knutzen, D. *et al.* (2008). CC2D2A is mutated in Joubert syndrome and interacts with the ciliopathy-associated basal body protein CEP290. *American Journal of Human Genetics* **83**, 559-71.

Gotlieb, A. I., May, L. M., Subrahmanyan, L. and Kalnins, V. I. (1981). Distribution of microtubule organizing centers in migrating sheets of endothelial cells. *Journal of Cell Biology* **91**, 589-94.

Gray, R. S., Abitua, P. B., Wlodarczyk, B. J., Szabo-Rogers, H. L., Blanchard, O., Lee, I., Weiss, G. S., Liu, K. J., Marcotte, E. M., Wallingford, J. B. *et al.* (2009). The planar cell polarity effector Fuz is essential for targeted membrane trafficking, ciliogenesis and mouse embryonic development. *Nature Cell Biology* **11**, 1225-32.

Griffiths, G. M., Tsun, A. and Stinchcombe, J. C. (2010). The immunological synapse: a focal point for endocytosis and exocytosis. *Journal of Cell Biology* **189**, 399-406.

Gros, J., Serralbo, O. and Marcelle, C. (2009). WNT11 acts as a directional cue to organize the elongation of early muscle fibres. *Nature* **457**, 589-93.

Guirao, B., Meunier, A., Mortaud, S., Aguilar, A., Corsi, J. M., Strehl, L., Hirota, Y., Desoeuvre, A., Boutin, C., Han, Y. G. *et al.* (2010). Coupling between hydrodynamic forces and planar cell polarity orients mammalian motile cilia. *Nature Cell Biology* **12**, 341-50.

Gundersen, G. G. and Bulinski, J. C. (1986). Microtubule arrays in differentiated cells contain elevated levels of a post-translationally modified form of tubulin. *European Journal of Cell Biology* **42**, 288-94.

Gundersen, G. G. and Bulinski, J. C. (1988). Selective stabilization of microtubules oriented toward the direction of cell migration. *Proceedings of the National Academy of Sciences of the United States of America* **85**, 5946-50.

Gundersen, G. G., Gomes, E. R. and Wen, Y. (2004). Cortical control of microtubule stability and polarization. *Current Opinion in Cell Biology* **16**, 106-12.

Gundersen, G. G., Kalnoski, M. H. and Bulinski, J. C. (1984). Distinct populations of microtubules: tyrosinated and nontyrosinated alpha tubulin are distributed differently in vivo. *Cell* **38**, 779-89.

Halbritter, J., Bizet, A. A., Schmidts, M., Porath, J. D., Braun, D. A., Gee, H. Y., McInerney-Leo, A. M., Krug, P., Filhol, E. and Davis, E. E. (2013). Defects in the IFT-B component IFT172 cause Jeune and Mainzer-Saldino syndromes in humans. *American Journal of Human Genetics* **93**, 915-25.

Hashimoto, M., Shinohara, K., Wang, J., Ikeuchi, S., Yoshiba, S., Meno, C., Nonaka, S., Takada, S., Hatta, K., Wynshaw-Boris, A. *et al.* (2010). Planar polarization of node cells determines the rotational axis of node cilia. *Nature Cell Biology* **12**, 170-6.

Haycraft, C. J., Banizs, B., Aydin-Son, Y., Zhang, Q., Michaud, E. J. and Yoder, B. K. (2005). Gli2 and Gli3 localize to cilia and require the intraflagellar transport protein polaris for processing and function. *PLoS Genetics* **1**, e53.

He, M., Subramanian, R., Bangs, F., Omelchenko, T., Liem, K. F., Jr., Kapoor, T. M. and Anderson, K. V. (2014). The kinesin-4 protein Kif7 regulates mammalian Hedgehog signalling by organizing the cilium tip compartment. *Nature Cell Biology* **16**, 663-72.

Heil-Chapdelaine, R. A., Adames, N. R. and Cooper, J. A. (1999). Formin' the connection between microtubules and the cell cortex. *Journal of Cell Biology* **144**, 809-11.

Heisenberg, C. P., Tada, M., Rauch, G. J., Saude, L., Concha, M. L., Geisler, R., Stemple, D. L., Smith, J. C. and Wilson, S. W. (2000). Silberblick/Wnt11 mediates convergent extension movements during zebrafish gastrulation. *Nature* **405**, 76-81.

Hernandez-Hernandez, V., Pravincumar, P., Diaz-Font, A., May-Simera, H., Jenkins, D., Knight, M. and Beales, P. L. (2013). Bardet-Biedl syndrome proteins control the cilia length through regulation of actin polymerization. *Human Molecular Genetics* **22**, 3858-68.

Hirokawa, N. (1998). Kinesin and dynein superfamily proteins and the mechanism of organelle transport. *Science* **279**, 519-26.

Ho, W. C., Allan, V. J., van Meer G., Berger, E. G. and Kreis, T. E. (1989) Reclustering of scattered Golgi elements occurs along microtubules. *European Journal of Cell Biology* **48**, 250-63.

Hofmann, C., Shepelev, M. and Chernoff, J. (2004). The genetics of Pak. *Journal of Cell Science* **117**, 4343-54.

Holy, T. E., Dogterom, M., Yurke, B. and Leibler, S. (1997). Assembly and positioning of microtubule asters in microfabricated chambers. *Proceedings of the National Academy of Sciences of the United States of America* **94**, 6228-31.

Horvath, G. and Sorscher, E. J. (2008). Luminal fluid tonicity regulates airway ciliary beating by altering membrane stretch and intracellular calcium. *Cell Motility and the Cytoskeleton* **65**, 469-75.

Hsiao, Y. C., Tong, Z. J., Westfall, J. E., Ault, J. G., Page-McCaw, P. S. and Ferland, R. J. (2009). Ahi1, whose human ortholog is mutated in Joubert syndrome, is required for Rab8a localization, ciliogenesis and vesicle trafficking. *Human Molecular Genetics* **18**, 3926-41.

Hu, E., Chen, Z., Fredrickson, T. and Zhu, Y. (2001). Molecular cloning and characterization of profilin-3: a novel cytoskeleton-associated gene expressed in rat kidney and testes. *Experimental Nephrology* **9**, 265-74.

Hu, Q., Milenkovic, L., Jin, H., Scott, M. P., Nachury, M. V., Spiliotis, E. T. and Nelson, W. J. (2010). A Septin Diffusion Barrier at the Base of the

Primary Cilium Maintains Ciliary Membrane Protein Distribution. *Science* **329**, 436-439.

Huang, L., Szymanska, K., Jensen, V. L., Janecke, A. R., Innes, A. M., Davis, E. E., Frosk, P., Li, C., Willer, J. R., Chodirker, B. N. *et al.* (2011). TMEM237 is mutated in individuals with a Joubert syndrome related disorder and expands the role of the TMEM family at the ciliary transition zone. *American Journal of Human Genetics* **89**, 713-30.

Huang, P. and Schier, A. F. (2009). Dampened Hedgehog signaling but normal Wnt signaling in zebrafish without cilia. *Development* **136**, 3089-98.

Huangfu, D. and Anderson, K. V. (2005). Cilia and Hedgehog responsiveness in the mouse. *Proceedings of the National Academy of Sciences of the United States of America* **102**, 11325-30.

Huangfu, D., Liu, A., Rakeman, A. S., Murcia, N. S., Niswander, L. and Anderson, K. V. (2003). Hedgehog signalling in the mouse requires intraflagellar transport proteins. *Nature* **426**, 83-7.

Hurtado, L., Caballero, C., Gavilan, M. P., Cardenas, J., Bornens, M. and Rios, R. M. (2011). Disconnecting the Golgi ribbon from the centrosome prevents directional cell migration and ciliogenesis. *Journal of Cell Biology* **193**, 917-33.

Iannicelli, M., Brancati, F., Mougou-Zerelli, S., Mazzotta, A., Thomas, S., Elkhartoufi, N., Travaglini, L., Gomes, C., Ardissino, G. L. and Bertini E. (2010). Novel TMEM67 mutations and genotype-phenotype correlates in meckelin-related ciliopathies. *Human Mutation* **31**, 1319-31.

Ishikawa, H., Kubo, A., Tsukita, S. and Tsukita, S. (2005). Odf2-deficient mother centrioles lack distal/subdistal appendages and the ability to generate primary cilia. *Nature Cell Biology* **7**, 517-24.

Ishikawa, H. and Marshall, W. F. (2011). Ciliogenesis: building the cell's antenna. *Nature Reviews Molecular Cell Biology* **12**, 222-34.

Ishizaki, T., Morishima, Y., Okamoto, M., Furuyashiki, T., Kato, T. and Narumiya, S. (2001). Coordination of microtubules and the actin cytoskeleton by the Rho effector mDia1. *Nature Cell Biology* **3**, 8-14.

Ishizaki, T., Naito, M., Fujisawa, K., Maekawa, M., Watanabe, N., Saito, Y. and Narumiya, S. (1997). p160ROCK, a Rho-associated coiled-coil forming protein kinase, works downstream of Rho and induces focal adhesions. *FEBS Letters* **404**, 118-24.

Janmey, P. A., Hvidt, S., Lamb, J. and Stossel, T. P. (1990). Resemblance of actin-binding protein/actin gels to covalently crosslinked networks. *Nature* **345**, 89-92.

Jeffery, P. K. and Reid, L. (1975). New observations of rat airway epithelium: a quantitative and electron microscopic study. *Journal of Anatomy* **120**, 295-320.

Jensen, V. L., Li, C., Bowie, R. V., Clarke, L., Mohan, S., Blacque, O. E. and Leroux, M. R. (2015). Formation of the transition zone by Mks5/Rpgrip1L establishes a ciliary zone of exclusion (CIZE) that compartmentalises ciliary signalling proteins and controls PIP2 ciliary abundance. *EMBO Journal* **34**, 2537-56.

Jessen, J. R., Topczewski, J., Bingham, S., Sepich, D. S., Marlow, F., Chandrasekhar, A. and Solnica-Krezel, L. (2002). Zebrafish trilobite identifies new roles for Strabismus in gastrulation and neuronal movements. *Nature Cell Biology* **4**, 610-5.

Joberty, G., Petersen, C., Gao, L. and Macara, I. G. (2000). The cell-polarity protein Par6 links Par3 and atypical protein kinase C to Cdc42. *Nature Cell Biology* **2**, 531-9.

Kakinuma, T., Ichikawa, H., Tsukada, Y., Nakamura, T. and Toh, B. H. (2004). Interaction between p230 and MACF1 is associated with transport of a glycosyl phosphatidyl inositol-anchored protein from the Golgi to the cell periphery. *Experimental Cell Research* **298**, 388-98.

Karmous-Benailly, H., Martinovic, J., Gubler, M. C., Sirot, Y., Clech, L., Ozilou, C., Auge, J., Brahimi, N., Etchevers, H., Detrait, E. *et al.* (2005). Antenatal presentation of Bardet-Biedl syndrome may mimic Meckel syndrome. *American Journal of Human Genetics* **76**, 493-504.

Katsanis, N., Ansley, S. J., Badano, J. L., Eichers, E. R., Lewis, R. A., Hoskins, B. E., Scambler, P. J., Davidson, W. S., Beales, P. L. and Lupski, J. R. (2001). Triallelic inheritance in Bardet-Biedl syndrome, a Mendelian recessive disorder. *Science* **293**, 2256-9.

Kaverina, I., Krylyshkina, O. and Small, J. V. (1999). Microtubule targeting of substrate contacts promotes their relaxation and dissociation. *Journal of Cell Biology* **146**, 1033-44.

Kaverina, I., Rottner, K. and Small, J. V. (1998). Targeting, capture, and stabilization of microtubules at early focal adhesions. *Journal of Cell Biology* **142**, 181-90.

Keating, T. J. and Borisy, G. G. (1999). Centrosomal and non-centrosomal MTs. *Biology of the Cell* **91**, 321-9.

Keating, T. J. and Borisy, G. G. (2000). Immunostructural evidence for the template mechanism of microtubule nucleation. *Nature Cell Biology* **2**, 352-7.

Kelley, C. A., Sellers, J. R., Gard, D. L., Bui, D., Adelstein, R. S. and Baines, I. C. (1996). Xenopus nonmuscle myosin heavy chain isoforms have different subcellular localizations and enzymatic activities. *Journal of Cell Biology* **134**, 675-87.

Khanna, H., Davis, E. E., Murga-Zamalloa, C. A., Estrada-Cuzcano, A., Lopez, I., den Hollander, A. I., Zonneveld, M. N., Othman, M. I., Waseem, N., Chakarova, C. F. *et al.* (2009). A common allele in RPGRIP1L is a modifier of retinal degeneration in ciliopathies. *Nature Genetics* **41**, 739-45.

Kikuchi, A., Yamamoto, H. and Sato, A. (2009). Selective activation mechanisms of Wnt signaling pathways. *Trends in Cell Biology* **19**, 119-29.

Kim, D. H. and Wirtz, D. (2013). Focal adhesion size uniquely predicts cell migration. *FASEB Journal* **27**, 1351-61.

Kim, J. C., Badano, J. L., Sibold, S., Esmail, M. A., Hill, J., Hoskins, B. E., Leitch, C. C., Venner, K., Ansley, S. J., Ross, A. J. *et al.* (2004). The Bardet-Biedl protein BBS4 targets cargo to the pericentriolar region and is required for microtubule anchoring and cell cycle progression. *Nature Genetics* **36**, 462-70.

Kim, J., Lee, J. E., Heynen-Genel, S., Suyama, E., Ono, K., Lee, K., Ideker, T., Aza-Blanc, P. and Gleeson, J. G. (2010). Functional genomic screen for modulators of ciliogenesis and cilium length. *Nature* **464**, 1048-51.

Kirjavainen, A., Laos, M., Anttonen, T. and Pirvola, U. (2015). The Rho GTPase Cdc42 regulates hair cell planar polarity and cellular patterning in the developing cochlea. *Biology Open* **4**, 516-26.

Kirschner, M. W. and Mitchison, T. (1986). Microtubule dynamics. *Nature* **324**, 621.

Kobayashi, T., Kim, S., Lin, Y. C., Inoue, T. and Dynlacht, B. D. (2014). The CP110-interacting proteins Talpid3 and Cep290 play overlapping and distinct roles in cilia assembly. *Journal of Cell Biology* **204**, 215-29.

Kodama, A., Karakesisoglou, I., Wong, E., Vaezi, A. and Fuchs, E. (2003). ACF7: an essential integrator of microtubule dynamics. *Cell* **115**, 343-54.

Kodani, A., Kristensen, I., Huang, L. and Sutterlin, C. (2009). GM130-dependent control of Cdc42 activity at the Golgi regulates centrosome organization. *Molecular Biology of the Cell* **20**, 1192-200.

Kollman, J. M., Merdes, A., Mourey, L. and Agard, D. A. (2011). Microtubule nucleation by gamma-tubulin complexes. *Nature Reviews Molecular Cell Biology* **12**, 709-21.

Koonce, M. P., Cloney, R. A. and Berns, M. W. (1984). Laser irradiation of centrosomes in newt eosinophils: evidence of centriole role in motility. *Journal of Cell Biology* **98**, 1999-2010.

Kozminski, K. G., Beech, P. L. and Rosenbaum, J. L. (1995). The Chlamydomonas kinesin-like protein FLA10 is involved in motility associated with the flagellar membrane. *Journal of Cell Biology* **131**, 1517-27.

Kozminski, K. G., Johnson, K. A., Forscher, P. and Rosenbaum, J. L. (1993). A motility in the eukaryotic flagellum unrelated to flagellar beating. Proceedings of the *National Academy of Sciences of the United States of America* **90**, 5519-23.

Krock B. L. and Perkins B. D. (2014). The Par-PrkC polarity complex is required for cilia growth in zebrafish photoreceptors. *PLoS One* **21**, e104661.

Krylyshkina, O., Kaverina, I., Kranewitter, W., Steffen, W., Alonso, M. C., Cross, R. A. and Small, J. V. (2002). Modulation of substrate adhesion dynamics via microtubule targeting requires kinesin-1. *Journal of Cell Biology* **156**, 349-59.

Kudryashova, E., Kudryashov, D., Kramerova, I. and Spencer, M. J. (2005). Trim32 is a Ubiquitin Ligase Mutated in Limb Girdle Muscular Dystrophy Type 2H that Binds to Skeletal Muscle Myosin and Ubiquitinates Actin. *Journal of Molecular Biology* **354**, 413-24.

Kurtulmus, B., Wang, W., Ruppert, T., Neuner, A., Cerikan, B., Viol, L., Sanchez, R. D., Gruss, O. J. and Pereira, G. (2015). WDR8 is a centriolar satellite and centriole-associate protein that promotes ciliary vesicle docking during ciliogenesis. *Journal of Cell Science* [Epub ahead of print].

Kuzhandaivel, A., Schultz, S. W., Alkhori, L. and Alenius, M. (2014). Cilia-mediated hedgehog signaling in *Drosophila*. *Cell Reports* **7**, 672-80.

Kyttälä, M., Tallila, J., Salonen, R., Kopra, O., Kohlschmidt, N., Paavola-Sakki, P., Peltonen, L. and Kestilä, M (2006). MKS1, encoding a component of the flagellar apparatus basal body proteome, is mutated in Meckel syndrome. *Nature Genetics* **38**, 155-7.

Lancaster, M. A. and Gleeson, J. G. (2010). Cystic kidney disease: the role of Wnt signaling. *Trends in Molecular Medicine* **16**, 349-60.

Lancaster, M. A., Schroth, J. and Gleeson, J. G. (2011). Subcellular spatial regulation of canonical Wnt signalling at the primary cilium. *Nature Cell Biology* **13**, 700-7.

Lauffenburger, D. A. and Horwitz, A. F. (1996). Cell migration: a physically integrated molecular process. *Cell* **84**, 359-69.

Lechler, T. and Fuchs, E. (2007). Desmoplakin: an unexpected regulator of microtubule organization in the epidermis. *Journal of Cell Biology* **176**, 147-54.

Lee, J. H., Silhavy, J. L., Lee, J. E., Al-Gazali, L., Thomas, S., Davis, E. E., Bielas, S. L., Hill, K. J., Iannicelli, M., Brancati, F. *et al.* (2012). Evolutionarily assembled cis-regulatory module at a human ciliopathy locus. *Science* **335**, 966-9.

Lee, M. S., Hwang, K. S., Oh, H. W., Ji-Ae, K., Kim, H. T., Cho, H. S., Lee, J. J., Yeong Ko, J., Choi, J. H., Jeong, Y. M. *et al.* (2015). IFT46 plays an essential role in cilia development. *Developmental Biology* **400**, 248-57.

Leightner, A. C., Hommerding, C. J., Peng, Y., Salisbury, J. L., Gainullin, V. G., Czarnecki, P. G., Sussman, C. R. and Harris, P. C. (2013). The Meckel syndrome protein meckelin (TMEM67) is a key regulator of cilia function but is not required for tissue planar polarity. *Human Molecular Genetics* **22**, 2024-40.

Leitch, C., Zaghloul, N. A., Davis, E. E., Stoetzel, C., Diaz-Font, A., Rix, S., Alfadhel, M., Lewis, R. A., Eyaid, W., Banin, E. *et al.* (2008). Hypomorphic mutations in syndromic encephalocele genes are associated with Bardet-Biedl syndrome. *Nature Genetics* **40**, 443-8.

Lemullois, M., Boisvieux-Ulrich, E., Laine, M. C., Chailley, B. and Sandoz, D. (1988). Development and functions of the cytoskeleton during ciliogenesis in metazoa. *Biology of the Cell* **63**, 195-208.

Lemullois, M., Klotz, C. and Sandoz, D. (1987). Immunocytochemical localization of myosin during ciliogenesis of quail oviduct. *European Journal of Cell Biology* **43**, 429-37.

Lerner, U. H. and Ohlsson C. (2015). The WNT system: background and its role in bone. *Journal of Internal Medicine* **277**, 630-49.

Leung, C. L., Sun, D., Zheng, M., Knowles, D. R. and Liem, R. K. (1999). Microtubule actin cross-linking factor (MACF): a hybrid of dystonin and dystrophin that can interact with the actin and microtubule cytoskeletons. *Journal of Cell Biology* **147**, 1275-86.

Levy, J. R. and Holzbaur, E. L. (2008). Dynein drives nuclear rotation during forward progression of motile fibroblasts. *Journal of Cell Science* **121**, 3187-95.

Li, M. G., Serr, M., Edwards, K., Ludmann, S., Yamamoto, D., Tilney, L. G., Field, C. M. and Hays, T. S. (1999). Filamin is required for ring canal assembly and actin organization during *Drosophila* oogenesis. *Journal of Cell Biology* **146**, 1061-74.

Li, R. and Gundersen, G. G. (2008). Beyond polymer polarity: how the cytoskeleton builds a polarized cell. *Nature Reviews Molecular Cell Biology* **9**, 860-73.

Li, Y. and Hu, J. (2011). Small GTPases and cilia. *Protein Cell* **2**, 13-25.

Lim, Y. S., Chua, C. E. and Tang, B. L. (2011). Rabs and other small GTPases in ciliary transport. *Biology of the Cell* **103**, 209-21.

Lin, C. M., Chen, H. J., Leung, C. L., Parry, D. A. and Liem, R. K. (2005). Microtubule actin crosslinking factor 1b: a novel plakin that localizes to the Golgi complex. *Journal of Cell Science* **118**, 3727-38.

Lin, S. X., Gundersen, G. G. and Maxfield, F. R. (2002). Export from pericentriolar endocytic recycling compartment to cell surface depends on stable, detyrosinated (glu) microtubules and kinesin. *Molecular Biology of the Cell* **13**, 96-109.

Ling, H., Hanashiro, K., Luong, T. H., Benavides, L. and Fukasawa, K. (2015). Functional relationship among PLK2, PLK4 and ROCK2 to induce centrosome amplification. *Cell Cycle* **14**, 544-53.

Liu, Y. P., Tsai, I. C., Morleo, M., Oh, E. C., Leitch, C. C., Massa, F., Lee, B. H., Parker, D. S., Finley, D., Zaghloul, N. A. *et al.* (2014). Ciliopathy

proteins regulate paracrine signaling by modulating proteasomal degradation of mediators. *The Journal of Clinical Investigation* **124**, 2059-70.

Lo, C. M., Buxton, D. B., Chua, G. C., Dembo, M., Adelstein, R. S. and Wang, Y. L. (2004). Nonmuscle myosin IIb is involved in the guidance of fibroblast migration. *Molecular Biology of the Cell* **15**, 982-9.

Locke, M., Tinsley, C. L., Benson, M. A. and Blake, D. J. (2009). TRIM32 is an E3 ubiquitin ligase for dysbindin. *Human Molecular Genetics* **18**, 2344-58.

Loktev, A. V., Zhang, Q., Beck, J. S., Searby, C. C., Scheetz, T. E., Bazan, J. F., Slusarski, D. C., Sheffield, V. C., Jackson, P. K. and Nachury, M. V. (2008). A BBSome subunit links ciliogenesis, microtubule stability, and acetylation. *Developmental Cell* **15**, 854-65.

Ludford-Menting, M. J., Oliaro, J., Sacirbegovic, F., Cheah, E. T., Pedersen, N., Thomas. S. J., Pasam, A., Iazzolino, R., Dow, L. E., Waterhouse, N. J., *et al.* (2005). A network of PDZ-containing proteins regulates T cell polarity and morphology during migration and immunological synapse formation. *Immunity* **22**, 737-48.

Ma, Z., Kanai, M., Kawamura, K., Kaibuchi, K., Ye, K. and Fukasawa, K. (2006). Interaction between ROCK II and nucleophosmin/B23 in the regulation of centrosome duplication. *Molecular Cell Biology* **26**, 9016-34.

Madrid, R., Aranda, J. F., Rodriguez-Fraticelli, A. E., Ventimiglia, L., Andres-Delgado, L., Shehata, M., Fanayan, S., Shahheydari, H., Gomez, S., Jimenez, A. et al. (2010). The formin INF2 regulates basolateral-to-apical transcytosis and lumen formation in association with Cdc42 and MAL2. *Developmental Cell* **18**, 814-27.

Maekawa, M., Ishizaki, T., Boku, S., Watanabe, N., Fujita, A., Iwamatsu, A., Obinata, T., Ohashi, K., Mizuno, K. and Narumiya, S. (1999). Signaling from Rho to the actin cytoskeleton through protein kinases ROCK and LIM-kinase. *Science* **285**, 895-8.

Magdalena, J., Millard, T. H. and Machesky, L. M. (2003). Microtubule involvement in NIH 3T3 Golgi and MTOC polarity establishment. *Journal of Cell Science* **116**, 743-56.

Mahuzier, A., Gaude, H. M., Grampa, V., Anselme, I., Silbermann, F., Leroux-Berger, M., Delacour, D., Ezan, J., Montcouquiol, M., Saunier, S. *et al.* (2012). Dishevelled stabilization by the ciliopathy protein Rpgrip1l is essential for planar cell polarity. *Journal of Cell Biology* **198**, 927-40.

Margaron, Y., Fradet, N. and Cote, J. F. (2013). ELMO recruits actin cross-linking family 7 (ACF7) at the cell membrane for microtubule capture and stabilization of cellular protrusions. *Journal of Biological Chemistry* **288**, 1184-99.

May, S. R., Ashique, A. M., Karlen, M., Wang, B., Shen, Y., Zarbalis, K., Reiter, J., Ericson, J. and Peterson, A. S. (2005). Loss of the retrograde motor for IFT disrupts localization of Smo to cilia and prevents the expression of both activator and repressor functions of Gli. *Developmental Biology* **287**, 378-89.

May-Simera, H. L., Petralia, R. S., Montcouquiol, M., Wang, Y. X., Szarama, K. B., Liu, Y., Lin, W., Deans, M. R., Pazour, G. J. and Kelley, M. W. (2015). Ciliary proteins Bbs8 and Ift20 promote planar cell polarity in the cochlea. *Development* **142**, 555-66.

Meng, W., Mushika, Y., Ichii, T. and Takeichi, M. (2008). Anchorage of microtubule minus ends to adherens junctions regulates epithelial cell-cell contacts. *Cell* **135**, 948-59.

Miller, P. M., Folkmann, A. W., Maia, A. R., Efimova, N., Efimov, A. and Kaverina, I. (2009). Golgi-derived CLASP-dependent microtubules control Golgi organization and polarized trafficking in motile cells. *Nature Cell Biology* **11**, 1069-80.

Mingle, L. A., Okuhama, N. N., Shi, J., Singer, R. H., Condeelis, J. and Liu, G. (2005). Localization of all seven messenger RNAs for the actin-polymerization nucleator Arp2/3 complex in the protrusions of fibroblasts. *Journal of Cell Science* **118**, 2425-33.

Mitchell, B., Jacobs, R., Li, J., Chien, S. and Kintner, C. (2007). A positive feedback mechanism governs the polarity and motion of motile cilia. *Nature* **447**, 97-101.

Mitchison, T. J. and Cramer, L. P. (1996). Actin-based cell motility and cell locomotion. *Cell* **84**, 371-9.

Mogensen, M. M., Malik, A., Piel, M., Bouckson-Castaing, V. and Bornens, M. (2000). Microtubule minus-end anchorage at centrosomal and non-centrosomal sites: the role of ninein. *Journal of Cell Science* **113 (Pt 17)**, 3013-23.

Mohri, H. (1968). Amino-acid composition of "Tubulin" constituting microtubules of sperm flagella. *Nature* **217**, 1053-4.

Morgan, N. V., Gissen, P., Sharif, S. M., Baumber, L., Sutherland, J., Kelly, D. A., Aminu, K., Bennett, C. P., Woods, C. G., Mueller, R. F. *et al.* (2002). A novel locus for Meckel-Gruber syndrome, MKS3, maps to chromosome 8q24. *Human Genetics* **111**, 456-61.

Mougou-Zerelli, S., Thomas, S., Szenker, E., Audollent, S., Elkhartoufi, N., Babarit, C., Romano, S., Salomon, R., Amiel, J., Esculpavit, C. *et al.* (2009). CC2D2A mutations in Meckel and Joubert syndromes indicate a genotype-phenotype correlation. *Human Mutation* **30**, 1574-82.

Mseka, T. and Cramer, L. P. (2011). Actin depolymerization-based force retracts the cell rear in polarizing and migrating cells. *Current Biology* **21**, 2085-91.

Mukai, H., Kitagawa, M., Shibata, H., Takanaga, H., Mori, K., Shimakawa, M., Miyahara, M., Hirao, K. and Ono, Y. (1994). Activation of PKN, a novel 120-kDa protein kinase with leucine zipper-like sequences, by unsaturated fatty acids and by limited proteolysis. *Biochemical and Biophysical Research Communications* **204**, 348-56.

Nachury, M. V., Loktev, A. V., Zhang, Q., Westlake, C. J., Peranen, J., Merdes, A., Slusarski, D. C., Scheller, R. H., Bazan, J. F., Sheffield, V. C. *et al.* (2007). A core complex of BBS proteins cooperates with the GTPase Rab8 to promote ciliary membrane biogenesis. *Cell* **129**, 1201-13.

Nachury, M. V., Seeley, E. S. and Jin, H. (2010). Trafficking to the ciliary membrane: how to get across the periciliary diffusion barrier? *Annual Review of Cell and Developmental Biology* **26**, 59-87.

Nakagawa, T., Tanaka, Y., Matsuoka, E., Kondo, S., Okada, Y., Noda, Y., Kanai, Y. and Hirokawa, N. (1997). Identification and classification of 16 new kinesin superfamily (KIF) proteins in mouse genome. *Proceedings of the National Academy of Sciences of the United States of America* **94**, 9654-9.

Nagae, S., Meng, W. and Takeichi, M. (2013). Non-centrosomal microtubules regulate F-actin organization through the suppression of GEF-H1 activity. *Genes to Cells* **18**, 387-96.

Nauta, J., Goedbloed, M. A., Herck, H. V., Hesselink, D. A., Visser, P., Willemsen, R., Dokkum, R. P., Wright, C. J. and Guay-Woodford, L. M. (2000). New rat model that phenotypically resembles autosomal recessive polycystic kidney disease. *Journal of the American Society of Nephrology* **11,** 2272-84.

Ng, D. H., Humphries, J. D., Byron, A., Millon-Fremillon, A. and Humphries, M. J. (2014). Microtubule-dependent modulation of adhesion complex composition. *PLoS One* **9**, e115213.

Nobes, C. D. and Hall, A. (1999). Rho GTPases control polarity, protrusion, and adhesion during cell movement. *Journal of Cell Biology* **144**, 1235-44.

Noor, A., Windpassinger, C., Patel, M., Stachowiak, B., Mikhailov, A., Azam, M., Irfan, M., Siddiqui, Z. K., Naeem, F., Paterson, A. D. *et al.* (2008). CC2D2A, encoding a coiled-coil and C2 domain protein, causes autosomal-recessive mental retardation with retinitis pigmentosa. *American Journal of Human Genetics* **82**, 1011-8.

Norris, D. P. and Grimes, D. T. (2012). Mouse models of ciliopathies: the state of the art. *Disease Models & Mechanisms* **5**, 299-312.

Nozawa, Y., Lin, C. and Chuang, P. T. (2013). Hedgehog signaling from the primary cilium to the nucleus: an emerging picture of ciliary localization, trafficking and transduction. *Current Opinion in Genetics & Development* **23**, 429-37.

Oda, T., Chiba, S., Nagai, T. and Mizuno, K. (2014). Binding to Cep164, but not EB1, is essential for centriolar localization of TTBK2 and its function in ciliogenesis. *Genes to Cells* **19**, 927-40.

Oh, E. C. and Katsanis, N. (2012). Cilia in vertebrate development and disease. *Development* **139**, 443-8.

Olbrich, H., Fliegauf, M., Hoefele, J., Kispert, A., Otto, E., Volz, A., Wolf, M. T., Sasmaz, G., Trauer, U., Reinhardt R *et al.* (2003). Mutations in a novel gene, NPHP3, cause adolescent nephronophthisis, tapeto-retinal degeneration and hepatic fibrosis. *Nature Genetics* **34**, 455-9.

Oleynikov, Y. and Singer, R. H. (1998). RNA localization: different zipcodes, same postman? *Trends in Cell Biology* **8**, 381-3.

Olson, K. R., McIntosh, J. R. and Olmsted, J. B. (1995). Analysis of MAP 4 function in living cells using green fluorescent protein (GFP) chimeras. *Journal of Cell Biology* **130**, 639-50.

Okuhara, K., Murofushi, H. and Sakai, H. (1989). Binding of kinesin to stress fibers in fibroblasts under condition of microtubule depolymerization. *Cell Motility and the Cytoskeleton* **12**, 71-7.

Omran, H., Fernandez, C., Jung, M., Häffner, K., Fargier, B., Villaquiran, A., Waldherr, R., Gretz, N., Brandis, M., Rüschendorf, F. *et al.* (2000). Identification of a new gene locus for adolescent nephronophthisis, on chromosome 3q22 in a large Venezuelan pedigree. *American Journal of Human Genetics* **66**, 118-27.

Online Mendelian Inheritance in Man, O. (2016). Phenotypic series: {249000}. *Johns Hopkins University, Baltimore, MD* **Date Accessed: {15/01/2016}**.

Ossipova, O., Tabler, J., Green, J. B. and Sokol, S. Y. (2007). PAR1 specifies ciliated cells in vertebrate ectoderm downstream of aPKC. *Development* **134**, 4297-306.

Otterbein, L. R., Graceffa, P. and Dominguez, R. (2001). The crystal structure of uncomplexed actin in the ADP state. *Science* **293**, 708-11.

Otto, E. A., Tory, K., Attanasio, M., Zhou, W., Chaki, M., Paruchuri, Y., Wise, E. L., Wolf, M. T., Utsch, B., Becker, C. *et al.* (2009). Hypomorphic mutations in meckelin (MKS3/TMEM67) cause nephronophthisis with liver fibrosis (NPHP11). *Journal of Medical Genetics* **46**, 663-70.

Paintrand, M., Moudjou, M., Delacroix, H. and Bornens, M. (1992). Centrosome organization and centriole architecture: their sensitivity to divalent cations. *Journal of Structural Biology* **108**, 107-28.

Palazzo, A. F., Cook, T. A., Alberts, A. S. and Gundersen, G. G. (2001a). mDia mediates Rho-regulated formation and orientation of stable microtubules. *Nature Cell Biology* **3**, 723-9.

Palazzo, A. F., Joseph, H. L., Chen, Y. J., Dujardin, D. L., Alberts, A. S., Pfister, K. K., Vallee, R. B. and Gundersen, G. G. (2001b). Cdc42, dynein, and dynactin regulate MTOC reorientation independent of Rho-regulated microtubule stabilization. *Current Biology* **11**, 1536-41.

Pan, J., You, Y., Huang, T. and Brody, S. L. (2007). RhoA-mediated apical actin enrichment is required for ciliogenesis and promoted by Foxj1. *Journal of Cell Science* **120**, 1868-76.

Park, T. J., Haigo, S. L. and Wallingford, J. B. (2006). Ciliogenesis defects in embryos lacking inturned or fuzzy function are associated with failure of planar cell polarity and Hedgehog signaling. *Nature Genetics* **38**, 303-11.

Park, T. J., Mitchell, B. J., Abitua, P. B., Kintner, C. and Wallingford, J. B. (2008). Dishevelled controls apical docking and planar polarization of basal bodies in ciliated epithelial cells. *Nature Genetics* **40**, 871-9.

Park, W. J., Liu, J., Sharp, E. J. and Adler, P. N. (1996). The *Drosophila* tissue polarity gene inturned acts cell autonomously and encodes a novel protein. *Development* **122**, 961-9.

Patla, I., Volberg, T., Elad, N., Hirschfeld-Warneken, V., Grashoff, C., Fassler, R., Spatz, J. P., Geiger, B. and Medalia, O. (2010). Dissecting the molecular architecture of integrin adhesion sites by cryo-electron tomography. *Nature Cell Biology* **12**, 909-15.

Pavalko, F. M., Roberts, T. M. and Holliday, L. S. (1988). Relationship between plasma membrane mobility and substrate attachment in the crawling movement of spermatozoa from *Caenorhabditis elegans*. *Cell Motility and the Cytoskeleton* **11**, 16-23.

Pazour, G. J. and Bloodgood, R. A. (2008). Targeting proteins to the ciliary membrane. *Current Topics in Developmental Biology* **85**, 115-49.

Pedersen, L. B. and Rosenbaum, J. L. (2008). Intraflagellar transport (IFT) role in ciliary assembly, resorption and signalling. *Current Topics in Developmental Biology* **85**, 23-61.

Perkins, L. A., Hedgecock, E. M., Thomson, J. N. and Culotti, J. G. (1986). Mutant sensory cilia in the nematode *Caenorhabditis elegans*. *Developmental Biology* **117**, 456-87.

Picariello, T., Valentine, M. S., Yano, J. and Van Houten, J. (2014). Reduction of meckelin leads to general loss of cilia, ciliary microtubule misalignment and distorted cell surface organization. *Cilia* **3**, 2.

Pinson, K. I., Brennan, J., Monkley, S., Avery, B. J. and Skarnes, W. C. (2000). An LDL-receptor-related protein mediates Wnt signalling in mice. *Nature* **407**, 535-8.

Pintado, P., Seixas, C., Barral, D. C. and Lopes, S. S. (Cilia 2014 Conference (unpublished)). Arl13b interferes with α-tubulin acetylation.

Pitaval, A., Tseng, Q., Bornens, M. and Thery, M. (2010). Cell shape and contractility regulate ciliogenesis in cell cycle-arrested cells. *Journal of Cell Biology* **191**, 303-12.

Plotkin, M. and Mudunuri, V. (2008). Pod1 induces myofibroblast differentiation in mesenchymal progenitor cells from mouse kidney. *Journal of Cellular Biochemistry* **103**, 675-90.

Pollard, T. D., Blanchoin, L. and Mullins, R. D. (2000). Molecular mechanisms controlling actin filament dynamics in nonmuscle cells. *The Annual Review of Biophysics and Biomolecular Structure* **29**, 545-76.

Pollard, T. D. and Borisy, G. G. (2003). Cellular motility driven by assembly and disassembly of actin filaments. *Cell* **112**, 453-65.

Prager-Khoutorsky, M., Lichtenstein, A., Krishnan, R., Rajendran, K., Mayo, A., Kam, Z., Geiger, B. and Bershadsky, A. D. (2011). Fibroblast polarization is a matrix-rigidity-dependent process controlled by focal adhesion mechanosensing. *Nature Cell Biology* **13**, 1457-65.

Prosser, S. L., Sahota, N. K., Pelletier, L., Morrison, C. G. and Fry, A. M. (2015). Nek5 promotes centrosome integrity in interphase and loss of centrosome cohesion in mitosis. *Journal of Cell Biology* **209**, 339-48.

Pruyne, D. and Bretscher, A. (2000). Polarization of cell growth in yeast. I. Establishment and maintenance of polarity states. *Journal of Cell Science* **113 (Pt 3)**, 365-75.

Qin, H., Wang, Z., Diener, D. and Rosenbaum, J. (2007). Intraflagellar transport protein 27 is a small G protein involved in cell-cycle control. *Current Biology* **17**, 193-202.

Quassollo, G., Wojnacki, J., Salas, D. A., Gastaldi, L., Marzolo, M. P., Conde, C., Bisbal, M., Couve, A. and Caceres, A. (2015). A RhoA Signaling Pathway Regulates Dendritic Golgi Outpost Formation. *Current Biology* **25**, 971-82.

Quinlan, R. J., Tobin, J. L. and Beales, P. L. (2008). Modeling ciliopathies: Primary cilia in development and disease. *Current Topics in Developmental Biology* **84**, 249-310.

Ramadani, H. M. and Nasrat, H. A. (1992). Prenatal diagnosis of recurrent Meckel syndrome. *International Journal of Gynaecology and Obstetrics* **39**, 327-32.

Ravanelli, A. M. and Klingensmith, J. (2011). The actin nucleator Cordon-bleu is required for development of motile cilia in zebrafish. *Developmental Biology* **350**, 101-11.

Reed, N. A., Cai, D., Blasius, T. L., Jih, G. T., Meyhofer, E., Gaertig, J. and Verhey, K. J. (2006). Microtubule acetylation promotes kinesin-1 binding and transport. *Current Biology* **16**, 2166-72.

Reiter, J. F., Blacque, O. E. and Leroux, M. R. (2012). The base of the cilium: roles for transition fibres and the transition zone in ciliary formation, maintenance and compartmentalization. *EMBO Reports* **13**, 608-18.

Reiter, J. F. and Skarnes, W. C. (2006). Tectonic, a novel regulator of the Hedgehog pathway required for both activation and inhibition. *Genes & Development* **20**, 22-7.

Ridley, A. J. (2006). Rho GTPases and actin dynamics in membrane protrusions and vesicle trafficking. *Trends in Cell Biology* **16**, 522-9.

Ridley, A. J., Paterson, H. F., Johnston, C. L., Diekmann, D. and Hall, A. (1992). The small GTP-binding protein rac regulates growth factor-induced membrane ruffling. *Cell* **70**, 401-10.

Rieder, C. L., Faruki, S. and Khodjakov, A. (2001). The centrosome in vertebrates: more than a microtubule-organizing center. *Trends in Cell Biology* **11**, 413-9.

Riento, K. and Ridley, A. J. (2003). Rocks: multifunctional kinases in cell behaviour. *Nature Reviews Molecular Cell Biology* **4**, 446-56.

Rios, R. M. (2014). The centrosome-Golgi apparatus nexus. *Philosophical Transactions of the Royal Society London B Biological Sciences* 369.

Rivero, S., Cardenas, J., Bornens, M. and Rios, R. M. (2009). Microtubule nucleation at the cis-side of the Golgi apparatus requires AKAP450 and GM130. *EMBO Journal* **28**, 1016-28.

Roberson, E. C., Dowdle, W. E., Ozanturk, A., Garcia-Gonzalo, F. R., Li, C., Halbritter, J., Elkhartoufi, N., Porath, J. D., Cope, H., Ashley-Koch, A. *et al.* (2015). TMEM231, mutated in orofaciodigital and Meckel syndromes, organizes the ciliary transition zone. *Journal of Cell Biology* **209**, 129-42.

Rohlich, P. (1975). The sensory cilium of retinal rods is analogous to the transitional zone of motile cilia. *Cell and Tissue Research* **161**, 421-30.

Rosenbaum, J. L. and Witman, G. B. (2002). Intraflagellar transport. *Nature Reviews Molecular Cell Biology* **3**, 813-25.

Ross, A. J., May-Simera, H., Eichers, E. R., Kai, M., Hill, J., Jagger, D. J., Leitch, C. C., Chapple, J. P., Munro, P. M., Fisher, S. *et al.* (2005).

Disruption of Bardet-Biedl syndrome ciliary proteins perturbs planar cell polarity in vertebrates. *Nature Genetics* **37**, 1135-40.

Roume, J., Genin, E., Cormier-Daire, V., Ma, H. W., Mehaye, B., Attie, T., Razavi-Encha, F., Fallet-Bianco, C., Buenerd, A., Clerget-Darpoux, F. *et al.* (1998). A gene for Meckel syndrome maps to chromosome 11q13. *American Journal of Human Genetics* **63**, 1095-101.

Rundle, D. R., Gorbsky, G. and Tsiokas, L. (2004). PKD2 interacts and co-localizes with mDia1 to mitotic spindles of dividing cells: role of mDia1 IN PKD2 localization to mitotic spindles. *Journal of Biological Chemistry* **279**, 29728-39.

Rybakin, V., Gounko, N. V., Spate, K., Honing, S., Majoul, I. V., Duden, R. and Noegel, A. A. (2006). Crn7 interacts with AP-1 and is required for the maintenance of Golgi morphology and protein export from the Golgi. *Journal of Biological Chemistry* **281**, 31070-8.

Rybakin, V., Stumpf, M., Schulze, A., Majoul, I. V., Noegel, A. A. and Hasse, A. (2004). Coronin 7, the mammalian POD-1 homologue, localizes to the Golgi apparatus. *FEBS Letters* **573**, 161-7.

Saadi-Kheddouci, S., Berrebi, D., Romagnolo, B., Cluzeaud, F., Peuchmaur, M., Kahn, A., Vandewalle, A. and Perret, C. (2001). Early development of polycystic kidney disease in transgenic mice expressing an activated mutant of the beta-catenin gene. *Oncogene* **20**, 5972-81.

Salaycik, K. J., Fagerstrom, C. J., Murthy, K., Tulu, U. S. and Wadsworth, P. (2005). Quantification of microtubule nucleation, growth and dynamics in wound-edge cells. *Journal of Cell Science* **118**, 4113-22.

Salonen, R. (1984). The Meckel syndrome: clinicopathological findings in 67 patients. *American Journal of Medical Genetics* **18**, 671-89.

Salonen, R. and Paavola, P. (1998). Meckel syndrome. *Journal of Medical Genetics* **35**, 497-501.

Salpingidou, G., Smertenko, A., Hausmanowa-Petrucewicz, I., Hussey, P. J. and Hutchison, C. J. (2007). A novel role for the nuclear membrane protein emerin in association of the centrosome to the outer nuclear membrane. *Journal of Cell Biology* **178**, 897-904.

Sanderson, M. J. and Sleigh, M. A. (1981). Ciliary activity of cultured rabbit tracheal epithelium: beat pattern and metachrony. *Journal of Cell Science* **47**, 331-47.

Santander, V. S., Bisig, C. G., Purro, S. A., Casale, C. H., Arce, C. A. and Barra, H. S. (2006). Tubulin must be acetylated in order to form a complex with membrane Na(+),K (+)-ATPase and to inhibit its enzyme activity. *Molecular and Cellular Biochemistry* **291**, 167-74.

Satir, P. and Christensen, S. T. (2007). Overview of structure and function of mammalian cilia. *Annual Review of Physiology* **69**, 377-400.

Satir, P., Pedersen, L. B. and Christensen, S. T. (2010). The primary cilium at a glance. *Journal of Cell Science* **123**, 499-503.

Sayer, J. A., Otto, E. A., O'Toole, J. F., Nurnberg, G., Kennedy, M. A., Becker, C., Hennies, H. C., Helou, J., Attanasio, M., Fausett, B. V. *et al.* (2006). The centrosomal protein nephrocystin-6 is mutated in Joubert syndrome and activates transcription factor ATF4. *Nature Genetics* **38**, 674-81.

Scheffler, K., Minnes, R., Fraisier, V., Paoletti, A. and Tran, P. T. (2015). Microtubule minus end motors kinesin-14 and dynein drive nuclear congression in parallel pathways. *Journal of Cell Biology* **209**, 47-58.

Schlessinger, K., McManus, E. J. and Hall, A. (2007). Cdc42 and noncanonical Wnt signal transduction pathways cooperate to promote cell polarity. *Journal of Cell Biology* **178**, 355-61.

Schmidt, K. N., Kuhns, S., Neuner, A., Hub, B., Zentgraf, H. and Pereira, G. (2012). Cep164 mediates vesicular docking to the mother centriole during early steps of ciliogenesis. *Journal of Cell Biology* **199**, 1083-101.

Schneider, L., Clement, C. A., Teilmann, S. C., Pazour, G. J., Hoffmann, E. K., Satir, P. and Christensen, S. T. (2005). PDGFRalphaalpha signaling is regulated through the primary cilium in fibroblasts. *Current Biology* **15**, 1861-6.

Schneider, M., Lu, W., Neumann, S., Brachner, A., Gotzmann, J., Noegel, A. A. and Karakesisoglou, I. (2011). Molecular mechanisms of centrosome and cytoskeleton anchorage at the nuclear envelope. *Cell and Molecular Life Sciences* **68**, 1593-610.

Schofield, A. V., Steel, R. and Bernard, O. (2012). Rho-associated coiled-coil kinase (ROCK) protein controls microtubule dynamics in a novel signaling pathway that regulates cell migration. *Journal of Biological Chemistry* **287**, 43620-9.

Scholey, J. M. (2003). Intraflagellar transport. *Annual Review of Cell and Developmental Biology* **19**, 423-43.

Sedmak, T. and Wolfrum, U. (2010). Intraflagellar transport molecules in ciliary and nonciliary cells of the retina. *Journal of Cell Biology* **189**, 171-86.

Sedmak, T. and Wolfrum, U. (2011). Intraflagellar transport proteins in ciliogenesis of photoreceptor cells. *Biology of the Cell* **103**, 449-66.

Seeley, E. S. and Nachury, M. V. (2010). The perennial organelle: assembly and disassembly of the primary cilium. *Journal of Cell Science* **123**, 511-8.

Sepulveda, W., Sebire, N. J., Souka, A., Snijders, R. J. and Nicolaides, K. H. (1997). Diagnosis of the Meckel-Gruber syndrome at eleven to fourteen weeks' gestation. *American Journal of Obstetrics and Gynecology* **176**, 316-9.

Seixas, C., Choi, S. Y., Polgar, N., Umberger, N. L., East, M. P., Zuo, X., Moreiras, H., Ghossoub, R., Benmerah, A., Kahn RA *et al.* (2016). Arl13b and the exocyst interact synergistically in ciliogenesis. *Molecular Biology of the Cell* **27**, 308-20.

Shah, A. S., Ben-Shahar, Y., Moninger, T. O., Kline, J. N. and Welsh, M. J. (2009). Motile cilia of human airway epithelia are chemosensory. *Science* **325**, 1131-4.

Shaheen, R., Almoisheer, A., Faqeih, E., Babay, Z., Monies, D., Tassan, N., Abouelhoda, M., Kurdi, W., Al Mardawi, E., Khalil, MM. *et al.* (2015). Identification of a novel MKS locus defined by TMEM107 mutation. *Human Molecular Genetics* **24**, 5211-8.

Shaheen, R., Faqeih, E., Alshammari, M. J., Swaid, A., Al-Gazali, L., Mardawi, E., Ansari, S., Sogaty, S., Seidahmed, M. Z., Al Motairi, M. I. *et al.* (2013). Genomic analysis of Meckel-Gruber syndrome in Arabs reveals marked genetic heterogeneity and novel candidate genes. *European Journal of Human Genetics* **21**, 762-8.

Shaheen, R., Faqeih, E., Seidahmed, M. Z., Sunker, A., Alali, F. E., Al Qahtani, K. and Alkuraya, F. S. (2011). A TCTN2 mutation defines a novel Meckel Gruber syndrome locus. *Human Mutation* **32**, 573-8.

Sharma, N., Berbari, N. F. and Yoder, B. K. (2008). Ciliary dysfunction in developmental abnormalities and diseases. *Current Topics in Developmental Biology* **85**, 371-427.

Sharma, N., Bryant, J., Wloga, D., Donaldson, R., Davis, R. C., Jerka-Dziadosz, M. and Gaertig, J. (2007). Katanin regulates dynamics of

microtubules and biogenesis of motile cilia. *Journal of Cell Biology* **178**, 1065-79.

Shelanski, M. L. and Taylor, E. W. (1967). Isolation of a protein subunit from microtubules. *Journal of Cell Biology* **34**, 549-54.

Shen, Q. T., Hsiue, P. P., Sindelar, C. V., Welch, M. D., Campellone, K. G. and Wang, H. W. (2012). Structural insights into WHAMM-mediated cytoskeletal coordination during membrane remodeling. *Journal of Cell Biology* **199**, 111-24.

Shina, M. C., Ünal, C., Eichinger, L., Müller-Taubenberger, A., Schleicher, M., Steinert, M. and Noegel, A. A. (2010). A Coronin7 Homolog with Functions in Actin-driven Processes. *Journal of Biological Chemistry* **285**, 9249-9261.

Simms, R. J., Eley, L. and Sayer, J. A. (2009). Nephronophthisis. *European Journal of Human Genetics* **17**, 406-16.

Simons, M., Gloy, J., Ganner, A., Bullerkotte, A., Bashkurov, M., Kronig, C., Schermer, B., Benzing, T., Cabello, O. A., Jenny, A. *et al.* (2005). Inversin, the gene product mutated in nephronophthisis type II, functions as a molecular switch between Wnt signaling pathways. *Nature Genetics* **37**, 537-43.

Sipe, C. W., Liu, L., Lee, J., Grimsley-Myers, C. and Lu, X. (2013). Lis1 mediates planar polarity of auditory hair cells through regulation of microtubule organization. *Development* **140**, 1785-95.

Small, J. V., Isenberg, G. and Celis, J. E. (1978). Polarity of actin at the leading edge of cultured cells. *Nature* **272**, 638-9.

Small, J. V., Stradal, T., Vignal, E. and Rottner, K. (2002). The lamellipodium: where motility begins. *Trends in Cell Biology* **12**, 112-20.

Smith, U. M., Consugar, M., Tee, L. J., McKee, B. M., Maina, E. N., Whelan, S., Morgan, N. V., Goranson, E., Gissen, P. and Lilliquist, S. (2006). The transmembrane protein meckelin (MKS3) is mutated in Meckel-Gruber syndrome and the wpk rat. *Nature Genetics* **38**, 191-6.

Sorokin, S. (1962). Centrioles and the formation of rudimentary cilia by fibroblasts and smooth muscle cells. *Journal of Cell Biology* **15**, 363-77.

Sorokin, S. P. (1968). Reconstructions of centriole formation and ciliogenesis in mammalian lungs. *Journal of Cell Science* **3**, 207-30.

Sotelo, J. R. and Trujillo-Cenoz, O. (1958). Electron microscope study on the development of ciliary components of the neural epithelium of the chick embryo. *Zeitschrift fur Zellforschung und Mikroskopische Anatomie* **49**, 1-12.

Spalluto, C., Wilson, D. I. and Hearn, T. (2013). Evidence for reciliation of RPE1 cells in late G1 phase, and ciliary localisation of cyclin B1. *FEBS Open Biology* **3**, 334-40.

Srour, M., Hamdan, F. F., Schwartzentruber, J. A., Patry, L., Ospina, L. H., Shevell, M. I., Desilets, V., Dobrzeniecka, S., Mathonnet, G., Lemyre, E. *et al.* (2012). Mutations in TMEM231 cause Joubert syndrome in French Canadians. *Journal of Medical Genetics* **49**, 636-41.

Starr, D. A. and Fridolfsson, H. N. (2010). Interactions between nuclei and the cytoskeleton are mediated by SUN-KASH nuclear-envelope bridges. *Annual Review of Cell and Developmental Biology* **26**, 421-44.

Stephen, L. A., Davis, G. M., McTeir, K. E., James, J., McTeir, L., Kierans, M., Bain, A. and Davey, M. G. (2013). Failure of centrosome migration causes a loss of motile cilia in talpid(3) mutants. *Developmental Dynamics* **242**, 923-31.

Stoetzel, C., Laurier, V., Davis, E. E., Muller, J., Rix, S., Badano, J. L., Leitch, C. C., Salem, N., Chouery, E., Corbani, S. *et al.* (2006). BBS10 encodes a vertebrate-specific chaperonin-like protein and is a major BBS locus. *Nature Genetics* **38**, 521-4.

Stowers, L., Yelon, D., Berg, L. J. and Chant, J. (1995). Regulation of the polarization of T cells toward antigen-presenting cells by Ras-related GTPase CDC42. *Proceedings of the National Academy of Sciences of the United States of America* **92**, 5027-31.

Stratigopoulos, G., Martin Carli, J. F., O'Day, D. R., Wang, L., Leduc, C. A., Lanzano, P., Chung, W. K., Rosenbaum, M., Egli, D., Doherty, D. A. *et al.* (2014). Hypomorphism for RPGRIP1L, a ciliary gene vicinal to the FTO locus, causes increased adiposity in mice. *Cell Metabolism* **19**, 767-79.

Symons, M. H. and Mitchison, T. J. (1991). Control of actin polymerization in live and permeabilized fibroblasts. *Journal of Cell Biology* **114**, 503-13.

Szymanska, K., Berry, I., Logan, C. V., Cousins, S. R., Lindsay, H., Jafri, H., Raashid, Y., Malik-Sharif, S., Castle, B., Ahmed, M. *et al.* (2012). Founder mutations and genotype-phenotype correlations in Meckel-Gruber syndrome and associated ciliopathies. *Cilia* **1**, 18.

Szymanska, K., Hartill, V. L. and Johnson, C. A. (2014). Unraveling the genetics of Joubert and Meckel-Gruber syndromes. *Journal of Pediatric Genetics* **3**, 65-78.

Takao, D., Dishinger, J. F., Kee, H. L., Pinskey, J. M., Allen, B. L. and Verhey, K. J. (2014). An assay for clogging the ciliary pore complex distinguishes mechanisms of cytosolic and membrane protein entry. *Current Biology* **24**, 2288-94.

Tallila, J., Jakkula, E., Peltonen, L., Salonen, R. and Kestilä, M. (2008). Identification of CC2D2A as a Meckel syndrome gene adds an important piece to the ciliopathy puzzle. *American Journal of Human Genetics* **82**, 1361-7.

Tammachote, R., Hommerding, C. J., Sinders, R. M., Miller, C. A., Czarnecki, P. G., Leightner, A. C., Salisbury, J. L., Ward, C. J., Torres, V. E., Gattone, V. H., 2nd *et al.* (2009). Ciliary and centrosomal defects associated with mutation and depletion of the Meckel syndrome genes MKS1 and MKS3. *Human Molecular Genetics* **18**, 3311-23.

Tanaka, Y., Okada, Y. and Hirokawa, N. (2005). FGF-induced vesicular release of Sonic hedgehog and retinoic acid in leftward nodal flow is critical for left-right determination. *Nature* **435**, 172-7.

Tang, N. and Marshall, W. F. (2012). Centrosome positioning in vertebrate development. *Journal of Cell Science* **125**, 4951-61.

Thurston, S. F., Kulacz, W. A., Shaikh, S., Lee, J. M. and Copeland, J. W. (2012). The ability to induce microtubule acetylation is a general feature of formin proteins. *PLoS One* **7**, e48041.

Thyberg, J. and Moskalewski, S. (1999) Role of microtubules in the organization of the Golgi complex. *Experimental Cell Research* **246**: 263-279.

Tongsong, T., Piyamongkol, W. and Pongsatha, S. (1999). Prenatal diagnosis of Meckel syndrome: a case report. *Journal of Obstetrics and Gynaecology Research* **25**, 339-42.

Tucker, R. W., Pardee, A. B. and Fujiwara, K. (1979a). Centriole ciliation is related to quiescence and DNA synthesis in 3T3 cells. *Cell* **17**, 527-35.

Tucker, R. W., Scher, C. D. and Stiles, C. D. (1979b). Centriole deciliation associated with the early response of 3T3 cells to growth factors but not to SV40. *Cell* **18**, 1065-1072.

Tsai, J. W., Lian, W. N., Kemal, S., Kriegstein, A. R. and Vallee, R. B. (2010). Kinesin 3 and cytoplasmic dynein mediate interkinetic nuclear migration in neural stem cells. *Nature Neuroscience* **13**, 1463-71.

Valente, E. M., Logan, C. V., Mougou-Zerelli, S., Lee, J. H., Silhavy, J. L., Brancati, F., Iannicelli, M., Travaglini, L., Romani, S., Illi, B. *et al.* (2010). Mutations in TMEM216 perturb ciliogenesis and cause Joubert, Meckel and related syndromes. *Nature Genetics* **42**, 619-25.

Valente, E. M., Silhavy, J. L., Brancati, F., Barrano, G., Krishnaswami, S. R., Castori, M., Lancaster, M. A., Boltshauser, E., Boccone, L., Al-Gazali, L. *et al.* (2006). Mutations in CEP290, which encodes a centrosomal protein, cause pleiotropic forms of Joubert syndrome. *Nature Genetics* **38**, 623-5.

van der Meel, R., Symons, M. H., Kudernatsch, R., Kok, R. J., Schiffelers, R. M., Storm, G., Gallagher, W. M. and Byrne, A. T. (2011). The VEGF/Rho GTPase signalling pathway: a promising target for anti-angiogenic/anti-invasion therapy. *Drug Discovery Today* **16**, 219-28.

Vaughan, S., Shaw, M. and Gull, K. (2006). A post-assembly structural modification to the lumen of flagellar microtubule doublets. *Current Biology* **16**, R449-50.

Vaughn, K. C. and Renzaglia, K. S. (2006). Structural and immunocytochemical characterization of the Ginkgo biloba L. sperm motility apparatus. *Protoplasma* **227**, 165-73.

Veland, I. R., Montjean, R., Eley, L., Pedersen, L. B., Schwab, A., Goodship, J., Kristiansen, K., Pedersen, S. F., Saunier, S. and Christensen, S. T. (2013). Inversin/Nephrocystin-2 is required for fibroblast polarity and directional cell migration. *PLoS One* **8**, e60193.

Veleri, S., Manjunath, S. H., Fariss, R. N., May-Simera, H., Brooks, M., Foskett, T. A., Gao, C., Longo, T. A., Liu, P., Nagashima, K. *et al.* (2014). Ciliopathy-associated gene Cc2d2a promotes assembly of subdistal appendages on the mother centriole during cilia biogenesis. *Nature Communications* **5**, 4207.

Verhey, K. J. and Gaertig, J. (2007). The tubulin code. *Cell Cycle* **6**, 2152-60.

Vladar, E. K. and Axelrod, J. D. (2008). Dishevelled links basal body docking and orientation in ciliated epithelial cells. *Trends in Cell Biology* **18**, 517-20.

von Tobel, L., Mikeladze-Dvali, T., Delattre, M., Balestra, F. R., Blanchoud, S., Finger, S., Knott, G., Muller-Reichert, T. and Gonczy, P. (2014). SAS-1 is a C2 domain protein critical for centriole integrity in *C. elegans*. *PLoS Genetics* **10**, e1004777.

Vorobjev, I. A. and Nadezhdina, E. S. (1987). The centrosome and its role in the organization of MTs. *International Review of Cytology* **106**, 227-93.

Vinogradova, T., Miller, P. M. and Kaverina, I. (2009). Microtubule network asymmetry in motile cells: role of Golgi-derived array. *Cell Cycle* **8**, 2168-74.

Wakida, N. M., Botvinick, E. L., Lin, J. and Berns, M. W. (2010). An intact centrosome is required for the maintenance of polarization during directional cell migration. *PLoS One* **5**, e15462.

Walker, R. A., O'Brien, E. T., Pryer, N. K., Soboeiro, M. F., Voter, W. A., Erickson, H. P. and Salmon, E. D. (1988). Dynamic instability of individual MTs analyzed by video light microscopy: rate constants and transition frequencies. *Journal of Cell Biology* **107**, 1437-48.

Wallar, B. J., Deward, A. D., Resau, J. H. and Alberts, A. S. (2007). RhoB and the mammalian Diaphanous-related formin mDia2 in endosome trafficking. *Experimental Cell Research* **313**, 560-71.

Wallingford, J. B. and Mitchell, B. (2011). Strange as it may seem: the many links between Wnt signaling, planar cell polarity, and cilia. *Genes & Development* **25**, 201-13.

Wallingford, J. B., Rowning, B. A., Vogeli, K. M., Rothbacher, U., Fraser, S. E. and Harland, R. M. (2000). Dishevelled controls cell polarity during Xenopus gastrulation. *Nature* **405**, 81-5.

Wang, M., Bridges, J. P., Na, C. L., Xu, Y. and Weaver, T. E. (2009). Meckel-Gruber syndrome protein MKS3 is required for endoplasmic reticulum-associated degradation of surfactant protein C. *Journal of Biological Chemistry* **284**, 33377-83.

Wang, J., Hamblet, N. S., Mark, S., Dickinson, M. E., Brinkman, B. C., Segil, N., Fraser, S. E., Chen, P., Wallingford, J. B. and Wynshaw-Boris, A. (2006). Dishevelled genes mediate a conserved mammalian PCP pathway to regulate convergent extension during neurulation. *Development* **133**, 1767-78.

Warner, J. F., McCarthy, A. M., Morris, R. L. and McClay, D. R. (2014). Hedgehog signaling requires motile cilia in the sea urchin. *Molecular Biology and Evolution* **31**, 18-22.

Watanabe, N. and Mitchison, T. J. (2002). Single-molecule speckle analysis of actin filament turnover in lamellipodia. *Science* **295**, 1083-6.

Waterman-Storer, C. M. and Salmon, E. D. (1999). Positive feedback interactions between microtubule and actin dynamics during cell motility. *Current Opinion in Cell Biology* **11**, 61-67.

Waters, A. M. and Beales, P. L. (2011). Ciliopathies: an expanding disease spectrum. *Pediatric Nephrology* **26**, 1039-56.

Weatherbee, S. D., Niswander, L. A. and Anderson, K. V. (2009). A mouse model for Meckel syndrome reveals Mks1 is required for ciliogenesis and Hedgehog signaling. *Human Molecular Genetics* **18**, 4565-75.

Wegner, A. (1982). Treadmilling of actin at physiological salt concentrations. An analysis of the critical concentrations of actin filaments. *Journal of Molecular Biology* **161**, 607-15.

Wei, Q., Ling, K. and Hu, J. (2015). The essential roles of transition fibers in the context of cilia. *Current Opinion in Cell Biology* **35**, 98-105.

Weisenberg, R. C. (1972). Microtubule formation in vitro in solutions containing low calcium concentrations. *Science* **177**, 1104-5.

Werner, M. E., Ward, H. H., Phillips, C. L., Miller, C., Gattone, V. H. and Bacallao, R. L. (2013). Inversin modulates the cortical actin network during mitosis. *American Journal of Physiology: Cell Physiology* **305**, C36-47.

Wheway, G., Abdelhamed, Z., Natarajan, S., Toomes, C., Inglehearn, C. and Johnson, C. A. (2013). Aberrant Wnt signalling and cellular over-proliferation in a novel mouse model of Meckel-Gruber syndrome. *Developmental Biology* **377**, 55-66.

Williams, C. L., Li, C., Kida, K., Inglis, P. N., Mohan, S., Semenec, L., Bialas, N. J., Stupay, R. M., Chen, N., Blacque, O. E. *et al.* (2011). MKS and NPHP modules cooperate to establish basal body/transition zone membrane associations and ciliary gate function during ciliogenesis. *Journal of Cell Biology* **192**, 1023-41.

Williams, C. L., McIntyre, J. C., Norris, S. R., Jenkins, P. M., Zhang, L., Pei, Q., Verhey, K. and Martens, J. R. (2014). Direct evidence for BBSome-

associated intraflagellar transport reveals distinct properties of native mammalian cilia. *Nature Communications* **5**, 5813.

Wloga, D. and Gaertig, J. (2010). Post-translational modifications of microtubules. *Journal of Cell Science* **123**, 3447-55.

Wolf, M. T. and Hildebrandt, F. (2011). Nephronophthisis. *Pediatric Nephrology* **26**, 181-94.

Wolfenson, H., Henis, Y. I., Geiger, B. and Bershadsky, A. D. (2009). The heel and toe of the cell's foot: a multifaceted approach for understanding the structure and dynamics of focal adhesions. *Cell Motility and the Cytoskeleton* **66**, 1017-29.

Wood, C. R., Huang, K., Diener, D. R. and Rosenbaum, J. L. (2013). The cilium secretes bioactive ectosomes. *Current Biology* **23**, 906-11.

Yamamoto, T., Tsukahara, T., Ishiguro, T., Hagiwara, H., Taira, M. and Takeda, H. (2015). The medaka dhc2 mutant reveals conserved and distinct mechanisms of Hedgehog signaling in teleosts. *BMC Developmental Biology* **15**, 9.

Yang, N., Higuchi, O., Ohashi, K., Nagata, K., Wada, A., Kangawa, K., Nishida, E. and Mizuno, K. (1998). Cofilin phosphorylation by LIM-kinase 1 and its role in Rac-mediated actin reorganization. *Nature* **393**, 809-12.

Yang, T. T., Su, J., Wang, W. J., Craige, B., Witman, G. B., Tsou, M. F. and Liao, J. C. (2015). Superresolution Pattern Recognition Reveals the Architectural Map of the Ciliary Transition Zone. *Scientific Reports* **5**, 14096.

Yee, L. E., Garcia-Gonzalo, F. R., Bowie, R. V., Li, C., Kennedy, J. K., Ashrafi, K., Blacque, O. E., Leroux, M. R. and Reiter, J. F. (2015). Conserved Genetic Interactions between Ciliopathy Complexes Cooperatively Support Ciliogenesis and Ciliary Signaling. *PLoS Genetics* **11**, e1005627.

Yin, Y., Bangs, F., Paton, I. R., Prescott, A., James, J., Davey, M. G., Whitley, P., Genikhovich, G., Technau, U., Burt, D. W. *et al.* (2009). The Talpid3 gene (KIAA0586) encodes a centrosomal protein that is essential for primary cilia formation. *Development* **136**, 655-64.

Young, K. G. and Copeland, J. W. (2010). Formins in cell signaling. *Biochimica et Biophysica Acta (BBA)* **1803**, 183-90.

Young, K. G., Thurston, S. F., Copeland, S., Smallwood, C. and Copeland, J. W. (2008). INF1 is a novel microtubule-associated formin. *Molecular Biology of the Cell* **19**, 5168-80.

Yu, W., Ahmad, F. J. and Baas, P. W. (1994). MT fragmentation and partitioning in the axon during collateral branch formation. *The Journal of Neuroscience* **14**, 5872-84.

Yuan, W. C., Lee, Y. R., Lin, S. Y., Chang, L. Y., Tan, Y. P., Hung, C. C., Kuo, J. C., Liu, C. H., Lin, M. Y., Xu, M. *et al.* (2014). K33-Linked Polyubiquitination of Coronin 7 by Cul3-KLHL20 Ubiquitin E3 Ligase Regulates Protein Trafficking. *Molecular Cell* **54**, 586-600.

Zamir, E., Katz, B. Z., Aota, S., Yamada, K. M., Geiger, B. and Kam, Z. (1999). Molecular diversity of cell-matrix adhesions. *Journal of Cell Science* **112 (Pt 11)**, 1655-69.

Zamir, E., Katz, M., Posen, Y., Erez, N., Yamada, K. M., Katz, B. Z., Lin, S., Lin, D. C., Bershadsky, A., Kam, Z. *et al.* (2000). Dynamics and segregation of cell-matrix adhesions in cultured fibroblasts. *Nature Cell Biology* **2**, 191-6.

Zahnleiter, D., Hauer, N. N., Kessler, K., Uebe, S., Sugano, Y., Neuhauss, S. C., Giessl, A., Ekici, A. B., Blessing, H., Sticht, H. *et al.* (2015). MAP4-dependent regulation of microtubule formation affects centrosome, cilia, and golgi architecture as a central mechanism in growth regulation. *Human Mutation* **36**, 87-97.

Zhang, Y.E. (2009). Non-Smad pathways in TGF-beta signaling. *Cell Research* **19**, 128-39.

Zhou, X., Fan, L. X., Li, K., Ramchandran, R., Calvet, J. P. and Li, X. (2014). SIRT2 regulates ciliogenesis and contributes to abnormal centrosome amplification caused by loss of polycystin-1. *Human Molecular Genetics* **23**, 1644-55.

Zhou, W., Dai, J., Attanasio, M. and Hildebrandt, F. (2010). Nephrocystin-3 is required for ciliary function in zebrafish embryos. *American Journal of Physiology. Renal Physiology* **299**, F55-62.

Zhu, X. and Kaverina, I. (2013). Golgi as an MTOC: making microtubules for its own good. *Histochemistry and Cell Biology* **140**, 361-7.

Zuo, X., Fogelgren, B. and Lipschutz, J. H. (2011). The small GTPase Cdc42 is necessary for primary ciliogenesis in renal tubular epithelial cells. *The Journal of Biological Chemistry* **286**, 22469-77.

APPENDIX 1: Centrosome positioning in non-dividing cells

The following paper was written during the course of my PhD, co-first authored with Dr Amy Barker, and additionally authored by Dr Helen Dawe. This is a review describing centrosome movement in contexts outside of cell division.

This paper has been appended as it provides a more detailed insight into centrosome movement during ciliogenesis and in relation to the Golgi and the nucleus, as covered more briefly in the introduction to this thesis. It also further describes centrosome movement during cell migration.